JOURNAL OF TELECOMMUNICATIONS AND INFORMATION TECHNOLOGY

4/2016

Traffic Engineering in Software Defined Networks: A Survey

M. R. Abbasi, A. Guleria, and M. S. Devi — *Paper* — *3*

Network Dimensioning with Maximum Revenue Efficiency for the Fairness Index

G. Zalewski and W. Ogryczak — *Paper* — *15*

Hybrid Models for the OWA Optimization

P. Olender — *Paper* — *22*

EVA as a Tool for Estimation of Management Efficiency and Value Creation in Polish Telecom Sector

W. Kamieniecki — *Paper* — *31*

Self-organization and Routing Algorithms for the Purpose of the Sensor Network Monitoring Environmental Conditions on a Given Area

K. Bronk, A. Lipka, B. Wereszko, J. Żurek, and K. Żurek — *Paper* — *39*

Focusing Operators and Tracking Moving Wideband Sources

M. Frikel, S. Safi, and Y. Khmou — *Reprint* — *53*

Implementation of Standardized Cooperation Environment for Intelligent Transport Systems

M. Kowalewski and A. Pękalski — *Paper* — *60*

L-SCANN: Logarithmic Subcentroid and Nearest Neighbor

T. Ahmad and K. Muchammad — *Paper* — *71*

(*Contents Continued on Back Cover*)

Editorial Board

Editor-in Chief: ..... ***Paweł Szczepański***

Associate Editors: ..... ***Krzysztof Borzycki***
Marek Jaworski

Managing Editor: ..... ***Robert Magdziak***

Technical Editor: ..... ***Ewa Kapuściarek***

Editorial Advisory Board

Chairman: ..... ***Andrzej Jajszczyk***
Marek Amanowicz
Hovik Baghdasaryan
Wojciech Burakowski
Andrzej Dąbrowski
Andrzej Hildebrandt
Witold Hołubowicz
Andrzej Jakubowski
Marian Kowalewski
Andrzej Kowalski
Józef Lubacz
Tadeusz Łuba
Krzysztof Malinowski
Marian Marciniak
Józef Modelski
Ewa Orłowska
Andrzej Pach
Zdzisław Papir
Michał Pióro
Janusz Stokłosa
Andrzej P. Wierzbicki
Tadeusz Więckowski
Adam Wolisz
Józef Woźniak
Tadeusz A. Wysocki
Jan Zabrodzki
Andrzej Zieliński

ISSN 1509-4553 on-line: ISSN 1899-8852

© Copyright by National Institute of Telecommunications
Warsaw 2016

Circulation: 300 copies

Sowa – Druk na życzenie, www.sowadruk.pl, tel. 22 431-81-40

JOURNAL OF TELECOMMUNICATIONS AND INFORMATION TECHNOLOGY

Preface

The growth of today's telecommunications induces wide spectrum of obstacles on various layers, from management of large networks with thousands of nodes to physical aspects that touch singular links. The current issue of *Journal of Telecommunications and Information Technology* brings a set of eleven articles that cover just such a broad range of problems.

The first four papers focus on issues related with network-operator level. To begin with, the article *Traffic Engineering in Software Defined Networks: A Survey* by M. R. Abbasi, A. Guleria and M. S. Devi gives an overview over traffic engineering methods, which are intended to optimize a network and improve network robustness. In addition to classic techniques, the authors present the state of the art in traffic engineering solutions proposed for novel network architecture, which is Software Defined Networking (SDN). They also highlight the research challenges and future directions for SDN-based traffic engineering.

G. Zalewski and W. Ogryczak in their article *Network Dimensioning with Maximum Revenue Efficiency for the Fairness Index* propose a new optimization method that maximizes the total flow on given pairs of nodes. The feature of the method is that it takes into account a revenue factor together with fairness criteria, thus preventing the problem of starvation of less attractive paths.

Optimization is also the subject of the third article, entitled *Hybrid Models for the OWA Optimization*. P. Olender analyzes the so-called Ordered Weighted Averaging (OWA) optimization models and introduces new general formulations for them. Furthermore, the author proposes some simple valid inequalities to improve the computational performance. Presented numerical results illustrate that in the case of certain problem types, the proposed hybrid formulations outperform other general models presented in literature.

The Economic Value Added (EVA) indicator allows for measuring company efficiency showing the income after deduction of full costs of capital. W. Kamieniecki in the article *EVA as a Tool for Estimation of Management Efficiency and Value Creation in Polish Telecom Sector* studies the usefulness of the EVA analysis for evaluation of telecom companies. Obtained results indicate that EVA sign and magnitude are in agreement with indicators based on data from financial books. In addition, the author investigates the effectiveness of using EVA for prediction of telecom's market capitalization with the conclusion that EVA cannot be considered as a more effective indicator of company value than other commonly used indicators.

The next three papers are devoted to applications of telecommunication systems, as Internet of Things and Intelligent Transport Systems. Vision of Internet of Things (IoT) binds the digital world with the real one, and IoT services will actively benefit from information about the physical environment. This information is collected through diverse sets of interconnected sensors, which exchange data without human interaction. Taking into account the limited capabilities of devices, such sensor networks require different mechanisms compared to traditional telecommunication networks. K. Bronk, A. Lipka, B. Wereszko, J. Żurek and K. Żurek in their paper *Self-organization and Routing Algorithms for the Purpose of the Sensor Network Monitoring Environmental Conditions on a Given Area* describe their implementation of wireless sensor network, which was designed to gather information about environmental conditions on a defined area. They selected the KNeigbours algorithm to provide self-organization feature in their network, and proposed own routing algorithm, which jointly with modifications of MAC layer introduced to network nodes, increases network efficiency and helps maintain connectivity in the network.

In many emerging IoT applications, such as smart cities or smart transportation, obtaining information about precise location of involved users or objects plays a key role. M. Frikel, S. Safi and Y. Khmou in their article *Focusing Operators and Tracking Moving Wideband Sources* investigate a new method for localization of mobile terminals, which bases on estimation of two DOA (direction of arrival) by using two different arrays of sensors. In addition, they propose an algorithm for prediction of the trajectory of moving terminal, which exploits ARMA model. Presented simulation results illustrate effectiveness of the method to estimate location and trajectory of moving terminal operating in GSM band.

One of the areas in which IoT can be of great importance is Intelligent Transport Systems (ITS). M. Kowalewski and A. Pękalski in their article *Implementation of Standardized Cooperation Environment for Intelligent Transport Systems* provide a comprehensive overview of standards related with ITS communication model, with special focus on European Standards.

Securing computer networks is considered one of the biggest challenges nowadays. Intrusion Detection System (IDS) is a technology that monitors network and/or computer system for security violations. In the article *L-SCANN: Logarithmic Subcentroid and Nearest Neighbor* T. Ahmad and K. Muchammad investigate a method for data classification in IDS. By reducing the search space in training data, the authors achieve higher efficiency of their IDS, in terms of lower processing time and greater accuracy, compared with IDS that uses known TANN method.

The next two papers are devoted to the issues of the physical layer of OSI model. R. Singh and M. Rawat in their article *Closed-form Distribution and Analysis of a Combined Nakagami-lognormal Shadowing and Unshadowing Fading Channel* deal with modeling problem of the realistic wireless channels that face shadowing and unshadowing fading in wireless signal propagation. The authors propose a new closed-form probability distribution function of a Nakagami-lognormal model of fading channel, which next allows them to derive the closed-form expression of combined Nakagami-lognormal shadowing and unshadowing fading. The obtained result facilitates carrying out the performance evaluation of wireless communication links.

T. Kossek, D. Czułek and M. Koba in *Long-term Absolute Wavelength Stability of Acetylene-stabilized Reference Laser at 1533 nm* measure the frequency of a laser emitting light in 1550 nm region against optical frequency of commercially available comb generator. Accurate optical frequency standards are important tool in development of fiber optic telecommunications. The authors propose the measuring method that provides high accuracy and high flexibility compared with methods presented in literature.

The last paper *Verification of Staff Proficiency in the Calibration Laboratory on Voltage, Frequency, Resistance and Capacity Measurements* by A. Warzec, M. Marszalec, and M. Lusawa, is concerned with determination of most appropriate algorithm of staff proficiency verification. The authors, with many years of experience gained in the Laboratory of Electrical, Electronic & Optoelectronic Metrology in National Institute of Telecommunications, present measurement systems used for verification, analysis of results or simulations, and show conclusions for selecting best solution.

Piotr Krawiec
Guest Editor

Paper

Traffic Engineering in Software Defined Networks: A Survey

Mohammad R. Abbasi[1], Ajay Guleria[2], and Mandalika S. Devi[1]

[1] *Department of Computer Science and Application, Panjab University, Chandigarh, India*
[2] *Computer Center, Panjab University, Chandigarh, India*

Abstract—An important technique to optimize a network and improve network robustness is traffic engineering. As traffic demand increases, traffic engineering can reduce service degradation and failure in the network. To allow a network to adapt to changes in the traffic pattern, the research community proposed several traffic engineering techniques for the traditional networking architecture. However, the traditional network architecture is difficult to manage. Software Defined Networking (SDN) is a new networking model, which decouples the control plane and data plane of the networking devices. It promises to simplify network management, introduces network programmability, and provides a global view of network state. To exploit the potential of SDN, new traffic engineering methods are required. This paper surveys the state of the art in traffic engineering techniques with an emphasis on traffic engineering for SDN. It focuses on some of the traffic engineering methods for the traditional network architecture and the lessons that can be learned from them for better traffic engineering methods for SDN-based networks. This paper also explores the research challenges and future directions for SDN traffic engineering solutions.

Keywords—application awareness, Software Defined Networking, traffic engineering.

1. Introduction

A major problem with underlying communication network is the dynamic nature of the network applications and their environment. This means that the performance requirements of the transferred data flows, like Quality of Service (QoS), can vary over time. The applications operate in a wide range of environments, i.e. wired and wireless with a variety of networking devices. For the applications to perform effectively, the underlying network should be flexible enough to dynamically change in response to any changes in the application requirements and their environment. The current approaches are either based on static or overprovisioned overlay networks, or require the applications to change in accordance with the network performance.

An important way to address this problem is through traffic engineering (TE). It is the process of analyzing the network state, predicting and balancing the transmitted data load over the network resources. It is a technique used to adapt the traffic routing to the changes in the network condition. The aim of traffic engineering is to improve network performance, QoS and user experience, by efficient use of resources, which can reduce operation cost too. The QoS techniques assign the available resources to the prioritized traffic to avoid congestion for this traffic. However, these techniques do not provide additional resources to the traffic that requires QoS. The traditional routing techniques do not provide any mechanism to allocate network resources in an optimal way.

To address this problem the research community started working on traffic engineering and proposed new ways to improve network robustness in response to the growth of traffic demands. Traffic engineering reduces the service degradation due to congestion and failure, e.g. link failure. Fault tolerance is an important property of any network. It is to ensure that if a failure exists in the network, still the requested data can be delivered to the destination.

Computer networks consist of numerous networking devices, such as switches, middle boxes (e.g. firewalls) and routers. Traditional network architecture is distributed, as shown in Fig. 1, where each networking device has both the control plane and the data plane. The control plane is the intelligent part of networking devices. It makes decision about forwarding and routing of data-flow. The data plane is the part of a networking device that carries user traffic. It executes the control plane's commands and forwards the data.

Network operators have to manually configure these multi-vendor devices to respond to a variety of applications and event in the network. Often they have to use limited tools such as command line interface (CLI) and sometimes scripting tools to convert these high-level configuration policies into low-level policies. This makes the management and optimization of a network difficult, which can introduce errors in the network. Other problems with this architecture can cause oscillations in the network, since control planes of the devices are distributed, innovation is difficult because the vendors prohibit modification of the underlying software in the devices.

To overcome these problems, the idea of network programmability was introduced, particularly with the introduction of Software Defined Networking (SDN) [1]. SDN allows a network to be programmed so that its behavior can

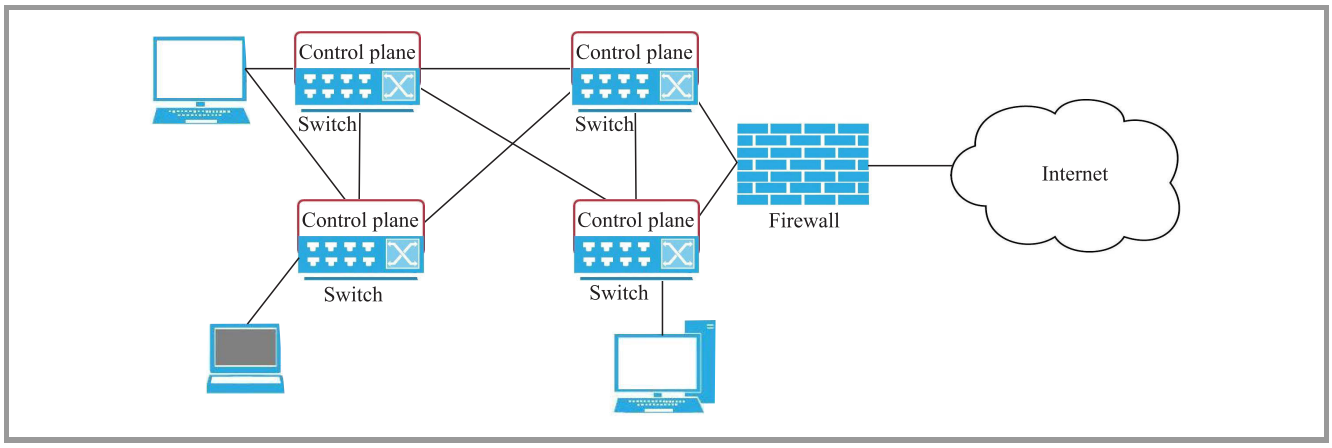

Fig. 1. Traditional network architecture.

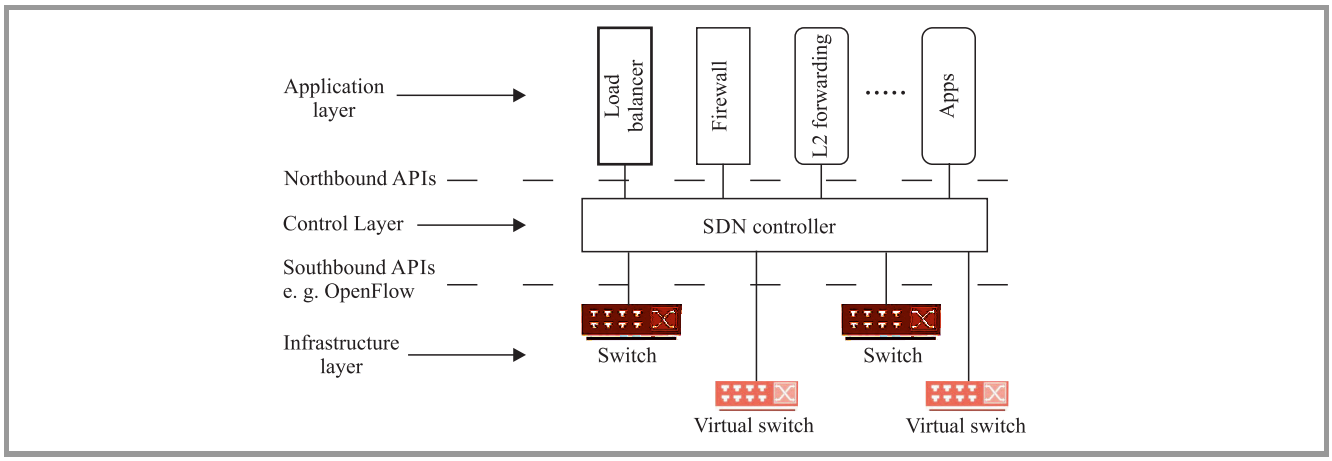

Fig. 2. An example of SDN architecture.

be changed actively on demand and in a fine-grained manner. It is a new networking model, where the control plane and the data plane are separated. The idea behind SDN is to simplify network management and enable innovation, i.e. to develop and deploy new network applications and services with ease, also to manage and optimize network performance through high-level policy enforcement.

To optimize these heterogeneous networks, both classic networks and SDN-based networks, a number of TE techniques have been introduced. Most are based on tweaking wide area TE and routing mechanism, such as Equal Cost Multi-Path routing (ECMP), Intermediate System to Intermediate System (IS-IS), and Multi protocol Label Switching (MPLS) [2], [3].

From traffic engineering point of view, even though these techniques perform well, they suffer from several limitations such as, they take routing decision locally, and it is difficult to change the link weights dynamically. In addition, while sending traffic these techniques consider few criteria, such as link capacity.

SDN separates the control plane and data plane of networking devices and introduces a well-defined interface, the OpenFlow protocol [4], between the two planes. The SDN architecture (Fig. 2) and the OpenFlow takes the intelligence, control functions, out of networking devices and place them in a centralized servers called controller, and provides centralized control over a network. The SDN/OpenFlow controller acts as an operating system for the network. It executes the control applications and services, such as routing protocols and L2 forwarding. This configuration abstracts the underlying network infrastructure. Therefore, it enables the applications and network services to treat the network as a logical entity.

One of the most widely used SDN enabler is the OpenFlow v.1.3 protocol. It allows the controller to manage the OpenFlow switches. The OpenFlow switches contain one or more flow tables, a group table, and a secure OpenFlow channel (Fig. 3). The flow tables and the group table are used for packet lookup and then to forward the packets. The OpenFlow channel is an abstraction layer. It establishes a secure link between each of the switches and the controller via the OpenFlow protocol. This channel abstracts the underlying switch hardware. As of OpenFlow version 1.5, a switch can have one or more OpenFlow channels that are connected to multiple controllers.

SDN is, generally, a flow-based control strategy. Through the OpenFlow a controller can define how the switches should treat the flows. In a SDN when a source node sends

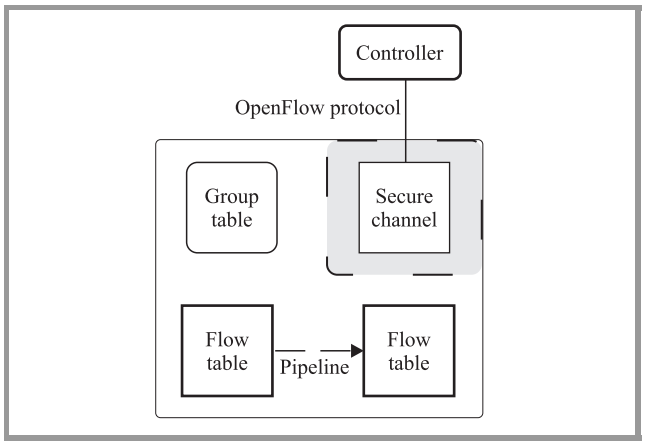

Fig. 3. Main OpenFlow switch components.

data to the destination, the switch sends the first packet to the controller, since it doesn't know how to treat this packet. The controller calculates the path for this packet and installs the appropriate rules in the switches on the packet's path. The new networking paradigm, SDN, has introduced new characteristics such as:

- separation of the control plane functionality, and the data plane functionality;
- centralized architecture allows the controller to have a central view of the deployed network. The controller has the global view of the network devices, servers, and virtual machines;
- network programmability, SDN provides an open standard, which allows external applications to program the network;
- facilitates innovation, new protocols and control applications can be introduced because OpenFlow provides the required abstractions, so we do not need to know the switch internals and configuration;
- flow management, through the OpenFlow a controller can define flows in different granularity, and how the switches should treat the flows.

The rest of the paper surveys some of the TE techniques, and it is organized as follows: Section 2 provides some of the TE mechanisms available for the classic network architecture and the assimilation from them. Section 3 describes an overview of SDN TE solutions. In Section 4, research challenges and future directions are discussed. Sections 5 and 6 conclude the paper.

2. Review of Classic Traffic Engineering Techniques

Classic traffic engineering techniques are based on tweaking wide area TE and routing mechanism such as ECMP or existing routing protocols such as IS-IS or MPLS [2], [3], [5], [6]. The Open Shortest Path First (OSPF) and IS-IS routing protocols do not adapt to the changes in the network condition because the link weights are static and these protocols lack any performance objectives while selecting the paths. The traffic engineering extensions to IS-IS and OSPF standard, extends these protocols by incorporating the traffic load while selecting a path. In these approaches during link state advertisements, routers advertise the traffic load along with link costs. After routers exchange link costs and traffic loads, then they calculate the shortest path for each destination. These standards require the routers to be modified to collect and exchange traffic statistics [5], [6].

Fortz *et al*. [7] propose a traffic engineering mechanism that monitors network wide view of the traffic pattern and network topology, then changes the link weights accordingly. This mechanism is based on the interior gateway protocols, like IS-IS. The authors says that classic inter-domain gateway protocols are effective traffic engineering tools in a network, and ensure robustness in terms of scalability and failure recovery. The introduced mechanism keeps the router and routing protocols unchanged. The mechanism is a centralized approach where it monitors the network topology and traffic, then optimizes the link costs to provide the best path possible to address the network goals. Routing protocols, like OSPF, select the path with minimum cost. If multiple paths with the same minimum cost are available then the traffic can be equally distributed among these paths. This is the concept behind ECMP. As depicted in Fig. 4, ECMP is a routing technique which balances the load over multiple paths by routing the packets to multiple-paths with equal cost. Various routing protocols such as OSPF and IS-IS explicitly support ECMP routing [8].

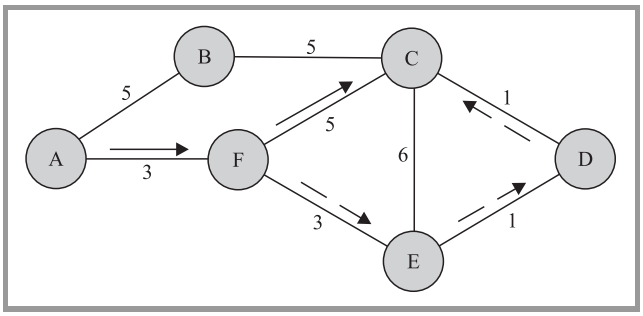

Fig. 4. An example of ECMP – there are two paths with equal cost to the destication node C, i.e. (A, F, C) and (A, F, E, D, C).

Multi-protocol Label Switching, MPLS, provides a tunneling mechanism. It creates end-to-end connections between the nodes. MPLS can integrate short path labels with IP routing mechanism, where the ingress routers assign short fixed labels to the packets, instead of long network addresses. The networking devices use this label to forward the packets to the destination through label-switched path (LSP). This reduces the routing table lookup overhead. The MPLS based traffic engineering, MPLS-TE, first reserve the resources for end-to-end path and then transfer the data. It establishes a labeled switched path over links

with sufficient bandwidth. This technique assures that enough resources are available for a flow. Since MPLS-TE works on available bandwidth in one aggregated class, it does not support QoS [9]. To provide QoS capability DiffServe-aware MPLS-TE techniques have been introduced, which combine both the Differentiated Services (DiffServ) and MPLS traffic engineering techniques to provide QoS [10]. Dongli *et al.* [9] analyze the QoS performance of DiffServe-aware MPLS traffic engineering techniques. The experimental results show that DiffServ-aware MPLS-TE can provide good QoS for traffics such as VoIP and other data, but due to the variable bit-rate property of the video data, these techniques cannot guarantee QoS for video data. As compared with conventional routing protocol MPLS is more flexible in selecting paths, since it sets up virtual circuit paths to send the traffic. The disadvantage of MPLS is that network operators need to manage the resource allocation to each path, and change the network configuration to adjust the path to the traffic condition. Because MPLS-TE transfers the aggregated traffics along allocated LSPs, it suffers from scalability and robustness [11]. In MPLS-TE it is necessary to use backup links so that if any link fails the traffic can be transferred through different paths.

An important way to balance the traffic over network resources is to disseminate the traffic over multiple paths. Gojmerac *et al.* [12] introduce an adaptive multi-path routing, which allows dynamic traffic engineering. Unlike other solutions, using global network information, the proposed technique focuses on local information in each node. This means the routers exchange information about links only to their immediate neighbors. So the nodes only have the information regarding their neighbors. During multi-path routing any neighboring node which is closer to the destination has a smaller cost than the current node. This neighboring node is considered as a viable candidate for the next hop. The advantage of taking routing decision based on local information is that it can reduce the signaling and memory overhead. The downside to the approach is, since the nodes do not have the global knowledge of the network state, it may not result in optimum routing of the traffic. Also due to the inherent limitation of the traditional network architecture it cannot adapt to the rapid changes in the traffic pattern and it can cause oscillation in the network.

Frank *et al.* in a [13] propose a content-aware traffic engineering technique for content distribution/delivery networks. The content providers duplicate the contents over distributed server infrastructures to provide better services to the users in different locations. The authors argue that it is essential for the content providers to know network topology and measure network state before mapping user request to the servers, which can introduce new challenges such as assigning users to the servers and performing traffic engineering. ISPs have the knowledge of the individual links status and network topology. This information can separate the server selection task from content delivery task, and help the content providers to focus on mapping the user to a server that provides better user experience. The introduced traffic engineering uses the information provided by ISPs along with the user's location to dynamically adapt to the traffic demand for the contents on the servers. This framework focuses on the traffic demand rather than routing, and uses the knowledge of the content providers (e.g. server status), and ISPs' knowledge (e.g. the network state and the user's location). For this reason this framework can complement the existing routing protocols and traffic engineering because it emphasizes on traffic demand rather than on traffic routing. Routing protocol such as OSPF and IS-IS are used to produce a routing matrix. With this matrix it tries to adjust a set of flow demands to reduce the maximum link utilization. The results of the experiments show that this framework has improved the user experience while reducing maximum link utilization and traffic delay.

Several energy-aware traffic engineering solutions have been proposed in [14]–[16]. These solutions incorporate traffic engineering to reduce the energy cost while trying to keep the network performance unaffected.

Vasic *et al.* [16] introduce an online traffic engineering technique. It spreads the load among multiple paths to reduce the energy consumption without affecting traffic rate. It presumes that energy-aware hardware is used in the network. These devices are capable to adjust its operating rate to its utilization, also they can sleep whenever it is possible to save energy. To enhance energy saving and keep the transfer rate steady, it transfers the data over multiple paths. The authors propose a number of techniques where they shift data to the links with low energy consumption, or they try to remove the traffic from as many possible links to allow the links and routers to sleep.

Most of the discussed approaches agree on the point that to engineer traffic in an efficient way a network-wide approach is required. When short-term changes happen in traffic volume the traffic engineering solution should quickly decide on how to route the traffic to different paths to balance link utilization. Under such circumstances where traffic pattern changes frequently, it is important for the traffic engineering solution to be stable. Otherwise, it can cause oscillation. Traffic oscillation can have a number of undesirable effects on the network, for example, switch-buffer overflow, out-of-order packets, poor allocation of network resources to the users, traffic delay and service degradation [17]. The solutions that have the above characteristics are difficult to implement in the traditional network architecture since we need to have access to global information in real-time, which is a tedious work in this paradigm. To find an optimal solution, most of the proposed solutions are based on local measurements, i.e. require the networking devices to decide independently on how to send the packets. In the traditional networks, generally, the link costs are kept static for a long period. Since the link cost is fixed, the traffic is transferred through the same path for a long period, until the link costs are changed.

For a traffic engineering technique to have an optimum effect on the network, it should have the following characteristics:

- it should utilize multi-path diversity in the network,
- it should make routing decisions based on the global view of the network,
- it should consider the flow values.

3. Review of Traffic Engineering Techniques in SDN

In SDN-based networks the controller can dynamically change the network state, for example, in traditional networks the link cost for routing protocols such as IS-IS are kept static for a long period. If congestion happens in the network it may lead to poor delivery of data till the link costs are changed or the problem is resolved. However, in SDN these values can be changed more dynamically to adapt to the changes. More innovative routing mechanism can be implemented, or the existing routing protocols can be modified, so that they can change dynamically as per network state to enhance resource utilization, avoid failure and congestion, and improve QoS. With the advances in SDN several traffic engineering techniques have been introduced by the research community. Table 1 summarizes some of the TE techniques in SDN.

To connect their Data Centers across the world and meet their performance requirements, Google introduced a Software Defined WAN architecture called B4 [18]. B4 is designed to resolve the problems in Wide Area Network (WAN) such as reliability, failures, and performance. It assigns bandwidth to the competing services, dynamically shifts traffic pattern, and overcomes network failure. B4 is designed to allow rapid deployment of new or standard protocols and control functions. One of such introduced functionalities is a traffic engineering mechanism, which allows applications to dynamically adapt in response to changes in the network behavior or failure. This architecture employs the routing and traffic engineering as separate services. The TE is layered on top of the routing protocols. This enables the network with a fallback strategy. If the TE service faced with a serious problem, it would be stopped so that the packets are forwarded using short path forwarding mechanism. This architecture consists of 3 logical layers:

- global layer, allows centralized control of the entire WAN through logically centralized applications such as the Central Traffic Engineering server (CTE) and SDN gateway (it allows centralized control of the network);
- site controller layer which includes the OpenFlow controller and network control applications such as routing services;
- switch hardware layer includes the switches, and performs traffic forwarding.

CTE is responsible for tasks such as measuring the unoccupied network bandwidth for multi-path forwarding, assigning and adjusting resource demands among the services, and actively relocating traffic from failed links and switches. SDN gateway provides the network topology graph for CTE. CTE uses this graph to compute the aggregated traffic at site to site edges. Then, an abstract of the computed result is fed to TE optimization algorithm to fairly allocate resources among the competing application groups/services. To achieve fairness it allocates resources using Min-Max fairness technique. Based on the applications' priority it allocates bandwidth to the applications. It uses hashed-based ECMP to balance the load among multiple links.

Hedera [19] is introduced to make an effective use of the bandwidth in a data center. Hedera detects the elephant-flows at the edge switches. The Hedera implementation uses periodic pulling, where it collects statistics every five seconds to detect large flows. At first switches send a new flow using its default flow matching rules on one of its equal-cost paths, until the flow size grows and meet the threshold. Then, the flow is marked as elephant-flow. The default threshold is 10% of network interface controller (NIC). At this point Hedera's central scheduler uses its global view of the network and calculates a better path for the flow and route the traffic. To effectively use the bandwidth the scheduler calculates the path in a way that it is non-conflicting, and it can accommodate the flow. This method can improve the bandwidth utilization, but because it uses periodic pulling, it can cause high resource utilization and overhead.

The main design goal of DevoFlow [20] is to improve network scalability and performance by keeping the flows in the data plane as much as possible without losing the centralized view of the network. This reduces the interaction between control plane and data plane. DevoFlow uses aggressive use of wildcards to reduce the controller and switches interactions. Therefore, switches take routing decision locally, while controller manages the overall control of the network and routes the significant flows, i.e. elephant-flows. It uses techniques such as packets sampling to collect switch statistic and detect the elephant-flows. The flows that have transferred a certain number of bytes is marked as large flow. The suggested threshold is 1–10 MB. In the beginning DevoFlow forwards the traffic using DevoFlow's multi-path wildcard rules. When an elephant flow is detected the controller will calculate the path that is least congested, and re-route the traffic to this path.

The flow detection mechanisms used in Hedera and Devoflow have high resource overhead. To overcome this problem Mahout [21] modifies the end-hosts to detect elephant-flows. It uses a shim layer in the operating system to mark the significant flows. The shim layer monitors the TCP socket buffer and marks the flows when in a given period the buffer exceeds the rate threshold. It

Table 1
Overview of traffic engineering techniques in SDN

Technique	Description	Routing	Comments
B4 [18]	• it uses a centralized TE, layered on top of the routing protocols, • to achieve fairness it allocates resources using Min-Max fairness technique.	• it uses hashed-based ECMP to balance the load among multiple links.	• if TE service can be stopped so that the packets are forwarded using short path forwarding mechanism.
Hedera [19]	• detects the elephant-flows at the edge switches, • if threshold is met, i.e. 10% of NIC bandwidth, the flow is marked as elephant flow, • uses periodic pulling, every 5 s.	• uses the global view of network and calculate the better paths, which are non-conflicting, for the elephant flows.	• it achieves 15.4 b/s throughput, • achieves better optimal bisection of bandwidth of network, in comparison to ECMP, • periodic pulling can cause high resource utilization in switches.
DevoFlow [20]	• detects the elephant-flows at the edge switches, • if threshold is met, i.e. 1–10 MB, it marks the flow as elephant-flow.	• it uses aggressive use of wild carded OpenFlow rules, and a static multi-path routing algorithm to forward the traffic.	• it can improve throughput up to 32% in CLOS network.
Mahout [21]	• detects the elephant-flows at end-host using a shim layer, the default threshold is 100 k, and then the flow is marked as elephant-flow, • it uses in-band signaling to inform the controller about the elephant-flows.	• it computes the best path for elephant-flow; otherwise it forwards other flows using ECMP, • it calculates the path that is least congested by pulling the elephant-flow statistics and link utilization from switches.	• it can detect elephant flow, if threshold is 100 k, in 1.53 ms, • it has 16% better bisection than ECMP.
MicroTE [22]	• detect the elephant flows at end-host, • it calculates the mean of traffic matrix between ToR-ToR, if the mean and traffic is between δ of each other, default is 20%, then it is predictable.	• uses short term predictability to route the traffic on multiple paths, • the remaining flows are routed by the EMCP scheme with heuristic threshold.	• if traffic is predictable it perform close to optimal performance otherwise it performs like ECMP.
MiceTrap [23]	• it addresses the mice-flows, • uses end-host elephant-flow detection to distinguish between mice-flows, and elephant-flows.	• it aggregates the mice-flows to improve scalability, • it route the mice-flows using a weighted multi.	• N/A.
Rethinking Flow Classification in SDN [26]	• it is a tag-based classification, • source-edge switch tags the packets based on the application classes.	• the tag is also an identifier for matching & forwarding the packets	• it is 3 ms faster than the OpenFlow field matching, • it requires introduction of new API's to the data plane.
Atlas [25]	• it classifies each application uniquely. • it uses C5.0 machine learning tool to classify the applications, • it requires user to install agents on their mobile devices to collect information to train ML trainer.	• it routes the flow based on applications, and network requirements.	• it has about 94% accuracy, • requires extension to OpenFlow.
MSDN-TE [32]	• it gathers network state information and considers the actual path's load to forward the flows on multiple paths.	• it dynamically selects the best shortest path among the available paths.	• it has better performance over other forwarding mechanisms such as Shortest Path First, • it reduced download time by 48%.

uses an in-band signaling mechanism to mark the flows as elephant-flows and inform the controller about the significant flows. Mahout uses ECMP to route normal traffic. When an elephant-flow is detected the controller calculates the best path for this flow. To calculate the best paths the controller pulls the elephant-flow statistics and link utilization from the switches to select the least congested path. This method can detect the elephant-flows faster, with lower

processing overhead than other method. But, it requires modification of the end-hosts.

In [22] Benson *et al.* present a traffic engineering mechanism for data center network called MicroTE, which uses an end-host elephant flow detection to detect the elephant flows. It exploits short-term prediction, and quickly adapts to the changes in traffic pattern. To efficiently handle the network load, it takes advantage of multiple paths in the network and coordinates traffic scheduling by using global view of traffic across the available network paths. The authors argue that the traffic nature of data center networks is bursty, and during long-run time the traffic is unpredictable, above 150 s, but it is predictable in short-time scale of 1–5 s. The TE methods for ISPs do not perform well in data center environments because they work on the granularity of hours, but TE for Data Centers should work on granularity of seconds.

Unlike MicroTE, MiceTrap [23] incorporates the end-host flow detection to handle mice-flows and uses OpenFlow group table (multi-path group type) to aggregate the incoming mice-flows for each destination. The authors believe that TE mechanism, which handles elephant-flows, can cause congestion to mice-flows, i.e. short-lived flows. Also the resources should be distributed according to flow values. Managing mice-flows using ECMP and giving preference to elephant flows can degrade QoS. MiceTrap architecture consists of end-host elephant flow detection module, multi-path aggregates implemented in OpenFlow switch, and a controller. It uses the kernel-level shim layer approach to mark the elephant flow detection. The shim layer method monitors the TCP socket buffer and marks the flows when in a given period the buffer exceeds the specified threshold. Multi-path Mice-flow Aggregator, aggregates the incoming mice-flows for each destination. This reduces the rules for traffic management because if each mice-flow is managed by an exact flow rule, it will cause a bottleneck and limit the scalability. The advantage of using group table is that it saves bandwidth since one single group message can update a set of flows when the traffic distribution is changed. It uses a weighted routing algorithm which forwards aggregated traffic into multiple paths by considering the current network load while calculating the paths.

These are effective solutions for data center networks, but they share the network resources based on the flow size and do not consider the flow-value. An important way to consider the flow-values is to classify the applications. Two promising techniques for application classification are Deep Packet Inspection (DPI) and Machine Learning (ML) classification method. In comparison to techniques such as port-based classification, these techniques have a high classification accuracy. DPI methods inspect the payload of packets and search for known patterns, keywords or regular expressions that are characteristic of a given application. These methods are more accurate, but with higher overhead (in terms of memory and processing). ML methods exploit several flow-level features to classify the traffic. To classify the flows these methods look for known flow behavior such as packet counts, data bytes, TCP flags, etc. [24].

In the work [25] Qazi *et al.* try to investigate how to integrate application awareness in SDN-based networks and how to classify traffics with high accuracy. A framework called Atlas is introduced, which is capable of classifying the traffic in the network and enforcing higher layer policies. The presented framework uses a ML tool called C5.0 to classify the flows based on the application types. It shows 94% accuracy. The Atlas framework can classify each specific application. It can classify each VoIP application uniquely rather than classifying them as a common VoIP flows. Such framework should be scalable so the application detection and enforcing application-aware policy is done in a smooth and uninterrupted manner. They have deployed the framework in the HP Lab wireless network. It requires the users to install software agents on their mobile devices. These agents collect information such as active network sockets, Netstat logs for each application. The agents send this information to the controller, where the controller runs machine learning trainer. The OpenFlow switch statistics are extended to store first n packet size of each flow and announce it to the controller. The controller collects such flow features along with the information sent by the agents to train the ML tool by using the ML trainer.

Hamid *et al.* in [26] introduce a tag-based classification architecture, where the source-edge switches tag the packets based on the application classes. This way the network operator can apply different policies for each of the application classes. The tag is also used as an identifier for matching the packets which reduce the matching overhead. After a tagged packet is delivered to the destination edge switch, the switch removes the tag and performs the required actions, if there is any action, and sends the packet to the destination host. The experimental result shows this tag-based approach is 3 ms faster than the hash-based field matching methods like OpenFlow field matching, and reduces processing overhead. To solve the backward compatibility, unlike MPLS, the tag is added to the end of packet instead of its middle. This way, if the variable length packet is supported, there is no need for whole packet parsing. Otherwise, the whole packet should be parsed. The downside of this approach is that it requires changes in the switch internal by introducing a new API to the switch data plane. This API is an application layer processor in the data plane.

A promising way to address challenges and problems in distributed environments, such as a computer network, is with the help of intelligent agents, i.e. Multi-Agent System (MAS) and mobile agents. Bieszczad *et al.* [27] describes how intelligent agents can be used to facilitate network management. It explains the potential of Intelligent Agents to tackle various difficulties in different network management areas such as fault management, security, performance management, accounting, etc. SDN provides a good platform for the agents to tackle such difficulties.

In [28] Skobelev *et al.* propose a task-scheduling system for SDN-based networks. This system incorporates MAS to overcome task-scheduling problems in the distributed systems, i.e. where the servers and computational resources are distributed. The MAS task scheduler associates the basic system entities with an agent. It consists of three main agents:

- task agent represents the task that should be processed with minimum cost by a server in the network,
- resource agent provides the system with a server to process tasks,
- commutator agent is responsible for providing information about network state and task allocation to the nodes.

This system is developed in C#, .NET framework, as a Windows application.

The research [29]–[31] show that by providing application-awareness and feedback from clients' machines to the network, the user Quality of Experience (QoE), and resource utilization can be improved. These works use agents on user side to collect information (like audio/video quality, waiting time, etc.) and send this information to the controller to adjust the network state accordingly to improve users' QoE.

To address traffic forwarding and traffic engineering in SDN, Dinh et al. [32] introduced a multipath-based forwarding traffic engineering mechanism called MSDN-TE. The goal of this mechanism is to forward the traffic in such a way that it avoids congestion on any link in the network. MSDN-TE dynamically selects the best available shortest paths and forwards the incoming traffic. This TE mechanism gathers network state information and considers the actual path's load to forward the flows on multiple paths. The MSDN-TE is a module which extends OpenDayLight controller. It consists of three components:

- a monitoring function which is used for gathering information about network states and flows in the network; for example, flow's static, link utilization, network topology, etc. The path matrices are refreshed every 10–15 s;
- the TE algorithm calculates n number of paths, which have the lowest traffic load, between the source and destination node. To select the shortest paths Eppstein [33] algorithm is used;
- the actuating function supports TE algorithm module. It takes certain actions and dynamically allots flows to the selected paths. Compared with the Shortest Path First and spanning tree, MSDN-TE shows better performance in regard to download time, delay and packet drops. For example, it reduced packet drops by 72.9% in AGIS [34] simulated topology and more than 90% in Abilene [34] simulated topology.

4. Traffic Engineering Research Challenges

As SDN becomes widely used, the research community and industry introduce new protocols and control applications like TE mechanisms. However, like any new technology the potential of SDN to simplify and improve network management comes with new challenges that need to be addressed. In this section, some of the challenges and future directions for traffic engineering in SDN are discussed, namely, fault-tolerance, energy-awareness, flow-update scheduling and consistency, and data-flow scheduling and dissemination.

4.1. High-availability

Fault tolerance is an important feature of any computer network. It means if an unexpected error or problem happens, like the failure of a link or a switch, the services in the network will continue to be accessible. The faults in a network can cause congestion and packet loss. These conditions can last for seconds due to the time it takes for TE mechanism to respond to the faults and update the network, i.e. update the topology and switches. In a SDN-based network two types of failure are control plane failure and data plane failure, like failure of links and switches. Besides physical/logical failure of control plane, control plane failure can also refer to a situation when the controller fails to update switches in the right time, so the switches continue to forward the traffic with the old rules. This can lead to congestion because the link capacity is not considered. There are two approaches to address the faults in the network: proactive where the paths are calculated and reserved beforehand, and reactive where the resources are not reserved until failure happens. The paths are calculated dynamically or decided in advance. Proactive approach has faster fault recovery since the paths are already calculated. When a fault occurs there is minimum interaction between the controller and the switch. This approach is about 5 times faster than reactive approach [35], [36]. But, reactive approach has a lower cost because the link capacity is not reserved, so it requires less memory in the control plane.

In [37] Liu *et al.* have introduced a proactive fault management TE mechanism, known as forward fault correction (FFC), which handles both data plane and control plane faults. In this approach if the number of faults is smaller than a configurable bound f, it can ensure protection against failure and congestion in the network. Depending on the value of f, and the traffic distribution flowing in the network, FFC provisions a certain amount of link capacity to avoid failure in the network. However, since the link capacity is pre-provisioned it can have lower throughput. Kim *et al.* in [38] introduced a fault-tolerance framework called CORONET, which uses a centralized controller to forward packets and can work with any network topology. CORONET recovers from switch or link failures in a short period. It uses multi-path routing methods. Its architecture

consists of modules to discover network topology, route planning, shortest-route path calculation, and traffic assignment. To simplify packet forwarding, and minimize the number of flow-rules CORONET uses VLANs mechanism in the switches. Therefore, it is also scalable.

A traffic engineering framework should detect faults in the network and re-route the sensitive applications' traffic by avoiding the failed areas to allow these applications to work seamlessly and avoid service degradation. SDN characteristics such as failover mechanism introduced in OpenFlow protocol, global view of network, and its capability to dynamically change network state facilitate failure recovery. However, it is still challenging since the controller needs to calculate the new paths and install the flow-rules in the switches. The TE should achieve low communication overhead with a trade-off between the latency and memory usage.

4.2. Energy-awareness

To guarantee QoS in a network, high-end networking devices that have a high power consumption are used. To reduce delay and increase reliability, these resources are usually over-provisioned to increase network capacity. However, this leads to concerns about greenhouse gas emission and power wastage. A number of researches show that non-negligible percentage of world power consumption and CO_2 emission is due to information and communication technologies [39]. This motivated the researchers to propose new algorithms and devices to address these difficulties [14]–[16]. These techniques adapt the network elements' active time according to the traffic load.

The techniques proposed for classical network architecture are not as effective as they can be. There are few studies on energy-aware techniques for SDN-based networks. In [40] Giroire *et al*. have introduced an energy-aware routing technique for SDN that gathers traffic matrix, calculate the routing paths to guarantee QoS, and put the idle links and nodes into sleeping mode. This technique considers both memory limitation of routers and link capacity. SDN features such as centralized view of network and network programmability can help to introduce new efficient centralized energy-aware TE techniques that allow a network to dynamically adapt to the traffic load and network condition with the goal of achieving good performance and use network resources effectively to reduce power consumption. The centralized TE mechanism can shut down a set of switches and links, when the traffic demand is low to reduce power utilization while satisfying user experience.

4.3. Data-flow Scheduling

After the rules are installed in the switches, a switch will match and send the incoming packets to the destination. An important way to ensure QoS in a network is flow scheduling, where the packets that require better QoS are scheduled and transferred first. Flow priority is the main scheduling method [41], [42]. In this method, the flows with higher priorities are sent first. SDN provides a good platform to introduce new software-controlled flow schedulers that are capable of flow-oriented multi-policy scheduling. This abstraction can help to introduce advanced network configurability.

Bo-Yu *et al*. [43] have introduced an Iterative Parallel Grouping Scheduling Algorithm, IPGA-scheduling. It is designed to address the prioritized flow scheduling problem, which is required for QoS differentiation among different prioritized flows, and also energy saving in data center networks. This system is a Compute Unified Device Architecture (CUDA) system within SDN controller. CUDA is a parallel computing architecture developed by Nvidia for graphics processing.

In [42] Rifai *et al*. proposes coarse-grained scheduling. The authors argue that the data center networks and the Internet traffic nature mostly consist of short flows and most of the flows are carried by TCP. Therefore, the emphasis of this scheduling system is on flow-size scheduling. This system uses switch's OpenFlow flow statistics to identify the flow-size along with multiple queues per port to implement 802.1p QoS. The 802.1p standard delegates 8 queues per port. Two size-based schedulers are introduced. Both of these schedulers have two queues per port, and it is assumed that they are managed by strict priority scheduler.

Using a scheduler can improve the network performance. The majority of the schedulers are developed around the idea of "one size fits all", or consider only the flow size, and the flow value. The type of the application is ignored. These approaches examine, mostly, packet's priority and port workload while assigning the flows to a port. For example, in a VoIP network, the VoIP applications need to have the highest priority to ensure QoS. Even though priority-based solutions can address these requirements, they require precise configuration of the network which is time-consuming and error-prone.

4.4. Flow-update

In an operating network, the controller may change the configuration of the switches several times through flow-updates. Flow-update refers to updating the current switch configurations, forwarding rules, with new configurations. Flow-updates are important for various tasks such as fault management, adapting to changes in traffic pattern, etc. Flow-update is a challenging task since improper update of multiple flows can cause problems such as congestion, service degradation, and inconsistency in the network. Hence, flow-update scheduling is an important issue to be addressed. If a new rule is assigned for each flow it can increase the resource cost (e.g. processing and memory) in both the data plane and control plane. Also, the time that it takes for a flow to be added in a switch adds to the latency. There should be a tradeoff between load-balancing and latency.

The most common approaches for flow-update scheduling problem is the two-phase update mechanism, where controller first installs the new forwarding-rules into the

switches, if all packets that require the old rules are transferred, then the new installed rules will be used and the old forwarding-rules are removed from the switches. Compared to the one-phase approach, the advantage of this approach is that the chance of the controller to fail in updating the switches is lower. However, Li *et al*. [44] argue that the two-phase update mechanism is not effective, since it does not consider the switch's flow-table size. Thus, to address the multi-flow update problem, a step-by-step approach is introduced. This problem is formulated as an optimization problem to minimize the maximum link utilization, which is an important network performance metric. In this approach the controller schedules the flow updates and then updates each flow step by step, i.e. the path of a flow is changed to the new one in a step, so if there are n flow updates then the process is completed in n steps. This method considers both the link capacity and the flow-table size.

In [45] Mahajan believe that flow-update, to ensure consistency, has a number of properties such as loop free, packet drop free, switch memory limitation, load balancing, etc. Depending on the type of a network, different consistency, or combination of the consistency properties are needed, for example load-balancing or loop free network.

5. Conclusion

In this paper we have reviewed literature in the field of traffic engineering for both traditional network architecture and SDN, and examined some of the TE challenges and future directions. SDN is a new networking paradigm which simplifies the network management and enables innovation. It tries to address many problems in the traditional network architecture by simplifying network management through centralized management of a network, introducing network programmability, and providing a global view of a network and its state. New traffic engineering techniques are required to exploit these features for better control and management of traffic. Different TE mechanism should be included in SDN to control congestion and manage traffic for different applications in various QoS-sensitive scenarios such as video or business data, and to provide required QoS while balancing the load among the available resources in a network. To improve the network load handling, a traffic engineering mechanism should enable a network to react in real-time and classify a variety of traffic types from different applications. Routing optimization is one of the main techniques in TE. It should take advantage of multiple paths in the network and coordinate traffic scheduling by using global view of traffic across the available network paths. Beside load-balancing and optimization of resources, other components of TE are QoS and resilience form failure. SDN is currently capable of enforcing policy for lower layers, i.e. Layer 2-4, but not many studies have explored the higher layer policy enforcement. By identifying the packets sent by the applications to the network, it is possible to enforce higher layer, application layer, policies. Higher layer policy enforcement can help to engineer resilient and flexible network. Such networks can be optimized for each application to provide a good QoS and improve user experience. The authors described how an end-host flow detection mechanism and Multi-Agent System can improve network performance and scalability while reducing complexity.

6. Future Work

In terms of future work, authors plan to propose an efficient traffic engineer framework, which makes the SDN-based networks more application-aware. In this work a multi-agent based software framework consisting of a number of algorithms for application classification, and data scheduling and dissemination will be developed. The agents are responsible for application classification of user's traffic. Then, the data scheduling and dissemination algorithms will calculate the best path and order to process and forward the flow to the destination. All these modules will work together to ensure high-availability, load-balancing and optimizing resource utilization, and also to ensure high-QoS rating for QoS sensitive applications. This framework can help to automate the network configuration to achieve high QoS for the desired applications. By combining techniques such as scheduling, application classification, and MAS, a network can deliver better services.

References

[1] B. Nunes, M. Mendonca, X.-N. Nguyen, K. Obraczka, and T. Turletti, "A survey of software-defined networking: Past, present, and future of programmable networks", *IEEE Commun. Surv. & Tutor.*, vol. 16, no. 3, pp. 1617–1634, 2014.

[2] B. Fortz and M. Thorup, "Internet traffic engineering by optimizing OSPF weights", in *Proc. 19th IEEE Ann. Joint Conf. of the IEEE Comp. & Commun. Soc. INFOCOM 2000*, Tel Aviv, Israel, 2000, vol. 2, pp. 519–528.

[3] X. Xiao, A. Hannan, B. Bailey, and L. M. Ni, "Traffic engineering with MPLS in the Internet", *Network*, vol. 14, no. 2, pp. 28–33, 2000.

[4] O. N. Foundation, "OpenFlow – open networking foundation" [Online]. Available: https://www.opennetworking.org/sdn-resources/openflow (accessed Aug. 23, 2016).

[5] K. Ishiguro, A. Lindem, A. Davey, and V. Manral, "Traffic engineering extensions to OSPF Version 3", RFC 5329, IETF Trust, 2008 [Online]. Available: https://tools.ietf.org/html/rfc5329

[6] T. Li and H. Smit, "IS-IS extensions for Traffic Engineering", RFC 5305, IETF Trust, 2008 [Online]. Available: https://tools.ietf.org/html/rfc5305

[7] B. Fortz, J. Rexford, and M. Thorup, "Traffic engineering with traditional IP routing protocols", *Commun. Mag.*, vol. 40, no. 10, pp. 118–124, 2002.

[8] D. Thale and C. Hopps, "Multipath issues in unicast and multicast next-hop selection", RFC 2991, IETF Trust, 2000 [Online]. Available: https://tools.ietf.org/html/rfc2991

[9] D. Zhang and D. Ionescu, "QoS performance analysis in deployment of DiffServ-aware MPLS Traffic Engineering", in *Proc. 8th ACIS Int. Conf. on Software Engin., Artif. Intell., Netw., & Parallel/Distrib. Comput. SNPD 2007*, Qingdao, China, 2007, vol. 3, pp. 963–967.

[10] F. Le Faucheur *et al.*, "Multi-Protocol Label Switching (MPLS) Support of Differentiated Services", RFC 3270, IEFT Trust, 2002 [Online]. Available: https://tools.ietf.org/rfc/rfc3270.txt

[11] I. F. Akyildiz *et al.*, "A new traffic engineering manager for DiffServ/MPLS networks: design and implementation on an IP QoS Testbed", *Computer Commun.*, vol. 26, no. 4, pp. 388–403, 2003.

[12] I. Gojmerac, T. Ziegler, F. Ricciato, and P. Reichl, "Adaptive multipath routing for dynamic traffic engineering", in Proc. Global Telecommun. Conf. GLOBECOM'03, San Francisco, CA, USA, 2003, vol. 6, pp. 3058–3062.

[13] I. Poese, B. Frank, G. Smaragdakis, S. Uhlig, A. Feldmann, and B. Maggs, "Enabling content-aware traffic engineering", *ACM SIGCOMM Comp. Commun. Rev.*, vol. 42, no. 5, pp. 21–28, 2012.

[14] M. Zhang, C. Yi, B. Liu, and B. Zhang, "GreenTE: Power-aware traffic engineering", in *Proc. 18th IEEE Int. Conf. on Netw. Protocols ICNP 2010*, Kyoto, Japan, 2010, pp. 21–30.

[15] E. Amaldi, A. Capone, L. G. Gianoli, and L. Mascetti, "A MILP-based heuristic for energy-aware traffic engineering with shortest path routing", in *Network Optimization*, J. Pahl, T. Reiners, and S. Voß , Eds. *LNCS*, vol. 6701, pp. 464–477. Springer, 2011.

[16] N. Vasić and Dejan Kostić, "Energy-aware traffic engineering", in *Proc. of the 1st Int. Conf. on Energy-Effic. Comput. & Netw. e-Energy'10*, Passau, Germany, 2010, pp. 169–178.

[17] L. Zhang and D. Clark, "Oscillating behavior of network traffic: A case study simulation", *Internetworking: Res. and Exper.*, vol. 1, no. 2, pp. 101–112, 1990.

[18] S. Jain *et al.*, "B4: Experience with a globally-deployed software defined WAN", *ACM SIGCOMM Comp. Commun. Rev.*, vol. 43, no. 4, pp. 3–14, 2013.

[19] M. Al-Fares, S. Radhakrishnan, B. Raghavan, N. Huang, and A. Vahdat, "Hedera: Dynamic Flow Scheduling for Data Center Networks", in *Proc. 7th USENIX Symp. on Netw. Syst. Design & Implemen. NSDI'10*, San Jose, CA, USA, 2010, vol. 10, pp. 19–19.

[20] A. R. Curtis, J. C. Mogul, J. Tourrilhes, P. Yalagandula, P. Sharma, and S. Banerjee, "DevoFlow: scaling flow management for high-performance networks", *ACM SIGCOMM Comp. Commun. Rev.*, vol. 41, no. 4, pp. 254–265, 2011.

[21] A. R. Curtis, W. Kim, and P. Yalagandula, "Mahout: Low-overhead datacenter traffic management using end-host-based elephant detection", in *Proc. 30th IEEE Int. Conf. Comp. Commun. IEEE INFOCOM 2011*, Shanghai, China, 2011, pp. 1629–163.

[22] T. Benson, A. Anand, A. Akella, and M. Zhang, "MicroTE: Fine grained traffic engineering for data centers", in *Proc. 7th Conf. on Emerg. Networking Experim. & Technol. Co-NEXT'11*, Tokyo, Japan, 2011, p. 8.

[23] R. Trestian, G.-M. Muntean, and K. Katrinis, "MiceTrap: Scalable traffic engineering of datacenter mice flows using OpenFlow", in *IFIP/IEEE Int. Symp. on Integr. Netw. Managem. IM 2013*, Ghent, Belgium, 2013, pp. 904–907.

[24] S. Valenti, D. Rossi, A. Dainotti, A. Pescapè, A. Finamore, and M. Mellia, "Reviewing traffic classification", in *Data Traffic Monitoring and Analysis*, E. Biersack, C. Callegari, and M. Matijasevic, Eds. *LNCS*, vol. 7754, pp. 123–147. Springer, 2013.

[25] Z. A. Qazi *et al.*, "Application-awareness in SDN", *ACM SIGCOMM Comp. Commun. Rev.*, vol. 43, no. 4, pp. 487–488, 2013.

[26] H. Farhadi and A. Nakao, "Rethinking flow classification in SDN", in *Proc. IEEE Int. Conf. on Cloud Engin. IC2E 2014*, Boston, MA, USA, 2014, pp. 598–603.

[27] A. Bieszczad, B. Pagurek, and T. White, "Mobile agents for network management", *Commun. Surveys*, vol. 1, no. 1, pp. 2–9, 1998.

[28] P. O. Skobelev, O. N. Granichin, D. S. Budaev, V. B. Laryukhin, and I. V. Mayorov, "Multi-agent tasks scheduling system in software defined networks", *J. of Physics: Conf. Series*, vol. 510, no. 1, p. 012006, 2014 (doi: 10.1088/1742-6596/510/1/012006).

[29] M. Jarschel, F. Wamser, T. Hohn, T. Zinner, and P. Tran-Gia, "SDN-based application-aware networking on the example of YouTube video streaming", in *Proc. 2nd Eur. Worksh. on Softw. Defined Netw. EWSDN 2013*, Berlin, Germany, 2013, pp. 87–92.

[30] P. Georgopoulos, Y. Elkhatib, M. Broadbent, M. Mu, and N. Race, "Towards network-wide QoE fairness using openflow-assisted adaptive video streaming", in *Proc. ACM SIGCOMM Worksh. on Future Human-Centric Multim. Netw. FhMN 2013*, Hong Kong, China, 2013, pp. 15–20.

[31] H. Nam, K.-H. Kim, J. Y. Kim, and H. Schulzrinne, "Towards QoE-aware video streaming using SDN", in *Proc. Global Commun. Conf. GLOBECOM 2014*, Austin, TX, USA, 2014, pp. 1317–1322.

[32] K. T. Dinh, S. Kukliński, W. Kujawa, and M. Ulaski, "MSDN-TE: Multipath Based Traffic Engineering for SDN", in *Intelligent Information and Database Systems. Asian Conference on Intelligent Information and Database Systems*, N. T. Nguyen, B. Trawiński, and R. Kosala, Eds. Springer, 2016, pp. 630–639.

[33] D. Eppstein, "Finding the *k*-shortest paths", *SIAM J. Comput.*, vol. 28, pp. 652–673. 1999.

[34] S. Knight, H. X. Nguyen, N. Falkner, R. Bowden, and M. Roughan, "The Internet topology zoo", *IEEE J. on Selec. Areas in Commun.*, vol. 29, no. 9, pp. 1765–1775, 2011.

[35] S. Sharma, D. Staessens, D. Colle, M. Pickavet, and P. Demeester, "Enabling fast failure recovery in OpenFlow networks", in *Proc. 8th Int. Worksh. on the Des. of Reliable Commun. Netw. DRCN 2011*, Kraków, Poland, 2011, pp. 164–171.

[36] D. Staessens, S. Sharma, D. Colle, M. Pickavet, and P. Demeester, "Software defined networking: Meeting carrier grade requirements", in *Proc. 18th IEEE Worksh. on Local & Metropolitan Area Networks LANMAN 2011*, Chapel Hill, NC, USA, 2011, pp. 1–6.

[37] H. H. Liu, S. Kandula, R. Mahajan, M. Zhang, and D. Gelernter, "Traffic engineering with forward fault correction", *ACM SIGCOMM Comp. Commun. Rev.*, vol. 44, no. 4, pp. 527–538, 2014.

[38] H. Kim, J. R. Santos, Y. Turner, M. Schlansker, J. Tourrilhes, and N. Feamster, "Coronet: Fault tolerance for software defined networks", in *Proc. 20th IEEE Int. Conf. on Network Prot. ICNP 2012*, Austin, TX, USA, 2012, pp. 1–2.

[39] R. Bolla, R. Bruschi, F. Davoli, and F. Cucchietti, "Energy efficiency in the future Internet: A survey of existing approaches and trends in energy-aware fixed network infrastructures", *Commun. Surveys & Tutor.*, vol. 13, no. 2, pp. 223–244, 2011.

[40] F. Giroire, J. Moulierac, and T. K. Phan, "Optimizing rule placement in software-defined networks for energy-aware routing", in *Proc. Global Commun. Conf. GLOBECOM 2014*, IEEE, Austin, TX, USA, 2014, pp. 2523–2529.

[41] F. Pop, C. Dobre, D. Comaneci, and J. Kołodziej, "Adaptive scheduling algorithm for media-optimized traffic management in software defined networks", *Computing*, vol. 98, no. 1-2, pp. 147–168, 2016 (doi: 10.1007/s00607-014-0406-9).

[42] M. Rifai, D. Lopez-Pacheco, and G. Urvoy-Keller, "Coarse-grained scheduling with software-defined networking switches", in *Proc. 2015 ACM Conf. on Spec. Interest Group on Data Commun. SIGCOMM'15*, London, UK, 2015, pp. 95–96. 2015.

[43] B. Y. Ke, P.-. Tien, and Y.-L. Hsiao, "Parallel prioritized flow scheduling for software defined data center network", in *Proc. 14th Int. Conf. on High Perform. Switch. & Rout. IEEE HPSR 2013*, Taipei, Taiwan, 2013, pp. 217–218.

[44] Y. Liu, Y. Li, Y. Wang, and J. Yuan, "Optimal scheduling for multi-flow update in Software-Defined Networks", *J. of Network & Computer Applications*, vol. 54, no. C, pp. 11–19, 215 (doi: 10.1016/j.jnca.2015.04.009).

[45] R. Mahajan and R. Wattenhofer, "On consistent updates in software defined networks", in *Proc. 12th ACM Worksh. on Hot Topics in Netw. HotNets-XII*, College Park, MD, USA, 2013, p. 20.

Mohammad Reza Abbasi received his MCA degree in Computer Science and Applications from Panjab University, Chandigarh, India, in 2013. He is currently pursuing his Ph.D. in Panjab University. His research interests include software defined networking, network management, and network virtualization.

E-mail: mabbasi@pu.ac.in
Department of Computer Science & Application
Panjab University
160014 Chandigarh, India

Ajay Guleria received his Ph.D. degree in Computer Science and Engineering from National Institute of Technology Hamirpur. Presently he is working as Senior System Manager in Panjab University Chandigarh. His current research areas of interest include software defined networking, information centric networking, network security and vehicular ad hoc networks. He is a member of IEEE, ISTE.

E-mail: ag@pu.ac.in
Computer Center
Panjab University
160014 Chandigarh, India

Mandalika S. Devi is a Professor in the Department of Computer Science and Applications, Panjab University, Chandigarh. She received her Ph.D. degree in Computer Science and Systems Engineering from Andhra University, Visakhapatnam and M.E. in Computer Science and Engineering, from NIT, Allahabad. She has completed M.Sc. in Applied Mathematics from Andhra University, Visakhapatnam. Before joining Panjab University, she served Indian Space Research Organization, Sriharikota, and National Institute of Technical Teachers' Training and Research, Chandigarh. Her areas of expertise include algorithms, image processing, distributed artificial intelligence and educational computing.

E-mail: syamala@pu.ac.in
Department of Computer Science & Application
Panjab University
160014 Chandigarh, India

Paper

Network Dimensioning with Maximum Revenue Efficiency for the Fairness Index

Grzegorz Zalewski[1] and Włodzimierz Ogryczak[2]

[1] *National Institute of Telecommunications, Warsaw, Poland*
[2] *Institute of Control and Computation Engineering, Warsaw University of Technology, Warsaw, Poland*

Abstract—Network dimensioning is a specific kind of the resource allocation problem. One of the tasks in the network optimization is to maximize the total flow on given pairs of nodes (so-called demands or paths between source and target). The task can be more complicated when different revenue/profit gained from each unit of traffic stream allocated on each demand is taken into account. When the total revenue is maximized the problem of starvation of less attractive paths can appear. Therefore, it is important to include some fairness criteria to preserve connections between all the demands on a given degree of quality, also for the least attractive paths. In this paper, a new bicriteria ratio optimization method which takes into account both, the revenue and the fairness is proposed. Mathematical model is built in a form of linear programming. The solutions are analyzed with some statistical measures to evaluate their quality, with respect to fairness and efficiency. In particular, the Gini's coefficient is used for this purpose.

Keywords—allocation problem, decision problems, dimensioning networks, fair optimization, linear programming, maximization, multi-criteria.

1. Introduction

A problem of fair allocation of some finite set of resources appears in various contexts, such as transport or other branches of economy. In general, network dimensioning could also be compared with the group of allocation problems. Let us consider the set of resources and set of possible allocations of them. Each allocation of the resource is more or less profitable. The main goal in fairness optimization is to treat equal each of these locations in some degree. Such a decision problems appear in society while distributing the public goods or allocation of public services. Interesting approach was proposed by Rawls [1] to treat justice as fairness in social problems and political decisions. The problem of equity is a complex idea encountered in society and many times it requires dedicated model of optimization [2]. While dimensioning the telecommunication wired networks, it is required to remember about a lot of restrictions. First of all, it is needed to obtain the highest possible value of total revenue, which is related to profit from each unit of allocated load on given demand. Demand can be called also as a path between source and target. There are resources such as bandwidth or traffic flow, which have to be allocated on given paths [3]. The main assumption in this kind of problems is to describe the path character and next to limit each connection with the value of capacity. Paths could be formulated in two ways. One is to define a set of single paths as chain of nodes or links. This approach does not allow for bifurcation of a path and requires some work to predefine the set of them. It is the so-called link-path approach. Another, the node-link approach does not need setting the path before the optimization process. It is based on maintaining the flow on source, target and transitive nodes. In this way the path is allowed to split up. The model choice is determined by established assumptions on traffic flow in the network. No matter which formulation has been chosen, there could appear a problem of blocking some of demands. When some path shares at least one link and has different unit revenue the solution maximizing the efficiency of the network will allocate whole bandwidth to more profitable paths. When the decision-maker is interested in keeping the same degree of quality on each demand, it is necessary to include the fairness criterion into the optimization problem [4]. There have been done a lot of work in area of fairness optimization. For example, it could be the Max-Min [5] or Lexicographic Max-Min [6], [7] concepts. These methods have high fairness index but in many cases they return not satisfying and sometimes even dominated solutions. Another concepts to gain a fair and more efficient solution are methods such as Proportional-Fairness (PF) [8], Reference Point Method (RPM) [9], Ordered Weighted Averages (OWA) [10], [11]. The latter methods ensure efficient solutions and, in general, allows to control the fairness degree by appropriate parameters.

In the paper a new method of fair optimization is proposed. The method is based on so-called ratio model. It allows to obtain the most satisfying solution with respect to two different and inversely proportional criteria. The model formulation guarantees to obtain the solution of maximum additional revenue from allocated traffic flow with minimal acceptable fairness. Considering the mean value of revenue obtained from allocated load on all demands as z, mean value of some percent of the most discriminated paths as z_0 and result of the solution which should be improved (for example Max-Min method) as τ the new ratio model of maximization could be written as follows:

$$\max\left\{\frac{z-\tau}{z_0}\right\}. \tag{1}$$

In the rest of the paper the model is described in details and the results of an example of intput data are shown. For verification there have been chosen the basic statistics and the Gini coefficient. Consider set D as set of given allocations (demands), h_d as value of allocated resource on d-th allocation and vector of revenues per unit gained from allocated resource p_d associated with d-th location. Typical function that is used to describe efficiency criterion in the easiest form is the total revenue gained from obtained solution:

$$T(\mathbf{y}) = \sum_{d \in D} h_d \cdot p_d, h_d \geq 0. \tag{2}$$

Just mentioned formulation of efficiency criterion, when $\bar{D}$ denotes the cardinality of set D, could be also written as the mean (average) outcome:

$$\mu(\mathbf{y}) = \frac{\sum_{d \in D} h_d \cdot p_d}{\bar{D}}. \tag{3}$$

Linear formulation maximizes one of mentioned objective functions (2), (3), always returning the most profitable solution but in the most cases it leads to unfair solution. The main reason of that is in using the rational model of preference like in the standard Pareto-optimal solution concept. The rational relation of strict preference is denoted with $\succ$, weak preference $\succeq$, indifference with $\cong$ [12]. It could be described using the vector inequalities denoted by $\leq$, $\leqq$ and $=$. In this notation the rational relation of preference is defined by the following formulas:

$$\mathbf{y}' \succeq \mathbf{y}'' \Leftrightarrow \mathbf{y}' \geqq \mathbf{y}'' \Leftrightarrow \mathbf{y}'_i \geqq \mathbf{y}''_i, \tag{4}$$

$$\mathbf{y}' \succ \mathbf{y}'' \Leftrightarrow \mathbf{y}' \geq \mathbf{y}'' \Leftrightarrow (\mathbf{y}'_i \geqq \mathbf{y}''_i \textit{ and not } \mathbf{y}'_i \leqq \mathbf{y}''_i), \tag{5}$$

where $\mathbf{y}_i$ is the i-th vector value. Additionally it meets the base assumptions of rational preference:

- reversible

$$\mathbf{y} \succeq \mathbf{y}, \tag{6}$$

- transitivity

$$(\mathbf{y}' \succeq \mathbf{y}'') \wedge (\mathbf{y}'' \succeq \mathbf{y}''') \Rightarrow (\mathbf{y}' \succeq \mathbf{y}'''), \tag{7}$$

- strict monotonicity

$$\mathbf{y} + \varepsilon e_i \succ \mathbf{y}, \varepsilon > 0\ ,\ i = 1,2,\ldots d, \tag{8}$$

  where e_i is the i-th objective function unit vector on decision area Y.

Many times it can appear a problem of starvation some less attractive paths (with respect to revenue/profit). It is often not acceptable by the decision-maker and in this case Pareto-optimal solution is not good enough. One way to preserve the fairness is to add constraints, which enforce the model to treat impartially (anonymously) all the demands. Such a model of preferences is well-defined when for each vector of allocated resources is fulfilled $(h_{\tau(1)}, h_{\tau(2)}, \ldots, h_{\tau(d)}) \cong (h_1, h_2, \ldots, h_d)$, for various permutation τ of set $D = 1,2,\ldots,d$. Fulfillment of the above assumptions allows us to obtain so-called anonymous rational relation of preferences. Additionally, fulfillment of another axiom, the Pigou-Dalton principle of transfers (9), leads to equitable relation of preferences.

$$y_{i'} > y_{i''} \Rightarrow y - \varepsilon e_{i'} + \varepsilon e_{i''} \succ y,\ 0 < \varepsilon < y_{i'} - y_{i''}. \tag{9}$$

Every optimal solution of anonymous and equitable aggregation of multiple criteria problem leads to a fairly efficient solution (or simply fair solution) [13]. The fairly efficient solution is also Pareto-optimal but not vice-versa.
To quantify the fairness of the system there are a lot of equality (or inequality) measures. According to work has been done by Lan and Chiang [14] in area of fairness optimization it should be noticed that there exist five fundamental axioms, which should not be omitted by fairness measure. Those axioms are:

- continuity,
- homogeneity,
- saturation,
- partition,
- starvation.

Over the years many of measures which meet those axioms have been proposed [15]–[18], [20], [21]. For example, there are:

- maximum absolute difference or the mean absolute difference,
- maximum absolute deviation or the mean absolute deviation
- standard deviation or the variance,
- the mean (downside), the standard (downside) or the maximum semi deviation,
- k-largest semi deviations,
- Gini coefficient,
- Jain's index.

The inequality measures take the value of 0 for perfectly equal outcomes and the higher positive values for more unequal solutions. The most frequently used is the Gini coefficient. It is formulated as relative mean difference and is given by the formula:

$$G(d) = \frac{\sum_{i \in D} \sum_{j \in D} |h_i - h_j|}{2\bar{D}^2 \mu(d)}. \tag{10}$$

Standard bicriteria mean-equity model takes into account both the efficiency with optimization of the mean outcome

$\mu(\mathbf{y})$ and the equity with minimization of an inequality measure (or maximization of the equality measure) $\rho(\mathbf{y})$. Each measure has its own characteristic features, unfortunately, sometimes not able to use it effectively in optimization process directly. However, for several inequality measures, the reward-inequality ratio optimization

$$\max \left\{ \frac{\mu(d)-\tau}{\rho(d)} \ , \ d \in Q \right\}, \tag{11}$$

guarantees fairness of the solutions. This applies, in particular, to the worst conditional semi deviation.

2. Mathematical Optimization Model

The optimization task refers to allocation the load (traffic flow) on the set of given demands D, and $d \in \{1,\ldots,\bar{D}\}$. Each demand is associated with vector of revenues per unit p_d. As example, the Polish backbone network is adopted. Each link existed in graph is included in the set L and is marked by $l \in \{1,\ldots,\bar{L}\}$. Similarly, the set N contains all nodes and each node is marked as $n \in \{1,\ldots,\bar{N}\}$. Traffic flow could come into each node and get out from it in the same value exact source and target nodes. The node-link approach was chosen for make the possibility of paths bifurcation. This requires additional parameters which values are included in the matrices of incidences between nodes and links. Parameter a_{nl} is an element of outcome links matrix and if l-th link comes out from n-th node takes value of 1 and 0 otherwise. The similar schema is in income links matrix case. Its parameter b_{nl} takes the value of 1 when l-th link comes into the n-th node and 0 otherwise. Such notation is frequently uses in directed graphs, like the model described in the paper. In undirected graph case the values of those matrices would be the same. In typical network dimensioning the goal is to maximize the total flow (traffic stream, volume of bandwidth allocation, etc.). This variable is described as h_d and refers to the volume of flow allocated on d-th demand. Ratio optimization mathematical model is formulated as follows:

$$\max \frac{z-\tau}{z_0}, \tag{12}$$

$$z - u + \frac{\sum_{d\in D} k_d}{\beta \cdot \bar{D}} = z_0, k_d \geq 0, \tag{13}$$

$$k_d + h_d \cdot p_d \geq u, \tag{14}$$

$$z = \frac{1}{\bar{D}} \sum_{d\in D} h_d \cdot p_d, \tag{15}$$

$$\sum_{l\in L} a_{nl} \cdot x_{ld} - \sum_{l\in L} b_{nl} \cdot x_{ld} = \begin{cases} h_d & \text{if } n = s_d \\ 0 & \text{if } n \neq s_d, t_d \\ -h_d & \text{if } n = t_d \end{cases}, \tag{16}$$

$$\sum_{d\in D} x_{ld} \leq c_l \ , \ \forall l \in L. \tag{17}$$

In the ratio model Eqs. (13) and (14) ensure the ordering of considered objective functions. They contain the non-negative k_d and unbounded u variables, which guarantee a best solution in refer to some fair degree. More precisely it guaranties a special treat of the least values of allocated traffic flow. In optimization process, when z_0 variable is tending to possibly minimal value, the u variable is in inversely proportional. Moreover, when the u parameter is getting greater values, the Eq. (14) maximizes some part of k_d variables, which could be treated as the most discriminated demands. In each iteration, as the given percentage of the most discriminated demands, a z_0 parameter is chosen. This percentage refers to one of the control parameter β [22]. Further, there are the mean of all of objective functions needed to improve, labeled as τ. It should be noted that τ in example included in article has been calculated using the Max-Min method but it is not necessary to do. Depending on the given β degree, τ could accept greater values then τ_{MaxMin} but never greater then maximal achievable mean value, which is obtained for the simple maximization of total system efficiency (τ_{MAX}). In other words decision maker could substitute as τ each value included in just mentioned interval. However, if the greater the τ parameter is, the less fair solution will be. To ensure the node-link model assumptions is formulated as (16) constraint. It is formulated for three cases of node types:

- source,
- target,
- and connection node.

It is also important to remember about maximum capacity of each link (c_l) in the network (17) – see Table 1.

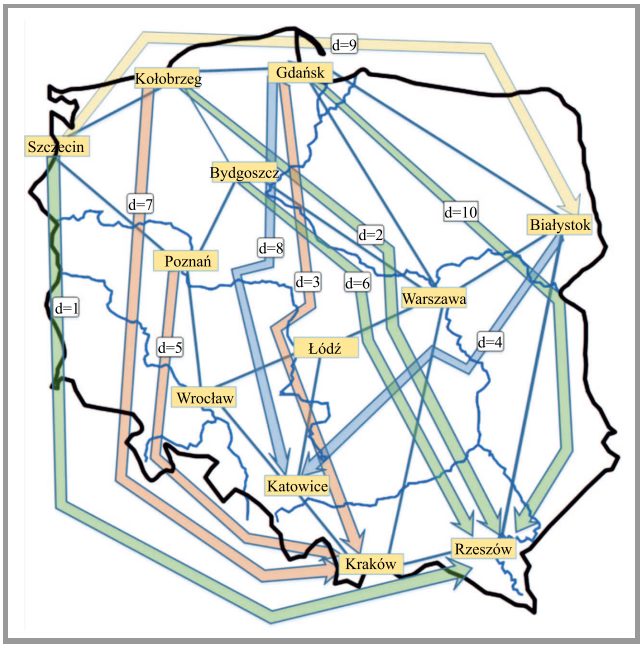

Fig. 1. An illustration of analyzed network.
(See color pictures online at www.nit.eu/publications/journal-jtit)

Table 1
Arc's characteristic

Arc ID	Start node	Target node	Capacity (c_l)
1	Kołobrzeg	Szczecin	150
2	Gdańsk	Kołobrzeg	100
3	Białystok	Gdańsk	100
4	Rzeszów	Białystok	150
5	Rzeszów	Kraków	100
6	Katowice	Kraków	80
7	Katowice	Wrocław	100
8	Wrocław	Poznań	150
9	Poznań	Szczecin	150
10	Bydgoszcz	Kołobrzeg	30
11	Warszawa	Gdańsk	80
12	Białystok	Warszawa	100
13	Warszawa	Kraków	100
14	Katowice	Łódź	80
15	Łódź	Wrocław	80
16	Poznań	Bydgoszcz	90
17	Warszawa	Bydgoszcz	200
18	Łódź	Warszawa	120
21	Szczecin	Kołobrzeg	150
22	Kołobrzeg	Gdańsk	100
23	Gdańsk	Białystok	100
24	Białystok	Rzeszów	150
25	Kraków	Rzeszów	100
26	Kraków	Katowice	80
27	Wrocław	Katowice	100
28	Poznań	Wrocław	150
29	Szczecin	Poznań	150
30	Kołobrzeg	Bydgoszcz	30
31	Gdańsk	Warszawa	80
32	Warszawa	Białystok	100
33	Kraków	Warszawa	100
34	Łódź	Katowice	80
35	Wrocław	Łódź	80
36	Bydgoszcz	Poznań	90
37	Bydgoszcz	Warszawa	90
38	Warszawa	Łódź	120

Model described above, unfortunately, cannot be used in the most of linear programming packages. It is caused by nonlinear dependencies in the main objective function (12). To face the problem variables $v = z/z_0$ and $v_0 = 1/z_0$ have been introduced. Next, all the constraints were divined by z_0 and the following submissions have been made: $\widetilde{h_d} = \frac{h_d}{z_0}$, $\widetilde{k_d} = \frac{k_d}{z_0}$, $\widetilde{u} = \frac{u}{z_0}$, $\widetilde{x_{ld}} = \frac{x_{ld}}{z_0}$. After that the ratio optimization model is written as the following linear program:

$$\max \; v - \tau \cdot v_0 \,, \tag{18}$$

$$v = \frac{1}{\bar{D}} \sum_{d \in D} \widetilde{h_d} \cdot p_d \,, \tag{19}$$

$$v - \widetilde{u} + \frac{\sum_{d \in D} \widetilde{k_d}}{\beta \cdot \bar{D}} = 1 \,, \tag{20}$$

$$\widetilde{k_d} + \widetilde{h_d} \cdot p_d \geq \widetilde{u} \;,\; \forall d \in D \,, \tag{21}$$

$$\sum_{l \in L} a_{nl} \cdot \widetilde{x_{ld}} - \sum_{l \in L} b_{nl} \cdot \widetilde{x_{ld}} = \begin{cases} \widetilde{h_d} & \text{if } \; n = s_d \\ 0 & \text{if } \; n \neq s_d, t_d \\ -\widetilde{h_d} & \text{if } \; n = t_d \end{cases} \;, \tag{22}$$

$$\sum_{d \in D} \widetilde{x_{ld}} \leq c_l \cdot v_0 \;,\; \forall l \in L \,. \tag{23}$$

The experiments are performed for example of Polish backbone network [23]. Arrangement of given demands is presented in Fig. 1.

3. Results

In computations the CPLEX package was used as optimization environment. In the paper the results have been obtained for several configurations of control parameters (such as β and τ) and are presented in the Table 4. Considering the algorithm of described dimensioning problem optimization, there has been done several iterations as it is shown in Fig. 2. First, the solution of ratio model has been obtained τ = MAXMIN(H). Next the value of τ, were taking greater values, obtained from previous solutions of ratio model optimization – RM(H). The steps were repeated until the receive of maximal value of τ related to simple maximization concept solution – MAX(H).

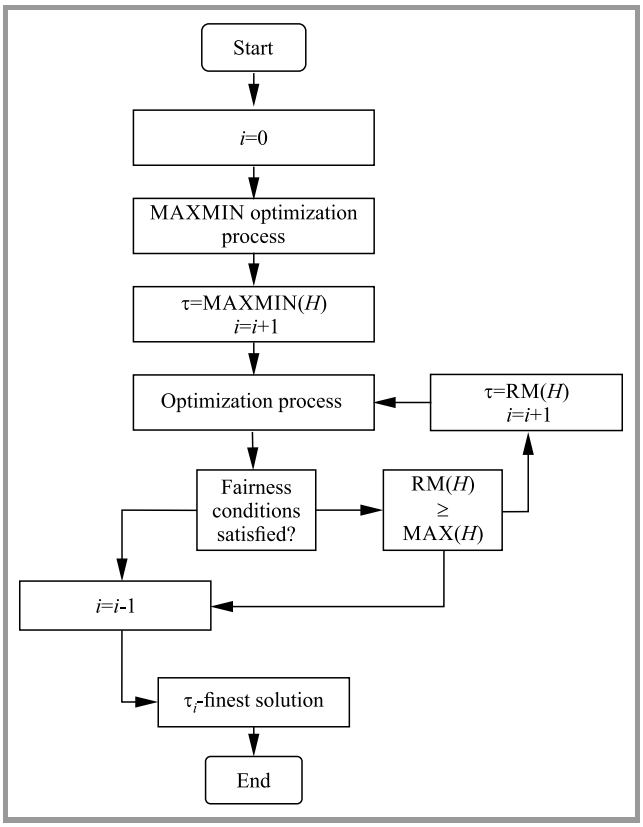

Fig. 2. An algorithm of decision process.

Table 2
Values of Gini coefficient for chosen control parameters

τ	$\beta = 0.1$	$\beta = 0.2$	$\beta = 0.3$	$\beta = 0.5$	$\beta = 0.8$
3667	0.10	0.10	0.10	0.10	0.10
3950	0.11	0.11	0.11	0.09	0.11
4000	0.56	0.45	0.51	0.63	0.51
4100	0.56	0.48	0.43	0.54	0.43
4200	0.66	0.50	0.53	0.49	0.53
4300	0.62	0.63	0.52	0.53	0.52
5000	0.49	0.53	0.59	0.60	0.59
6500	0.66	0.51	0.62	0.64	0.62
7800	0.56	0.51	0.62	0.62	0.62

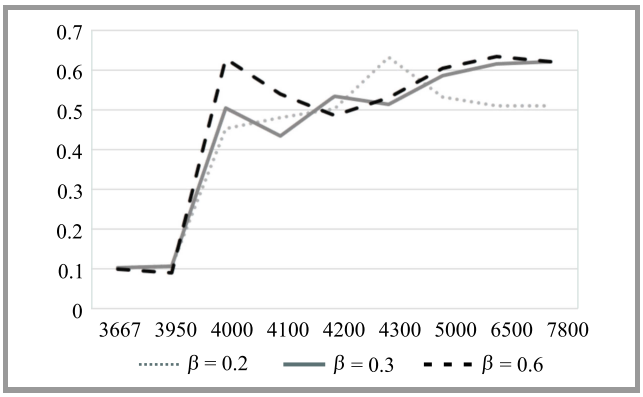

Fig. 3. A plot illustrating the course of Gini coefficient.

Table 3
Values of the mean traffic flow of obtained solutions

τ	$\beta = 0.1$	$\beta = 0.2$	$\beta = 0.3$	$\beta = 0.5$	$\beta = 0.8$
3667	4258	4258	4258	4400	4400
3950	4288	4288	4288	5040	5040
4000	6269	6269	6269	5040	5040
4100	6269	6269	6269	5040	5040
4200	7900	7900	6823	7505	6840
4300	7900	7900	7900	7660	7560
5000	7900	7900	7900	7660	7560
6500	7900	7900	7900	7660	7640
7800	7900	7900	7900	7900	7900

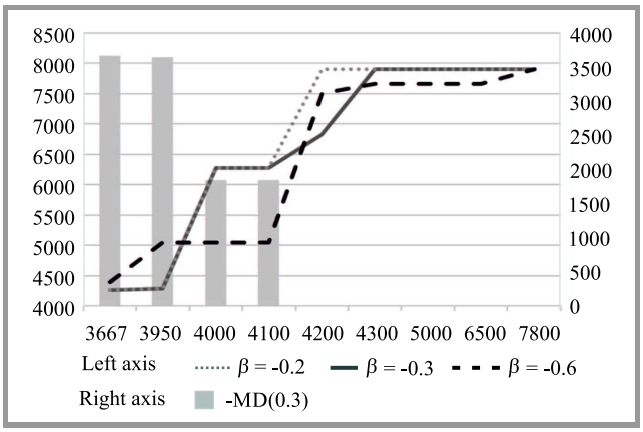

Fig. 4. A plot illustrating the course of mean value.

Considering the algorithm of described dimensioning problem optimization, there has been done several iterations. First, the solution of ratio model has been obtained τ = MAXMIN(H). Next the value of τ is taking greater values, obtained from previous solutions of ratio model optimization. The steps are repeated until the receive of maximal value of τ related to simple maximization concept solution MAX(H). Values presented in Tables 2 and 3 are in reference to several control parameters configurations. β parameter is related to percent of the most discriminated demands and it affects the dynamic of the mean value changes. Different situation is for the values of the Gini coefficient. The changes of β parameter have not impact for this inequality measure. Ratio model gives a capability of obtain some set of solutions in reference to chosen τ values and shows a spectrum of it, from more to less fair. The goal of each iteration of optimization process is to return the

Table 4
Detail table of solution obtained for $\beta = 0.3$ and given values of τ

d	p_d	$\tau = 3667$	$\tau = 3950$	$\tau = 4000$	$\tau = 4100$	$\tau = 4200$	$\tau = 4300$	$\tau = 5000$	$\tau = 6500$	$\tau = 7800$
1	200	3666.67	3647.06	2461.54	9076.92	16000	20000	12000	32000	16000
2	50	3666.67	3647.06	1846.15	1846.15	0	0	0	0	0
3	150	3666.67	3647.06	1846.15	1846.15	1846.15	12000	9000	9000	9000
4	100	6166.67	6000	11000	10692.3	7923.08	12000	8000	6000	6000
5	60	3666.67	3647.06	1846.15	1846.15	1846.15	0	0	0	0
6	200	3666.67	4000	24000	18000	24000	18000	34000	18000	34000
7	50	3666.67	3647.06	1846.15	1846.15	1846.15	0	0	0	0
8	150	5750	6000	6000	6000	6000	6000	9000	9000	9000
9	100	5000	5000	10000	9692.31	6923.08	11000	7000	5000	5000
10	60	3666.67	3647.06	1846.15	1846.15	1846.15	0	0	0	0

highest possible grow of efficiency of the system with the lowest possible loss of fairness. Figures 3 and 4 presents a graphs of changes of just mentioned values according to value of τ. Additional in Fig. 4 are added bars to visualize the changes of most discriminated value for value of $\beta = 0.3$ MD(0.3). Just mentioned degrees are suitable for the assessment of obtained solution but it not include the information about assigned 0 values to given demands. In some cases the situation such that (where at least one of objective function vector value gets 0) provides the non-acceptable judgment in the terms of justice. Considering solutions obtained for $\beta = 0.3$ the most visible growth of the mean value and the Gini index, according to increase of τ, is for the third iteration. Table 4 presents the solutions for this value of β in details. The outcome vectors which contains all non-zero values were assigned for the four first iterations of considered values of τ. It is necessary to decide if the solution which takes a 0 for at least one value of objective functions is automatically not fair. If such an assumption is made, according to Table 4 the solutions obtained for $\tau \geq 4200$ should be rejected in terms of fairness criterion. In calculations, the algorithm was stopped when τ parameter reached the value equal to simple maximization solution. Considering Figs. 3 and 4, the algorithm should be stopped some steps earlier. However, in the paper there was presented approach of finding the spectrum of solutions more or less fair, to demonstrate the range of options from the most fair to the most efficient. Next step belongs to the decision-maker who has his own preferences and may decide about the fairness degree of the selected solution.

References

[1] J. Rawls, *Theory of Justice*. Cambridge: Harvard Univ. Press, 1971.

[2] H. P. Young, *Equity in Theory and Practice*. Princeton: Princeton Univ. Press, 1994.

[3] M. Pióro and D. Medhi, *Routing, Flow and Capacity Design in Communication and Computer Networks*. San Francisco: Morgan Kaufmann, 2004.

[4] W. Ogryczak and A. Wierzbicki, "On multi-criteria approaches to bandwidth allocation", *Control and Cybernet.*, vol. 33, no. 3, pp. 427–448, 2004.

[5] J. Kleinberg, Y. Rabani, and E. Tardos, "Fairness in routing and load balancing", *J. Comput. Syst. Sci.*, vol. 63, no. 1, pp. 2–21, 2001.

[6] W. Ogryczak, M. Pióro, and A. Tomaszewski, "Telecommunications network design and Max-Min optimization problem", *J. of Telecommun. & Inform. Technol.*, no. 3, pp. 43–56, 2005.

[7] H. Luss, "On equitable resource allocation problems: A lexicographic minimax approach", *Operation Res.*, vol. 47, no. 3, pp. 361–378, 1999.

[8] F. Kelly, A. Mauloo, and D. Tan, "Rate control for communication networks: Shadow prices, proportional fairness and stability", *J. Oper. Res. Soc.*, vol. 49, pp. 206–217, 1997.

[9] R. Denda, A. Banchs, and W. Effelsberg, "The fairness challenge in computer networks", *Lect. Notes Comp. Sci.*, vol. 1922, pp. 208–220, 2000.

[10] R. R. Yager, "On ordered weighted averaging aggregation operators in multicriteria decision making", *IEEE Trans. on Systems, Man, and Cybernet.*, vol. 18, no. 1, pp. 183–190, 1988.

[11] R. R. Yager, J. Kacprzyk, and G. Beliakov, *Recent Developments in the Ordered Weighted Averaging Operators: Theory and Practice*. Springer, 2011.

[12] M. M. Kostreva and W. Ogryczak, "Linear optimization with multiple equitable criteria", *RAIRO Oper. Res.*, vol. 33, no. 3, pp. 275–297, 1999.

[13] W. Ogryczak, "Bicriteria models for fair and efficient resource allocation", in *Social Informatics*, L. Bolc, M. Makowski, A. Wierzbicki, Eds. *LNCS*, vol. 6430, pp. 140–159. Springer, 2010.

[14] T. Lan, D. Kao, M. Chiang, and A. Sabharwal, "An axiomatic theory of fairness in network resource allocation", in *Proc. 29th Conf. on Comp. Commun. IEEE INFOCOM 2010*, San Diego, CA, USA, 2010, pp. 1–9.

[15] W. Ogryczak, "Inequality measures and equitable approaches to location problems", *Eur. J. Oper. Res.*, vol. 122, no. 2, pp. 374–391, 2000.

[16] M. Dianati, X. Shen, and S. Naik, "A new fairness index for radio resource allocation in wireless networks", *Proc. IEEE Wirel. Commun. & Networking Conf. WCNC 2005*, New Orleans, LA, USA, 2005, vol. 2, pp. 712–717.

[17] W. Ogryczak, "Inequality measures and equitable locations", *Annals of Oper. Res.*, vol. 167, no. 1, pp. 61–86, 2009.

[18] W. Ogryczak and M. Zawadzki, "Conditional median: a parametric solution concept for location problems", *Annals of Oper. Res.*, vol. 110, no. 3, pp. 167–181, 2002.

[19] W. Ogryczak and A. Tamir, "Minimizing the sum of the k largest functions in linear time", *Inform. Processing Lett.*, vol. 85, no. 3, pp. 117–122, 2003.

[20] A. B. Atkinson, "On the measurement of inequality", *J. Econom. Theory*, vol. 2, pp. 244–263, 1970.

[21] R. Jain, D. Chiu, and W. Hawe, "A quantitative measure of fairness and discrimination for resource allocation in shared computer system", *Eastern Res. Lab., Digital Equipment Corp.*, 1984.

[22] W. Ogryczak and T. Śliwiński, "On equitable approaches to resource allocation problems: The conditional minimax solutions", *J. of Telecommun. & Inform. Technol.*, no. 3, pp. 40–48, 2002.

[23] S. Orłowski, R. Wessaly, and M. Pióro, and A. Tomaszewski, "SNDlib 1.0 – survivable network design library", *Networks*, vol. 55, no. 3, pp. 276–286, 2009.

Grzegorz Zalewski works as specialist in Institute of Telecommunications in Warsaw in Advanced Informations Technologies Department. He got M.Sc. at Faculty of Transport of Warsaw University of Technology in 2005. He completed postgraduate studies of Programming Architecture and Engineering at Military University of Technology in 2014. At 2015 he began doctoral studies at Warsaw University of Technology at Faculty of Electronics and Information Technology in Warsaw in the domain of networks optimization models. Exactly he is interested in deploying fair methods in networks dimensioning.

E-mail: G.Zalewski@itl.waw.pl
National Institute of Telecommunications
Szachowa st 1
04-894 Warsaw, Poland

Włodzimierz Ogryczak is Professor of Computer Science and Director of the Institute of Control and Computation Engineering at the Warsaw University of Technology, Poland. He received both his M.Sc. (1973) and Ph.D. (1983) in Mathematics from Warsaw University, and D.Sc. (1997) in Computer Science from Polish Academy of Sciences. His research interests are focused on models, computer solutions and interdisciplinary applications in the area of optimization and decision making with the main stress on: multiple criteria optimization and decision support, decision making under risk, location and distribution problems. He has published four books and numerous research articles in international journals.

E-mail: wogrycza@ia.pw.edu.pl
Institute of Control and Computation Engineering
Warsaw University of Technology
Nowowiejska st 15/19
00-665 Warsaw, Poland

Paper

Hybrid Models for the OWA Optimization

Paweł Olender

National Institute of Telecommunications, Warsaw, Poland

Abstract—When dealing with multicriteria problems, the aggregation of multiple outcomes plays an essential role in finding a solution, as it reflects the decision-maker's preference relation. The Ordered Weighted Averaging (OWA) operator provides a flexible preference model that generalizes many objective functions. It also ensures the impartiality and allow to obtain equitable solutions, which is vital when the criteria represent evaluations of independent individuals. These features make the OWA operator very useful in many fields, one of which is location analysis. However, in general the OWA aggregation makes the problem nonlinear and hinder its computational complexity. Therefore, problems with the OWA operator need to be devised in an efficient way. The paper introduces new general formulations for OWA optimization and proposes for them some simple valid inequalities to improve efficiency. A hybrid structure of proposed models makes the number of binary variables problem type dependent and may reduce it significantly. Computational results show that for certain problem types, some of which are very useful in practical applications, the hybrid models perform much better than previous general models from literature.

Keywords—location problem, mixed integer (linear) programming, multiple criteria, ordered weighted averaging.

1. Introduction

In many practical problems we have to deal with multiple conflicting criteria. Typically, there does not exist unique optimal solution for such problems and we need to use decision-maker's preference to solve them. We have to be able to compare different alternatives and decide, which one is better from a decision-maker point of view. A common approach is to aggregate all original criteria by some scalarizing function into one overall objective function. In this solution concept an aggregation is crucial, as it provides the preference model, and thus determines preference relation between alternatives. The so-called Ordered Weighted Averaging (OWA) operator provides a parameterized aggregation function that generalized many scalarizing functions, including the most popular the average and the maximum (minimum) along with many other cases. The OWA operator, introduced by Yager [1], is a special weighted average, where weights are assigned to the ordered values of outcomes (i.e. to the largest value, the second largest and so on) rather than to the specific outcomes.

The OWA operator not only generalizes various objective functions, but also ensures impartial and in some circumstances equitable solutions. It plays an essential role when the distribution of outcomes is more important than values' assignment to specific outcomes. It is the case when we deal with outcomes that express, for example, the evaluation of multiple independent users or scenarios. Thus, the OWA aggregation has been widely applied in different domains [2]–[4]. However, when we aggregate the variable criteria by the OWA operator, we get the nonlinear problem, even if the original problem has a linear formulation. Yager [5] showed that this type of nonlinearity can be transformed into a Mixed Integer Linear Programming (MILP) problem. Furthermore, in [6] it was proofed that the OWA optimization with appropriate monotonic weights can be expressed as linear programming (LP) problem of higher dimension, allowing to improve solution techniques for many related problems [7].

The outcomes distribution is important in location analysis when we deal with independent clients [8]. Within this field the so-called Ordered Median (OM) function was developed and analyzed [9], which in fact corresponds to the OWA operator. Thus, several models and some dedicated solution methods for the OWA optimization were developed within the location analysis, including branch and bound [10] or branch and cut [11], [12] approaches. A significant improvement in computational efficiency has been made. However, the solution times are still not satisfactory. Besides, some of these formulations take advantage of specific assumptions such as free self-service.

In this paper a new general MILP model for the OWA optimization is introduced, which is the extension of the LP formulation [6] and can be applied to any non-negative preference weights $\mathbf{w}$. Some similar concept of LP formulation extension has been recently applied for the weighted OWA aggregation [13]. Due to hybrid structure with the linear and the mixed integer linear parts, the number of binary variables in our new formulations depend on problem type and can be substantially reduced for some of them. We evaluate new models for the discrete location problems, but we do not exploit any specific structure and assume only the non-negativity of the outcomes for some results. We also propose some simple valid inequalities to improve the computational performance of new formulations, which we set together with one of the most efficient general model for OWA optimization (see comparison in [14]).

The paper is organized as follows. In Sections 2 and 3 the problem is formally defined and the hybrid models for the OWA optimization are developed. In Section 4 the ex-

perimental procedure is described and results are presented. Section 5 concludes and proposes some further research directions.

2. Problem Formulations

We consider uncapacitated discrete location problem [15], which can also be defined as network location problem, where facilities are allowed to be placed only on vertices (or subset of vertices) of the underlying network. Given a set of m clients and a set of potential facility locations, which without loss of generality can be assumed to be identical sets, we have to place n facilities ($n \leq m$) and assign them to clients to meet the demand. We aim at optimizing a given objective function, which is usually based on abstract distances (e.g. geographic distances, service costs, service times) between the clients and the facilities. We assume no capacity limit of facilities, so each client is assigned the closest facility. The model can be formally expressed in the following form:

$$\min \quad (y_1, y_2, \ldots, y_m), \tag{1a}$$

$$\text{s.t.} \quad y_i = \sum_{j=1}^{m} c_{ij} x'_{ij} \qquad \forall i, \tag{1b}$$

$$\sum_{j=1}^{m} x_j = n, \tag{1c}$$

$$\sum_{j=1}^{m} x'_{ij} = 1 \qquad \forall i, \tag{1d}$$

$$x'_{ij} \leq x_j \qquad \forall i, j, \tag{1e}$$

$$x_j \in \{0, 1\} \qquad \forall i, j, \tag{1f}$$

$$x'_{ij} \geq 0 \qquad \forall i, j, \tag{1g}$$

where c_{ij} denotes the cost of satisfying the total demand of client i from facility j. The main decisions are described by binary variables x_j ($j = 1, 2, \ldots, m$) equal 1 if a facility is placed at site j and equal 0 otherwise. Additional binary variables represent allocation decisions: x'_{ij} ($i, j = 1, 2, \ldots, m$) is equal to 1 if the demand of client i is satisfied by facility j and 0 otherwise. Due to lack of capacity restriction, each client will be assigned to the closest facility, and therefore variables x'_{ij} can be relaxed to continuous variables. The auxiliary variable y_i (1b) expresses the cost of satisfying the demand of client i. Constraint (1c) enforces that exactly n facilities are placed. Constraint (1d) limits each client to be assigned only one facility and constraint (1e) ensures that the assignment is done to the existing facilities. Thus, constraints (1c)–(1g) define the set of feasible solutions Q, which is mapped into the set of attainable outcome (cost) vectors $\mathbf{y}$ by constraint (1b).

We want to obtain efficient solutions of problem (1) in the sense of outcomes $y_i = f_i(\mathbf{x})$ for $i = 1, 2, \ldots, m$ using the OWA operator. To define the OWA aggregation of a vector $\mathbf{y} = (y_1, y_2, \ldots, y_m)$ more formally, let us introduce the ordering map Θ: $R^m \to R^m$ such that $\Theta(\mathbf{y}) = (\theta_1(\mathbf{y}), \theta_2(\mathbf{y}), \ldots, \theta_m(\mathbf{y}))$ satisfies $\theta_1(\mathbf{y}) \geq \theta_2(\mathbf{y}) \geq \ldots \geq \theta_m(\mathbf{y})$ and there exist a permutation τ of set I such that $\theta_i(\mathbf{y}) = y_{\tau(i)}$ for $i = 1, 2, \ldots, m$. Then for a given preference weight vector $\mathbf{w} = (w_1, \ldots, w_m)$ with $w_i \geq 0$ for all i, the OWA operator takes the form

$$A_{\mathbf{w}}(\mathbf{y}) = \sum_{i=1}^{m} w_i \theta_i(\mathbf{y}). \tag{2}$$

Finally, we apply formula (2) to problem (1) and receive the following optimization problem

$$\min\{A_{\mathbf{w}}(\mathbf{y}) \colon \ \mathbf{y} = \mathbf{f}(\mathbf{x}), \ \mathbf{x} \in Q\}.$$

3. Optimization Models

At first we recall the LP formulation for the OWA optimization [6] that can be used with appropriate monotonic weights (non-increasing in case of minimization). Then we extend it by mixed integer linear part, and thus making it valid to any non-negative preference weights.

3.1. LP Model for OWA

The ordering operator Θ in the OWA aggregation is nonlinear and, in general, it leads to complex optimization models. However, in special case with non-increasing weights the OWA aggregation is piecewise linear convex function and can be minimized using the linear programming form [6]. This so-called deviational model exploits the linear programming representation of the cumulated ordered outcomes $\bar{\Theta}(\mathbf{y}) = (\bar{\theta}_1(\mathbf{y}), \bar{\theta}_2(\mathbf{y}), \ldots, \bar{\theta}_m(\mathbf{y}))$, where

$$\bar{\theta}_k(\mathbf{y}) = \sum_{i=1}^{k} \theta_i(\mathbf{y}) \quad \forall k$$

expresses the total of the k largest outcomes. These quantities can be determined as

$$\bar{\theta}_k(\mathbf{y}) = k\theta_k(\mathbf{y}) + \sum_{i=1}^{k-1} (\theta_i(\mathbf{y}) - \theta_k(\mathbf{y})) \quad \forall k,$$

where the k-th largest outcome $\theta_k(\mathbf{y})$ is treated as a reference value to which its deviations from greater outcomes are added. Provided we introduce the explicit variables d_{ik} for deviations, each $\bar{\theta}_k(\mathbf{y})$ for any given $\mathbf{y} \in R^m$ and $k = 1, \ldots, m$ can be found by solving the following LP problem:

$$\bar{\theta}_k(\mathbf{y}) = \min_{t_k, d_{ik}} \quad (kt_k + \sum_{i=1}^{m} d_{ik}), \tag{3a}$$

$$\text{s.t.} \quad d_{ik} \geq y_i - t_k \qquad \forall i, \tag{3b}$$

$$d_{ik} \geq 0 \qquad \forall i. \tag{3c}$$

Variable t_k corresponds to k-th largest outcome (strictly speaking in optimal solution $\theta_{k+1}(\mathbf{y}) \leq t_k^* \leq \theta_k(\mathbf{y})$ for $k = 1, \ldots, m-1$ and $t_m^* \leq \theta_m(\mathbf{y})$; and $t_k^* = \theta_k(\mathbf{y})$ provided that at most $k-1$ variables $d_{ik} > 0$).

The ordered outcomes can be determined as differences $\theta_k(\mathbf{y}) = \bar{\theta}_k(\mathbf{y}) - \bar{\theta}_{k-1}(\mathbf{y})$ for $k = 2,\ldots,m$ and $\theta_1(\mathbf{y}) = \bar{\theta}_1(\mathbf{y})$. Hence the OWA aggregation $\sum_{k=1}^{m} w_k\theta_k(\mathbf{y})$ with weights w_k can be replaced by $\sum_{k=1}^{m} w'_k\bar{\theta}_k(\mathbf{y})$, where $w'_m = w_m$ and $w'_k = w_k - w_{k+1}$ for $k = 1,2,\ldots,m-1$. Therefore, as shown in [6], in case of non-increasing and non-negative original weights ($w_1 \geq w_2 \geq \ldots \geq w_m \geq 0$), the OWA optimization problem can be formulated as follows:

$$\min_{t_k,d_{ik},y_i} \quad \sum_{k=1}^{m} w'_k(kt_k + \sum_{i=1}^{m} d_{ik}), \tag{4a}$$

$$\text{s.t.} \quad d_{ik} \geq y_i - t_k \qquad \forall i,k, \tag{4b}$$

$$d_{ik} \geq 0 \qquad \forall i,k, \tag{4c}$$

$$\mathbf{y} = \mathbf{f}(\mathbf{x}),\ \mathbf{x} \in Q. \tag{4d}$$

3.2. Hybrid Model for OWA

In LP formulation (4) we minimize the upper bound of function $kt_k + \sum_{i=1}^{m} d_{ik}$ for each $k = 1,2,\ldots,m$. We then multiply these bounds by modified weights w'_k in the objective function (4a). If original weights w_k do not satisfy monotonicity condition (non-increasing), some weights w'_k are negative and then the problem (4) is unbounded. To make it valid for general case, we need to apply a lower bound for function $kt_k + \sum_{i=1}^{m} d_{ik}$.

The cumulative sum of the k-th largest outcomes $\bar{\theta}_k(\mathbf{y})$ can be determined in a similar way like in (3) by using a lower bound of function $kt_k + \sum_{i=1}^{m} d_{ik}$. However, it requires binary variables. For any $\mathbf{y} \in R^m$ and $k = 1,\ldots,m$ the problem is as follows:

$$\bar{\theta}_k(\mathbf{y}) = \max_{\rho_k,t'_k,d'_{ik},z_{ik}} \quad \rho_k, \tag{5a}$$

$$\text{s.t.} \quad \rho_k \leq kt'_k + \sum_{i=1}^{m} d'_{ik}, \tag{5b}$$

$$t'_k + d'_{ik} \leq y_i + M(1 - z_{ik}) \qquad \forall i, \tag{5c}$$

$$d'_{ik} \leq Mz_{ik} \qquad \forall i, \tag{5d}$$

$$\sum_{i=1}^{m} z_{ik} = k, \tag{5e}$$

$$z_{ik} \in \{0,1\} \qquad \forall i. \tag{5f}$$

For any $k = 1,\ldots,m$ there are m binary variables z_{ik}. They determine which constraints (5c) are relaxed by adding large constant M and which variables d'_{ik} are non-zero according to (5d). If $z_{ik} = 1$, then for respective i constraint (5c) becomes active and d'_{ik} may take positive values. Thus, according to maximization, $t'_k + d'_{ik}$ becomes equal to y_i. Solving this problem amounts to selecting k variables z_{ik} ($i = 1,\ldots,m$), which take value 1 in order to make the respective sums $t'_k + d'_{ik}$ as large as possible. Therefore, in optimal solution the value 1 is taken by k variables z_{ik} that correspond to the k largest outcomes y_i. Variable t'_k is not greater than k-th largest outcome due to k active constraints (5c); and k respective variables d'_{ik} complete t'_k to the k largest outcomes.

Formulation (5) can be simplified by removing the binary component from formula (5c). The character of t'_k changes a little bit, but the optimal value still equals the sum of the k largest outcomes.

Proposition 1: For any given vector $\mathbf{y} \in R^m$, the sum of its k largest components $\bar{\theta}_k(\mathbf{y})$ can be found as the optimal value of the following MILP problem:

$$\bar{\theta}_k(\mathbf{y}) = \max_{\rho_k,t'_k,d'_{ik},z_{ik}} \quad \rho_k, \tag{6a}$$

$$\text{s.t.} \quad \rho_k \leq kt'_k + \sum_{i=1}^{m} d'_{ik}, \tag{6b}$$

$$t'_k + d'_{ik} \leq y_i \qquad \forall i, \tag{6c}$$

$$d'_{ik} \leq Mz_{ik} \qquad \forall i, \tag{6d}$$

$$\sum_{i=1}^{m} z_{ik} = k, \tag{6e}$$

$$z_{ik} \in \{0,1\} \qquad \forall i. \tag{6f}$$

Proof: In order to proof the proposition, we will show that the optimal value of problem (6) is the same as that of problem (5). First of all, we may notice that problem (6) is a restriction of problem (5). Every feasible solution of (6) is also a feasible solution of (5). Consider any feasible solution of (5). Let $I_k^1 = \{i\colon z_{ik} = 1\}$ be the subset of $i \in I$ for which $z_{ik} = 1$ and respectively $I_k^0 = I \setminus I_k^1$. For each $i \in I_k^1$, constraint (5c) simplifies to (6c), and thus any feasible solution of (5) satisfies (6c) for $i \in I_k^1$. If feasible solution of (5) additionally satisfies (6c) for $i \in I_k^0$, then it is also a feasible solution of (6). Otherwise, there is some number s of $i \in I_k^0$ for which $t'_k + d'_{ik} > y_i$. According to (5d), as $d'_{ik} \leq 0$ for $i \in I_k^0$ then $t'_k > y_i$ for some s of $i \in I_k^0$. However, each such solution can be replaced by equally good or better alternative, which violates at most $s-1$ constraints (6c) for $i \in I_k^0$. We can determine

$$\delta = \min_{\substack{i \in I_k^0, \\ y_i < t'_k}} (t'_k - y_i), \tag{7}$$

replace t'_k by $\check{t}'_k = t'_k - \delta$ and d'_{ik} by $\check{d}'_{ik} = d'_{ik} + \delta$ for these i's for which $\check{d}'_{ik} \leq Mz_{ik}$ is satisfied. It holds at least for all $i \in I_k^1$ as follows

$$\begin{aligned} \check{d}'_{ik} = d'_{ik} + \delta &\leq y_i - t'_k + \delta && \text{by (5c)}, \\ &\leq y_i - \theta_m(\mathbf{y}) && \text{by (7)}, \\ &\leq \theta_1(\mathbf{y}) - \theta_m(\mathbf{y}) \leq M. \end{aligned}$$

So $\check{d}'_{ik} \leq Mz_{ik}$ is satisfied at least for $i \in I_k^1$, and thus at least $r \geq k$ variables d'_{ik} can be replaced by $\check{d}'_{ik}$, obtaining

$$k\check{t}'_k + \sum_{i=1}^{m} \check{d}'_{ik} = kt'_k + \sum_{i=1}^{m} d'_{ik} + (r-k)\delta \geq kt'_k + \sum_{i=1}^{m} d'_{ik}.$$

It means that for any feasible solution of (5), reducing the number of violated constraints (6c) for $i \in I_k^0$, we can obtain not worse corresponding feasible solution of (6). In conclusion, the optimal value of problem (6), similarly like

the optimal value of problem (5), determines the sum of the k largest components of any given vector $\mathbf{y} \in R^m$. ■

From proposition (1), we can also conclude that for any $k = 1, \ldots, m$, one of the optimal solution of problem (6) is one with $t_k'^* = \theta_m(\mathbf{y})$ and $d_{ik}'^* = y_i - \theta_m(\mathbf{y})$ for these i's that correspond to the k largest outcomes y_i, and $d_{ik}'^* = 0$ for the rest of i's. In general, the following holds:

Lemma 2: For any given vector $\mathbf{y} \in R^m$ and any given value $\zeta \leq \theta_m(\mathbf{y})$, there exists the optimal solution of problem (6) with $t_k'^* = \zeta$.

Proof: As stated above, problem (6) has the optimal solution with $t_k'^* = \theta_m(\mathbf{y})$. We will show that the value of the objective function is constant for $t_k' \leq \theta_m(\mathbf{y})$ for any $k = 1, \ldots, m$. The objective function of problem (6) can be expressed as

$$g(t_k') = kt_k' + \sum_{i \in I_k^1} \min(y_i - t_k', M) + \sum_{i \in I_k^0} \min(y_i - t_k', 0), \quad (8)$$

where $I_k^1 = \{i\colon z_{ik} = 1\}$ with $|I_k^1| = k$ and $I_k^0 = I \setminus I_k^1$ with $|I_k^0| = m - k$. For any given $t_k' \leq \theta_m(\mathbf{y})$, provided that constant M is large enough, function (8) can be simplified to

$$g(t_k') = kt_k' + \sum_{i \in I_k^1} (y_i - t_k') = \sum_{i \in I_k^1} y_i, \quad (9)$$

and thus the value of the $g(t_k')$ is constant in the considered interval. ■

Using problem (6), we can now propose the optimization model of OWA for any weights $w_k \geq 0$, which is based on function $kt_k + \sum_{i=1}^m d_{ik}$.

$$\min_{\rho_k, t_k, d_{ik}, t_k', d_{ik}', z_{ik}, y_i} \quad \sum_{k=1}^m w_k' \rho_k, \quad (10a)$$

$$\text{p.o.} \quad kt_k + \sum_{i=1}^m d_{ik} \leq \rho_k \qquad \forall k, \quad (10b)$$

$$t_k + d_{ik} \geq y_i, \; d_{ik} \geq 0 \qquad \forall i, k, \quad (10c)$$

$$\rho_k \leq kt_k' + \sum_{i=1}^m d_{ik}' \qquad \forall k, \quad (10d)$$

$$t_k' + d_{ik}' \leq y_i \qquad \forall i, k, \quad (10e)$$

$$d_{ik}' \leq M z_{ik} \qquad \forall i, k, \quad (10f)$$

$$\sum_{i=1}^m z_{ik} = k \qquad \forall k, \quad (10g)$$

$$z_{ik} \in \{0, 1\} \qquad \forall i, k, \quad (10h)$$

$$\mathbf{y} = \mathbf{f}(\mathbf{x}), \; \mathbf{x} \in Q. \quad (10i)$$

Formulation (10) is a valid optimization model for OWA. However, we do not need to use both lower and upper bound for each $k = 1, \ldots, m$. We need constraints (10b) and (10c) only for k for which $w_k' \geq 0$. What is more important, we need constraints (10d)–(10h) only for k for which $w_k' < 0$. It significantly reduces the number of variables too. Variables t_k, d_{ik} are defined only for $w_k' \geq 0$, whereas t_k', d_{ik}' and z_{ik} only for $w_k' < 0$. Taking advantage of above observations, the OWA optimization problem takes the following form:

$$\min_{\substack{\rho_k, t_k, d_{ik}, \\ t_k', d_{ik}', z_{ik}, y_i}} \quad \sum_{k=1}^m w_k' \rho_k, \quad (11a)$$

$$\text{s.t.} \quad kt_k + \sum_{i=1}^m d_{ik} \leq \rho_k \qquad \forall k; w_k' \geq 0, \quad (11b)$$

$$t_k + d_{ik} \geq y_i, \; d_{ik} \geq 0 \qquad \forall i, k; w_k' \geq 0, \quad (11c)$$

$$\rho_k \leq kt_k' + \sum_{i=1}^m d_{ik}' \qquad \forall k; w_k' < 0, \quad (11d)$$

$$t_k' + d_{ik}' \leq y_i \qquad \forall i, k; w_k' < 0, \quad (11e)$$

$$d_{ik}' \leq M z_{ik} \qquad \forall i, k; w_k' < 0, \quad (11f)$$

$$\sum_{i=1}^m z_{ik} = k \qquad \forall k; w_k' < 0, \quad (11g)$$

$$z_{ik} \in \{0, 1\} \qquad \forall i, k; w_k' < 0, \quad (11h)$$

$$\mathbf{y} = \mathbf{f}(\mathbf{x}), \; \mathbf{x} \in Q. \quad (11i)$$

It is clear now that problem (11) has hybrid structure and consists of linear part with constraints (11b)–(11c), and of mixed integer linear part with constraints (11d)–(11h). The linear part, for $w_k' \geq 0$, is in fact the LP problem (4). The mixed integer linear part is much more computationally expensive. However, it is worth to notice that the number of binary variables is proportional to the number of negative weights w_k'. If we define this set as $K^- = \{k\colon w_k' < 0, k = 1, \ldots, m\}$, the total number of binary variables equals $|K^-|m$. Taking into account that preference weights $w_k \geq 0$ and $w_m' = w_m$, $w_k' = w_k - w_{k+1}$, the cardinality of set K^- may be at most $m - 1$. Therefore, it seems that hybrid model can be an interesting alternative for other general MILP formulations for OWA optimization, where the number of binary variables is of order m^2 independently of problem type (for instance, models M1 and M2, compared in [14]). On the other hand, here we have $O(m^2)$ additional continuous variables, whereas other MILP formulations usually introduce $O(m)$ continuous variables. Moreover, the formulation has more constraints – in both cases the number of constraints is of order m^2, but in our formulation the proportional factor is greater. Due to these observations, formulation (11) seems interesting for problems with small number of negative weights w_k'. It is especially true for trimmed mean problems, where only one weight w_k' is negative. Trimmed mean problems are used when we want to discard some of the largest and smallest outcomes, and are ones of the most useful among problems with non-monotonic weights.

To improve the computational efficiency of formulation (11), we consider some simple valid inequalities for the mixed integer linear part. From now on, we also assume that the outcome vector is non-negative, i.e. $\mathbf{y} \geq 0$. This is very general assumption that holds not only in location problems but also in many others.

Proposition 3: There exists an optimal solution of (11) that satisfies the following constraints:

(i) non-negativity of d'_{ik}

$$d'_{ik} \geq 0 \qquad \forall i,k; w'_k < 0, \tag{12}$$

(ii) non-negativity of t'_k

$$t'_k \geq 0 \qquad \forall k; w'_k < 0, \tag{13}$$

(iii) non-decreasing order of binary variables z_{ik} for each i

$$z_{ik} \leq z_{ik'} \qquad \forall i,k; k \in \{K^- \setminus \max\{K^-\}\}; k' = suc(k), \tag{14}$$

where $suc(k) = \min\{k' : k' \in K^- \wedge k' > k\}$ is the successor function within set K^-.

Proof: There exists an optimal solution of (11) that satisfies constraints (12)–(13) if for any $k = 1,\ldots,m$ for which $w'_k < 0$ there exists an optimal solution of (6) that satisfies constraints (12)–(13). We will consider a specific optimal solution of (6) for any $k = 1,\ldots,m$. To show constraint (14) holds, we will consider relation between optimal solutions of (6) for different $k,k' = 1,\ldots,m$ ($k' > k$).
Due to Lemma 2 for any $\mathbf{y} \in R^m$ and any value $\zeta \leq \theta_m(\mathbf{y})$, there exists the optimal solution of (6) with $t'^*_k = \zeta$. Since we have assumed $\mathbf{y} \geq 0$, our consideration can be limited to $\zeta \in [0, \theta_m(\mathbf{y})]$. Lets consider the optimal solution with $t'^*_k = \theta_m(\mathbf{y})$. It follows directly that the optimal solution satisfies (13). Then, for any $k = 1,\ldots,m$

$$d'^*_{ik} = \begin{cases} \min(y_i - \theta_m(\mathbf{y}), 0) = 0 & \text{for } \ i \in I^0_k, \\ \min(y_i - \theta_m(\mathbf{y}), M) = y_i - \theta_m(\mathbf{y}) \geq 0 & \text{for } \ i \in I^1_k, \end{cases}$$

and the optimal solution satisfies (12).
Inequality (14) is defined only if $|K^-| \geq 2$. Due to formula (9) of the objective function, we know that for any k, indices $i \in I^1_k$ will correspond to k largest components of outcome vector $\mathbf{y}$. So, if y_i is one of the k largest outcomes, then $z^*_{ik} = 1$. If we consider formulation (6) for the same $\mathbf{y}$ and any $k' > k$, it follows that y_i is also one of the k' largest outcomes, and thus $z^*_{ik'} = 1$. The reverse implication is analogous. If y_i is not one of the k' largest outcomes, then it is not one of the $k < k'$ largest outcomes, and thus when $z^*_{ik'} = 0$, it follows that $z^*_{ik} = 0$. So, for the same $\mathbf{y}$ and any $k,k' = 1,\ldots,m$ ($k' > k$), the optimal solutions of (6) satisfies inequality $z^*_{ik} \leq z^*_{ik'}$ for any $i = 1,\ldots,m$. Thus, the optimal solution of (11) with $t'^*_k = \theta_m(\mathbf{y}^*)$ satisfies (14) for all $k \in K^-$.
We can conclude that there exists the optimal solution of (11) that satisfies constraints (i)–(iii). ■

Formulation (6) can be further modified by reducing the number of variables and simplifying some constraints.

Proposition 4: For any given vector $\mathbf{y} \geq 0$, the sum of its k largest components $\bar{\theta}_k(\mathbf{y})$ can be found as the optimal value of the following MILP problem:

$$\bar{\theta}_k(\mathbf{y}) = \max_{\rho_k, y'_{ik}, z_{ik}} \quad \rho_k, \tag{15a}$$

$$\text{s.t.} \quad \rho_k \leq \sum_{i=1}^{m} y'_{ik}, \tag{15b}$$

$$y'_{ik} \leq y_i \qquad \forall i, \tag{15c}$$

$$y'_{ik} \leq M z_{ik} \qquad \forall i, \tag{15d}$$

$$\sum_{i=1}^{m} z_{ik} = k, \tag{15e}$$

$$z_{ik} \in \{0,1\} \qquad \forall i. \tag{15f}$$

Proof: We will show that the optimal value of problem (15) is the same as that of problem (6).
By Lemma 2, we know that for any value $\zeta \leq \theta_m(\mathbf{y})$ there exists the optimal solution of problem (6) with $t'^*_k = \zeta$. As $\mathbf{y} \geq 0$, we may set t'_k equal to any value from interval $[0, \theta_m(\mathbf{y})]$, and the optimal value of problem (6) still equals the sum of the k largest components of outcome vector $\mathbf{y}$. Let $t'_k = 0$ in problem (6), then we get problem (15), where variables d'_{ik} are replaced by y'_{ik}. This change in notation follows the change in variables interpretation. Variables d'_{ik} stand for deviations of k largest outcomes from reference value. When we set the reference value to 0, these variables represent in fact the k largest outcomes.
In conclusion, the optimal value of problem (15), similarly like that of problem (6), is equal to the sum of the k largest components of outcome vector $\mathbf{y}$. ■

Analyzing problem (15), we can see now that consraints (15c) and (15d) form a linearization of formula

$$y'_{ik} \leq y_i z_{ik} \qquad \forall i.$$

We can use problem (15), similarly like problem (6), to determine the sum of the k largest components of outcome vector $\mathbf{y}$ for k for which $w'_k < 0$. The general model for the OWA optimization is as follows:

$$\min_{\substack{\rho_k, t_k, d_{ik}, \\ y'_{ik}, z_{ik}, y_i}} \quad \sum_{k=1}^{m} w'_k \rho_k, \tag{16a}$$

$$\text{p.o.} \quad k t_k + \sum_{i=1}^{m} d_{ik} \leq \rho_k \qquad \forall k; w'_k \geq 0, \tag{16b}$$

$$t_k + d_{ik} \geq y_i, \ d_{ik} \geq 0 \qquad \forall i,k; w'_k \geq 0, \tag{16c}$$

$$\rho_k \leq \sum_{i=1}^{m} y'_{ik} \qquad \forall k; w'_k < 0, \tag{16d}$$

$$y'_{ik} \leq y_i \qquad \forall i,k; w'_k < 0, \tag{16e}$$

$$y'_{ik} \leq M z_{ik} \qquad \forall i,k; w'_k < 0, \tag{16f}$$

$$\sum_{i=1}^{m} z_{ik} = k \qquad \forall k; w'_k < 0, \tag{16g}$$

$$z_{ik} \in \{0,1\} \qquad \forall i,k; w'_k < 0, \tag{16h}$$

$$\mathbf{y} = \mathbf{f}(\mathbf{x}), \ \mathbf{x} \in Q. \tag{16i}$$

Problem (16) is another version of hybrid model and in comparison to (11) has slightly fewer continuous variables (by the number of negative weights w'_k). The structure of

Table 1
Problem types defined by the vector of preference weights **w** with respect to the number of clients m and the number of facilities n ($\lceil a \rceil$, $\lfloor a \rfloor$ denote the ceil and floor of a, respectively)

Type	Name/description	Weighting vector **w**
T1	k_1+k_2-trimmed mean	$(\underbrace{0,\ldots,0}_{k_1},1,\ldots,1,\underbrace{0,\ldots,0}_{k_2})$ $k_1=\lceil \frac{m}{10} \rceil$, $k_2=\lceil n+\frac{m}{10} \rceil$
T2	Alternating 0's and 1's, beginning with 1	$(1,0,1,0,1,0,\ldots)$
T3	Alternating 0's and 1's, beginning with 0	$(0,1,0,1,0,1,\ldots)$
T4	Repeating the sequence $(1,1,0)$	$(1,1,0,1,1,0,\ldots)$
T5	Repeating the sequence $(1,0,0)$	$(1,0,0,1,0,0,\ldots)$
T6	From 1 increasing by 1	$(1,2,\ldots,m-1,m)$
T7	Ending with $3m$ and decreasing towards beginning in a piecewise linear manner, k weights by 3, next k weights by 2 and rest by 1	$(\ldots,3m-5k-2,3m-5k-1,$ $\underbrace{3(m-k)-2k,\ldots,3(m-k)-2}_{k},$ $\underbrace{3(m-k),\ldots,3(m-1)}_{k},3m)$ $k=\lfloor \frac{m}{3} \rfloor$

constraints (16d) and (16e) is simpler than that of (11d) and (11e), respectively.
For problem (16), we also consider an impact of valid inequality (14). The proof that it is a valid inequality for (16) is analogous to that in Proposition 3.

4. Computational Tests

To investigate the computational performance of the proposed formulations, we have applied them to various location problems and compared their results. We have used CPLEX solver to solve problems. The experimental scheme has been analogous to that presented in [16]. We have considered some parameters of location problems and have defined the set of their possible values. Then we have generated various testing instances as the combinations of parameters' values. We have taken into account the following parameters: the number of sites (clients), the number of facilities to be placed, and the type of problem defined by the vector of preference weights.
The number of sites (clients) m determines the size of the problem. Six different values are considered $m \in \{8,10,12,15,20,25\}$. The second parameter, the number of facilities n, is defined as proportional to the problem size, and the following cases are examined: $\lceil \frac{m}{4} \rceil$, $\lceil \frac{m}{3} \rceil$, $\lceil \frac{m}{2} \rceil$ and $\lceil \frac{m}{2}+1 \rceil$, where $\lceil a \rceil$ is the smallest integer value not smaller than a. The last parameter is the vector of preference weights **w**, which defines the problem type (the objective function) and determines the structure, and thus the complexity of the problem. We consider seven problem types with non-monotonic or increasing weights, which are defined in Table 1. In case of non-increasing weights, our hybrid models simplify to LP formulation (4), which performs much better than MILP models and was studied for location problems in [14]. The trimmed mean problem (T1) discard some of the largest and smallest outcomes and is considered as a robust objective. Problem types T2–T5 are artificial and are mainly used to check the computational efficiency for very irregular preference weights. The last two problem types, T6 and T7, represent increasing weights and can be treated as extended version of difficult min-min problems.
We have generated 15 cost matrices, for each size case, with zero on the main diagonal (Free Self-Service, FSS) and remaining entries randomly generated from a discrete uniform distribution on the interval $[1,100]$. These matrices have been combined with each combination of parameters with the corresponding problem size. Thus, we have received 15 problem instances differing in cost matrices for each combination of the number of sites, the number of facilities and the problem type. To solve them, we have applied the CPLEX 12.4 from IBM ILOG CPLEX Optimization Studio [17]. Computation have been carried out on a machine with the Intel Core2 Duo 2.53 GHz (mobile) and 4 GB of RAM. A time limit of 600 s has been imposed on maximum solution time for a single problem instance.
We have investigated the following formulations:

- $MH1_1$ – basic problem (11),
- $MH1_2$ – problem (11) with inequality (12),
- $MH1_3$ – problem (11) with inequality (13),
- $MH1_4$ – problem (11) with inequality (14),
- $MH1_5$ – problem (11) with inequalities (13), (14),
- $MH2_1$ – basic problem (16),
- $MH2_2$ – problem (16) with inequality (14).

Table 2
Average solution times of hybrid models and one of the most efficient general previous MILP model M1
(upper index depicts the number of instances out of 15 that reached the limit of 600 s;
"–" means that all 15 instances reached the time limit)

Problem			CPU[s]							
Type	m	n	M1	$MH1_1$	$MH1_2$	$MH1_3$	$MH1_4$	$MH1_5$	$MH2_1$	$MH2_2$
T1	8	2	0.35	0.05	0.05	0.06	0.05	0.06	0.08	0.08
		3	0.29	0.05	0.05	0.07	0.05	0.07	0.07	0.06
		4	0.15	0.05	0.05	0.06	0.05	0.06	0.06	0.06
		5	0.06	0.05	0.04	0.05	0.05	0.05	0.05	0.05
	10	3	1.85	0.08	0.09	0.15	0.09	0.15	0.15	0.15
		4	1.33	0.09	0.09	0.14	0.09	0.14	0.13	0.13
		5	0.67	0.11	0.11	0.11	0.11	0.12	0.11	0.11
		6	0.28	0.10	0.10	0.10	0.10	0.10	0.09	0.10
T2	8	2	0.09	52.48	51.39	10.22	3.97	2.69	10.98	2.62
		3	0.07	53.16	54.28	7.02	3.63	2.39	7.58	2.10
		4	0.04	50.14	53.76	5.06	3.61	1.48	5.74	1.38
		5	0.04	52.74	52.91	4.68	4.26	1.23	4.91	1.20
	10	3	0.32	–	–	–	167.56	103.15	–	108.89
		4	0.15	–	–	–	160.29	83.34	–	96.73
		5	0.12	–	–	–	157.81	72.70	–	82.83
		6	0.06	–	–	–	152.06	56.88	–	58.92
T3	8	2	0.28	148.20	151.27	18.73	6.36	2.53	19.88	2.73
		3	0.20	177.86	189.57	14.01	6.42	2.02	14.05	1.88
		4	0.14	170.15	199.93	11.29	6.65	2.25	11.41	2.17
		5	0.06	163.80	159.00	8.66	6.44	1.32	7.13	1.30
	10	3	0.94	–	–	–	294.08	91.91	–	96.32
		4	0.84	–	–	–	321.08	84.96	–	90.87
		5	0.51	–	–	–	313.26	72.61	–	74.96
		6	0.39	–	–	–	297.26	68.36	–	70.64
T4	8	2	0.10	1.41	1.72	0.21	0.68	0.19	0.19	0.18
		3	0.09	2.06	2.29	0.19	0.63	0.19	0.17	0.17
		4	0.05	1.71	1.81	0.13	0.53	0.13	0.13	0.12
		5	0.03	1.50	1.49	0.11	0.53	0.11	0.11	0.11
	10	3	0.24	^{1}346.19	^{2}393.42	12.78	22.12	6.25	10.21	6.11
		4	0.18	^{1}327.38	^{1}364.44	6.66	20.24	4.35	6.34	4.61
		5	0.13	310.17	260.00	5.54	23.00	3.08	4.32	3.49
		6	0.07	207.92	226.05	2.03	19.51	1.53	1.93	1.63
T5	8	2	0.10	2.57	2.85	0.83	0.80	0.65	0.76	0.62
		3	0.08	2.33	2.30	0.93	0.69	0.58	0.89	0.59
		4	0.06	2.17	2.40	0.64	0.63	0.49	0.62	0.45
		5	0.03	1.90	1.99	0.33	0.54	0.33	0.38	0.32
	10	3	0.28	^{3}416.97	^{2}416.28	45.31	25.34	11.81	43.93	12.12
		4	0.15	^{1}287.87	311.06	36.27	24.31	9.77	31.67	9.37
		5	0.12	291.73	289.73	34.71	25.30	9.44	30.62	9.10
		6	0.09	293.54	310.41	26.53	24.76	8.06	27.82	7.68
T6	8	2	0.30	–	–	0.28	8.88	0.22	0.26	0.21
		3	0.22	–	–	0.18	14.44	0.15	0.16	0.14
		4	0.11	–	–	0.11	19.69	0.09	0.09	0.09
		5	0.04	–	–	0.06	24.00	0.05	0.05	0.04
	10	3	1.81	–	–	2.68	^{4}490.57	0.68	3.36	0.66
		4	0.79	–	–	0.65	^{14}593.68	0.40	0.54	0.35
		5	0.46	–	–	0.30	–	0.21	0.26	0.19
		6	0.16	–	–	0.15	–	0.13	0.13	0.11
T7	8	2	0.12	^{12}536.72	^{11}528.55	0.13	3.47	0.11	0.12	0.10
		3	0.08	–	–	0.09	7.50	0.07	0.06	0.08
		4	0.04	–	–	0.05	11.19	0.05	0.05	0.05
		5	0.03	–	–	0.03	15.50	0.03	0.03	0.03
	10	3	0.42	–	–	0.38	195.78	0.32	0.52	0.27
		4	0.19	–	–	0.18	^{1}361.19	0.17	0.16	0.14
		5	0.10	–	–	0.09	^{7}518.86	0.09	0.09	0.09
		6	0.05	–	–	0.07	^{14}589.66	0.06	0.06	0.06

Table 3
Average solution times of the most efficient hybrid and previous MILP models for selected problem types (upper index depicts the number of instances out of 15 that reached the limit of 600 s; "–" when all 15 instances reached the time limit)

Problem			CPU[s]	
Type	m	n	M1	$MH2_2$
T1	12	3	11.80	0.64
		4	7.86	0.39
		6	2.11	0.37
		7	1.33	0.33
	15	4	162.75	0.90
		5	94.90	0.81
		8	11.70	0.77
		9	5.56	0.73
	20	5	–	2.47
		7	–	2.31
		10	^{12}551.73	3.03
		11	^{4}305.99	2.93
	25	7	–	24.37
		9	–	32.14
		13	–	43.77
		14	–	44.54
T6	12	3	11.79	3.64
		4	10.95	1.61
		6	1.77	0.46
		7	0.54	0.20
	15	4	156.83	37.00
		5	101.02	7.54
		8	11.19	0.91
		9	3.05	0.54
	20	5	–	^{13}574.93
		7	–	^{5}297.77
		10	–	10.45
		11	^{7}476.59	5.67
	25	7	–	^{14}595.39
		9	–	^{12}532.15
		13	–	64.75
		14	–	37.10
T7	12	3	1.47	1.29
		4	0.71	0.46
		6	0.20	0.16
		7	0.10	0.12
	15	4	5.59	6.18
		5	2.61	1.85
		8	0.27	0.53
		9	0.15	0.35
	20	5	100.52	^{8}356.07
		7	29.00	^{1}73.42
		10	4.97	4.08
		11	1.71	3.12
	25	7	^{8}480.75	^{11}480.85
		9	^{3}252.69	^{4}277.26
		13	24.44	14.56
		14	12.89	8.78

4.1. Results

Table 2 presents solution times for instances with 8 and 10 locations. Solution times for model MH1 vary widely between different types of problem and inclusion of some valid inequalities. In general, valid inequalities allow to improve the performance and reduce the solution time. An exception is inequality (12), which hardly influence the computational performance. Inequalities (13) and (14) in most cases shorten the solution time of one or two orders of magnitude. The best results are obtained for trimmed mean problems (T1), and it is consistent with our expectation. In this case, valid inequalities do not influence the solution time significantly. In fact, inequality (14) is not defined for T1 problems as there is only one negative weight w'_k. The valid inequalities significantly improve results for problems T2–T5. However, the solution times for these problems are much longer than for other types. Interesting situation is for problems T6 and T7, which in theory are the most difficult as there are the maximum number of negative weights w'_k. Basic model $MH1_1$, indeed, performs very poorly. However, formulations with valid inequality (14) and especially with (13) achieve much shorter solution times, even of three orders of magnitude.

Analyzing model MH2, we see that its basic formulation $MH2_1$ performs much better than basic formulation $MH1_1$ of model MH1. In fact, basic formulation $MH2_1$ performs similar to formulation $MH1_3$, and formulation $MH2_2$ achieves similar solution times to formulation $MH1_5$. Generally, formulations $MH1_5$ and $MH2_2$ seem to be the best ones from examined hybrid models.

We have also compared the hybrid models with one of the most efficient MILP model for the OWA optimization from literature (see model $M1_3$ from [14]). Table 2 shows clearly that the hybrid models perform much worse for problem types T2–T5. On the other hand, for problem types T6 and T7 they obtain similar or shorter solution times. For trimmed mean problem (T1) the results show the advantage of hybrid models even more (formulation $MH2_2$). To investigate it a little more, Table 3 presents the results for problems T1, T6 and T7 with 12–25 locations. It reveals that hybrid model has much better performance for trimmed mean problems, presents the substantial advantage for T6 problems and has similar efficiency for T7 problems. So the hybrid models are specially useful for trimmed mean problems, which seems to be one of the most important for practical application from all non-monotonic problem types, to which linear model can not be applied.

5. Conclusions

The paper analyzes the OWA optimization models for discrete location problems. The OWA operator provides a parametrized preference model that generalizes many objective functions and allows to obtain impartial solution, what is important when we consider independent clients. Unfortunately, the ordering operator hinders the problem

increasing its computational complexity. Therefore, the efficient formulations for OWA optimization are sought. We introduce general MILP models that can be applied for any non-negative preference weights. It extends the LP formulation, adding the mixed integer part. We also propose some simple valid inequalities to improve the computational performance. The results show the advantage of proposed new hybrid formulations over other general MILP models from literature for some specific problem types. The greatest improvement is obtained for trimmed mean problems. This is particularly important as trimmed mean problems seems to be one of the most useful in practical applications from all other problem types with non-monotonic preference weights, which can not be solved by LP model. On the other hand, hybrid models perform very poorly for problem types T2–T5. However, these types represent rather artificial objective functions (preferences) with little practical value. The proposed models perform surprisingly well for problems with increasing weights, which require the largest number of binary variables. For example, considering problems T6, the hybrid models obtain much shorter solution times than previous general formulations.

The presented new models shorten solution times for some specific problems, but there is still room for improvement. As mentioned before, presented formulations are general and can be applied to various multicriteria problems (for MH2 and inequality (13) we only require the non-negativity of the outcomes). Some modifications and valid inequalities that exploit specific problem structure (such as free self-service assumption) may increase the computational efficiency.

As the location problem with OWA objective is an *NP*-hard problem, heuristic methods seems a reasonable approach. Despite this fact, the literature on approximation algorithms for these problems is rather limited. Thus, it is also the area where we are currently carrying out some research.

Acknowledgements

The author is grateful to Prof. Włodzimierz Ogryczak from the Institute of Control and Computation Engineering at the Warsaw University of Technology for the comments and suggestions at the early stage of research presented in this paper.

Research conducted by P. Olender was partially supported by the National Institute of Telecommunications under the grant 06.30.001.6.

References

[1] R. R. Yager, "On ordered weighted averaging aggregation operators in multicriteria decisionmaking", *IEEE Trans. on Systems, Man, and Cybernet.*, vol. 18, no. 1, pp. 183–190, 1988.

[2] R. R. Yager, J. Kacprzyk, and G. Beliakov, Eds., *Recent Developments in the Ordered Weighted Averaging Operators: Theory and Practice*, vol. 265 of *Studies in Fuzziness and Soft Computing.* Springer, 2011.

[3] W. Ogryczak, T. Śliwiński, and A. Wierzbicki, "Fair resource allocation schemes and network dimensioning problems", *J. Telecommun.& Inform. Technol.*, no. 3, pp. 34–42, 2003.

[4] M. Köppen, K. Yoshida, M. Tsuru, and Y. Oie, "Annealing heuristic for fair wireless channel allocation by exponential ordered-ordered weighted averaging operator maximization", in *Proc. 11th Ann. Int. Symp. on Applications and the Internet SAINT 2011*, Munich, Germany, 2011, pp. 538–543.

[5] R. R. Yager, "Constrained OWA aggregation", *Fuzzy Sets and Syst.*, vol. 81, no. 1, pp. 89–101, 1996.

[6] W. Ogryczak and T. Śliwiński, "On solving linear programs with the ordered weighted averaging objective", *Eur. J. of Operat. Res.*, vol. 148, no. 1, pp. 80–91, 2003.

[7] W. Ogryczak and A. Tamir, "Minimizing the sum of the k largest functions in linear time", *Inform. Process. Lett.*, vol. 85, no. 3, pp. 117–122, 2003.

[8] W. Ogryczak, "On the distribution approach to location problems", *Comp. & Indust. Engin.*, vol. 37, no. 3, pp. 595–612, 1999.

[9] S. Nickel and J. Puerto, *Location Theory: A Unified Approach.* Berlin: Springer, 2005.

[10] N. Boland, P. Domínguez-Marín, S. Nickel, and J. Puerto, "Exact procedures for solving the discrete ordered median problem", *Comp. & Operat. Res.*, vol. 33, no. 11, pp. 3270–3300, 2006.

[11] A. Marín, S. Nickel, J. Puerto, and S. Velten, "A flexible model and efficient solution strategies for discrete location problems", *Discr. Appl. Mathem.*, vol. 157, no. 5, pp. 1128–1145, 2009.

[12] A. Marín, S. Nickel, and S. Velten, "An extended covering model for flexible discrete and equity location problems", *Mathem. Methods of Operat. Res.*, vol. 71, no. 1, pp. 125–163, 2010.

[13] W. Ogryczak and P. Olender, "Ordered median problem with demand distribution weights", *Optimization Lett.*, vol. 10, no. 5, pp. 1071–1086, 2016.

[14] W. Ogryczak and P. Olender, "On MILP models for the OWA optimization", *J. Telecommun. & Inform. Technol.*, no. 2, pp. 5–12, 2012.

[15] P. B. Mirchandani and R. L. Francis, *Discrete Location Theory*. New York: Wiley, 1990.

[16] P. Domínguez-Marín, *The Discrete Ordered Median Problem: Models and Solution Methods*. Springer, 2003.

[17] IBM, *IBM ILOG CPLEX Optimization Studio* [Online]. Available: http://www-03.ibm.com/software/products/en/ibmilogcpleoptistud/

Paweł Olender is an Assistant Professor in the National Institute of Telecommunications in Warsaw. He received his M.Sc. and Ph.D. in Computer Science from the Warsaw University of Technology, Poland, in 2008 and 2015, respectively. He has participated in projects related to data warehousing and analysis for a telecommunication operator. His research interests are focused on modeling, decision support, optimization, machine learning and data mining.

e-mail: P.Olender@itl.waw.pl
National Institute of Telecommunications
Szachowa st 1
04-894 Warsaw, Poland

Paper

EVA as a Tool for Estimation of Management Efficiency and Value Creation in Polish Telecom Sector

Wojciech Kamieniecki

Research and Academic Computer Network (NASK), Warsaw, Poland

Abstract—The paper presents results of empirical study on creation of added value in Polish telecom sector, based on Economic Value Added (EVA) indicator. First, an EVA analysis was performed for publicly traded telecom companies. Next, the effectiveness of EVA itself in management of telecom companies was evaluated. A statistical analysis was made to investigate dependence between EVA and other indicators of company value, confirming that EVA sign and magnitude are in agreement with indicators based on data from financial books. Finally, the effectiveness of using EVA for prediction of market capitalization of telecom companies was investigated. Overall results do not give a clear picture and cannot allow to state that EVA is a better determinant of value of telecom company than financial indicators like Earnings Per Share (EPS).

Keywords—Economic Value Added, empirical study, statistical analysis, telecom sector.

1. Introduction

The purpose of this analysis was to evaluate the creation of added value and usefulness of the Economic Value Added (EVA) indicator in Polish telecom companies in the 2007–2015 period.

EVA is an indicator of company efficiency developed in the 1980s by J. Stern i G. Bennett Stewart III at Stern Stewart & Co [1]. The economic value added is a measure of company efficiency showing the income after deduction of full costs of capital. EVA is a tool used for corporate financial management. The economic value added is understood as a true profit generated by given company after taking into account all costs, including interest, taxes and fees for capital invested by the owners [2]. According to some economists, EVA is the best available indicator of company efficiency in a one-year timeframe, and EVA-based financial management systems allow to make decisions bringing gains for the owners and generating economic profits for the company [3]. At the same time, multiple empirical studies do not confirm such positive evaluation of this indicator.

This analysis is focused on evaluation of efficiency of using the EVA indicator in Polish telecom sector. In the first phase, EVA was used to evaluate the creation of added value by Polish telecom enterprises between 2007 and 2015. Next, EVA values were compared to other efficiency indicators of telecom companies. Finally, the dependence between EVA and market capitalization of each company listed at the Warsaw Stock Exchange was analyzed in attempt to estimate to what extent the economic value added can be a basis for predicting the future value of telecom company.

2. Evolution of EVA of Polish Telecom Companies

The study was carried out by means of financial and statistical analysis of publicly available data, included in financial reports and annual reports published by telecom companies active in Poland. The sample for analysis comprised of eight telecom companies listed on the Warsaw Stock Exchange: Orange, Netia, MNI, Hyperion, Easy Call, Mediatel, Telestrada, and Open-NET (reports available only for the 2010–2015 period). The study covered a group of listed companies belonging to different sections of telecom market – representing different scale of business, resources, and experience, providing different services and operating in accordance with different business models.

The EVA indicator was calculated according to a standard formula [4]:

$$\mathrm{EVA} = \mathrm{NOPAT} - \mathrm{IC} \cdot \mathrm{WACC}, \tag{1}$$

where: NOPAT denotes the net operating profit after tax, IC the invested capital and WACC the weighted average cost of capital. They are explained in details in the following subsections.

2.1. Net Operating Profit After Tax

The basis for calculation of the EVA indicator in Eq. (1) for a given year is the net operating profit after tax (NOPAT). $\mathrm{NOPAT} = \mathrm{EBIT} \cdot (1-T)$, in turn, is calculated as an operating profit reduced by a standard tax rate ($T = 19\%$ in Poland); in case of an operating loss the tax equals $T = 0$[1]. The net operating profit after tax shall, in accordance with EVA assumptions, reflects the true value generated by company operations. Therefore, the value included in financial reports in accordance with Polish accounting law – the operating profit (or loss) was subject to several corrections,

[1] According to annual reports of companies studied for the 2007–2015 period.

Table 1

Corrections to operating profit during calculation of EVA and their effects

Correction	Description	Evaluation of scale and effect on NOPAT
Proceedings from sale of durable assets during a given year	Profit generated by sale of durable assets reduced the value of net operating profit used in EVA calculation, while a loss increased this value. Sale of assets is excluded from calculation of NOPAT due to being a one-time event and termination of company activity in a given field.	A half (four) of telecom companies analyzed in this study sold some assets during this period. Two of them – Mediatel and Hyperion made large transactions that had a substantial influence on operating profit.
Subsidies and grants	Proceedings from subsidies and grants were excluded from the result as they are not a result of company operations.	Despite use of grants by some of analyzed companies, a substantial effect on operating profit was recorded only by EasyCall in 2014 and 2015.
Write-offs updating the value of assets	Operating profit was corrected of value of write-offs updating the value of company assets.	Write-offs updating the value of assets were made during the 2007–2015 period by all subjects analyzed. Material influence on operating profit occurred in smaller companies: Mediatel, Hyperion, Open-NET, EasyCall, and Telestrada. In most cases, exclusion of updating write-offs improved the operating profit.
Effects of extraordinary events	The effects of extraordinary events in a given year (e.g. compensation received and paid, settlements with trading partners, cancelations of receivables and payments) were removed from the operating profit.	Extraordinary events were recorded in large and medium companies, usually as result of court settlements between companies (Orange, Netia, Mediatel) and cancelations of receivables and payments (Orange, Mediatel, Hyperion). Influence of extraordinary events on operating profit is particularly visible in case of Mediatel and Netia (one-time effect at Netia in 2014 was as much as 141 million PLN due to settlements with Orange).
Interest included in the operating profit	In calculations here, also the interest received and paid as results of loans made to dependent companies or received form them, and included in the operating profit was removed. The interest, being a result of financial operations, does not belong to operating profit as defined in analysis of EVA.	Interest on loans made to dependent companies were present only in case of Netia. The correction had no meaningful effect of operating profit.
Variations in currency exchange rates	Effects of variations in currency exchange rates included in the operating profit were excluded from EVA calculations, similarly as interest.	Variations in currency exchange rates were included in operating profit reported by Orange, Netia and Mediatel. The influence of related corrections on operating profit of companies studied was small.
Excessive deprecation	The methodology of EVA calculation assumes standard deprecation rates. Excessive (above standard) values were excluded form results for a given period.	This correction applies only to Mediatel for the 2008–2010 period. Due to additional deprecation in this period, the correction had positive influence on operating profit of this company.
Costs of research and development activities	Costs related to R&D activities in a given year were excluded from calculation of operating profit. In accordance with methodology of EVA calculation, R&D costs were removed from result for a given year and added, in a capitalized form, to value of capital invested, increasing own capital of given company.	R&D cost were include only in financial reports and annual reports of Orange, and suitable corrections were made for this company only.

as defined in the methodology of calculating the Economic Value Added [5], [6]. Calculations made for the purposes of this study included corrections for the following:

- proceedings from sale of durable assets during a given year,
- subsidies and grants,
- write-offs updating the value of assets,
- extraordinary events,
- interest included in the operating profit,
- variations in currency exchange rates,
- excessive deprecation,
- research and development costs [7].

Detailed list of corrections made in the course of analysis, together with evaluation of their scale and influence on results of the study is presented in Table 1.
Corrections made allowed to correctly estimate the operating profits of telecom companies being a subject of this study. It needs to be noted, that influence of these corrections on final values of EVA was relatively small.
Values of NOPAT calculated this way were subsequently re-calculated into theoretical net values by subtraction of 19% tax on operating profit. In case of operating loss, no taxes were calculated.

2.2. Invested Capital

The invested capital (IC) in Eq. (1) reflects funds engaged in company operations in order to generate the net operating profit after tax – NOPAT [8]. The invested capital is a sum of company own capital, in accordance to balance sheet and debt incurring interest (without taking into account reserves and commercial or formal/legal obligations)[2]. For the purpose of this analysis, the value of invested capital was estimated as balance sheet value of company own[3] and balance sheet value of debts incurring financial costs (credits, loans, obligations, leasing).

2.3. Weighted Average Cost of Capital

In general, the weighted average cost of capital (WACC) is a sum of costs of n sources of a company financing weighted by a share of each source in the total financing [9].

$$\mathrm{WACC} = \sum_{i=1}^{n} s_i C_i \,, \tag{2}$$

where s_i and C_i denote respectively, the share and cost of the i-th capital, n the number of sources of the company financing.

[2]Values used during analysis were taken from annual reports and financial reports of companies studied for the 2007–2015 period.

[3]For Orange, the value of capitalized R&D costs was included in company own capital.

For the purpose of the presented analysis, the weighted average cost of capital was calculated in accordance with the following formula:

$$\mathrm{WACC} = \frac{E}{V} C_E + \frac{D}{V} C_C \cdot (1 - T) \,, \tag{3}$$

$$V = D + E \,,$$

where E denotes the cost of the own capital (equity), D the cost of the external capital (debt), C_E the cost of equity, C_D the cost of debt and T the corporate tax rate.

In the presented paper the cost of debt D was calculated from real interest rates paid by companies in a given year, related to an average amount of debt at the end of a given year and preceding one. This approach is simplified, but accurate enough to well reflect costs of financing company with debt.
The cost of the equity E was calculated according to Capital Assets Pricing Model (CAPM), the Bond Yeld Plus version [9]:

$$E = Rf + Mp \cdot B \,, \tag{4}$$

where Rf denotes the risk free interest rate equal to yield of government obligations, Mp – the market premium and B – the beta factor.

In this paper the risk free interest rate Rf was calculated based on the data published by "market-risk-premia" portal

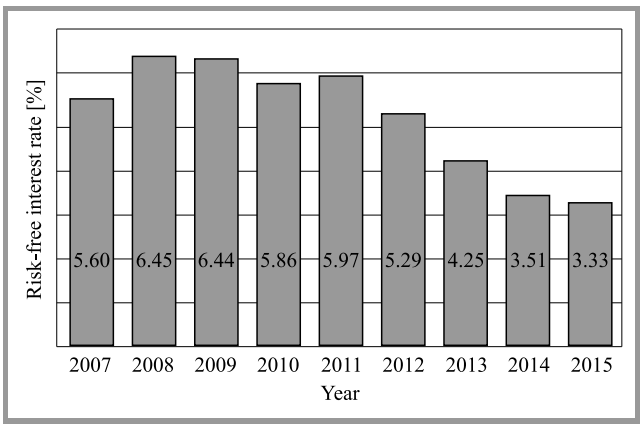

Fig. 1. Risk-free interest rate included in the analysis.

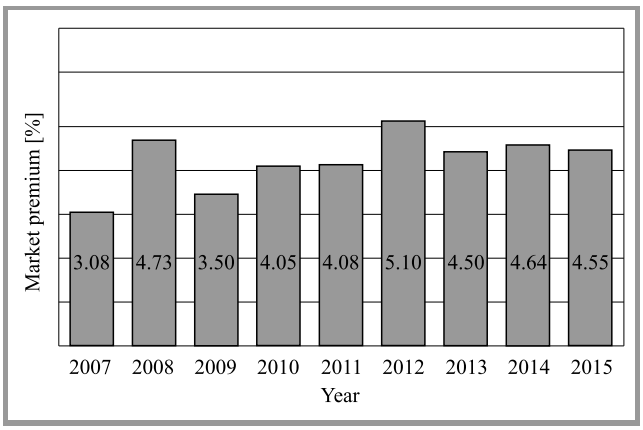

Fig. 2. Market premium used for EVA calculations.

Table 2
Values of beta factor used in this study

Company	Reuters	Stockwatch	Infinancials	Barron's	Average
Orange	0.75	–	0.78	0.59	0.707
Netia	–	0.62	0.32	0.57	0.503
Mediatel	1.55	–	–	0.51	1.030
MNI	0.89	0.51	0.61	0.61	0.655
Hyperion	–	0.15	0.25	0.15	0.183
Open-NET	–	0.44	–	–	0.440
EasyCall	–	0.27	–	–	0.270
Telestrada	–	–	0.20	–	0.200

Table 3
EVA values for individual telecom companies, 2007–2015 (thousands PLN)

Company	2007	2008	2009	2010's	2011	2012	2013	2014	2015
Orange	761,338	428,738	–28,908	–809,716	284,933	–149,498	–545,461	–171,229	–411,149
Netia	–223,946	–269,559	–157,600	47,025	1,603	–230,254	–176,708	–201,264	–133,515
Mediatel	–7,309	–2,432	3,067	–9,229	–745	–585	–6,419	–14,664	–15,732
MNI	–7,779	2,455	5,988	16,592	6,382	–36,180	–25,416	–23,609	–40,368
Hyperion	3,593	3,525	–2,568	–3,715	–6,104	–2,918	5,857	–7,452	–6,720
Open-NET	–	–	–	–253	–795	–979	554	1,663	2,217
EasyCall	5	–37	128	114	–282	136	1,404	301	–3,176
Telestrada	40	–39	922	2,306	2,714	2,980	2,621	959	5,651

for the Polish market in 2007–2015 [10]. Evolution of Rf with time is presented in Fig. 1.

The market premium (Mp) is a standard value reflecting average (for a given market) expectations of investors with respect to return on capital invested in stocks compared to yield generated by investment in risk-free financial instruments. Again, calculations were based on data published by [10]. Evolution of market premium with time is presented in Fig. 2.

The beta factor (B) is a factor reflecting price variability of a given stock compared to market as a whole. Values used in this analysis are average values for each company, taken from publicly available sources[4]. Values of beta factor being considered are listed in Table 2.

EVA values for the period of 9 years were estimated in accordance with rules presented above, using data taken directly from annual reports and financial reports published by eight telecom companies being subject of this study.

3. EVA Values in Telecom Companies

The same procedure of calculating the EVA was applied to all companies for each year from 2007 to 2015 (except for Open-NET, whose data are available only for the 2010–2015 period). Resulting EVA values for each company are shown in Table 3.

According to rules developed by the creators of EVA methodology, the values of this indicator shall be interpreted as follows:

- the company generates value for shareholders in a given years for EVA > 0,
- the company behaves neutrally for EVA = 0,
- the company destroys value for shareholders for EVA < 0.

The EVA for analyzed telecom companies in Poland during the 2007–2015 period were both positive and negative. Negative values, however, were more frequent, meaning that telecom companies listed on Warsaw Stock Exchange more often generated loss (39 out of 69 observations) than profit (30 out of 69 observations) for their shareholders. The direction and rate of EVA change were different for each company.

It is interesting that a clear tendency of fall in average EVA has emerged among large (Orange, Netia) and medium (MNI, Mediatel, Hyperion) companies beginning from 2012, while it was absent among small companies (Telestrada, Open-NET, EasyCall). On particular interest is

[4]Analysis presented was based on values of beta factor published at Reuters, Barrons, Stockwatch and Infinancials websites; average values published for each company were used in calculations.

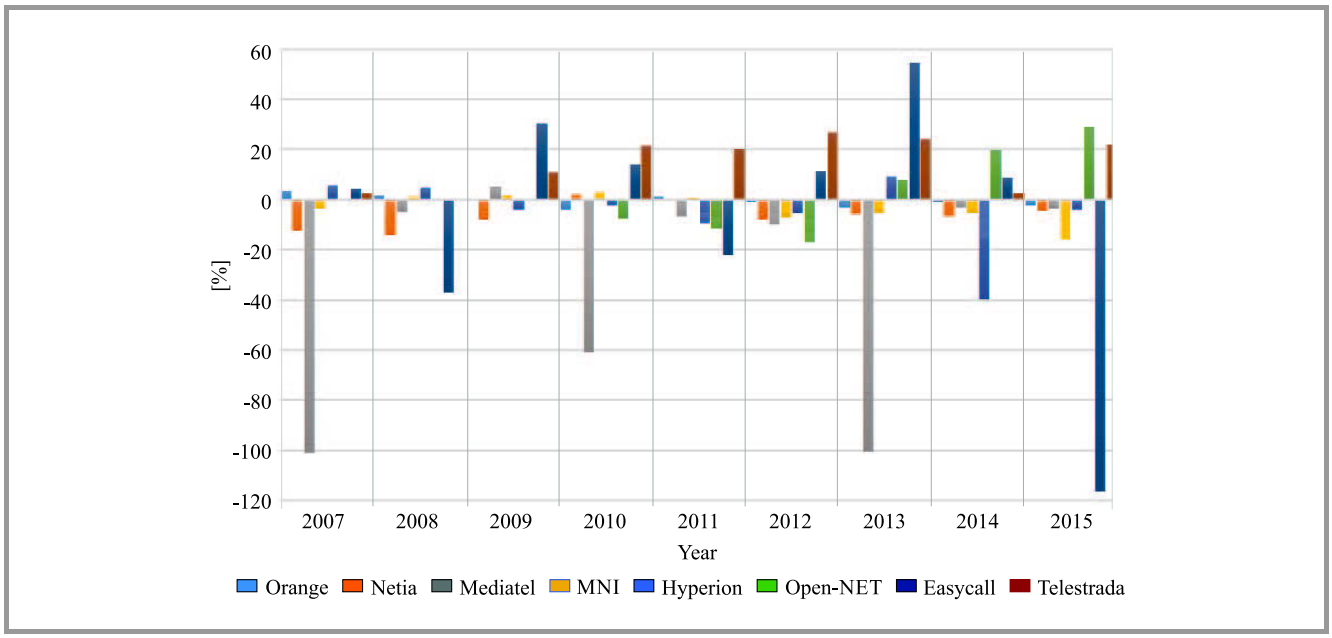

Fig. 3. EVA/IC return rate for individual companies in 2007–2015 period. (See color pictures online at www.nit.eu/publications/journal-jtit)

Telestrada, which had positive EVA during 8 out of 9 years, and its EVA has been rising[5].

At the same time, no relationship between EVA values for individual companies studies was observed – both when it comes to values in particular years, and trends of EVA changes – values recorded were divergent. The lack of relationship is confirmed by average Pearson factor of –0.08. This means conditions specific to telecom sector had little effect on EVA.

Global values of EVA cannot be meaningfully compared due to very different size of companies studied (from hundreds of millions PLN in case of Orange to few thousands PLN in case of EasyCall). Therefore, an EVA return rate with respect to invested capital (EVA/IC) was used instead. Its values are presented in Fig. 3.

The best results (measured as relative values) were achieved by Telestrada. For this company, the average return rate defined as ratio of generated EVA to invested capital over the study period was 14.4%. The only other company with a positive result was Open-NET showing average EVA/IC of 3.5%. All other companies have lost value for shareholders, with negative economic results. The outstanding bad performer was Mediatel with average EVA/IC of –31.7%. Return rates for other companies ranged from –0.5% for Orange to –6.3% for Netia.

Average return rate for the whole group of companies included in this study was –4.7%. This is a relatively low value, suggesting a poor operational efficiency of telecom companies in Poland. Studies conducted in other countries indicate a long-term tendency of EVA/IC to approach 0%, usually exhibiting small negative values [11].

[5]The dependence between size of company and EVA was analyzed in a later part of this study.

4. Comparison between EVA and Other Indicators of Operational Efficiency

This section of analysis was devoted to relations between EVA and other indicators of company efficiency, especially those based on accounting data: income from sales, earnings per share (EPS), return on assets (ROA) and return on equity (ROE).

The analysis included, again, search for correlation between factors investigated.

Analysis of relationship between income from sales and EVA confirmed a positive correlation between those variables. For most of companies studied, the respective correlation factor was between 0.40 and 0.91, proving a fairly strong relationship (Fig. 4). The average correlation factor for the whole group was 0.458, indicating a medium

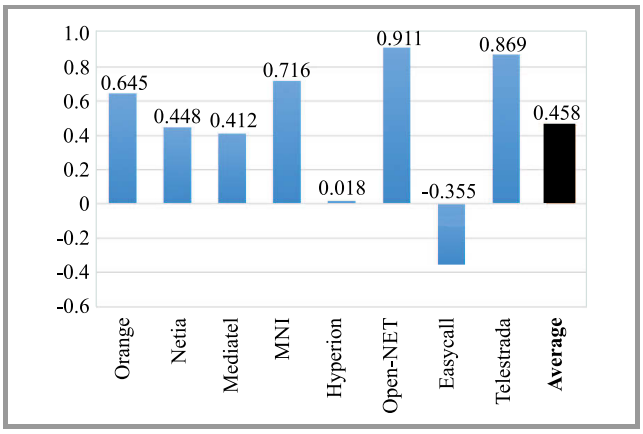

Fig. 4. r-Pearson correlation factor between EVA and income from sales (2007–2015).

level of correlation. This average was significantly lowered by results for EasyCall – correlation factor for this company was –0.355, indicating a weak negative link (rising sales resulting in fall of EVA) and Hyperion, whose correlation factor of 0.018, meaning no dependence between sales and EVA. A rejection of those two extreme sets of data would increase the correlation factor between income from sales and EVA to 0.58, corresponding to a relatively strong relationship.

The next step was to probe correlation between EVA and the most common measure of operating efficiency of publicly traded companies – Earnings Per Share (EPS). Values of respective correlation factors for telecom companies studied ranged from 0.309 for Mediatel to 0.957 for Orange (Fig. 5). Average value for the whole group was 0.659, indicating a strong correlation between earnings per share and EVA.

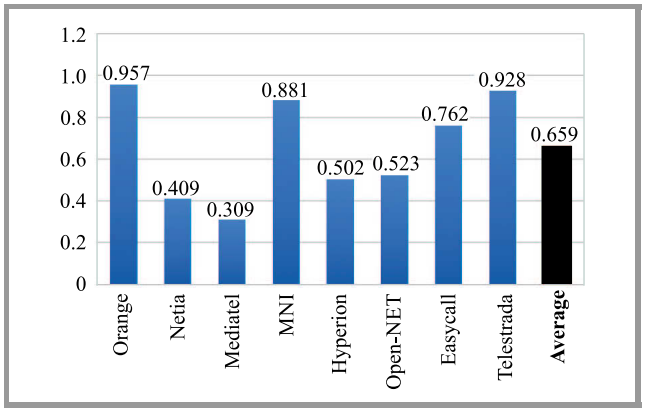

Fig. 5. r-Pearson correlation factor between EVA and earnings per share EPS (2007–2015).

Interestingly, the differences between individual companies were relatively small. Standard deviation of correlation factor was 0.253, with most of values in the 0.4–0.9 range. This confirms strong relationship between EVA and EPS in Polish telecom companies.

Similar analysis done for ROA (return on assets – net profit divided by value of all assets) and ROE (return on equity – net profit divided by book value of company own capital) confirms that values of EVA are in agreement with other indicators of company efficiency. Average value of correlation factor for relationship between EVA, and ROA or ROE is 0.577 in both cases, indicating a medium level of inter-dependence (Fig. 6).

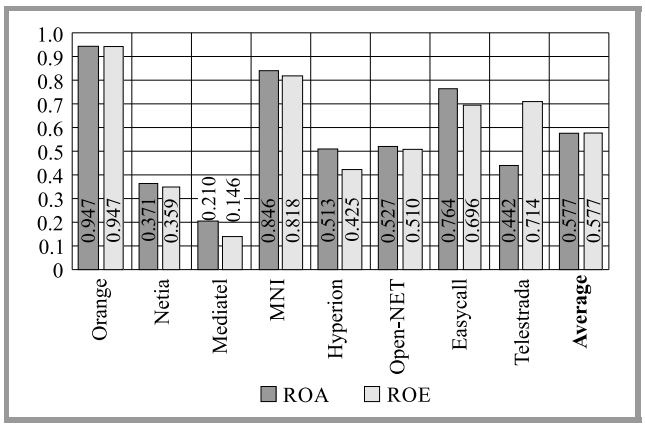

Fig. 6. r-Pearson correlation factor between EVA, and ROA/ROE of telecom companies (2007–2015).

Most of telecom companies studied exhibit a strong ROA – EVA and ROE – EVA dependence. In case of Orange and MNI values of both correlation factors exceed 0.8. Average values for the whole group are driven down by Mediatel and Netia, whose values of correlation factors were markedly lower than for other companies.

The analysis presented above confirms that EVA values are changing in the same direction as indicators of current operational efficiency (profitability) of telecom company – income from sales, earning per share, ROE and ROA.

5. EVA Influence on Company Evaluation

The final stage of analysis was investigation of relationship between EVA and capitalization of telecom companies at the end of each year. Investigation of correlation factor and R^2 (R squared) coefficient of determination was performed to verify the assumption that EVA is a good indicator of company value.

It was assumed that a high degree of correlation between company capitalization and EVA value for a given year means a dependence between EVA and evaluation of company own capital. Company capitalization (market evaluation of company own capital) was established by multiplying its share price on the last day of a given year by number of shares in circulation. Next, the values of EVA and capitalization for each company were compared. Results are inconsistent, ranging from a strong correlation for a number of companies to very weak one for several others. Graphs of EVA – capitalization dependence for two extreme cases: MNI – where capitalization was strongly correlated with EVA, and Hyperion, for which the r-Pearson value was only 0.16, are shown in Figs. 7 and 8.

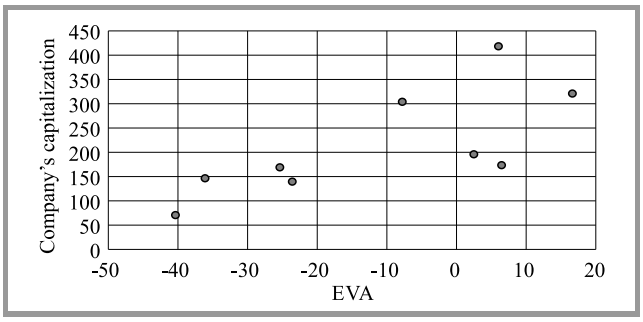

Fig. 7. Dependence between EVA and capitalization at the end of each year (2007–2015) for the MNI company (r-Pearson = 0.73).

The analysis is further complicated by the fact that for two companies – Mediatel and Open-NET the dependence

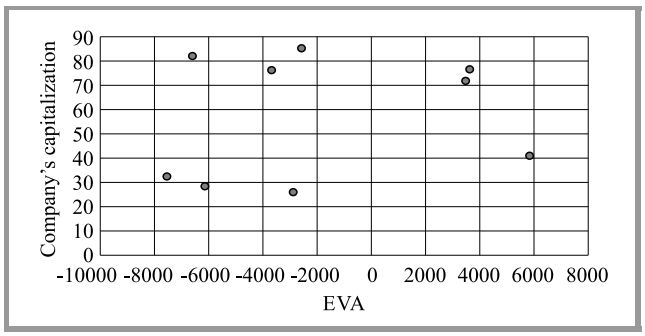

Fig. 8. Dependence between EVA and capitalization at the end of each year (2007–2015) for the Hyperion company (r-Pearson = 0.16).

between EVA and capitalization was a negative one – increase of EVA corresponded to reduced company capitalization.

Average value of correlation factor for the whole group of telecom companies studied was 0.338, indicating a weak dependence and limited impact of EVA on capitalization. Comparison of correlation factors for all companies is shown in Fig. 9.

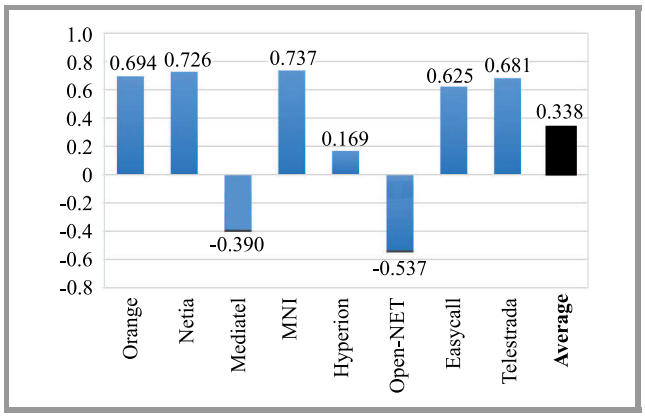

Fig. 9. r-Pearson correlation factor between EVA and company's capitalization at the end of the year (2007–2015).

Because of highly variable results (standard deviation ±0.53) it is impossible to clearly state that EVA is a good indicator of value of telecom company in Poland. However, there are cases when EVA provides much better explanation of changes in company valuation that standard indicators like earnings per share (EPS). Among them are Netia – where the R squared coefficient of determination was 58% for EVA, while the same coefficient for EPS was only 25%, and Telestrada, where the same values were 46% and 17%, respectively. This means using EVA for prediction of value of company own capital is more than twice as effective than EPS.

6. Conclusion

The analysis presented above revealed that analyzed Polish telecom companies more often destroyed than created value for their owners in the 2007–2015 period. Values of EVA for individual telecom companies listed at the Warsaw Stock Exchange were more often negative than positive, and average return rate calculated as ratio of EVA to invested capital was 4.9% during the same period.

EVA values calculated for companies active in the telecom sector exhibited signs and trends of change in agreement with other indicators of company value such as income from sales, EPS, ROA or ROE. Particularly strong correlation was observed in case of return on assets (ROA) and return on equity (ROE). Results for sales and earnings per share (EPS) are not clear due to high variability between different companies analyzed.

Because of similarly high variability, it is not possible to unequivocally evaluate the effectiveness of using EVA as a determinant of market value of telecom companies in Poland. Results obtained in this study cannot prove that EVA is a better indicator of company value than simpler to calculate earnings per share (EPS).

To summarize, while EVA finds use in evaluation of telecom companies, it cannot be regarded a more effective indicator of company value than other commonly used indicators.

References

[1] G. Friedl and L. Deuschinger, "A note on Economic Value Added (EVA)", Technische Universität Muenchen, Nov. 2008.

[2] R. Lewis and W. H. Leavel, "Economic Value Added", Working Paper, no. 95-17G, Sam Houston State University, 1995.

[3] E. Maćkowiak, *Ekonomiczna Wartość Dodana* (*Economic Value Added*). Warsaw: PWE, 2009 (in Polish).

[4] A. Ehrbar, *EVA Strategia Tworzenia Wartości Przedsiębiorstwa* (*The Strategy of Company Value Creation*). WIG-Press, 2000 (in Polish).

[5] M. Sierpińska, "Zysk ekonomiczny jako miernik stopnia realizacji celów spółki (Economic profit as indicator of a degree of achieving company goals)", in *Proc. of Int. Conf. "Restructuring and Improvement of Company Economic Efficiency"*, Zakopane, Poland, 1998.

[6] K. Jagiełło, "Ekonomiczna wartość dodana EVA w systemie mierników finansowych wykorzystywanych w zrównoważonej karcie wyników (Economic Value Added in the System of Financial Indicators Used in Balanced Chart of Results)", *Zeszyty Naukowe MWSE w Tarnowie*, no. 6, 2004, pp. 51–65 (in Polish).

[7] K. J. Liapis, "The residual value models: A framework for business administration", *Eur. Res. Studies*, vol. XIII, no. 1, pp. 83–102, 2010.

[8] A. Cwynar, "Wycena przedsiębiorstwa metodą zdyskontowanych zysków ekonomicznych (EVA)", in *Wycena Przedsiębiorstwa od Teorii do Praktyki* (*Valuation of a Company Using the Method of Discounted Economic Profits* (*EVA*), M. Panfil and A. Szablewski, Eds. Warsaw: Poltext, 2011.

[9] M. Pęsyk, "Kalkulacja kosztu kapitału", in *Wycena Przedsiębiorstwa od Teorii do Praktyki* (*Valuation of a Company Using the Method of Discounted Economic Profits* (*EVA*), M. Panfil and A. Szablewski, Eds. Warsaw: Poltext, 2011.

[10] Market Risk Premia – Application of Valuation Parameters in Practice [Online]. Available http://www.market-risk-premia.com/

[11] S. O'Byrne, "EVA and market value", *J. of Appl. Corp. Finance*, vol. 9, no. 1, pp. 116–126, 1996.

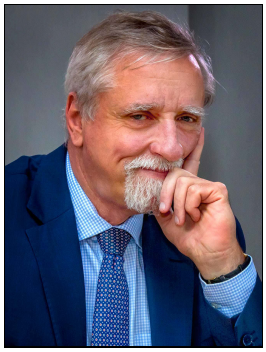

Wojciech Kamieniecki received his M.Sc. in Electronic from the Faculty of Automation and Computer Science of Silesian University of Technology in 1981. He completed Ph.D. studies at the University of Szczecin Faculty of Economics and Management in 2002. He is Director of Research and Academic Computer Network (NASK). He has many years of experience in running businesses and managing large projects in the area of telecommunications. His research interests focus on management efficiency and value creation of company, especially in telecom sector. He was involved in a number of business development projects providing by the biggest Polish telecoms (e.g. TeleNet, Exatel, Multimedia) as well as start-up projects (Nordisk Polska, Fiberia).

E-mail: wojciechk@nask.pl
Research and Academic Computer Network (NASK)
Kolska st 12, 01-045 Warsaw, Poland

Paper

Self-organization and Routing Algorithms for the Purpose of the Sensor Network Monitoring Environmental Conditions on a Given Area

Krzysztof Bronk[1], Adam Lipka[1], Błażej Wereszko[1], Jerzy Żurek[2], and Krzysztof Żurek[1]

[1] *Wireless Systems and Networks Department, National Institute of Telecommunications, Gdańsk, Poland*
[2] *National Institute of Telecommunications, Warsaw, Poland*

Abstract—The article describes an implementation of wireless sensor network (WSN) based on the IEEE 802.15.4-2006 standard, which was designed to monitor environmental conditions (e.g. temperature, humidity, light intensity, etc.) on a given area. To carry out this task, a self-organization algorithm called KNeighbors was selected. It exhibits low computational complexity and is satisfactory with respect to energy consumption. Additionally, the authors proposed a novel routing algorithm and some modifications to the MAC layer of the IEEE 802.15.4 standard. The article discusses the selected algorithms and procedures that were implemented in the network.

Keywords—network management, network self-organization, sensor networks.

1. Introduction

One of the main benefits of the sensor networks is the fact they offer a myriad of various applications. In fact it is also one of the reasons why they evolve so dynamically. The applications or purposes for which a sensor network is intended to be used determine the requirements such network needs to satisfy. The engineer is faced with a complex problem of selecting the most suitable hardware and software platforms as well as the algorithms and parameters which should ensure the correct – i.e. compliant with the predefined criteria – operation of the sensor network.

The selected mean of communications between the nodes should always reflect the network's characteristics, the method of data acquisition and also the method this data will be used in the future. The most common techniques employed in the wireless sensor networks (WSNs) are the ZigBee and 6LoWPAN, which are based on the IEEE 802.15.4 standard. Identification of the optimal self-organization and routing algorithms is also one the most crucial stages of the WSN development.

In the last years, many algorithms of the transport layer have been proposed, which in assumption should ensure the reliability and congestion control. Some of them have been designed for the node-sink transmission (ESRT [1], RMST [2]), the others for the sink-nodes transmission (GARUDA [3], PSFQ [4]) or for both directions (ART [5], STCP [6]). The comparative study of these protocols can be found in paper [7].

In contrast to the algorithms mentioned above, the algorithm proposed in this paper is used to collect data from as many nodes as possible and the loss of some packets is acceptable, because it does not result in data degradation for the whole monitored area. These assumptions were taken into account during development process. A query is sent from the sink node and answers are sent back by every node to which the query arrived. In the proposed solution, there is no mechanism for ensuring reliability of transmission between node and sink. The reliability is achieved in every hop by sending ACK in MAC layer. Congestion control is also made locally by time-out periods in nodes or by changing the packet destination node.

The following paper describes a practical implementation of the sensor network based on the IEEE 802.15.4-2006 standard, which was built for monitoring of environmental conditions (e.g. temperature, air humidity, light intensity) on a defined area. This network may operate efficiently even when some of the nodes cannot communicate or are damaged. Due to the purpose of the proposed WSN, it should satisfy the following requirements:

- long operational time,
- low sensitivity to communication problems with single nodes,
- scalability and remote configurability,
- communication with the network using the Internet,
- resistance to dynamic modifications of the topology (changes of the nodes' quantity and their location) and operational conditions,
- low price of the network node.

To satisfy the above, several assumptions have been formulated:

- the network configuration can be modified dynamically (via self-organization procedures), depending on the number of nodes and the transmission parameters,

Table 1
Functions performed by the nodes

Node type	Function
Master node, connected to the Internet	1. It receives: a request for data and parameters of the network configuration. 2. It sends a request for measurement data to the slave nodes. 3. The request mentioned in "2" additionally includes the network parameters. 4. It formats the received data. 5. It does not participate in the network self-organization. 6. It acts as a server for the network data.
Slave node, equipped with sensors and GPS	1. At master's request, it sends the measurement data from the sensors and the GPS-based position. 2. It participates in the network self-organization.
Slave node, without sensors	1. It passes data packets from other network nodes. 2. It participates in the network self-organization.

- nodes should be powered using solar power systems,
- network should be configurable remotely through commands transmitted by the primary node,
- the primary node should be connected to the Internet,
- the master-slave architecture should be utilized, where the primary (master) node demands the data, and the other (slave) nodes respond by sending the required data (measurement results) to the master,
- routing should be based on the self-organization procedure,
- hardware requirements for the node's processor should be kept low,
- information (data) is collected from each and every network node (nodes have not assigned IP addresses so it is not possible to collect the data from a specific node).

To implement those assumptions, the authors created their own, novel routing algorithm. Additionally, they proposed some modifications of the 802.15.4 MAC layer. In the next step, those algorithms and procedures have been implemented on a hardware platform designed and built for the purpose of this project, and the resulting solution has been subjected to a measurement campaign. The whole process of the WSN development and testing has been described in the subsequent sections.

2. Architecture of the Proposed Network

The research process was initiated by a review of the existing solutions. In paper [8], the authors analyzed the following self-organization algorithms: LMST (Local Minimum Spanning Tree) [9], CBTC (Cone-Based Topology Control) [10], DistRNG (Distributed Relative Neighbor Group) [11], KNeighbors (k-Neighbors) [12], LINT (Local Information No Topology) [13] and LILT (Local Information Link-state Topology) [13]. In that paper it was shown the KNeighbor algorithm will be the most suitable one to be implemented in the target sensor network. Its major benefits are: a relatively low energy consumption and implementation simplicity. Moreover, it exhibits low computational complexity, since it does not require a precise calculation of the nodes' position or the signal's direction of arrival. With a sufficient number of neighbors (6 or more), alternative routes (of packet transmission) can be ensured in case of nodes' failure. In this way, the problem of losing a full connectivity in the network can be substantially marginalized.

On the basis of the initial assumptions and requirements for the projected WSN and using the simulation comparative analysis of several self-organization algorithms [8]–[13], a general concept of the network architecture was developed [14].

The discussed sensor network is composed of two types of nodes:

- master node,
- slave nodes.

Functions performed by those are listed in Table 1.

The packets transmitted in the network are assigned a type denoted by an ASCII code inserted in the first payload's byte (MAC payload) of each packet. Designations of the packets and their brief description can be found in Table 2. The terms "packet" and "command" are used interchangeably in the following text.

After the reception of the packet, the node checks its type and acts accordingly. Table 2 includes all the commands to be used in the network. The ACK column indicates

Table 2
Commands transmitted in the network

Packet designation	Description	ACK	Number of bytes
W	The packet sent by a node that is searching for its neighbors. The recipient verifies the quality of the received command and if it is above a threshold, responds by sending an "A" type packet. The "W" packet includes the value of power it was transmitted with.	No	50
A	A response for the "W" packet. It contains: • LQI value (range 0–255) of the received "W" packet, which indicates the quality of connection, • ID from the "W" packet, • the value of power the "A" packet was transmitted with.	No	4
O	A packet which contains measurement data obtained by the node, including position information from the GPS.	Yes	Max. 80
o	A packet which contains measurement data sent to the master node. The "o" command is a response to the "s" command. The packet is transmitted with a maximum power.	Yes	Max. 80
S	A request for measurement data sent by the network node to its neighbors. The packet also contains network configuration parameters.	No	13
s	A request for measurement data sent by the master node. The packet is transmitted with a maximum power and it contains network configuration parameters.	Yes	4

whether the transmission of a certain packet has to be acknowledged by the recipient (by ACK frame), or not.

2.1. Network Layer Model

The following subchapter introduces the communication protocols of the self-organization and network layers, which manage the packet routing. The physical and MAC layers are generally compliant with the IEEE 802.15.4 standard [15], with the exception of some MAC layer modifications: the number of attempts to transmit a packet has been increased and the mechanism of power control has been altered.
The layer model of the discussed sensor network is presented in Fig. 1.

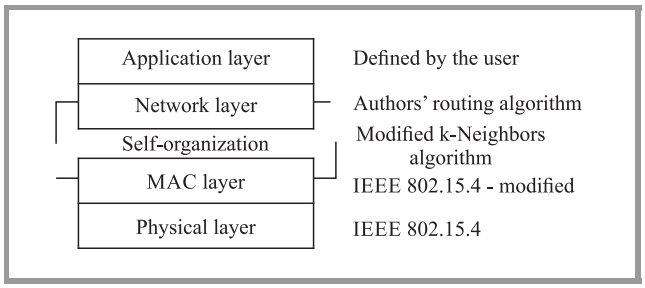

Fig. 1. Network's layer model.

The self-organization layer is located between the MAC and the network layer. The direct output of the self-organization procedure in a given network node is a table of its neighbors, later utilized by the network layer for routing.

2.1.1. Self-organization Layer

In the discussed network, the term "self-organization" should be understood as the node's activity which results in a list of neighbors connected with that node through a radio link of a certain quality with minimum node's transmit power. As it was mentioned, the output of the self-organization procedure is a table with neighbors' addresses and the current value of transmitted power, which will be used to send data request packets ("S" type packets) and data packets ("O" type packets). A given node in a given moment can generally communicate only with its neighbors. There are, however, two exceptions to this rule:

– any node within the range of the master node can attempt to communicate directly with it,

– a node, which does not have any neighbors, is still capable of sending messages.

As it was mentioned previously, the KNeighbor algorithm [12] has been selected as the most suitable one to be implemented in the discussed sensor network, due to its simplicity and satisfactory performance [16]. The general algorithm of neighbor searching is depicted in Fig. 2.
The procedure of the self-organization is initiated in each node after the time Ts, which is one of the network parameters. After the node has been powered on, the first self-organization starts after a random time in the range of 0 to Ts. This approach was taken to reduce the probability that self-organization procedures performed by neighboring nodes will overlap.

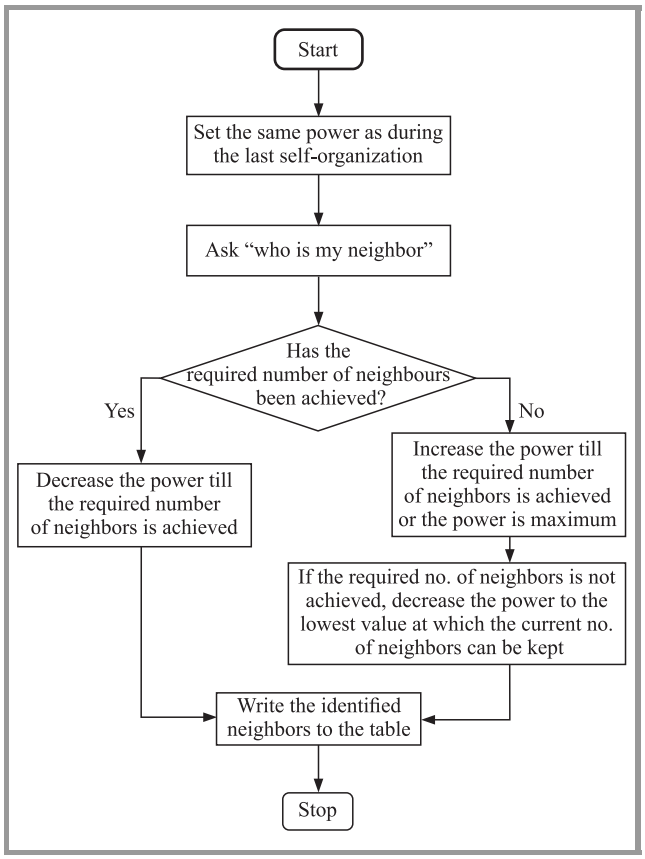

Fig. 2. *k*-Neighbors self-organization algorithm.

The node searching for its neighbors performs the following tasks:

- it sets the transmitter power to the value used during the previous self-organization,
- it sends the "W" packet (with 45 additional bytes to improve the link quality assessment),
- it waits for approx. 1 s, and during this period it collects responses from the neighboring nodes,
- it checks how many nodes actually responded for the "W" packet,
- if the number of the nodes that responded is too small, it increases the transmitted power and resends the "W" packet,
- If the required number of neighbors has been found, it decreases transmitted power and keeps resending the "W" packet. This procedure is repeated until further power decrease would cause the number of neighbors dropping below the desired threshold.

The node, which receives the "W" packet, acts according to the following procedure:

- it evaluates the quality of the received "W" packet;
- if the quality is better than the assumed threshold, it responds (by sending the "A" packet to the "W" packet-sender) with the transceiver power set to the value contained in the received "W" packet. The response also includes the LQI of the received "W" packet.

The procedure of the self-organization ends when:

- the node reaches the minimum or maximum power,
- the number of identified neighbors is at least equal to the desired threshold and any further decrease of the transmitted power would reduce the number of responding nodes.

The result of the self-organization is a table of the node's neighbors and the transmitted power obtained during the procedure. The determination of the transmitted power before sending the "W" and "A" packets is performed in the link layer, which is a modification of the 802.15.4 standard.

2.1.2. Example of Self-organization Procedure

A sample procedure of the self-organization procedure is shown in Fig. 3. The following network configuration parameters have been assumed:

– maximum number of neighbors to be found: MAX_N = 3,

– minimum expected transmission LQI: MIN_LQI = = 30.

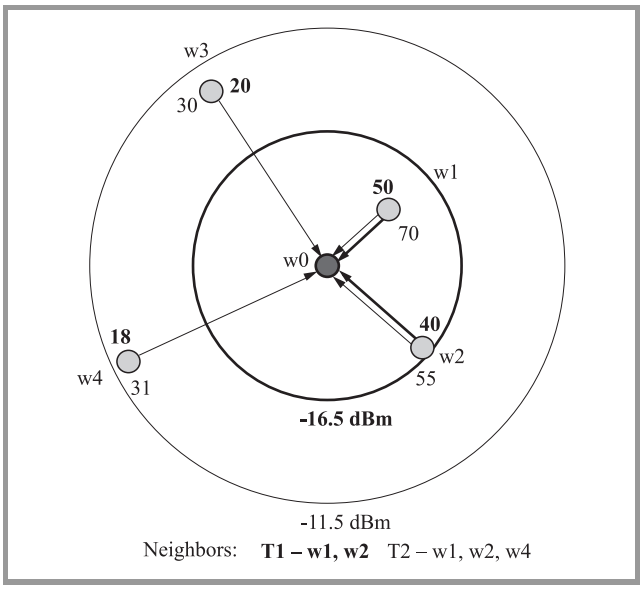

Fig. 3. Sample self-organization procedure.

In the instant T1, the w0 node initiates the procedure, by sending the "W" packet with a power of –16.5 dBm and a recipient address set to broadcast.
The packet is received by every node shown in the Fig. 3, with the following values of LQI: 50 at w1 node, 40 at w2 node, 20 at w3 node and 18 at w4 node. The LQI value

exceeded LQI_MIN only in the cases of w1 and w2 nodes, so only these two respond by sending the "A" packet to the n0 node.
After 1 s, the w0 node checks, how many nodes responded. Since only 2 did, w0 increases transmitted power to –11.5 dBm and resends the "W" packet in the instant T2. In this case, the LQIs were as follows: 70 at w1, 55 at w2, 30 at w3, 31 at w4. Therefore, all of these nodes respond with the "A" packet addressed to the w0 node.
While receiving the "A" packets, the w0 node adds nodes with the highest LQI to its neighbors list. As a result, the searching procedure ends with w1, w2 and w4 nodes identified as w0's neighbors and the transmitted power set to –11.5 dBm.

2.1.3. Network Layer

The network layer is responsible for the routing of packets with measurement data ("O" and "o" packets) and packets with data request ("S" and "s" packets). For the proposed sensor network, the authors created their own novel routing algorithms which should ensure:

- distribution of data requests and configuration parameters to as many nodes as possible,
- delivery of packets with data to the master node.

To make sending the data possible in the network, each node needs to know a specific address called *RoutingNode* (RN). It is the node's address, to which all the measurement data should be sent. The method used for RN's selection will be discussed later.
In the following paragraphs, novel routing algorithms, proposed by the authors, for different types of packets will be introduced.

2.1.4. Request for measurement data sent by the Master Node

The request for measurement data is sent by the master node to the broadcast address, i.e. 0xFFFF. This command is marked as "s" and is transmitted with maximum power. The command contains the following fields:

- "s" packet identification (8 bits),
- message ID, 16-bits random number,
- number of hops, increased by 1 after every successive packet transmission (16 bits),
- network configuration fields discussed in the following part.

The procedure of the "s" packet routing is shown in Fig. 4. The node which received the "s" packet, sets the master's address as its RN and sends its measurement data at this address. This node also sends the received "s" packet to its neighbors, but the packet type is changed to "S". It is the only case when the RoutingNode is not one of the neighbors. The master node is not a neighbor of any node, because it does not participate in the self-organization procedures. Consequently, it cannot be added to any neighbors' list.

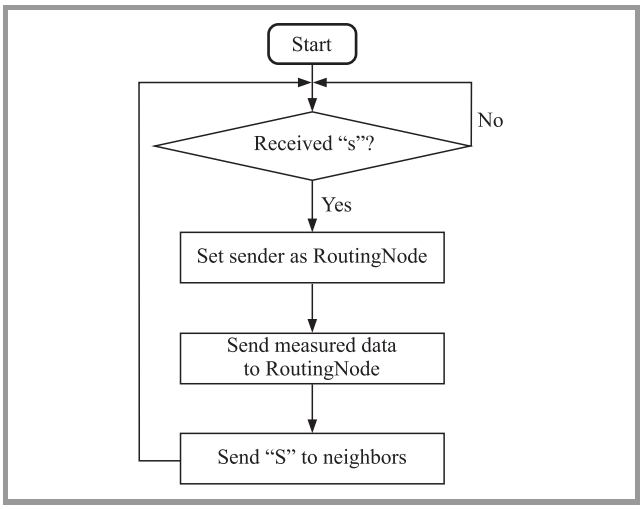

Fig. 4. Routing of the data request sent by the master node.

2.1.5. Request for data Sent by the Slave Node

A slave node is any node in the network that is not a master node. Every node that received the "s" packet, sends its measurement data back to the sender and then – if the node has neighbors – it sends the "S" packet to them. Data requests originated by the slave node are treated differently than the packets from the master:

- they do not need to be sent with maximum power,
- packet sender will not be set as RN, if it is not the recipient's neighbor.

The procedure of the "S" packet routing is shown in Fig. 5. The node, which receives the "S" packet, acts according to the following procedure:

- it checks if the number of hops is less or greater than the maximum acceptable value; if it is greater, the nodes will ignore the message;
- it reads the ID and checks if it has already received a message with an identical ID. If it has not, it writes the ID to the table; on the other hand, if such an ID is already in the table – another RN is selected;
- it checks if the sender is its neighbor; if yes – it sets the sender as RN;
- it sends its measurement data to the RN;
- it increases the number of hops by 1;
- it sends "S" to its neighbors.

2.1.6. Sending Measurement Data

Measurement data ("O" or "o" packets) are always sent to the RoutingNode: with the same transmitted power as the one used during the previous self-organization, or with

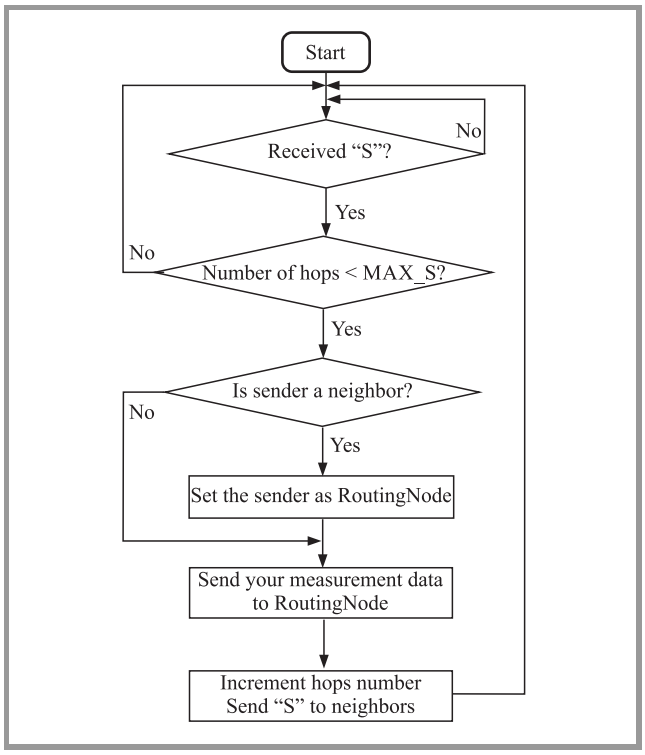

Fig. 5. Routing of the "S" packets.

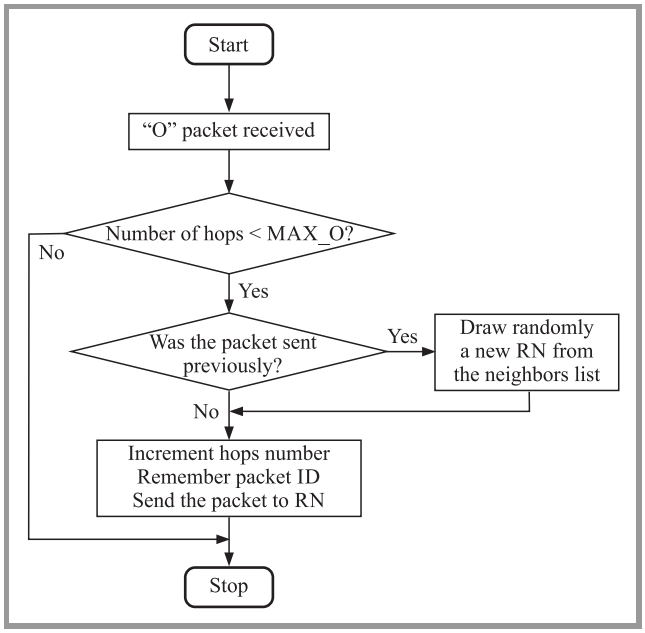

Fig. 6. Routing of the measurement data packets.

maximum power if the data is addressed to the master node. The routing of the packets carrying the measurement data is depicted in Fig. 6.

2.1.7. Determination of the RoutingNode

The RoutingNode is selected in the following way:

- it is the master node, from which the "s" packet was received,
- it is the neighbor node, from which the "S" packet was received,
- if the packet with measurement data is returned to sender, a different neighbor node has to be selected as RN,
- if the node which does not have any neighbors receives the "S" packet, it sets the packet sender as RN.

Measurement data packets have a hop counter, which is incremented (increased by 1) after every successive packet transmission. If the hop counter value in the packet is greater than the accepted threshold, such a packet will be ignored by the node that received it. The "o" packet (sent directly to the master node) should always have the hop counter value set at zero.

2.1.8. Exchange of Data Request Packets and Data Packets – Sample Scenario

In this scenario, it was assumed that in a given moment of time, only one node can be granted access to the radio channel. It was also assumed that nodes have the following neighbors:

Node w1: w4 and w2,

Node w2: w3, w4 and w5,

Node w3: w2 and w5,

Node w4: w1, w2, w5,

Node w5: w2, w3 and w4.

Figure 7a depicts 13 subsequent steps of the scenario (numbers in brackets next to the arrows indicate the step's number), additionally all the events are presented in Fig. 7b.
In the first instant of time, the master node transmits the "s" packet which is received by nodes w1, w2 and w3. These three nodes set the master's address as RN.
In the next instant of time, the node w1 is granted access to the radio link and sends the measurement data obtained by its sensors to the RN. After that, it sends the "S" packet to the node w4. W4 sets the address of w1 to be its RN. In the fourth instant of time, the node w4 sends its measurement data back to w1.
The precise time sequence of the whole procedure is shown in Fig. 7b. The numbers visible in the first column are the numbers of subsequent steps.
In the procedure depicted in Fig. 7, the w5 node received the "S" packet from the w4 node, and the w4 node had previously received this same packet from w1 – consequently there were two hops of the packet ("S" was originally sent from the master, which constituted the zeroth hop). As a result, number 2 (number of hops) is inserted by w4 to the specific field of the "S" packet.
One can observe, the message containing data from w5 took the longest path. It was delivered to w0 via nodes w4 and w1. The heaviest traffic was served at node w1, which sent its own data and the data from nodes w5 and w4. Obviously, the channel access is granted randomly, so

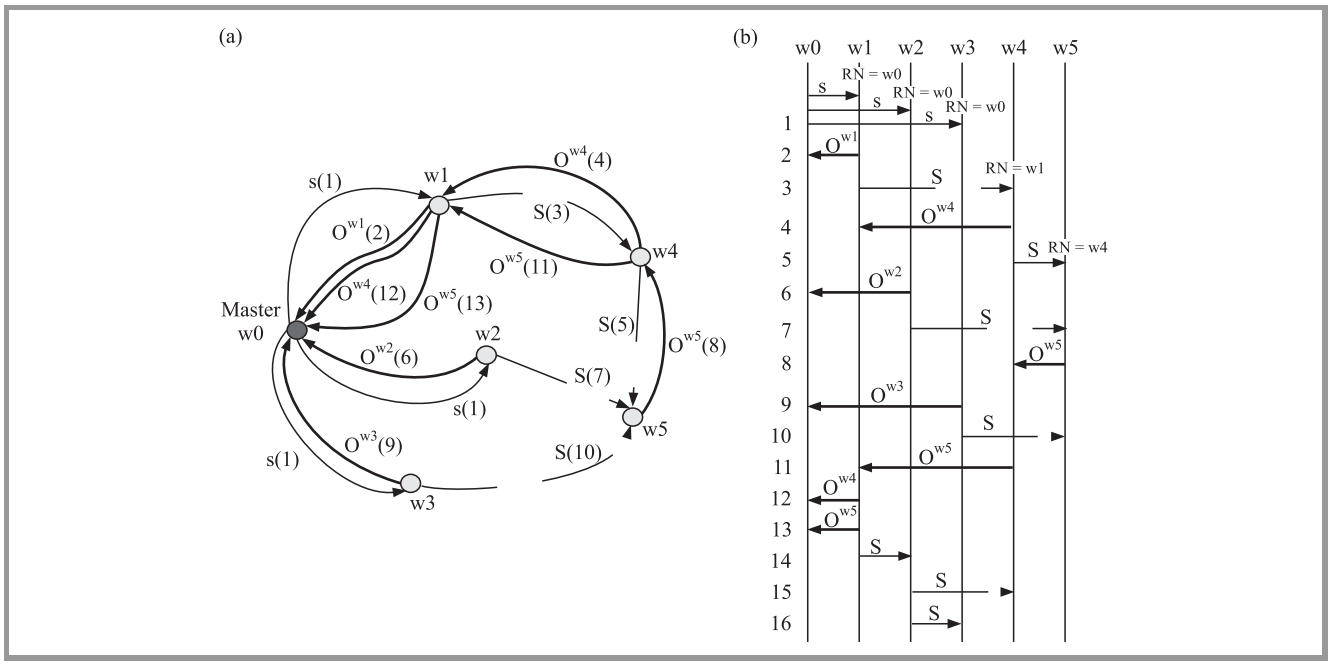

Fig. 7. Data routing scenario.

Table 3
Structure of the "S" and "s" data request packet

No.	Field	Description	Example	Bytes
1	Packet type	Data request command	"S"	1
2	MAX_S	Maximum number of hops for the "S" packet	100	2
3	MAX_O	Maximum number of hops for the "O" packet	200	2
4	T_S	Time between self-organization procedures, max. 72 hours	10	2
5	T_GPS	Time between position readings from the GPS, max. 72 hours	30	2
6	LQI_MIN	Minimum LQI in the self-organization procedure	20	1
7	MAX_N	Maximum number of neighbors, from 1 to 10	3	1
8	CRC	CRC checksum	0x1C	1
			Total	12

in the next steps, the routing can be handled in a different way.

2.2. Network Configuration

One of the main features of the presented sensor network is the capability to be configured remotely, which also ensures a certain level of scalability. The network configuration is performed through a distribution of the "S" and "s" packets, which contain fields with the network's parameters. The structure of the data request packets is introduced in Table 3.

The MAX_S field defines the maximum number of hops for the "S" packet. This parameter allows to modify the range of the packet distribution and consequently to modify the area from which the data can be collected.

The MAX_O field defines the maximum number of hops for the "O" packet.

The T_S field defines the time that has to elapse between two subsequent self-organization procedures. To determine the value of this parameter, the changes of nodes' positions should be considered: if the nodes are moving, self-organization should occur more frequently than in the case of fixed nodes.

The T_GPS field defines how often the position is read from the GPS receiver. After the position has been obtained, the receiver is switched off (or goes into idle mode) to reduce power consumption of the node.

The LQI_MIN field contains a value (in the range of 1 to 255) defining a minimum LQI at which the node will still respond to the "W" packet sent by another node. Besides the MAX_N, this parameter is the most crucial with respect to the resulting network topology. A low value of LQI_MIN results in a greater number of neighbors (i.e. bigger network connectivity), but at the same time it might result in a low quality of connections between the nodes.

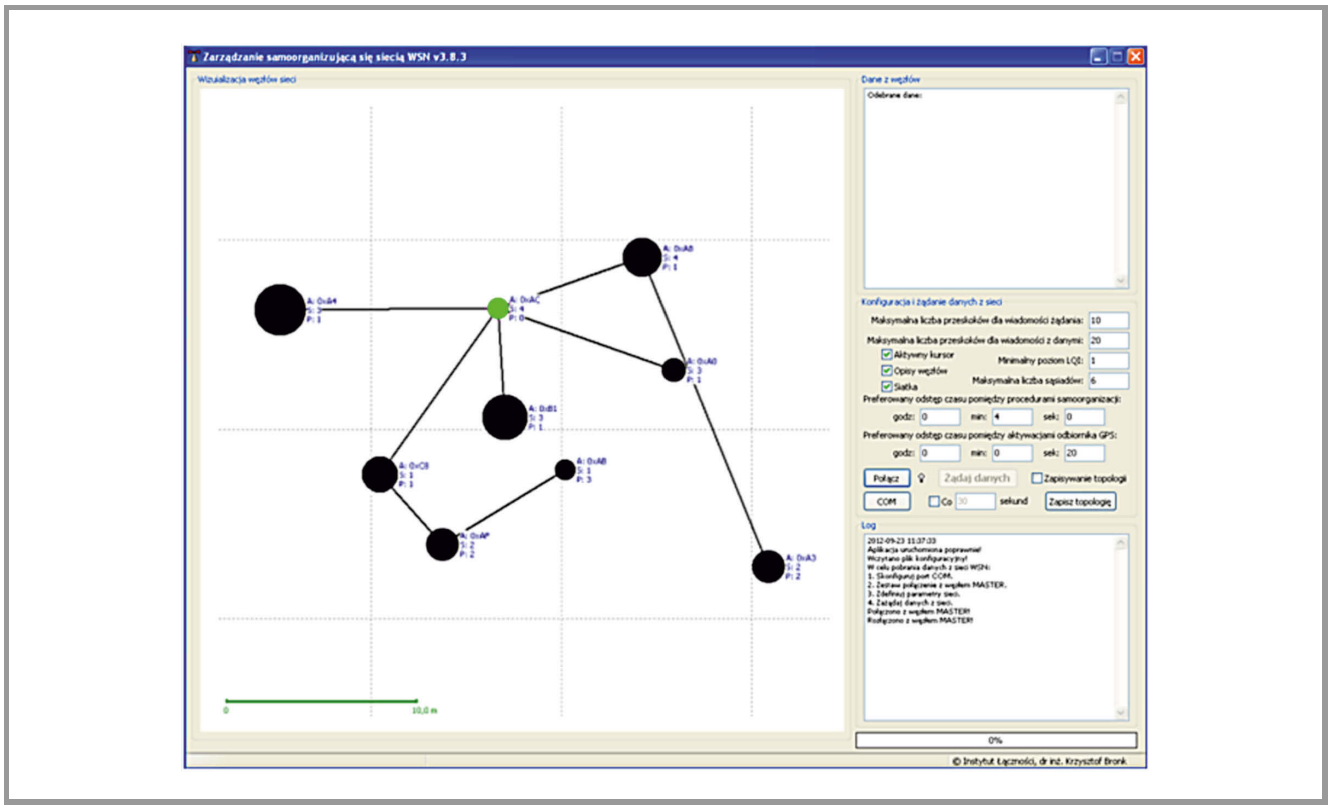

Fig. 8. Software tool for the network management. (See color pictures online at www.nit.eu/publications/journal-jtit)

The MAX_N field defines the maximum number of neighbors that can be found in the self-organization procedure.

As it was previously mentioned, the network topologies resulting from the self-organization mostly depend on the MAX_N and LQI_MIN parameters (when the nodes' position and terrain condition are known and remain constant). Low value of the MAX_N can lead to local clusters of nodes that remain "hidden" and separated from the rest of the network. On the other hand, high values of this parameter make the self-organization procedure longer and increase the nodes' transmitted power, which may result in heavy traffic and increase of the network interference. These two factors will in turn worsen the self-organization efficiency so the node will possibly be able to discover fewer neighbors than it was supposed to.

2.3. Hardware Implementation

On the basis of all the assumptions, simulations results [8] and concepts discussed above, as well as the analysis of the relevant references and state of the art, a hardware implementation of the wireless sensor network has been created. The network comprises of ten RCB128RFA1 radio modules with additional sensors, and one master node connected to the Internet. To enable acquisition of the data from the network and its visualization and also to facilitate network configuration, a software tool for network management was developed. The user interface of the tool is depicted in Fig. 8.

The visualization of the network activity includes the following factors:

- the node's position calculated using the GPS data,
- the size of the node corresponds to the node's transmitted power,
- nodes are depicted by three different colors: green – a node that transmits directly to the master, black – other nodes, red – nodes whose power voltage is below 3.225 V.
- the nodes which exchange data with one another are connected with lines.

2.3.1. Master Node

The master node (see Fig. 9) is implemented using the Ethernet module with the RTL8019AS controller and the

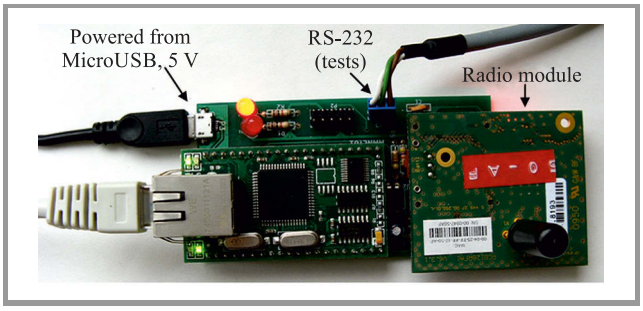

Fig. 9. Master node with the Ethernet interface.

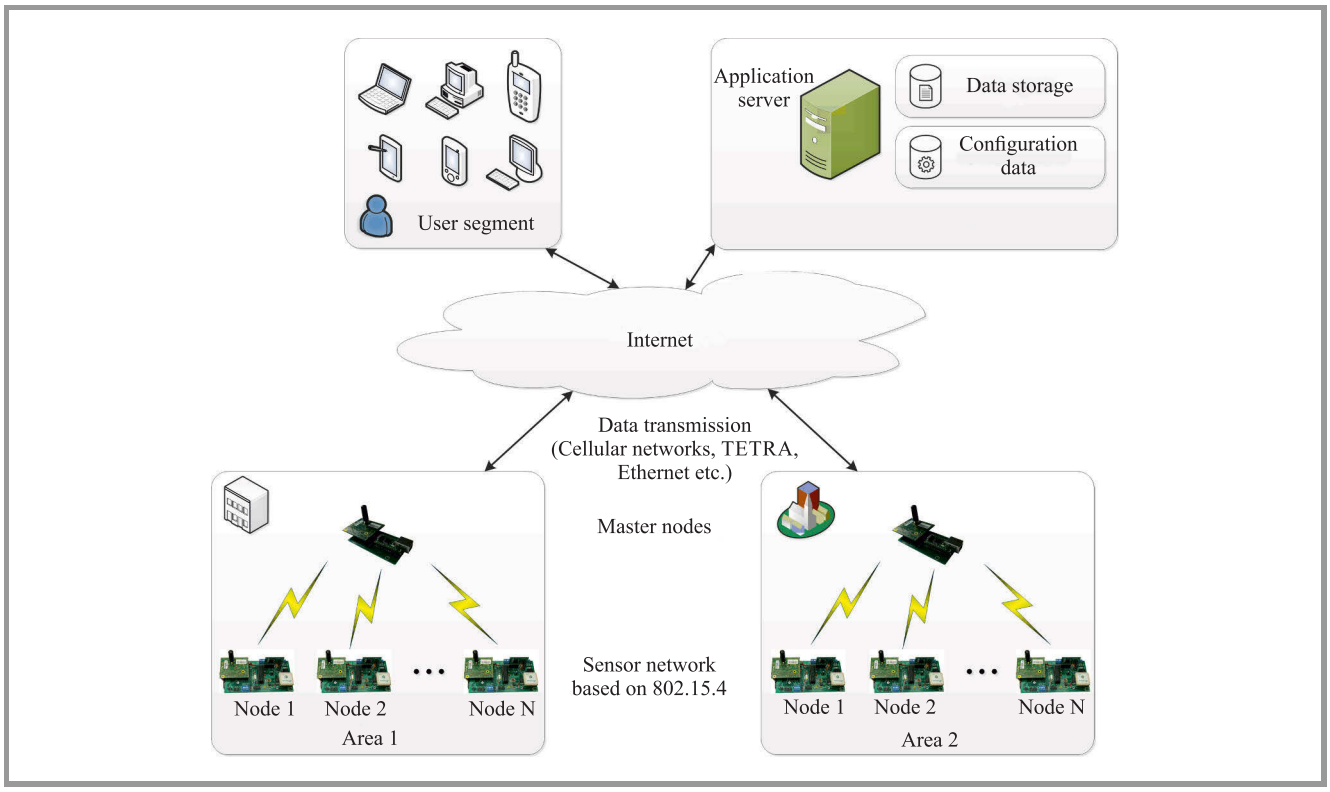

Fig. 10. Connection of the sensor network to the Internet.

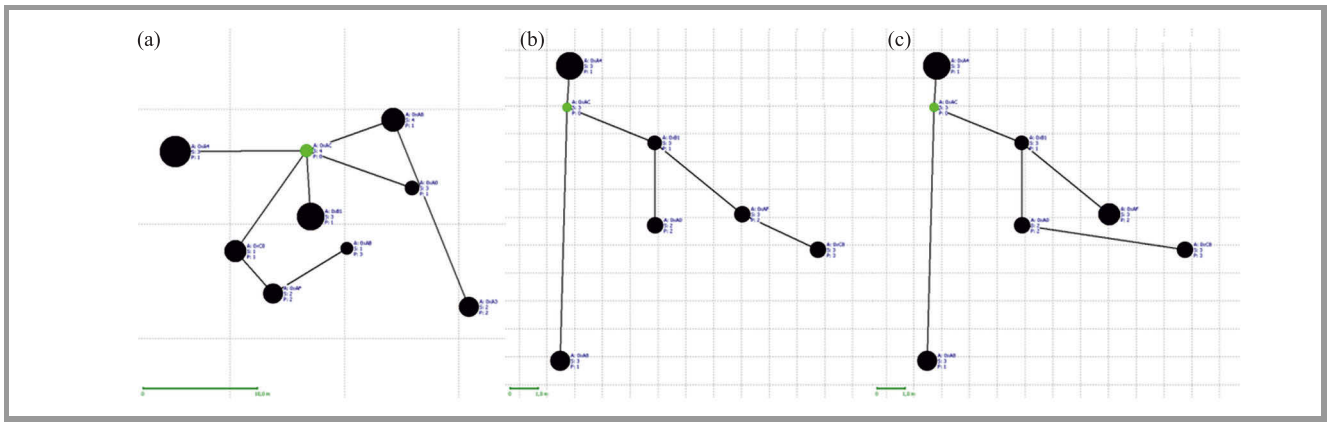

Fig. 11. Sample topologies created during the WSN measurements.

RCB128RFA1 radio module by the Dresden Elektronik. Both these components have been assembled on a single printed circuit board. The node is powered with 5 V from the microUSB port.

The Ethernet module operates under control of the real time system FreeRTOS with the TCP/IP stack called LwIP (A Lightweight TCP/IP stack [17]).

2.3.2. Connecting the Network to the Internet

The proposed network is connected to the Internet through the master node. This approach is illustrated in Fig. 10. As it has been previously mentioned, in the discussed network, no node-to-node communication has been employed, i.e. it is not possible to communicate with a specific network node. Instead the authors utilized the master-to-node communication. In this case, establishing a connection to the master is essentially establishing a connection with the whole network, and consequently, in the best-case scenario, data from all the nodes can be collected. Such an approach was taken due to the target purpose of the proposed network (monitoring of the environmental parameters on large areas), in which the ability to obtain the data from as many nodes as possible is the top priority.

2.3.3. Initial Measurements of the Network

The network management software tool allows to collect data from the network and to perform network configuration. Additionally, the master node acts as a Webserver

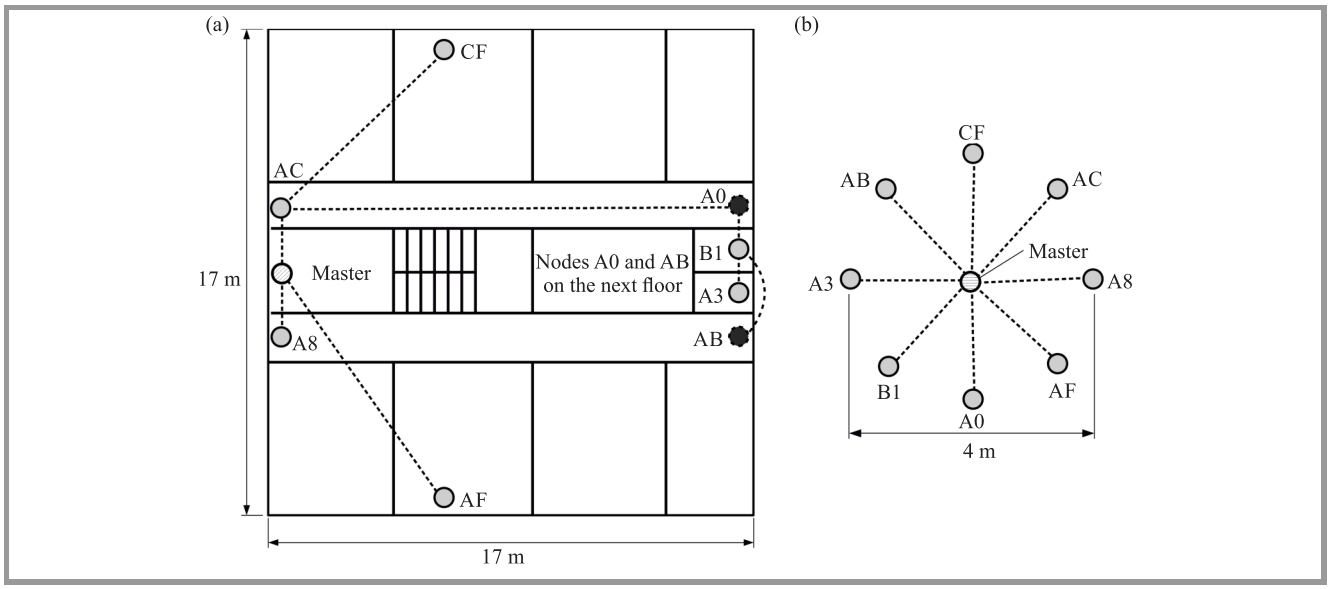

Fig. 12. Network topologies.

to enable remote observation of the parameters measured by the sensor nodes. The acquired data are presented in the table and can be accessed e.g. in an Internet browser.
A few examples of the topologies obtained during the tests are depicted in Fig. 11.
These topologies are generated in the software tool on the basis of the received data. The black circles represent the nodes and their size (diameter) is proportional to the transmitted power. Obviously, the greater the diameter, the higher the transmitter power. In this particular case the largest diameter is equivalent to the power of 3.5 dBm. Green circles are the nodes communicating directly with the master node. Their diameter corresponds to the power determined in the self-organization procedure, but the transmission to the master is always performed with the maximum power. Positions of the nodes are obtained from GPS receiver mounted on every node. The lines between nodes denote the paths over which packets are routed.
It should be stated, Fig. 11a, depicts a scenario where nodes were located on a rectangular plane of 17×17 m (the roof of the National Institute of Telecommunications (NIT) building in Gdańsk), whereas in the cases of Figs. 11b and 11c, the nodes were located in rooms and corridors of the same building. As we can observe, Figs. 11b and 11c depict the same arrangement of the nodes, but two different paths of the packets originating from the rightmost node.

3. Functional Network Tests

3.1. Network Configuration During the Tests

The measurement tests of the resulting sensor network have been performed in the NIT office in Gdańsk, using eight slave nodes and one master node. The tests have been carried out for two network's configurations: the mesh (Fig. 12a) and the star (Fig. 12b).

The mesh topology was obtained by placing the nodes in different rooms on the same floor, with the exception of nodes A0[1] and AB, which were located on a higher level. By doing so, some of the nodes were outside the master node's range and data requests could be delivered to them only via other nodes in the network.
On the other hand, the star topology was obtained by placing all the nodes in the same room, approximately 2 meters from the master node. Consequently, all the nodes were in the master's range and each of the node was in the range of all other nodes. The tests of the star topology were performed for the purpose of comparison with the mesh.
All the simulations have been carried out using the following network settings:

- requested number of neighbors: 1, 2, 3, 4 and 5,
- maximum number of hops for the request packets: 10,
- maximum number of hops for the data packets: 12,
- minimum LQI: 50,
- maximum number of attempts to send the message: 2,
- self-organization procedure initiated every 120 s,
- data requests from the network sent every 15 s.

The measurement series have been repeated ten times, and each of them comprised approx. 200 requests being sent to the network, which accounted for a total of roughly 2000 requests.

3.2. Measurements Results

In this section, the measurements results – averaged for the entire network – are presented. The testing procedure

[1]In the paper, in order to address the node, only the last byte of its 8-byte address was used. It could be done, because the nodes' addresses only differed in this last byte.

covered such parameters as: the delay, number of packets, number of hops, availability and number of discovered neighbors. Additionally, the availability was analyzed separately for every network's node.

3.2.1. Delay

The delay in the network – measured by the software application – is defined as the time that elapsed from the moment the data request packet was prepared (by the application) to the moment the data packet was received. According to that definition, the following "events" account for the delay: (a) packet processing by the computer, (b) packet multi-hop transmission, (c) packet processing by the recipient node, (d) transmission of the response and its reception by the master node, (e) packet forming and its transmission to the computer via the USART interface and (f) time needed by the computer to deliver the packet to the software application.
The tests performed for the scenario of the connectivity with just one node, show that the minimum reachable delay for this configuration is 218 ms. That analysis was performed using the exact same computer that was later employed in the actual measurements of the network (2-cores Pentium R 3.4 GHz processor, 64-bit Windows 7).

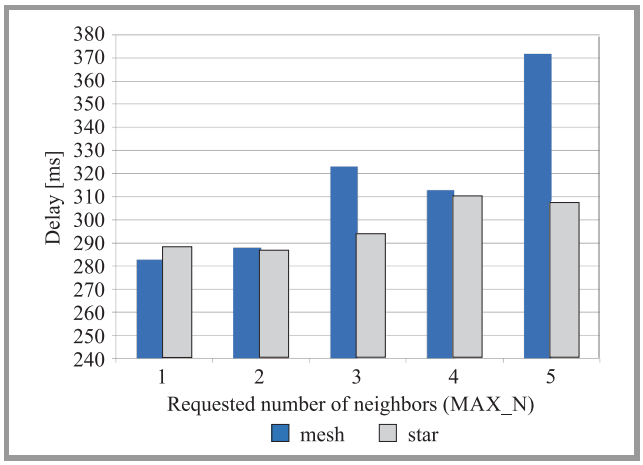

Fig. 13. Average delay in the network.

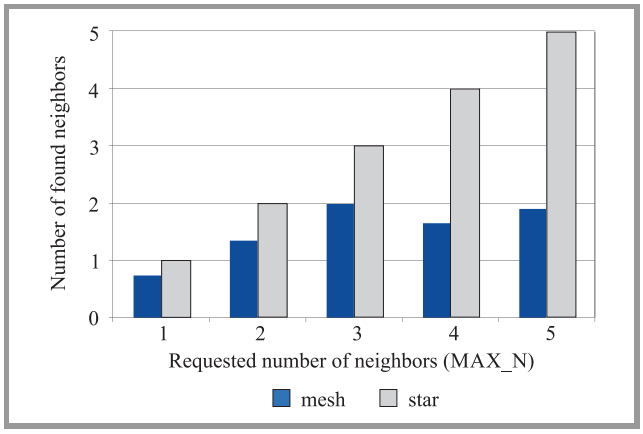

Fig. 14. Number of discovered neighbors.

The measured values of the delay are presented in Fig. 13. The delay for the mesh topology increases as the number of neighbors increases, with the only exception being the case of 4 neighbors. It can be explained by the fact that when the requested number of neighbors is 4 (MAX_N=4), the number of actually discovered neighbors drops (see Fig. 14), which decreases the number of transmitted messages and consequently – reduces the delay in the network as well.

3.2.2. Number of Discovered Neighbors

The average number of the discovered (found) neighbors is shown in Fig. 14.
In case of the star topology, where each node is in the range of every other node, the nodes are able to discover as many neighbors as required. On the other hand, in case of the mesh topology, the highest average number of neighbors can be found for the parameter MAX_N=3.
In the mesh topology, where the node is in the range of only some of the nodes, neighbors' discovery requires a higher number of requests sent with higher power, which could translate into greater interference inside the network and longer duration of the whole procedure. As a result, the self-organization fails more frequently and the node is then unable to find the required number of neighbors.
Consequently, it might be stated that increasing the MAX_N parameter value can often prove counterproductive and in such a case, the actual neighbors' number will more likely start to drop rather than grow. This observation can be confirmed in Fig. 14 for MAX_N=4 and MAX_N=5. The same picture clearly indicates the optimal value of the MAX_N parameter is 3.

3.2.3. Number of Packets

Figure 15 shows the average number of packets transmitted in the network per single request. The term "packets transmitted in the network" should be understood as every packet sent by the node, including data requests, data packets and messages utilized in the self-organization algorithm.
In case of the star topology, the number of packets grows linearly as the required number of neighbors' increases. It

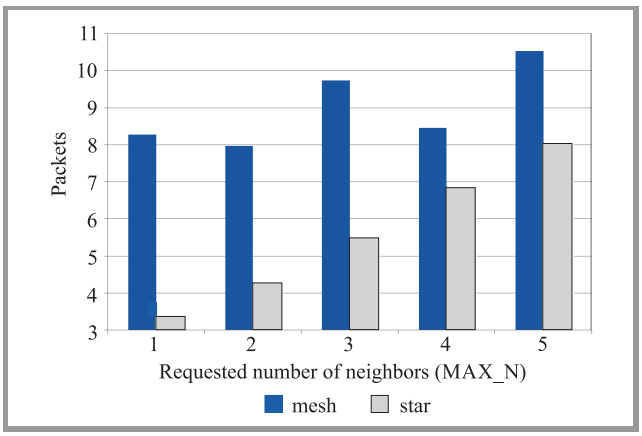

Fig. 15. Number of packets sent in the network per single request.

is caused by the fact that the requests are broadcast to the increasing number of neighbors. Hence, if the required number of neighbors is increased by one, the number of transmitted packets grows accordingly.
For the mesh topology, the growth of the packet number is less significant, which is caused by the problems with finding the required number of neighbors in this particular topology (see Subsection 3.2.2).

3.2.4. Number of Hops

Figure 16 indicates an average number of hops for data packets. If the number of hops is zero, it means the packet is sent directly to the master node. In case of the star topology, hops occur quite rarely, because the nodes send their data directly to the master.

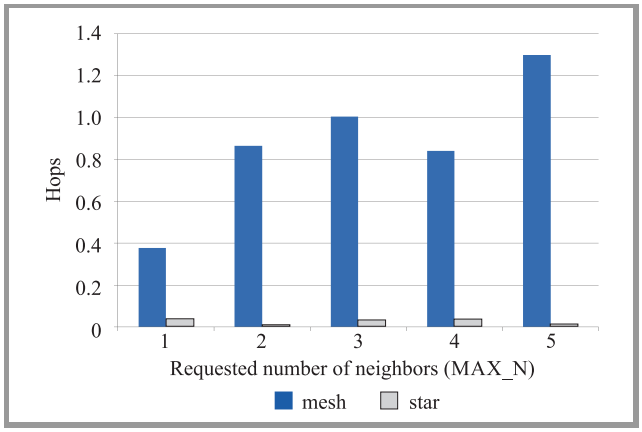

Fig. 16. Average number of hops for data packets.

In case of the mesh topology, the number of hops grows as the MAX_N parameter grows, even though the nodes' positions remain unchanged. This might suggest that the paths for the data messages are not chosen optimally. Unfortunately, this is a weakness of the assumed solution, where the first node from which the data request has been received is appointed to be the node to which the data packets are sent back – without the actual path length to the master node being calculated. On the other hand, that issue has been known already at the development stage and – from a practical point of view – it does not represent any significant problem for the network in its current form and it does not interfere with its primary purpose i.e. environmental parameters' monitoring.

3.2.5. Availability

The node's availability is defined here as a ratio of the number of responses to the number of requests. For example, if 100 requests have been sent to the network, and 80 responses have been received from a certain node, that node's availability is 0.8 (or 80%).
In Fig. 17, the availability for the whole network was presented, whereas in Fig. 18, the same parameter was shown separately for every analyzed node.
The maximum availability is observed for the requested number of neighbors MAX_N=3. For MAX_N<3, local

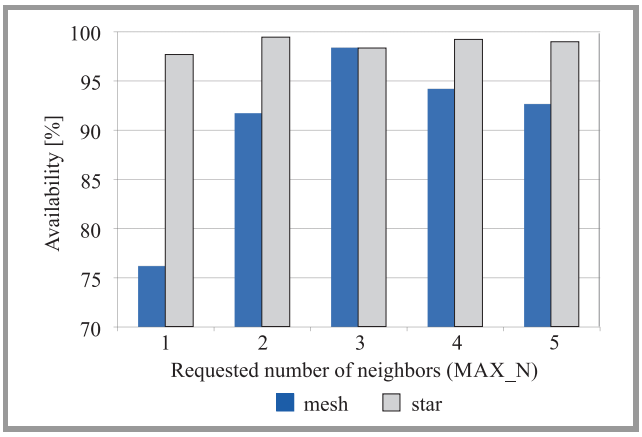

Fig. 17. Nodes' availability in the network.

nodes' clusters are formed, the messages are unable to be transmitted outside this cluster and consequently, they are unable to reach the master node. Obviously, in such a scenario the availability of the nodes belonging to such a cluster drops – it can be observed particularly for the nodes A3 and AB at MAX_N=1 (Fig. 18).

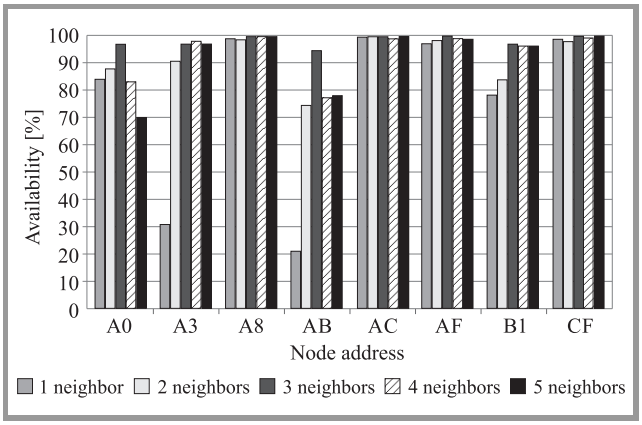

Fig. 18. Availability of every analyzed node.

For MAX_N>3, the number of messages transmitted in the network goes up, which also reduces the nodes' availability. Those mechanisms that occur when MAX_N is not equal to 3 result in the fact that some nodes – especially those far away from the master (i.e. AB, A3, B1 and A0) – lose their connectivity.

4. Conclusions

In the article, a wireless sensor network based on the IEEE 802.15.4-2006 standard has been introduced. The network was developed to monitor various environmental parameters on a defined (potentially large) area. The authors employed the approach in which the data are collected from the whole network via a single primary node, instead of a more common practice where every node is assigned an IP address. Owing to that, the resulting network works efficiently even when some of nodes lose connection or are damaged.

In the network implementation phase, the authors identified the KNeighbors algorithm as the base for the self-organization mechanisms. In comparison to similar algorithms, it exhibits small computational complexity and reasonable energy consumption. Additionally, the authors proposed their own routing algorithm and introduced some modification to the MAC layer of the IEEE 802.15.4 standard, which is one of the main achievements of this work. The article discusses in detail those algorithms and presents the complete network hardware implementation.

The conducted measurement research performed using the hardware platform mentioned above – showed that the implemented self-organization and routing algorithms are effective and allow to maintain connectivity in the network. During the measurement test, the nodes' availability of 98% was observed, but that value strongly depends on the parameter MAX_N (the number of requested neighbors). It is caused by two main mechanisms: for MAX_N<3 local groups of nodes occur, and for MAX_N>3 the number of packets sent in the network increases.

On the basis of those observations, the following goals for the future network development can be identified:

- the configuration of the network should not be performed "manually". Instead, the adaptive mechanisms should be introduced to identify optimal network parameters;
- the number of transmitted messages should be reduced;
- the shortest path for the data packets should be selected.

The implementation of the above factors will make the network more efficient and will enable to use it in wide range of various applications. Nevertheless, it is necessary to recall one more time the original purpose of the wireless sensor network presented in this article – i.e. the monitoring of environmental conditions on a given area. The tests have proven that for this specific purpose, the network in its current configuration and architecture is more than sufficient and does not require any substantial modifications.

References

[1] Y. Sankarasubramaniam, O. Akan, and I. Akyildiz, "ESRT: Event-to-sink reliable transport in wireless sensor networks", in *Proc. 4th Int. Symp. on Mob. Ad Hoc Netw. & Comput. MobiHoc 2003*, Annapolis, MD, USA, 2003, s. 177–188 (doi: 10.1145/778415.778437).

[2] F. Stann and J. Heideman, "RMST: Reliable data transport in sensor networks", in *Proc. 1st IEEE Int. Worksh. Sensor Netw. Protoc. & Appl. SNPA 2003*, Anchorage, AK, USA, 2003, pp. 102–113.

[3] S. Park, R. Vedantham, R. Sivakumar, and I. Akyildiz, "A scalable approach for reliable downstream data delivery in wireless sensor networks", in *Proc. 5th Int. Symp. on Mob. Ad Hoc Netw. & Comput. MobiHoc 2004*, Tokyo, Japan, 2004, pp. 78–89 (doi: 10.1145/989459.989470).

[4] C.-Y. Wan, A. T. Campbell, and L. Krishnamurthy "PSFQ: A reliable transport protocol for sensor networks", in *Proc. 1st ACM Int. Worksh. on Wirel. Sensor Netw. & Appl. WSNA 2002*, Atlanta, GA, USA, 2002, pp. 1–11 (doi: 10.1145/570738.570740).

[5] N. Tezcan and W. Wang, "ART: An asymmetric and reliable transport mechanism for wireless sensor networks", *Int. J. of Sensor Netw.*, Special Issue on Theoretical and Algorithmic Aspects in Sensor Networks, vol. 2, no. 3-4, pp. 188–200, 2006.

[6] Y. G. Iyer, S. Gandham, and S. Venkatesan, "STCP: A generic transport layer protocol for wireless sensor networks", in *Proc. 14th Int. Conf. on Comp. Commun. & Netw. ICCCN 2005*, San Diego, CA, USA, 2005, pp. 449–454.

[7] A. Karanjawane, A. W. Rohankar, S. D. Mali, and A. A. Agarkar, "Transport layer protocol for urgent data transmission in WSN", *Int. J. of Res. in Engin. & Technol.*, vol. 2, no. 11, pp. 81–89, 2013.

[8] K. Bronk, A. Lipka, and B. Wereszko, "Analysis of the topology control algorithms for the purpose of the hardware implementation", *Przegląd Telekomunikacyjny i Wiadomości Telekomunikacyjne*, vol. 4, pp. 364–367, 2012 (in Polish).

[9] N. Li, J.C. Hou, and L. Sha, "Design and analysis of an MST-based topology control algorithm", in *Proc. 22nd Ann. Joint Conf. . IEEE Comp. & Commun. INFOCOM 2003*, San Francisco, CA, USA, 2003, pp. 1702–1712.

[10] M. Bahramgiri, M. Hajiaghayi, and V. S. Mirrokni, "Fault-tolerant and 3-dimensional distributed topology control algorithms in wireless multi-hop networks", in *Proc. 11th Int. Conf. on Comp. Commun. & Netw. ICCCN 2002*, Miami, FL, USA, 2002, pp. 392–397.

[11] S. A. Borbash and E. H. Jennings, "Distributed topology control algorithm for multihop wireless networks", in *Proc. Int. Joint Conf. on Neural Netw. IJCNN'02*, Honolulu, Hawaii, USA, 2002, pp. 355–360.

[12] D. M. Blough, M. Leoncini, G. Resta, and P. Santi, "The *k*- Neighbors approach to interference bounded and symmetric topology control in ad hoc network, *IEEE Trans. on Mob. Comput.*, vol. 5, no. 9, pp. 1267–1282, 2006.

[13] K. Wu and W. Liao, "Revisiting topology control for multi-hop wireless ad hoc networks", *IEEE Trans. on Wirel. Commun.*, vol. 7, no. 9, pp. 3498–3506, 2008.

[14] K. Bronk, A. Lipka, B. Wereszko, and K. Żurek, "Hardware implementation of the self-organizing sensor network to monitor of the environmental parameters", *Przegląd Telekomunikacyjny i Wiadomości Telekomunikacyjne*, vol. 6, pp. 246–249, 2013 (in Polish).

[15] IEEE Std 802.15.4-2006: Wireless Medium Access Control (MAC) and Physical Layer (PHY) Specifications for Low-Rate Wireless Personal Area Networks (LR-WPANs), IEEE, New York, 2006.

[16] R. Niski, K. Bronk, J. Żurek, A. Lipka, B. Wereszko, and K. Żurek, "A hardware demonstrator of the self-organizing sensor network to monitor condition and hydro-meteorological threats at sea – Stage 1", National Institute of Telecommunications, Gdańsk, 2011 (in Polish).

[17] lwIP 2.0.0 LightweightIPstack [Online]. Available: http://www.nongnu.org/lwip/

Krzysztof Bronk holds Ph.D. (2010) and is an Assistant Professor in National Institute of Telecommunications. He is an author or co-author of more than 30 reviewed scientific articles and publications and about 20 R&D technical documents and studies. His research is mainly centered on the field of radiocommunication systems and networks designing and planning, software defined and cognitive radio systems development, multi-antenna technology, cryptography, propagation analysis, transmission

and coding techniques as well as positioning systems and techniques. His interests includes also multithread and object oriented applications, devices controlling applications, DSP algorithms and quality measurement solutions.

E-mail: K.Bronk@itl.waw.pl
National Institute of Telecommunications
Wireless Systems and Networks Department
Jaśkowa Dolina st 15
80-252 Gdańsk, Poland

Adam Lipka received the M.Sc. and Ph.D. degrees in Telecommunication from the Gdańsk University of Technology in October 2005 and June 2013, respectively. Since January 2006, he has been working in the National Institute of Telecommunications in its Wireless Systems and Networks Department in Gdańsk (currently as an Assistant Professor). His scientific interests include contemporary transmission techniques, MIMO systems and radio waves propagation. He is an author or co-author of over 40 scientific papers and publications.

E-mail: A.Lipka@itl.waw.pl
National Institute of Telecommunications
Wireless Systems and Networks Department
Jaśkowa Dolina st 15
80-252 Gdańsk, Poland

Błażej Wereszko received the M.Sc. in Electronics and Telecommunications from Gdańsk University of Technology in 2011. Since 2010 he works in the Wireless Systems and Networks Department of the National Institute of Telecommunications. His scientific interests focus on wireless communications, radio waves propagation, radiolocation and cognitive radio technology. He is an author or co-author of over 10 scientific papers and publications in the field of radiocommunication.

E-mail: B.Wereszko@itl.waw.pl
National Institute of Telecommunications
Wireless Systems and Networks Department
Jaśkowa Dolina st 15
80-252 Gdańsk, Poland

Jerzy Żurek received his M.Sc. and Ph.D. degrees in Telecommunication from the Gdańsk University of Technology in 1990 and 2005, respectively. Since 2005, he is employed at the National Institute of Telecommunications, Poland, (as an Assistant Professor) and since July 2014 he is also the Director of the Institute. He has also been associated with the Gdynia Maritime University. His research interest includes wireless systems theory, digital signals processing and radio propagation. He is a member of Polish Government delegation to IMO COMSAR Subcommittee in London.

E-mail: J.Zurek@itl.waw.pl
National Institute of Telecommunication
Szachowa st 1
04-894 Warsaw, Poland

Krzysztof Żurek is employed at the National Institute of Telecommunications in Wireless Systems and Networks Department in Gdańsk as an R&D specialist. Currently he is also concluding his Ph.D. thesis at the Gdańsk University of Technology. His research interest include the theory of automatic control, sensor networks and wireless systems.

E-mail: K.Zurek@itl.waw.pl
National Institute of Telecommunication
Wireless Systems and Networks Department
Jaśkowa Dolina st 15
80-252 Gdańsk, Poland

Paper

Focusing Operators and Tracking Moving Wideband Sources

Miloud Frikel[1], Said Safi[2], and Youssef Khmou[2]

[1] *GREYC Lab UMR 6072 CNRS, ENSICAEN, Caen, France*
[2] *Department of Mathematics and Informatics, Polydisplinary faculty, Beni Mellal, Morocco*

Abstract—In this paper, the localization of wideband source with an algorithm to track a moving source is investigated. To locate the wideband source, the estimation of two directions of arrival (DOA) of this source from two different arrays of sensors is used, and then, a recursive algorithm is applied to predict the moving source's position. The DOA is estimated by coherent subspace methods, which use the focusing operators. Practical methods of the estimation of the coherent signal subspace are given and compared. Once the initial position is estimated, an algorithm of tracking the moving source is presented to predict its trajectory.

Keywords—DoA, localization, tracking, wideband signal.

1. Introduction

In many problems in signal processing, the received data can be considered as a superposition of a finite number of elementary source signals and an additive noise. Generally, in a multi-sensor environment application, such as sonar, radar, and underwater acoustics, the objective is the estimation of the number and the direction of arrival (DOA) or radiating sources bearing. In the 1990s, an eigenstructure based methods [1]–[5] yield resolution have been proposed to the problem of wideband sources bearing estimation. Over the last years other approaches were published [6]–[14], some of these propositions are popular, such as Test of Orthogonality of Projected Subspaces (TOPS) [8]. TOPS is the most recent wideband DOA method and estimates DOAs by measuring the orthogonal relation between the signal and noise subspaces of multiple frequency components of the sources. However, TOPS is different from coherent methods that form a general coherent correlation matrix using focusing angles and it is different from usual incoherent methods since it takes advantage of subspaces from multiple frequencies simultaneously. Another well-known approach, the Weighted Average of Signal Subspaces (WAVES) [13] combines a robust near-optimal data-adaptive statistic. This method is used with an enhanced design of focusing matrices to ensure statistically robust preprocessing of wideband data. The DOA estimation is used to locate a mobile systems, Hence it is great deal of interest in wireless communication systems [15]–[17]. Most conventional location techniques, based on the angle, or the time of signal arrival, use the signal being transmitted by a mobile to determine its location [15]. For practical reasons, the reception points are usually existing base stations [15], [16] using array of sensors. However, to estimate the direction of arrival of a mobile, the line of sight (LOS) is required. In the case of non-line of sight (NLOS), the accuracy drastically decreases.

In the classical array processing (narrow-band signals), the parameter of interest is the direction of arrival of the radiating sources from the recorded data [1]. However, all the wideband array processing methods for DOA are based on the well-studied algorithms for narrow band sources. Indeed, two approaches were developed in the 1990s: some methods sample the frequency spectrum to create narrow band signals [2], then at each frequency bin a narrow band signal methods are used to estimate the DOA – that is the incoherent method. The other approach is the coherent signal subspace method. The cross-spectral matrices at different frequency bins are combined to form an average cross-spectral matrix. Then, the high-resolution algorithm, such as Music [3]–[5], is used to estimate the DOA. In the coherent signal subspace method, the combination of the narrow-band samples is done through the observation vector or the cross-spectral matrices, this is called focusing. The focusing operator is a matrix that transforms the location matrix at a sampling frequency to the location matrix at the focusing frequency. An improved version of the coherent signal subspace method is also reported in the [5] that uses unitary focusing matrices. A two-sided transformation is applied on the data spectral matrices.

To locate mobile station, the DOA geolocation method [17] uses simple geometrical principle to solve transmitter position. The receiver measures the direction of received wideband signals from the target transmitter using antenna arrays. DOA measurements at two receivers will provide a position fix but the accuracy of the position estimation depends on the transmitter location with respect of the two receivers, multi-path propagation etc. As a result, more than two receivers are normally needed to improve the position accuracy.

In this paper authors propose an algorithm to perform the prediction of the trajectory of a moving source. This approach will use the ARMA modeling movement of the object. Its trajectory is described by a series of coordinates calculated, previously, from two DOAs and from two arrays. The convergence of this algorithm is given.

This rest of this paper is organized as follows. In Section 2 the problem formulation is given. In Section 3, some fo-

cusing operators for wideband localization are presented. Localization of DOA and mobile location is given in the Section 4. The simulation performance is presented in the Section 5.

2. Problem Formulation

The estimation of the angle of arrival for a known signal is the main function for location systems. The conventional approach for estimating the DOA in a wireless communication system is based on transmitting a known signal, i.e. pulse (wide-band signal), and performing correlation or parametric estimations of DOA.

Let us consider an array of N sensors, which receives the waveforms generated by P wide-band sources, with M frequency bins, in the presence of an additive noise. The received signal vector in the frequency domain is given by:

$$r(f_n) = A(f_n)s(f_n) + n(f_n), \quad n = 1, \ldots, M, \tag{1}$$

where r_n is the Fourier transform of the array output vector, s_n is the $P \times 1$ vector of complex signals of P wavefronts: $s_n = [s_1(f_n), s_2(f_n), \ldots, s_P(f_n)]^T$.$n_n$ is the $N \times 1$ vector of additive noise $n_n = [n_1(f_n), n_2(f_n) \ldots, n_N(f_n)]^T$, and $A_n(\theta)$ is the $N \times P$ transfer matrix of the source-sensor array systems with respect to some chosen reference point, given by:

$$A_n(\theta) = [A_n(\theta_1), A_n(\theta_2), \ldots, A_n(\theta_P)] \ ,$$

where $A_n(\theta_i)$ is the steering vector of the array toward the direction θ_i at frequency f_n.

For simplification reason, r_n is used instead of $r(f_n)$, the same for $A(f_n)$, $s(f_n)$ and $n(f_n)$: A_n, s_n, n_n, respectively.

For example, the steering vector of a linear uniform array with N sensors is:

$$A(f_n, \theta_i) = \left[1 \ \mathrm{e}^{j\varphi_i} \ \mathrm{e}^{2j\varphi_i} \ldots \ \mathrm{e}^{(N-1)j\varphi_i}\right]^T ,$$

where: $\varphi_i = 2\pi f_n \frac{d}{c} \sin(\theta_i)$, d – sensor spacing, θ_i – direction of arrival (DOA) of the i-th source as measured from the array broadside, c – velocity wave propagation, f_n – analysis frequency.

Assume that the signals and the additive noise are stationary and ergodic zero mean complex valued random processes. In addition, the noise is assumed to be uncorrelated between sensors, and have different variances $\sigma_i^2(f_n)$ at each sensor. It follows from these assumptions that the spatial $(N \times N)$ cross-spectral matrix of the observation vector at frequency f_n is:

$$\begin{cases} \Gamma_n = E[r_n r_n^+] \\ \Gamma_n = A_n \Gamma_n^s A_n^+ + \Gamma_n^n \\ \Gamma_n^n = \sigma_n^2 I \end{cases} ,$$

where $E[.]$ denotes the expectation operator, the superscript $^+$ represents conjugate transpose, $\Gamma_n^s = E[s_n s_n^+]$ is the $P \times P$ sources cross-spectral matrix, $\Gamma_n^n = E[n_n n^+(f_n)]$ is the $P \times P$ noise cross-spectral matrix, and σ_i^2 are the noise variances at sensor i. Authors assume that the number of the sources P is supposed known. For locating the wideband sources several solutions have been proposed in the literature and are summarized as:

- the incoherent subspace methods – the analysis bandwidth is divided into several frequency bins and then at each frequency the treatment is applied and obtained results are combined to obtain the final result,
- the coherent subspace methods – the different subspaces are transformed in a predefined subspace using the focusing matrices [2]–[5].

3. Focusing Operators

The focusing matrices F_n^o's are the solution of the equations: $F_n^o A_n = A_o$, $\forall f_n \in L$, where f_o is the focusing frequency and A_o is the focusing location matrix.

The matrices A_o and A_n are function of the DOA's θ. An ordinary beamforming pre-process gives an estimate of the angles-of-arrival that can be used to form A_o. Using the focusing matrices F_n^o, the observation vectors at different frequency bins are transformed into the focusing subspace.

3.1. Coherent Signal Subspace Method

Hung and Kaveh [2] have shown that the focusing is lossless if F_n^o's are unitary transformations and proposed use of the transformation matrices obtained by the constrained minimization problem:

$$\begin{cases} \min\limits_{F_n^o} \| A_o - F_n^o A_n \| \\ F_n^{+o} F_n^o = I \end{cases} . \tag{2}$$

The focusing matrix F_n^o that solves Eq. (2) is $F_n^{Hung} = V_n W_n^+$, where the singular value decomposition of $A_o A_n^+$ is represented by $V_n \Sigma_n W_n^+$ [2].

3.2. Adaptive Focusing Operator

The focusing matrices [3] are based on signal subspace rotation at each frequency to the signal subspace at focusing frequency. The focusing matrix presented in [3] is $F_{Adaptive}^o = V_o V_n^+$, where V_o and V_n are the eigenvector matrices of Γ_o and Γ_n, respectively: $\Gamma_n = V_n \Delta_n V_n^+$, with Δ_n is the diagonal eigenvalue matrix of Γ_n.

3.3. TCT Method

In [5], the Two-sided Correlation Transformation (TCT) approach is based on transformation of the matrices $P_n = A_n \Gamma_{Sn} A_n^+$, where P_n is the cross-spectral matrix of the received data at the n-th frequency bin in a noise-free environment. Let P_o be the focusing noise-free cross-spectral

matrix. The TCT focusing matrices can be found by minimizing:

$$\begin{cases} \min\limits_{F_n^o} \| P(f_o) - F_n^o P_n F_n^{o+} \| \\ F_n^{o+} F_n^o = I \end{cases} . \tag{3}$$

It is shown [5] that the optimal solution of (3) is given by the eigenvectors of the cross-spectral matrix at the frequencies f_o and f_n. The solution of the equation system (3) is [5]:

$$F^o_{CTn} = X_o X_n^+ , \tag{4}$$

where X_o and X_n are the eigenvector matrices of P_o and P_n, respectively, $P_n = X_n \Pi_n X_n^+$, with Π_n is the eigenvalue diagonal matrix.

3.4. Fast TCT Method

In this section, the focusing operator [4] based in the rotation of the source subspace is presented (only at the frequency f_n to the source subspace at the focusing frequency f_o). This limitation to the transformation of the signal subspace reduces the computational load, and has, almost, the same performance than the TCT method.

Let the partition of the eigenvector matrix $X_n = \left[X_n^S \mid X_n^B\right]$, where X_n^S is $(N \times P)$ of P largest eigenvectors, and X_n^B is $N \times (N-P)$ of $(N-P)$ smallest eigenvectors of the cross-spectral matrix P_n. The eigenvalues of the cross-spectral of the received data P_n is:

$$\Pi_n^S = \begin{bmatrix} \Pi_n^S & 0 \\ 0 & \Pi_n^B \end{bmatrix} , \tag{5}$$

where Π_n^S is $P \times P$ of P largest eigenvalues, and Π_n^B is $(N-P) \times (N-P)$ of $(N-P)$ smallest eigenvalues of P_n. The proposed focusing operator is [4]:

$$F^o_{FTCTn} = X_o^S X_n^{S+} . \tag{6}$$

Then average cross-spectral matrix is:

$$\widetilde{P}_o = \frac{1}{M} \sum_{n=1}^{M} F_n^{So} P_n F_n^{So+} .$$

It is shown in [1] that the noise and signal subspaces are orthogonal, hence $X_n^{S+} X_n^B = X_n^{B+} X_n^S = 0$.

The P eigenvectors corresponding to the P largest eigenvalues of the cross-spectral matrix of the observation are orthonormalized [1], so we have $X_n^{S+} X_n^S = I$. Using the above properties:

$$\widetilde{P}_o = X_o^S \left[\frac{1}{M} \sum_{n=1}^{M} \Pi_n^S \right] X_o^{S+} .$$

This formula shows that the proposed operator focuses the signal subspace into the focusing frequency f_o, all the power of the different signal subspaces of the analysis band. The eigendecomposition of $\widetilde{P}^o$ is $\widetilde{P}_o = \widetilde{X}_o \widetilde{\Pi}_o \widetilde{X}_o^+$, and the partition of the eigenvector matrix $\widetilde{X}_o$: $\widetilde{X}_o = \left[\widetilde{X}_o^S \mid \widetilde{X}_o^B\right]$.

Because $\widetilde{X}_o^S$ and $\widetilde{X}_o^B$ are orthogonal, this property is used to estimate the DOA [1].

The focusing matrices could be extracted from the received cross-spectral matrix Γ_n [4]. The partition of the eigenvector matrix V is $V_n = \left[V_n^S \mid V_n^B\right]$, where V_n^S is $(N \times P)$ of P first eigenvectors, and V_n^B is $N \times (N-P)$ of $(N-P)$ last eigenvectors.

Therefore, the proposed focusing operator is then: $F^o_{FTCTn} = V_o^S V_n^{S+}$

4. TOPS Method

The test of orthogonality of projected subspaces (TOPS) [8] estimates DOAs by measuring the orthogonal relation between the signal and the noise subspaces of multiple frequency components of the sources. TOPS can be used with arbitrary shaped one-dimensional (1D) or two-dimensional (2D) arrays. Unlike other coherent wideband methods, such as the coherent signal subspace method and WAVES, this method doesn't require any preprocessing for initial values. This algorithm is summarized as follows:

1. Divide the sensor output into M identical sized blocks.
2. Compute the temporal Discrete Fourier Transform (DFT) of the M blocks.
3. For the m-th block, select $x_{m,k}$, at preselected ω_k, where $k = 0, 1, \ldots, K-1$ and $m = 0, 1, \ldots, M-1$.
4. Compute the signal subspace $V_{s,1}$ and the noise subspace $V_{n,k}$ for $k = 1, \ldots, K-1$ by Singular Value Decomposition (SVD) of estimated cross spectral matrices $\Gamma_{n,k}$.
5. Generate for each hypothesized DOA φ:
   $\Pi_i(\varphi) = I - (a_i(\varphi)^+ a_i(\varphi))^{-1} a_i(\varphi) a_i(\varphi)^+$,
   $V_{s,i}(\varphi)^{\ddagger} = \Pi_i(\varphi) V_{s,i}(\varphi)$,
   $D(\varphi) = [V_{s,1}^{+\ddagger} V_{n,1} \mid V_{s,2} +\ddagger V_{n,2} \mid, \ldots, \mid V_{s,K-1} +\ddagger V_{n,K-1}]$.
6. Estimate $\theta = \arg\max\limits_{\varphi} \dfrac{1}{\sigma(\varphi)}$, where $\sigma(\varphi)$ is the smallest singular value of $D(\varphi)$; the estimation is now to find P local maxima by doing a one-dimensional search.

TOPS method is different from coherent methods that form a general coherent correlation matrix using focusing angles. It is also different from usual incoherent methods since it takes advantage of subspaces from multiple frequencies simultaneously.

5. Mobile Localization

The FTCT algorithm is summarized as follows. First, an ordinary estimator is used to scan the space and find an initial estimate of the DOA.

1. Form $\widehat{A}_n$ and estimate
$$\widehat{\Gamma}_n^S = \left(\widehat{A}_n^+\widehat{A}_n\right)^{-1}\widehat{A}_n^+\left[\widehat{\Gamma}_n^{NS}\right]\times\widehat{A}_n\left(\widehat{A}_n^+\widehat{A}_n\right)^{-1},$$
where $\widehat{\Gamma}_n^{NS}$ is the noiseless received data.

2. Obtain the average the source cross-spectral matrices:
$$\widetilde{\Gamma}_o^S = \frac{1}{M}\sum_{n=1}^{M}\widehat{\Gamma}_n^S.$$

3. Estimate the cross-spectral matrix of the received data: $\widetilde{\Gamma}_o = \widehat{A}_o\widetilde{\Gamma}_o^S\widehat{A}_o + \widehat{\sigma}_o^2 I$.

4. Find $\widetilde{P}_o = \widehat{A}_o\widetilde{\Gamma}_o^S\widehat{A}_o^+$, and $\widehat{P}_n = \widehat{\Gamma}_n - \widehat{\sigma}_n^2 I, n = 1,\ldots,M$.

5. Determine the focusing operator. Multiply these matrices by the sample cross-spectral matrices, and average the results: $\widetilde{P}_o = X_o^S\left[\frac{1}{M}\sum_{n=1}^{M}\Pi_n^S\right]X_o^{S+}$.

6. Apply a localization method e.g. MUSIC [1] to find the DOA of the source.

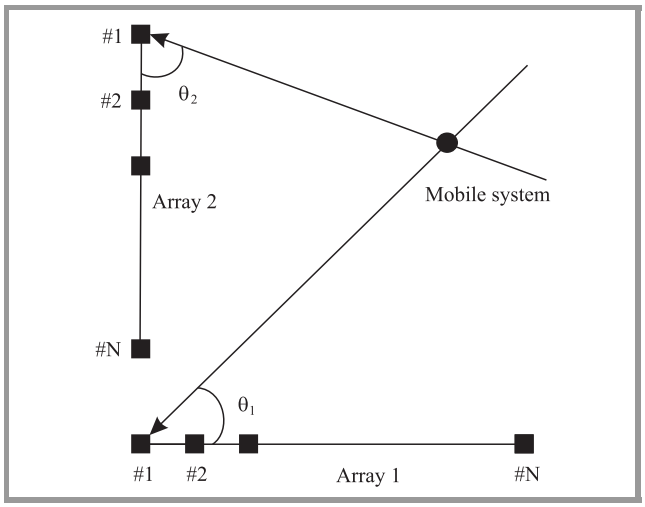

Fig. 1. Geolocation by angulation.

Finally, once these DOAs are estimated from two arrays of sensors, as shown in Fig. 1, the angulation technique is then used to estimate the moving source position.

6. Tracking a Moving Source

It is desired to perform the trajectory prediction of a moving source on a map. This approach will use the ARMA modeling object movement. Moving source on a map is observed. Its trajectory is described by a series of coordinates stored in a file containing the following information. These coordinates were calculated from two DOAs estimated from two arrays. The goal here is to anticipate the best path of the source position and to predict the source location at to time $t+1$ using known values. We denote $\xi(t+1)$ the x and y coordinates of the source. The coordinates are estimated from two DOAs estimated below, and $\widehat{\xi}(t+1|t)$ of the prediction $\xi(t+1)$ knowing the position of the object until a time t. This prediction can be considered as a filtering performed by:

$$\widehat{\xi}(t+1|t) = H(z^{-1})\xi(t),$$

with

$$H(z^{-1}) = H_0 + H_1.z^{-1} + \cdots + H_n.z^{-L},$$

where L is the filter order and H_i is the dimension of 2×2. This trajectory modeling is a modeling type Auto Regressive (AR). This prediction $\widehat{\xi}(t+1|t)$ can be rewritten as least squares formalism as:

$$\widehat{\xi}(t+1|t) = \widehat{\Omega}_t^T\varphi(t), \tag{7}$$

where $\varphi(t)$ is a vector of dimension $2(L+1)$ and $\widehat{\Omega}_t$ is a matrix $2\times 2(L+1)$, respectively, and given by:

$$\varphi(t) = \begin{pmatrix} \xi(t) \\ \xi(t-1) \\ \cdots \\ z(t-L) \end{pmatrix} \quad \text{and} \quad \widehat{\Omega}_t = \begin{pmatrix} H_0 \\ H_1 \\ \cdots \\ H_L \end{pmatrix}.$$

Let

$$\begin{cases} \widehat{\omega}_t = col(\widehat{\Omega}_t^T) \\ \phi(t) = \varphi(t)\otimes I_2 \end{cases},$$

where $\widehat{\omega}_t = col(\widehat{\Omega}_t^T)$ is a column vector of dimension $4(L+1)$, $\phi(t) = \varphi(t)\otimes I_2$ a matrix of dimension $4(L+1)\times 2$, and $\otimes$ is the Kronecker product. The equation (7) can also be put in a more general form as:

$$\widehat{\xi}(t+1|t) = \phi^T(t)\widehat{\omega}_t. \tag{8}$$

To enable a recursive estimation of $\widehat{\omega}_t$ vector parameter and therefore a correct prediction $\xi(t+1)$ is proposed to use the least-squares algorithm with recursive forgetting factor. The adapted version of the algorithm of multivariable problem (the output is a vector with 2 dimensions) has the following form:

1. $\widehat{\xi}(t+1|t) = \phi(t)^T\widehat{\omega}_t$,
2. $\varepsilon(t+1|t) = \xi(t+1) - \widehat{\xi}(t+1|t)$,
3. $K_t = P_t\phi(t)(\phi(t)^T P_t\phi(t) + \lambda I_2)^{-1}$,
4. $\widehat{\omega}_{t+1} = \widehat{\omega}_t + K_t\varepsilon(t+1|t)$,
5. $P_{t+1} = \frac{1}{\lambda}(P_t - K_t\phi(t)^T P_t)$.

where $0<\lambda<1$ is the forgetting factor. The algorithm converges rapidly for high value of λ but with an important variance. However, for a very low λ one can notice the weak variance with the very slow convergence.

7. Simulation Results

To analyze the performance of the presented focusing operators, the normalized root mean-square error (NRMSE) is employed as a performance tool of the input estimates, it is given by:

$$\text{NRMSE} = \frac{1}{\|\theta\|} \quad \frac{1}{K}\sum_{i=1}^{K}\|\hat{\theta}_i - \theta\|^2\Bigg)^{\frac{1}{2}}, \tag{9}$$

where K is the number of the trials and $\hat{\theta}_i$ is the estimated DOA from the i-th trial.

A linear array of $N = 5$ omnidirectional sensors at the base station in order to have a spatial diversity with equal inter-element spacing $d = \frac{c}{2f_o}$ is used, where f_o is the center frequency and c is the propagation velocity. The source signals are temporally stationary zero-mean bandpass white Gaussian processes with the center frequency $f_o = 902.5$ MHz and the same bandwidth $B_w = 25$ MHz.

The distance d between two consecutive sensors at the base station is 16.62 cm, hence the total distance of the array is 66.48 cm. The noise is stationary zero-mean bandpass (the same pass-band as that the signals) white gaussian process, independent of the signals, and statistically independent and identical. One moving punctual source impinging from the angle $-55°$ at the array 1 and from $10°$ at the array 2, with a SNR of 3 dB is used for this simulation. Figures 2 and 3 represent the results of localization functions $f(\theta)$ of the FTCT method by two arrays.

In the second part of the simulation, the performance of TCT, FTCT, adaptive and Hung methods was compared, where the SNR varies from 0 dB to 35 dB, the results of the NRMSE are presented in Fig. 4.

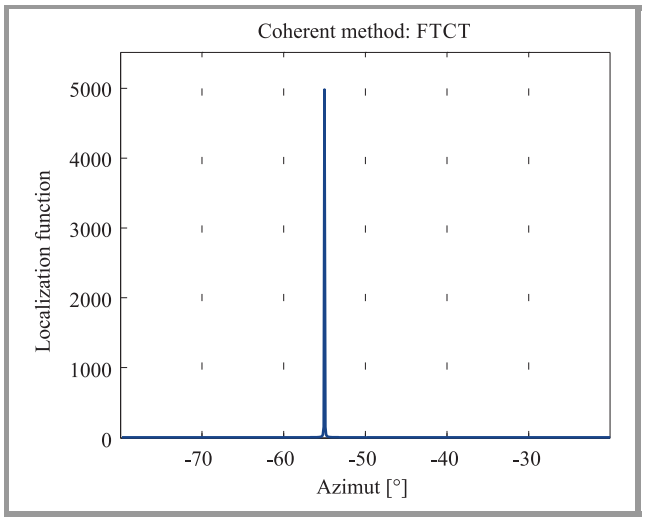

Fig. 2. Estimation of the DOA of the source from Array 1, SNR = 3 dB.

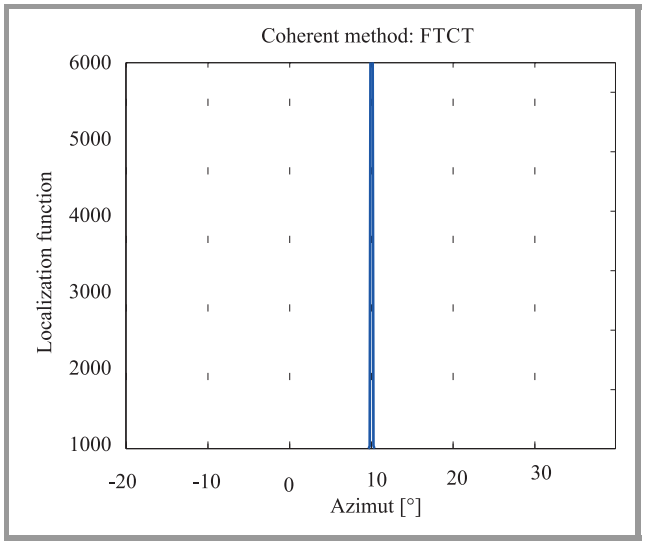

Fig. 3. Estimation of the DOA of the source from Array 2, SNR = 3 dB.

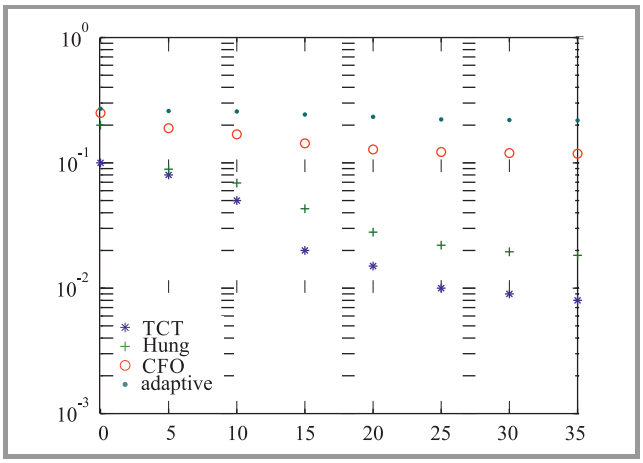

Fig. 4. NRMSE of one mobile location (y axis) vs. SNR (x axis) for different focusing operators.

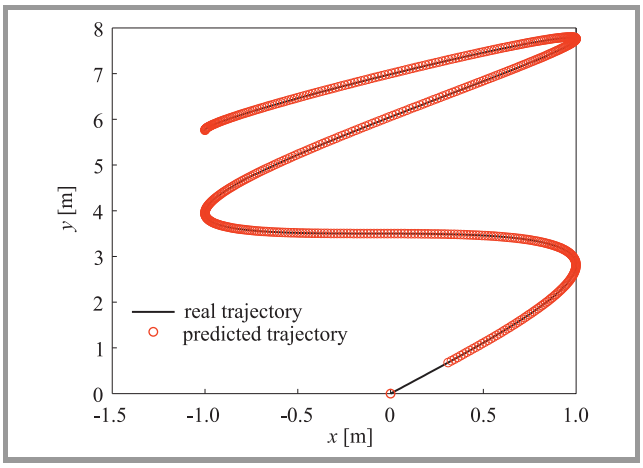

Fig. 5. Estimation of the trajectory of moving punctual source.

The TCT and Hung's operator achieve a higher performance compared to the adaptive and FTCT methods. However, this last method is very interesting in term of computational load because only one part of the eigenvectors are used to built the focusing operators.

In the case of moving punctual radiating source, such as a robot with single transmitting antenna, the arrays system and the moving object are in the same horizontal plane. The following parametric model for the trajectory is proposed:

$$\begin{cases} \vec{r}(t) = x(t)\vec{e}_x + y(t)\vec{e}_y \\ x(t) = \sin(\omega_1 t) \\ y(t) = x(t) + 7\sin(\omega_2 t) \end{cases}, \tag{10}$$

where $\vec{r}(t)$ is the position of the punctual source at instant t, $\omega_1 = \pi$ rad/s and $\omega_2 = 0.5234$ rad/s, the initial position $r(t=0) = 0$ m, corresponds to the solution of the angulation technique from the DOAs $\theta_1 = -55°$ and $\theta_2 = 10°$. The least mean square algorithm is used to predict the trajectory of the moving source with forgetting factor $\lambda = 0.99$. The results of the prediction proces, for a period $T = 3.5$ s, are given in Fig. 5 and Fig. 6. Finally, in Fig. 7, the convergence rate of the first parameter $\omega_t(1)$ is presented.

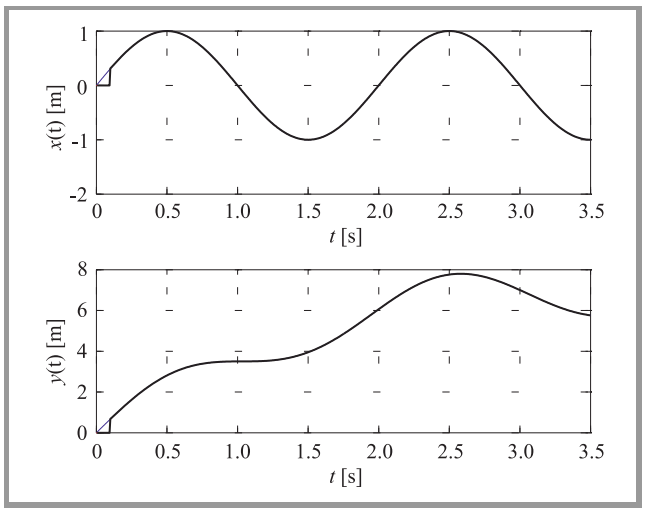

Fig. 6. *x-y* coordinates of moving punctual source.

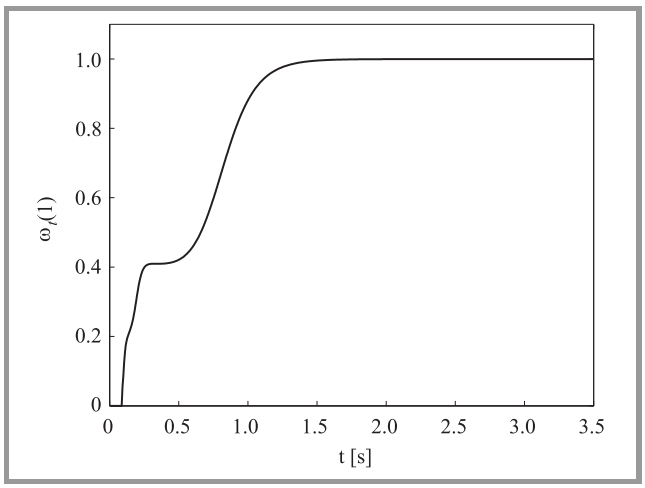

Fig. 7. Convergence of the 1st parameter $\omega_t(1)$.

8. Conclusion

In this paper a class of focusing operators were studied, and their numerical performances were evaluated. The obtained results show the efficiency of the eigenvectors focusing operators in term of accurate angles. These operators were used to estimate the DOAs of a known pulse and to locate mobile station. Once two directions of arrival of wideband source is estimated at instant t, an algorithm of LMS is used to track this moving source.

References

[1] R. O. Schmidt, "Multiple emitter location and signal parameters estimation", *IEEE Trans. Antenn. and Propagat.*, vol. AP-34, no. 3, pp. 276–280, 1986 (doi: 10.1109/TAP.1986.114830).

[2] H. Hung and M. Kaveh, "Focusing matrices for coherent signal-subspace processing", *IEEE Trans. ASSP*, vol. 36, no. 8, pp. 1272–1281, 1988 (doi: 10.1109/29.1655).

[3] S. Bourennane, C. Fossati, and J. Marot, "About noneigenvector source localization methods", *EURASIP J. on Adv. in Sig. Process.*, ID 480835:13, 2008 (doi: 10.1155/2008/480835).

[4] M. Frikel and S. Bourennane, "Traitement large bande: Opérateurs de focalisation", *Annals of Telecommun.*, vol. 52, no. 5–6, pp. 339–348, 1997 (in French).

[5] S. Valaee and P. Kabal, "Wideband array processing using a two-sided correlation transformation", *IEEE Trans. on Sig. Process.*, vol. 43, no. 1, pp. 160–172, 1995.

[6] M. Agrawal and S. Prasad, "DOA estimation of wideband sources using a harmonic source model and uniform linear array", *IEEE Trans. on Instr. and Measur.*, vol. 47, no. 3, pp. 619–629, 1999 (doi: 10.1109/78.747780).

[7] F. Sellone, "Robust auto-focusing wide-band DOA estimation", *Signal Process.*, vol. 86, no. 1, pp. 17–37, 2006 (doi: 10.1016/j.sigpro.2005.04.009).

[8] Y.-S. Yoon, M. Kaplan, and J. H. McClellan, "Tops: New DOA estimator for wideband signals", *IEEE Trans. on Sig. Process.*, vol. 54, no. 6, pp. 1977–1989, 2006 (doi: 10.1109/TSP.2006.872581).

[9] L. Zhou, Y. J. Zhao, and Hao Cuin, "High resolution wide-band DOA estimation based on modified music algorithm" in *Proc. Int. Conf. on Inform. & Autom. ICIA 2008*, Changsha, China, 2008, vol. 54, pp. 20–22 (doi: 10.1109/ICINFA.2008.4607961).

[10] W. Cui, H. Lim, and K. Eom, "DOA estimation for wideband signal: Multiple frequency bins versus multiple sensors", in *Proc. 7th Ann. IEEE Consumer Commun. & Netw. Conf. CCNC 2010*, Las Vegas, NV, USA, 2010, vol. 54, pp. 1–5, (doi: 10.1109/CCNC.2010.5421847).

[11] L. Lu and H.-C. Wu, "Novel robust direction-of-arrival-based source localization algorithm for wideband signals", *IEEE Trans. on Wirel. Commun.*, vol. 11, no. 11, pp. 3850–3859, 2012.

[12] Z.-M. Liu, Z.-T. Huang, and Y.-Y. Zhou, "Direction-of-arrival estimation of wideband signals via covariance matrix sparse representation", *IEEE Trans. on Sig. Process.*, vol. 59, no. 9, pp. 4256–4270, 2011.

[13] E. D. Di Claudio and G. Jacovitti, "Wideband source localization by space-time music subspace estimation", in *Proc. 8th Int. Symp. on Image and Sig. Process. & Anal. ISPA 2013*, Trieste, Italy, 2013, pp. 331–336, Sept. 2013.

[14] K. Yu, M. Yin, J. Luo, M. Bao, Y.-H. Hu, and Z. Wang, "A direct wideband direction of arrival estimation under compressive sensing", in *IEEE 10th Int. Conf. on Mob. Ad-Hoc and Sensor Syst. MASS 2013*, Hangzhou, China, 2013, pp. 603–608.

[15] J. J. Caffery and G. L. Stuber, "Overview of radiolocation in CDMA cellular systems", *IEEE Commun. Mag.*, vol. 36, no. 4, pp. 38–45, Apr. 1998.

[16] T. Rappaport, *Wireless Communications: Principles and Practice.* Prentice Hall, NJ, 1996.

[17] M. Frikel and B. Barroso, "Mobile positioning: Angle of arrival estimation", in *Proc. 4th Conf. on Telecommun. ConfTele'2003*, Aveiro, Portugal, 2003, pp. 235–238.

Miloud Frikel received his Ph.D. degree from the center of mathematics and scientific computation CNRS URA 2053, France, in array processing. Currently, he is with the GREYC laboratory (CNRS URA 6072) and the ENSI-CAEN as Assistant Professor. From 1998 to 2003, he was with the Signal Processing Lab, Institute for Systems and Robotics, Institute Superior Tecnico, Lisbon, as a researcher in the field of wireless location and statistical array processing, after been a research engineer in a software company in Munich, Germany. He worked in the Institute for Circuit and Signal Processing of the Technical University of Munich. His research interests span several areas, including statistical signal and array processing, cellular geolocation (wireless location), space-time coding, direction finding and source localization, blind channel identification for wireless communication systems, and MC-CDMA systems.

E-mail: mfrikel@greyc.ensicaen.fr
GREYC UMR 6072 CNRS
Ecole Nationale Supérieure d'Ingénieurs
de Caen (ENSICAEN)
B. Maréchal Juin 6
14050 Caen, France

Said Safi received the B.Sc. degree in Physics (option Electronics) from Cadi Ayyad University, Marrakech, Morocco in 1995, M.Sc. and Doctorate degrees from Chouaib Doukkali University and Cadi Ayyad Univerrsity, in 1997 and 2002, respectively. He has been a Professor of information theory and telecommunication systems at the National School for Applied Sciences, Tangier, Morocco, from 2003 to 2005. Since 2006, he is a Professor of applied mathematics and programming at the Faculty of Science and Technics, Beni Mellal, Morocco. In 2008 he received the Ph.D. degree in Telecommunication and Informatics from the Cadi Ayyad University. His general interests span the areas of communications and signal processing, estimation, time-series analysis, and system identification – subjects on which he has published 14 journal papers and more than 60 conference papers. Current research topics focus on transmitter and receiver diversity techniques for single- and multi-user fading communication channels, and wide-band wireless communication systems.

E-mail: safi.said@gmail.com
Department of Mathematics and Informatics
Beni Mellal, Morocco

Youssef Khmou obtained the B.Sc. degree in Physics in 2010, M.Sc. degree in 2012 and Ph.D. degree in 2015 from Sultan Moulay Slimane University, Morocco. His research interests include statistical signal and array processing and statistical physics.

Email: khmou.y@gmail.com
Department of Mathematics and Informatics
Beni Mellal, Morocco

Paper

Implementation of Standardized Cooperation Environment for Intelligent Transport Systems

Marian Kowalewski and Andrzej Pękalski

National Institute of Telecommunications, Warsaw, Poland

Abstract—Many of Intelligent Transport Systems (ITS) solutions are using components that dynamically change in time and space. Among these, there occur changes of location, movement parameters, components configuration, external environment influence, automation use, etc. Standard facilities in ITS communication model are useful base for implementation of the services in such variable environment. Such features have an influence on the implementation of the services and requirements for the lower communication layers.

Keywords—C-ITS, communication, facilities, services.

1. Introduction

In each phase of the transportation and logistic actions (e.g. loading goods, transferring, the unloading etc.) a relevant information is exchanged. Thus, present transport needs reliable communications as essential part of such activity.

The communication is gaining the even greater significance in transport systems using information and communication technology (ICT) solutions, acting in the automated or full automatic way. One can say, that sophisticated communication is a key to intelligent transport systems cooperation with each other Cooperative ITS (C-ITS).

ITS information exchange requirements are similar to the communication requirements generally used in other ICT applications such as: capacity, response time, reliability, etc. However, in certain instances a special requirements are applied, and, from a point of view of purposes and activity conditions of the transport system, they are often critical. These particular requirements cover: the knowledge of local conditions, the adaptation to them, the speed, the certainty of acting, etc. Implementation of the application responsible for the safety or programming automatic reaction to circumstances of the environment can depends on these local conditions, e.g. weather conditions, infrastructure state, breakdowns, other object behavior, etc.

Such issues are important especially in application in moving vehicles which have to cooperate with applications located in other vehicles as vehicle to vehicle – V2V relation, or with applications located in transport infrastructure as vehicle to infrastructure – V2I relation or infrastructure to vehicle – I2V relation, generally V2X relation.

In ITS solutions, the mechanisms to provide the communication for applications in varying conditions are used. This is an effect of standardization, so that all transport services can use them in different circumstances.

Implementation of ITS services on the standard base needs:

- methodology of defining ITS components, their description and principles of cooperation with other platforms,
- service solutions adapted to real conditions, including local experience from their usage,
- tools needed for the implementation of standardized solutions.

Such standardized solutions are described in public documents, i.e. European Standards (EN). Knowledge of these solutions is necessary for implementation C-ITS services in Poland.

Communication processes in ITS are important for not only the completion of separate transport processes, but also for the integration and the cooperation of transport systems, which are based on various platforms. The good knowledge of communication environment will accelerate designing and manufacturing of big ICT systems in ITS area.

The facilities layer takes an essential role in the standardized architecture of the ITS communication [1]. This layer executes shared functions, allowing actions and cooperation integration. The communications means, required by the facilities layer, are seen as the network and the transport layer.

Action presentation and problems indication connected to realization, especially in the layer of facilities, are significant steps for implementing ITS systems. The Polish national environment should be also considered. However, it is significant, that presented solutions are in the course of creation (even they are placed in approved documents). Therefore, in many places there appear remarks on the incomplete statements and follow-up works on standard documents.

Methods and solutions proposal, presented here are taken from standards. This study is an attempt of the synthesis of the certain essential fragment of the ITS standardization results. It is also an attempt to locate these issues in Polish context for better assimilation in professional environment.

2. Application Requirements

The aim of ITS are transport services where ICT applications take an important part. It means that ITS is cooperative product of transport entities as well as ICT technologies.

From institutional point of view, ITS applications issues and their communication requirements were an object of the activity many international projects, inspired by industry as well as by state administrations. An example of powerful and fruitful activity is CAR 2 CAR Communication Consortium, created by major automotive companies from Europe, USA and Far East regions. This consortium prepared a document [2] where visions of the communication were framed in ITS systems. These visions were developed and experimentally verified as part of other projects [3]. Their result, are standardization documents.

One of that document is ETSI TR 102 638 report [4], which defines Basic Set of ITS Applications (BSA). According to ETSI methodology, this document supports beginning of the technical specifications and standards development process. List of the services and applications included in BSA along with the proposal of their Polish translation and definitions were placed in [5]. BSA is important, in case of statement of fundamental assumptions in relation to the structure of the homogeneous environment for the set of ITS specific services. This set of services remains open. However, functional requirements resulting from it were transferred into methodology solutions for building the application layer, especially layers of common facilities of the ITS communication model.

In this section is shown how requirements are formulated, leading to the completion of services from components, supposed to ensure execution of the services in the dynamically changing environment.

2.1. ITS Applications Functional Requirements Statement

Functional requirements description rules are based on ETSI TS 102 637-1. They are divided into two groups: application requirements and use case requirements.

Application functional requirements: General application functional requirements, which applies for all use cases of this application. Application functional requirements are signed as **[FR_application_#_stationtype]**, where:

- **FR** means functional requirement,
- **application** provide acronym of application to which the requirement applies,
- # is sequence number of requirement,
- **stationtype** indicates ITS station type to which the requirement applies; it could missed when the requirement is not correspond to any specific station type.

Use case (UC) functional requirements: Functional requirements for specific use cases, do not apply to other use cases of the same or other applications. Use case functional requirements are signed as **[FR_UC#_#_stationtype]**, where:

- **FR** means functional requirement,
- **UC#** is designation of use case, to which the requirement applies,
- # is sequence number of requirement,
- **stationtype** indicates ITS station type to which the requirement applies; it could missed when the requirement is not correspond to any specific station type.

Station types defined in ITS communication architecture are:

- CS – central station,
- VS – vehicle station,
- RS – roadside station,
- PS – personal station.

An example of an application of the functional requirements is the Cooperative Awareness (CA) application. Its implementation is based on exchange of messages named Cooperative Awareness Message (CAM) and Decentralized Environment Notification Message (DENM), in the ITS network, in V2X relations. These messages transfer information on vehicles attributes and their nearest surroundings. Details of these messages proceedings will be shown hereinafter.

Table 1 provides list of functional CA applications requirements (to be verified in real conditions) connected to driver support[6].

The next specification stage is use case requirements set for one use case included in CA application, e.g. UC003: Intersection collision warning, shown in Table 2 [6]. It should be noted that at this detail level are required interfaces to technical means, like transmission media or Human Machine Interface (HMI).

2.2. Identification of Facilities for ITS Applications

Functional requirements implementation is common for many use cases and applications, and is addressed to the facilities layer of ITS communication model, located directly below the application layer. This is so-called facilities layer serves typical operations and applications specified on higher layer.

ETSI TS 102 894-1 [7] identified two groups of facilities for ITS applications: common facilities and domain fa-

Table 1
An example of Cooperative Awareness application functional requirements

FR_CA_001	An ITS station shall announce its presence to its vicinity
FR_CA_002	An ITS station shall broadcasts its position, speed and moving direction to its vicinity
FR_CA_003_VS	A vehicle ITS station shall broadcast its basic dynamics and status information to its vicinity
FR_CA_004	CAM shall provide the position information with a confidence level that is sufficient for the all use cases
FR_CA_005_VS	Vehicle ITS station shall have access to the in vehicle system to obtain the required information for the CAM construction
FR_CA_006	A receiving ITS station should update the position of the sending ITS station
FR_CA_007	Information included in CAM shall allow receiving ITS station to estimate the relevance of the information and the risk level
FR_CA_008	An ITS station shall be able to modify the sending interval of two consecutive CAMs
FR_CA_009	CAM shall be set with high priority for transmission
FR_CA_010	ITS station shall provide one hop broadcasting functionality for CAM

Table 2
An example of use case functional requirements for UC003: Intersection collision warning

FR_UC003_001	Unique use case identifier shall be defined in this use case
FR_UC003_002	Unique event identifier shall be defined for this use case If the “intersection collision” event can be divided into multiple sub event types, a unique event identifier shall be defined to each of the sub event type
FR_UC003_003	The application at the originating ITS station shall be able to request the construction and the transmission of an “intersection collision warning” DENM in complementary of CAM
FR_UC003_004	If DENM is sent, the originating ITS station shall be able to detect the vehicle positions and movements within the intersection area
FR_UC003_005	If DENM is sent, the originating ITS station shall be able to verify whether the “intersection collision warning” event that may be a risk
FR_UC003_006	If DENM is sent, the application at the originating ITS station shall be able to provide required information for the “intersection collision warning” DENM construction
FR_UC003_007	If DENM is sent, the application at the originating ITS station shall define the transmission rate of the “intersection collision warning” DENM
FR_UC003_008	If DENM is sent, the application at the origination ITS station shall define the transmission area of the “intersection collision warning” DENM and provide to the network and transport layer
FR_UC003_009	If DENM is sent, the application at the originating ITS station shall define the transmission latency requirement and the priority of the “intersection collision warning” DENM
FR_UC003_010	If DENM is sent, the application at the ITS station shall provide the estimated intersection collision position as the event position
FR_UC003_011	If DENM is sent, the application at the originating ITS station shall be able to stop sending the DENMs when the “intersection collision” event is terminated
FR_UC003_012_VS	The vehicle ITS stations shall include the vehicle type and size information in CAM
FR_UC003_013_VS	Information in CAM or DENM shall allow the application at the receiving vehicle ITS station to check the relevance of the information and estimate the risk level
FR_UC003_014_VS	The application at the receiving ITS station shall decide whether a warning or information of “intersection collision” event is provided to the driver via HMI
FR_UC003_015_VS	The application at the vehicle ITS station should present the “intersection collision warning” to the driver via HMI at an appropriate timing
FR_UC003_016_VS	The application at the vehicle ITS station may further broadcast its itinerary to pass the intersection

Table 3
List of common facilities

Classification	Identifier	Facility name	Short description
Management	CF001	Traffic class management	Manage assignment of traffic class value for the higher layer messages
	CF002	ITS-S ID management	Manage ITS-S identifiers used by the application and the facilities layer
	CF003	AID management	Manage the application ID used by the application and the facilities layer
	CF004	Security access	Deal with the data exchanged between the application and facilities layer with the security entity
Application support	CF005	HMI support	Support the data exchanges between the applications and HMI devices
	CF006	Time service	Provide time information and time synchronization service within the ITS-S
	CF007	Application/facilities status management	Manage the functioning of active applications and facilities within the ITS-S
	CF008	SAM processing	Support the transmission and receiving of the service announcement message (SAM)
Information support	CF009	Station type/capabilities	Manage the ITS-S type and capabilities information
	CF010	ITS-S positioning service	Calculate the real time ITS-S position and provides the information to the applications/facilities layers
	CF011	Location referencing	Calculate the location referencing information and provide the data to the applications/facilities layers
	CF012	Common data dictionary	Data dictionary for messages
	CF013	Data presentation	Message encoding/decoding support
Communication support	CF014	Addressing mode	Select addressing mode for messages transmission
	CF015	Congestion control	Facilities layer decentralized congestion control functionalities

cilities. Common facilities (CF) (Table 3) are required for ITS station (ITS-S) operation and/or support for communication interoperability. Additionally, certain common facilities transfer cross layer information to the management and security entities.
The common facilities from Table 3 are identified by unique number CF#. For each facility a set of functions and interfaces is identified.
Function is denoted by an identifier [CF#_F#], where:

- CF# identifies of common facility,
- F# indicates of function number.

Interface is denoted an identifier [CF#_IN#], where:

- CF# identifies of common facility,
- IN# indicates of interface number.

Domain Facilities (DFs) are services and functions for one or more BSA applications or for one or more ITS station types. Domain facilities could be optional for other ITS applications and other ITS-S types. Table 4 provides list of domain facilities identified in standardization documents [7].

Domain facility is identified by unique number **DF#**. For each facility a set of functions and interfaces is defined.
Function is denoted by an identifier **[DF#_F#]**, where:

- DF# identifies of domain facility,
- F# indicates a function number.

Interface is denoted by an identifier **[DF#_IN#]**, where:

- DF# identifies of domain facility,
- IN# indicates a interface number.

As an example, functional requirements two facilities are presented, which are the base for implementation of use case UC003: Intersection collision warning, such as requirements for DF001: DEN basic service and DF002: CA basic service.

2.3. Functional Requirements Identification Example

The domain facility DF001 executes Decentralized Environment Notification Message (DENM) protocol associated

Table 4
List of domain facilities

Classification	Identifier	Facility name	Short description
Application support	DF001	DEN basic service	Support the protocol processing of the DENM
	DF002	CA basic service	Support the protocol processing of the CAM
	DF003	EFCD	Aggregation of CAM/DENM data at the road side ITS-S and provide to the central ITS-S
	DF004	Billing and payment	Provide service access to billing and payment service provider
	DF005	SPAT basic service	Support the protocol processing of the Signal Phase and Timing Message
	DF006	TOPO basic service	Support the protocol processing of the Road Topology Message
	DF007	IVS basic service	Support the protocol processing of the In Vehicle Signage Message
	DF008	Community service user management	Manage the user information of a service community
Information support	DF009	Local dynamic map	Local Dynamic Map database and management of the database
	DF010	RSU management and communication	Manage the Road Side Units from the central ITS-S and communication between the central ITS-S and road side ITS
	DF011	Map service	Provide map matching functionality
Communication support	DF012	Session support	Support session establishment, maintenance and closure
	DF013	Web service support	High layer protocol for Web connection, SOA application protocol support
	DF014	Messaging support	Manage ITS services messages based on message priority and client services/use case requirements
	DF015	E2E geocasting	Deal with the disseminating of information to ITS vehicular and personal ITS stations based on their presence in a specified geographical area

with this message. DENM is used in cooperative road hazard applications mainly in order to inform other road users about detected events.

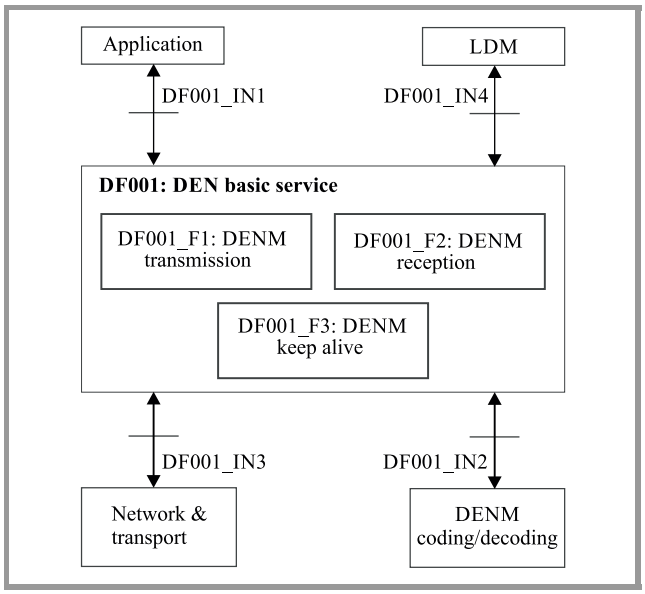

Fig. 1. Block diagram of DF001: DEN basic service according to ETSI TS 102 894-1.

The source of the DENM is the ITS station, which have detected an event. The application provides attributes data of detected event: type, duration, location, as well as DENM destination dissemination area to DEN basic service. The DEN service constructs the DENM and provides it to network and transport layer. At the reception, DEN service filters not valid messages. Further received information is provided to application directly or via common database (Local Dynamic Map – LDM). Keep alive function may forward valid messages to protect their dissemination in the case of dynamic events.

Figure 1 shows DEN service functional configuration and external interfaces [7].

Table 5 provides functional requirements and Table 6 provides interfaces to external components descriptions addressed to DEN basic service according to ETSI TS 102 894-1 [7].

2.4. Functional Requirements Example Set out for DF002 CA Basic Service

The Cooperative Awareness (CA) basic service is a facilities layer entity providing the management of facilities layer data, needed for ITS stations cooperation. It executes the protocol associated with CAM. In BSA, this

Table 5
Functional requirements for DF001: DEN basic service

Function	Requirements
[DF001_F1]	The function shall execute the DENM transmission protocol. It constructs a DENM when receiving a request from application, and initiates the DENM transmission. The DENM format shall be as specified in ETSI EN 302 637-3 [8]. The DENM transmission protocol shall include functionalities to enable the DENM initiation, DENM updates and DENM termination from originator ITS-S.
[DF001_F2]	The function shall execute the DENM reception protocol. It decodes a received DENM, manages its lifetime according to a validity time and provides the DENM content to the applications and/or to the LDM when requested. The DENM reception protocol shall include functionalities to discard the outdated DENM and to provide the update DENM content to the ITS applications.
[DF001_F3]	The function shall execute a forwarding of a DENM which is still valid within a specific area and specific duration (keep alive). This function is optional.

Table 6
Interfaces of DF001: DEN basic service

Interface	Related component	Direction	Information exchanged over the interface
[DF001_IN1]	Application, LDM or other facilities	In/out	In: Request from application for the transmission of new DENM, updated DENM or DENM termination, together with the data related to the detected event and the DENM dissemination requirements. Out: Content of the received DENM.
[DF001_IN2]	Data presentation	In/out	Data required for the DENM encoding/decoding, as supported by the data presentation common facility.
[DF001_IN3]	ITS network and transport layer	In/out	In: Received DENM content from the Network & Transport (N&T) layer. Out: DENM content to the N&T layer for DENM transmission.
[DF001_IN4]	LDM or other facilities	Out	Content of the received DENM.

Table 7
Functional requirements for DF002: CA basic service

Function	Requirements
[DF002_F1]	The function shall collect data required to construct a CAM. The CAM format shall be as specified in ETSI EN 302 637-2 [9].
[DF002_F2]	The function shall manage the CAM transmission frequency according to the congestion level.
[DF002_F3]	The function shall transmit the CAM to the networking and transport layer.
[DF002_F4]	The function shall process the received CAMs

facility is relevant to vehicle ITS-S and roadside ITS-S. It is expected that other ITS-S may use the CAM in the future.

CA basic service periodically constructs and transmits CAM. It cooperates with other facilities in order to collect the data needed for CAM. In case of CAM reception, the service decodes the message and transfer received data to the application and/or to LDM, which is common local facilities layer database. CAM is a heartbeat message of the facilities layer. Interval of CAM transmission may vary from several hundred milliseconds to one second. It depends on application requirements and/or network congestion level. Figure 2 shows CA service functional configuration and external interfaces [7].

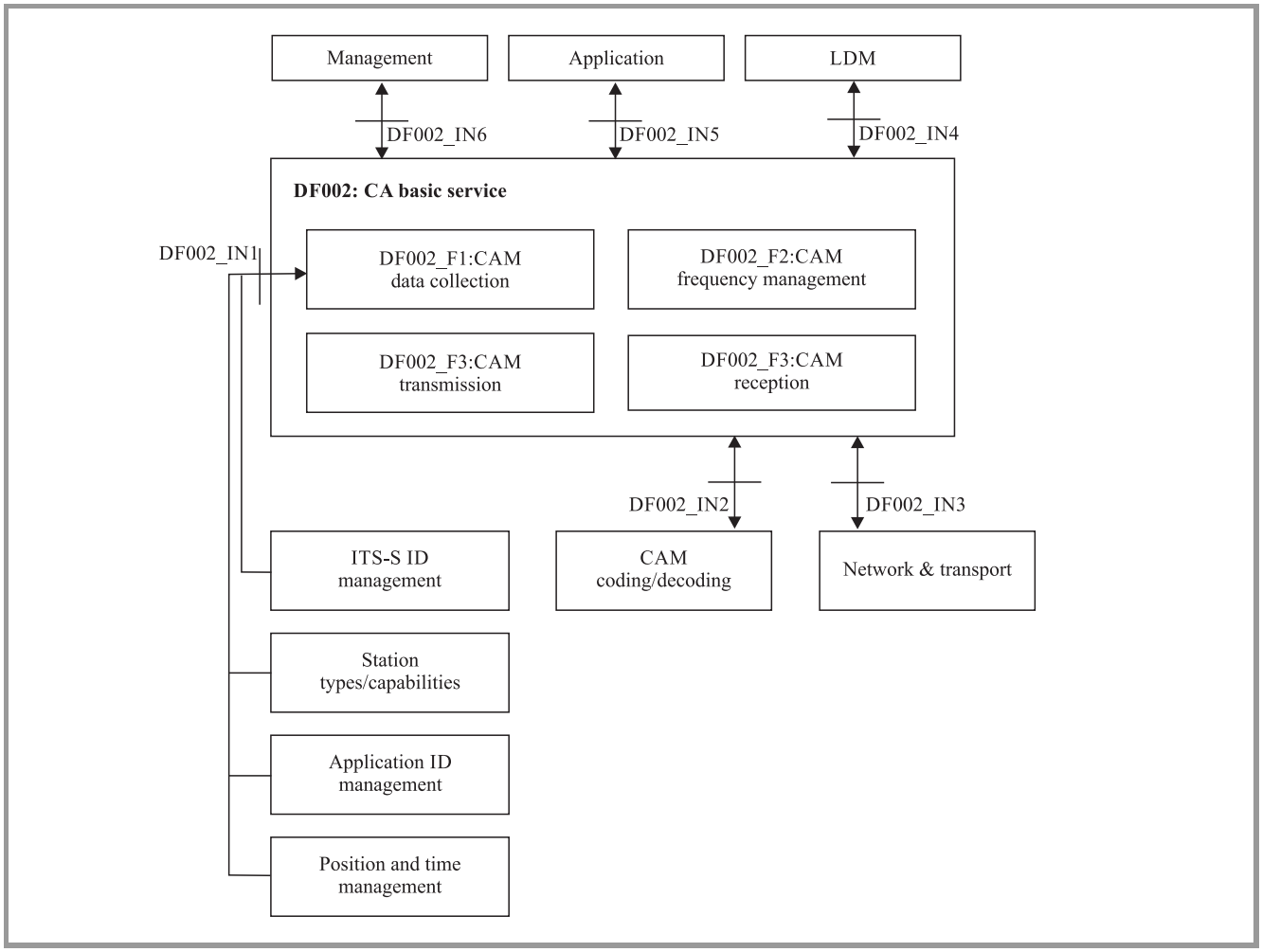

Fig. 2. Block diagram of DF002: CA basic service.

Table 8
Interfaces of DF002: CA basic service

Interface	Related component	Direction	Information exchanged over the interface
[DF002_IN1]	• station type/capabilities, • application ID management, • position and time management, • ITS-S ID management,	In	Data required for the construction of CAM: • station type, • in vehicle data (for vehicle CAM), • application ID information of CAM, • current position and time information of the ITS-S, • ITS-S ID information, • other information included in CAM as specified in ETSI EN 302 637-2 [9].
[DF002_IN2]	Data presentation	In/out	Data presentation and message encoding/decoding support.
[DF002_IN3]	Network & transport	In/out	Out: CAM delivered to network and transport layer for transmission; In: Received CAM delivered by the networking and transport layer.
[DF002_IN4]	LDM	Out	Content of the received CAMs to the LDM.
[DF002_IN5]	Application	In/out	In: Application requirements, if applicable; Out: Content of the received CAMs to the LDM and/or to the application.
[DF002_IN6]	Management	In/out	Data required by the management layer and/or information of the congestion level.

Table 7 provides functional requirements and Table 8 showsinterfaces to external components descriptions addressed to CA basic service [7].

3. Facility Layer Services Implementation

The implementations aspects of facilities, generally defined earlier, are shown here on the example of DEN and CA services.

It is worth to note that CA and DEN services are standardized in Europe and they are specified in EN class documents. It means that these documents were voted by European Union member state standardization bodies (i.e. Polski Komitet Normalizacji in Poland) and recognized as Polish Standards – PN-EN. It is the base for ITS solutions manufacturing unification and services interoperability operations, at least throughout Europe. The process of standard document recognition does not cover other document classes, i.e. Technical Specifications (TS) or Technical Report (TR).

It should be noted that this standard area is still during the work process – new documents are under preparation and old ones have new versions, some documents are not fully cohesive or there are differences among them. It involves some problems during implementation of the standardized services.

3.1. DEN Basic Service Implementation

DENM transfers information on the road events that could have impact on road user safety and traffic conditions. The event could have the following attributes: event type, event position, event detection time and time duration. This attributes may change over space and over time [9].

DEN basic service constructs and process DENM. DENM construction is initiated by ITS station application after event detection in order to inform about that other ITS stations. The message ready to distribution is transferred to network and transport layer. It triggers all communications facilities services. Usually DENM is distributed to ITS stations located in area of direct communication between different vehicles and between vehicles and roadside infrastructure.

In case of DENM received from network and transport layer, DEN basic service processes the message and presents the content to ITS application. The application can show information about danger or traffic conditions. Then the driver could react accordingly.

DENM transmission could be repeated when the event takes place or, in some cases, even when originating ITS station left the event location but event is not ended (e.g. the case of ice or fog). DEN basic service protocol was design to serve composed situations. For this purpose, the following DENM types were defined.

New DENM is generated by the DEN basic service after the event detection by originating ITS station. New DENM is denoted by new identifier and provides defined event attribute like position, type, detection time and others. Update DENM is generated by the same station, which had generated new DENM for the same event. It updates event information.

Cancellation DENM is generated by the same station which had generated new DENM for the same event. It informs on event termination. Negation DENM is generated by the ITS station, which is able to detect event termination, previously announced by another station.

DENM contains one common ITS Protocol Data Unit (PDU) header and several data containers, see Fig. 3.

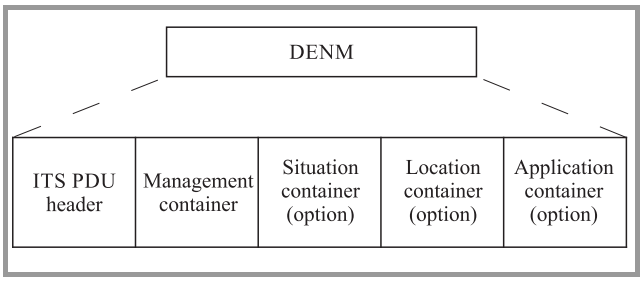

Fig. 3. General DENM structure.

ITS PDU header is common unit in all messages that includes protocol version information, message type and source ITS station identifier.

DENM work part consists of four data containers in fixed order for management, situation, location and application information.

Management container transfers information related to DENM management and DENM protocol. Situation container describes event type. Location container contains information on event location and position data. Application container contents uses case information required additionally and is not filled in previous containers.

Each container is composed of a sequence of optional or mandatory Data Elements (DE) and/or Data Frames (DF). DEs and DFs are mandatory unless specified otherwise. Detailed descriptions of all DE and DF in the CAM context are in normative annex B to PN-ETSI EN 302 637-3 [8]. DE and DF not defined in PN-ETSI EN 302 637-3 [8] should be searched in common data dictionary (i.e. [10]). Formal ASN.1 CAM specification is included in normative annex A to PN-ETSI EN 302 637-3 [8]. DENM basic service protocol operation formal specification is include in clause 8 of PN-ETSI EN 302 637-3 [8].

3.2. CA Service Implementation

CA basic service implements requirements and specifications described earlier. The PN-ETSI EN 302 637-2 [9] shows the service execution in more details. The service is constructed on the base of CAM processing.

CAMs are exchanged in ITS network between ITS stations, in order to maintenance of mutual knowledge and cooperation of vehicles on the common roads. CAM contains information about source ITS station attributes needed for actions of specific applications. Set of information depends on station type and information itself. This information could be used by applications for mapping of road situation, for prediction of the situation development and for calculation of risk.

For example ITS-S could calculate a risk of road collision between vehicles. The driver can receive the message, via HMI, and decide on specific actions. In case of automatic actions applied, the breaks could be activated automatically.

CAM contains one common ITS Protocol Data Unit (PDU) header, basic data container and many optional (conditional) data containers, see Fig. 4. ITS PDU header is common unit in all messages that includes protocol version information, message type and source ITS station identifier. Basic container include basic information on source ITS station. High frequency (HF) container includes information that is changing frequently. Low frequency (LF) container includes static or not frequently changed information of source ITS station. Special vehicle containers include information connected to specific role of vehicles represented by ITS station.

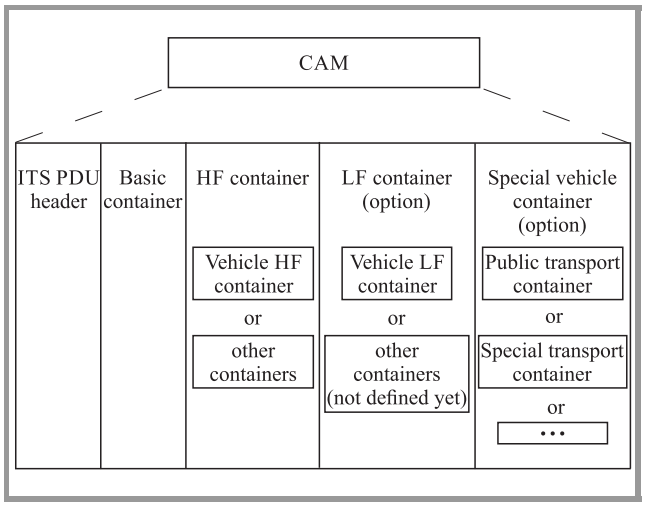

Fig. 4. General CAM structure.

Each container is composed by the sequence of optional or mandatory Data Elements (DE) and/or Data Frames. DEs and DFs are mandatory unless specified otherwise. Detailed descriptions of all DE and DF in the CAM context are in normative annex to PN-ETSI EN 302 637-2 [9]. DEs and DFs not defined in PN-ETSI EN 302 637-2 [9] should be searched in common data dictionary [10]. Formal Abstract Syntax Notation One (ASN.1) CAM specification is included in normative annex A to PN-ETSI EN 302 637-2 [9]. Informative annexes C, D and E to PN-ETSI EN 302 637-2 [9] include framework of CA basic service protocol operation formal specification. Up to date CAM content is specified for vehicle ITS stations. It is expected that CAM content and format specifications for other ITS stations will be added in future.

3.3. Common Solutions on Syntax and Data Dictionaries

There are some common methods of specifications applied to ITS services implementation.

Messages syntax is defined using ASN.1 notation according to ITU-T Recommendation X.680 (11/08)/ISO/IEC 8824-1) [11] and others from this series. For messages coding and decoding should be applied Packed Encoding Rules according to ITU-T Recommendation X.691/ISO/IEC 8825-2 [12]. Messages syntax, defined using above-mentioned rules, is formal and could be used as a part of software of service protocols and applications using the information transferred by the messages.

Information transferred by messages is located in containers in form of Data Elements and/or Data Frames. Data sources and destinations included in data elements are other facilities layer entities as well as applications. Syntax invokes all the data elements in specific order.

Common data dictionary is a tool for integration of DE and DF in all messages. Usually descriptions of all DEs and DFs in the specific message context are included in standardization documents of the message. DE and DF not defined in the message context should be taken from common data dictionary specified in ETSI TS 102 894-2 [10]. It covers the description of data meaning included in specific data elements. The dictionary includes also data elements specification in ASN.1 notation. It is possible to import the ASN.1 specification to message encoding procedures.

4. Summary

In this paper definition tool of ITS services and environment of their execution have been shown. They should allow an implementation that would assure services efficient execution. Implementation of facilities layer is important as it has an impact on the realization of many different services. Using standardized solutions, especially international, can assure that specific products may be designed, manufactured and provided with vehicles by different subjects and cooperate with each other as well as with road infrastructure in different countries.

Standardization documents and international product development are full of knowledge and solution proposals. There are many references to real experience. As presented, ITS services implementation and deployment require general knowledge of the final services and their execution environment.

One of the implementation tools is dissemination of concepts and solutions, as presented, in ITS professional environment. In some cases, it requires verification against implementation conditions. Some parts need to be more precise. In particular it is addressed to:

- definition and description methodology of specific solutions (including adequate terminology). It means needs of standards, including technical reports and technical specification localized in national and local law, business, administration and professional environments;
- verification of proposed solutions whether they are complete, capacious and they sense their applications. As an example see CAM content definitions for ITS stations other than vehicle stations;
- workout of missing solutions and/or solutions for specific requirements, such as data security and data privacy in the context of public road and transport operations;
- specification and making or purchase of tools for ITS solutions implementation, deployment and operations, e.g. ASN.1 notation and/or common data dictionary usage.

The standards have the particular role. Hence, there is no formal obligation for their application but mode of their preparation in international environment, that justify their treatment as a base for implemented solutions. Moreover, there is a need to track the standards development, where ITS is a nascent area where occur rapid changes in the standard requirements. See clause 3.4.5 in Rolling Plan for ICT Standardization in [13].

Still before implementation of selected ITS services, specific conditions have to be fulfilled. In particular the following:

- determination of real ITS services deployment strategy with its law and organization context of execution,
- indication of specific technical solutions, especially transport infrastructure (roads, vehicles), which assure efficient ITS services deployment.

European Commission has noticed that there is a need to discount earlier experience and practically support common implementation of C-ITS throughout Europe. At the first stage, a review report was prepared [14]. Key issues for C-ITS implementation are indicated and described in this report. Next stages of this platform activity are planned as answers for questions asked by C-ITS implementers and questions emerged by the current needs of ITS users.

The paper presented the framework of standards implementation. Common understanding of the ITS implementation processes is an essential for real cooperation of ITS.

References

[1] ETSI EN 302 665 V1.1.1: Intelligent Transport Systems (ITS); Communications Architecture.

[2] CAR 2 CAR Communication Consortium, Manifesto, Overview of the C2C-CC System; Version 1.1, 2007.

[3] ETSI TR 102 698 V1.1.2: Intelligent Transport Systems (ITS); Vehicular Communications; C2C-CC Demonstrator 2008; Use Cases and Technical Specifications.

[4] ETSI TR 102 638 V1.1.1 (2009-06) Intelligent Transport Systems (ITS); Vehicular Communications; Basic Set of Applications; Definitions.

[5] M. Kowalewski, A. Pękalski, and M. Siergiejczyk, "Normalizacja współpracy inteligentnych systemów transportowych w pojazdach (Standardization of cooperation of intelligent transport systems in vehicles)", *Drogi i Mosty*, no. 13, pp. 357–378, 2014 (in Polish).

[6] ETSI TS 102 637-1 V1.1.1: Intelligent Transport Systems (ITS); Vehicular Communications; Basic Set of Applications; Part 1: Functional Requirements.

[7] ETSI TS 102 894-1 V1.1.1: Intelligent Transport Systems (ITS); Users and applications requirements; Part 1: Facility layer structure, functional requirements and specifications.

[8] ETSI EN 302 637-3 V1.2.2: Intelligent Transport Systems (ITS); Vehicular Communications; Basic Set of Applications; Part 3: Specifications of Decentralized Environmental Notification Basic Service.

[9] ETSI EN 302 637-2 V1.3.2: Intelligent Transport Systems (ITS); Vehicular Communications; Basic Set of Applications; Part 2: Specification of Cooperative Awareness Basic Service.

[10] ETSI TS 102 894-2 V1.2.1: Intelligent Transport Systems (ITS); Users and applications requirements; Part 2: Applications and facilities layer common data dictionary.

[11] ITU-T Recommendation X.680: Information technology – Abstract Syntax Notation One (ASN.1): Specification of basic notation.

[12] ITU-T Recommendation X.691: Information technology – ASN.1 encoding rules: Specification of Packed Encoding Rules (PER).

[13] European Commission, Directorate-General for Internal Market, Industry, Entrepreneurship and SMEs Innovation and Advanced Manufacturing, KETs, Digital Manufacturing and Interoperability, Rolling Plan for ICT Standardization 2016.

[14] The Platform for the Development of Cooperative Intelligent Transport Systems in European Union (C-ITS Platform) Final report, January 2016 (with annexes).

Marian Kowalewski graduated from the Military Academy of Telecommunications in Zegrze (1975), and was academic teacher, research worker and vice-chancellor for education and research at the same Academy (1975–1997), deputy director for science and general matters in NIT (1997–2004). He is Professor at the National Institute of Telecommunications and at Warsaw University of Technology. He is the Chairmen of the NIT Scientific Council. Head of TETRA project in NIT (since 2002), scientific manager of the IT System of the State Protection Against Extraordinary Threats project (ISOK) in NIT (2011-2012), Intelligent Transport Systems (ITS) in NIT (2011–2013). Organizer and co-organizer of many seminars and scientific conferences, author of numerous textbooks, academic course books, articles and R&D works concerning telecommunications problems. His scientific interests are planning and developing of telecommunications, telematics systems, and their efficiency.

E-mail: M.Kowalewski@itl.waw.pl
National Institute of Telecommunications
Szachowa st 1
04-894 Warsaw, Poland

Andrzej Pękalski received his M.Sc. degree in Telecommunication from Warsaw University of Technology in 1975. He has been working at Polska Pocz-, ta Telegraf i Telefon (PPTiT), National Institute of Telecommunications, Alcatel, Telekokomunikacja Polska as an R&D engineer. He has been attending works of ITU-T and Telemanagement Forum. Currently he is employed at the National Institute of Telecommunications, Electronic Communications Technologies Applications and Power Systems Department. He is Technical Committee for Telecommunication chairman of Polish Committee for Standardization (PKN). He has published several papers in scientific journals on communications technology applications.

E-mail: A.Pekalski@itl.waw.pl
National Institute of Telecommunications
Szachowa st 1
04-894 Warsaw, Poland

Paper

L-SCANN: Logarithmic Subcentroid and Nearest Neighbor

Tohari Ahmad and Kharisma Muchammad

Department of Informatics, Institut Teknologi Sepuluh Nopember, Surabaya, Indonesia

Abstract—Securing a computer network has become a need in this digital era. One way to ensure the security is by deploying an intrusion detection system (IDS), which some of them employs machine learning methods, such as *k*-nearest neighbor. Despite its strength for detecting intrusion, there are some factors, which should be improved. In IDS, some research has been done in terms of feature generation or feature selection. However, its performance may not be good enough. In this paper, a method to increase the quality of the generated features while maintaining its high accuracy and low computational time is proposed. This is done by reducing the search space in training data. In this case, the authors use distance between the evaluated point and the centroid of the other clusters, as well as the logarithmic distance between the evaluated point and the subcentroid of the respective cluster. Besides the performance, the effect of homogeneity in extracting centroid and subcentroid on the accuracy of the detection model is also evaluated. Based on conducted experiment, authors find that the proposed method is able to decrease processing time and increase the performance. In more details, by using NSL-KDD 20% dataset, there is an increase of 4%, 2%, and 6% from those of TANN in terms of accuracy, sensitivity and specificity, respectively. Similarly, by using Kyoto 2006 dataset, proposed method rises 1%, 3%, and 2% than those of TANN.

Keywords—clustering, feature transformation, information security, network security.

1. Introduction

Transferring data through a computer network has become an essential need in this digital era. This has made it easy for people to communicate each other. Since the data are transmitted in a public network, the security should have more attention. It is because anyone may have access to it. This works especially to sensitive data whose access must be restricted to legitimate users only. Moreover, these private data, such as medical and financial data, may become a target of attacks. Therefore, there must be a mechanism to protect it.

Based on its objective, data protection can be divided into two categories. The first is securing data in a file or transaction. This is done by using either encryption [1], transformation [2] or steganography [3]. The second is protecting data which reside in a network. In this case, the control is usually carried out by an intrusion detection system (IDS). Based on [4], IDS can be grouped into two categories. The first is signature-based IDS, which uses records of known attack. If an activity matches with any of that record, then the IDS will trigger an alarm. The second is anomaly-based IDS, which uses a model representing a normal activity. Any flow that deviates too far from the model will trigger an alarm.

That first type of IDS has lower resource consumption than the second. However, it needs constantly update the signatures, which have been stored in the database. Different from this, the second type of IDS does not need signatures to detect specific packets. So, it is able to detect unknown attacks to some degree. Nevertheless, it has a slightly higher false positive rate than the first [4].

There is some research, which have been introduced to solve those problems. Their results, however, may not be so optimal. In more details, there are at least two factors that the anomaly-based IDS should be improved, those are [5]:

- outlier detection – in common anomaly-based IDS, the detection model only uses normal data. It is assumed that data which are outside of the detection model is anomaly, as specified in [6]. In real life, however, this assumption may not be realistic;

- cost of false alarm – unlike other applications of machine learning, such as hand written recognition or product recommendation, in this case false alarm requires much time and energy to verify. Ignoring an alarm is not a good idea since a true alarm can cause the whole system down.

Some research, such as [7] and [8], has proposed a feature transformation method to reduce the false alarm rate and at the same time maintain high detection rate. This method needs to use whole training data for the final classification step. If the training data is too large, then the time needed to classify an activity rises greatly. In authors' previous research [9], a method to reduce the size of training data and to transform them for the classification purpose have been proposed. This is done by measuring the distance between the respective point and centroids, as well as and logarithmic distance between the respective point and subcentroid. In this paper, we expands and further validate this method.

The rest of this paper is organized as follows. Section 2 contains previous works, which relate to this research. Section 3 explains the proposed method. The Sections 4 and 5 describe the experimental design and result, respectively. Finally, the conclusions in the Section 6 are drawn.

2. Related Works

Some research has been introduced to classify data by using distance to the centroid. This includes [7], [8], [10]–[14], which have used that distance to generate features. The basic idea of those methods is similar, that is, the distance between a point and the respective centroid is used to differentiate data within dataset. The differences between that researches are how the centroid is extracted and how that distances is used. Some methods use *k*-means by using the previously defined number of clusters [7], [8], [14] and by partitioning the dataset based on their label and by extracting the centroids according to their average features in each partition [10], [11], [13].

The research [7] and [8] are proposed in order to address problems in [5]. Both methods have achieved a relatively low false positive rate while maintaining its high detection rate. Here, they employ feature transformation to extract new features and to classify the data by using *k*-Nearest Neighbor (*k*NN). For handling the dynamic nature of the data stream, some research such as [15], [16] propose to use the affinity propagation [17] for selecting exemplars. This is to be applied to the on line clustering algorithms. Some methods, which are often used for classification, are described as follows.

2.1. TANN

Triangle Area and Nearest Neighbor (TANN) is proposed in [8]. It works by assuming that the centroid of a dataset can be used to differentiate data, and the distance of unknown data to centroid of other clusters can be used for classification. This method generates features by using data, which have been extracted, and by utilizing any 2 out of 5 centroids. This method requires a parameter *k*, similar to that used in *k*NN. The overall framework of this method can be observed in Fig. 1. Here, TANN works as follows:

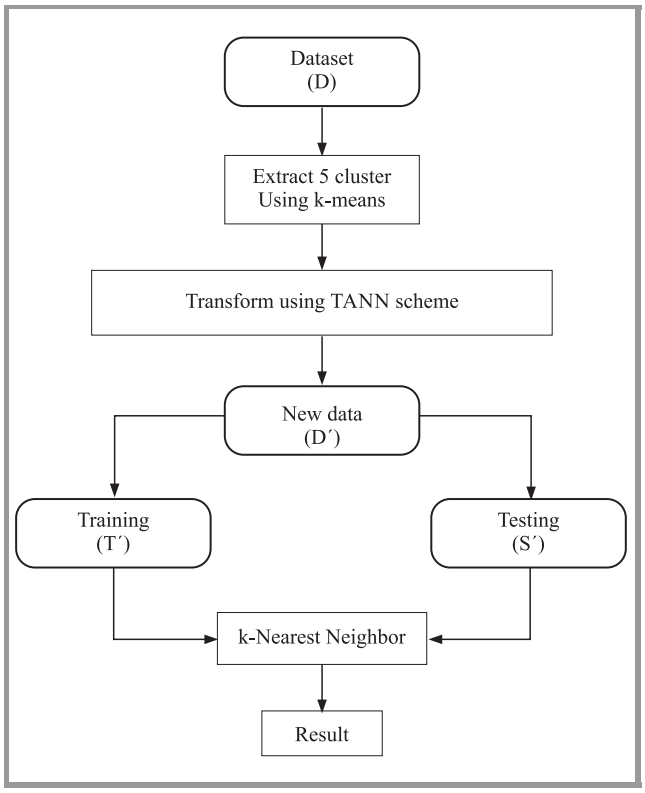

Fig. 1. TANN workflow.

1. **Extracting centroids** – by using *k*-means, this method extract 5 centroids. This number is chosen by assuming that there are 5 classes: 1 normal and 4 type of attacks.
2. **Generating new features** – the transformed data are generated by summing the area of all possible triangles formed by using the old data and any two of five centroids, which have been extracted in step 1. Possible triangles, which are formed are depicted in Fig. 2.
3. **Training and testing *k*NN** – the new data are divided into training and testing sets. Next, the testing set is classified by using *k*NN.

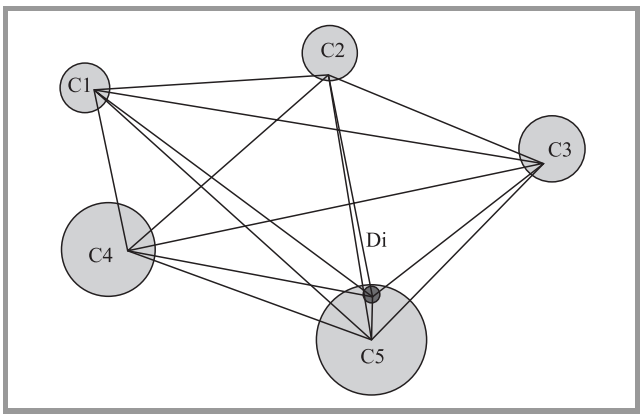

Fig. 2. TANN scheme.

A common problem of TANN is that it needs to use all training data in order to classify the testing or other data. Consequently, if the size of the training data is large, the time needed to process rises significantly. To overcome this problem, some applications use parallel searching by using Graphic Processing Unit (GPU) such as [18] and [19]. However, not all computers have GPU, which is able to do it. Therefore, reducing the search space is one of the feasible solution for this problem.

2.2. Bisecting k-Means

This clustering method is proposed by [20] to classify documents. It works as follows:

1. Pick a cluster to split. In this case, they use the largest cluster.
2. Split the selected cluster into two clusters by using ordinary *k*-means.

3. Repeat step 1 and 2 until the desired number of clusters has been reached.

In [20], authors also propose to use the centroids, which have been extracted from those steps as initial centroids for basic k-means. In addition, they believe that their method works better than simple agglomerative clustering. This is because the agglomerative clustering sometimes merges data from different classes, which may happen in the early clustering step. If so, then this mistake cannot be fixed. Divisive clustering on the other hand, may split clusters whose members actually have same labels. Fortunately, this mistake can be fixed in later phases.
A weakness of this method is, similar to that of k-means, we need to know the number of required clusters. Unfortunately, we may not have this information every time.

3. Proposed Method

The proposed method is inspired by TANN [8], CANN [7], and comparison of clustering techniques [20]. Similar to [8] and [7], the distance between the evaluated point and the respective centroid is used to transform data while the difference is on how the extraction of centroid is performed. In more details, the proposed method differs in the extraction process and in treating the subcentroid to add differentiating power to the classification method. The overall proposed method is depicted in Fig. 3, where T is training dataset, S is testing dataset and $D = T \cup S$.
The proposed method is developed based on authors' previous research [9]. In this paper, the scope is extended as follows.

1. The dataset used here is bigger than that in [9].

2. The use of entropy is explored as well as Gini impurity index. Additionally, their combination is also investigated.

3. The use of bisecting k-means and logarithmic distance in the transformation process is investigated. This is intended to evaluate their effect on the performance.

As shown in Fig. 3, the first step is to divide the dataset into testing and training. In the experiment, authors further divide the data into 10 partitions. This is to carry out cross validation with each partition whose composition is proportional.
Next is to cluster the training data by using a modified variant of bisecting k-means whose diagram is presented in Fig. 4. This method works as follows:

1. Split the dataset to two clusters by using k-means.

2. If the impurity of any resulting cluster is higher than the user defined threshold U, then split it by using ordinary k-means into two clusters.

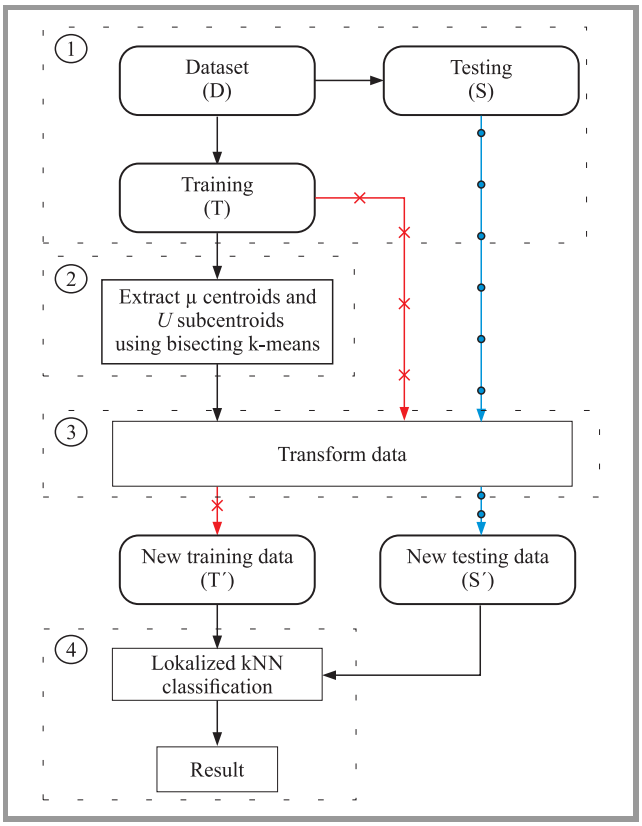

Fig. 3. L-SCANN workflow.

3. Repeat step 2 until there is no cluster whose impurity is higher than U, or no more impurity can be reduced. At this stage, the number of clusters n has been obtained.

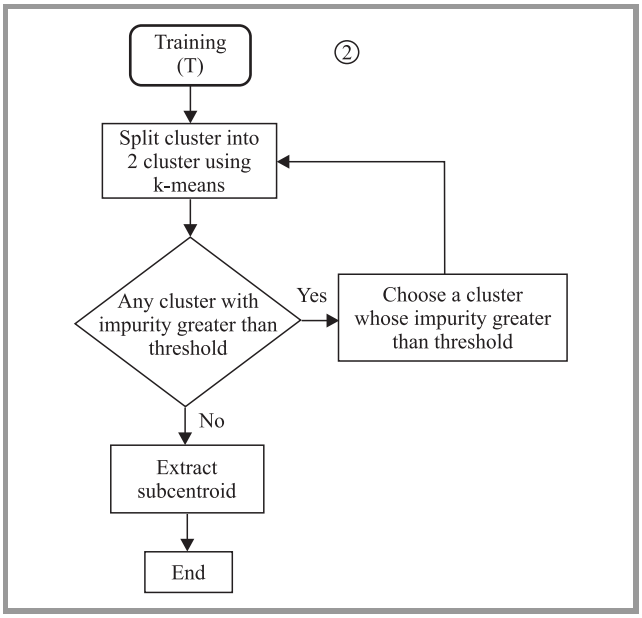

Fig. 4. Variant of bisecting ki-means used.

This step is intended to solve the problems experienced by previous research, such as [7] and [8]. That is, the number

of needed clusters to give decent performance is not always available. In addition, data with a same label is not always grouped into one cluster.

Different from other research, such as [21], which uses a genetic algorithm to iteratively search the best centroid in partially labeled data, a variant of bisecting k-means is employed. Furthermore, they make use of Gini impurity index, mean square error and combination of both for measuring the quality of the generated clusters. Here, authors take Gini impurity index, entropy and combination of them as stopping criteria as previously described.

Let O and be m be the number of specified subcentroids in each cluster whose value is obtained from an experiment, and the number of members in a cluster, respectively. There are three possibilities of subcentroids according to those O and m values:

- $m > O$ – subcentroids are extracted by using k-means whose k is equal to O,
- $m = O$ – each member of the clusters is treated as subcentroid,
- $m = O$ – in this paper, we assumed that the cluster is homogeneous. So, there is no subcentroid, which can be extracted.

The following step is transforming the data such that the distance of the evaluated data can be collected. In authors' previous works [9], the transformation of the data is done by summing two types of distance: between the point and centroids, and between the point and the subcentroids in the same cluster. Let D_i be the i-th data being evaluated, C_j be the j-th centroid of each cluster, L_k be the k-th subcentroid of the respective cluster. It is shown in Fig. 5 that D_i is closer to C_5 than to other centroids. Therefore, C_5 is firstly assigned as its centroid.

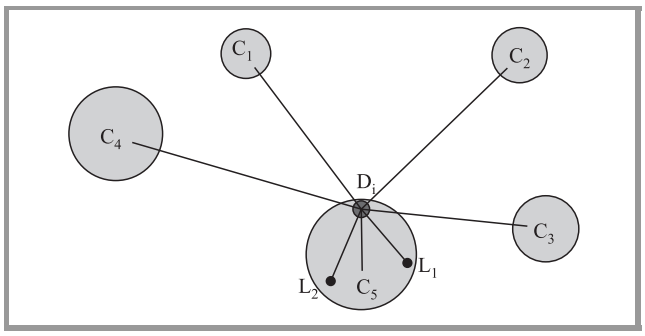

Fig. 5. L-SCANN scheme.

Let $Dist1_i$ be the distance between the i-th data and all centroids in each cluster, n be the number of clusters extracted from the clustering step, and $||C_j - D_i||$ be the Euclidean distance between D_i and C_j. This distance can be depicted in Eq. (1). Next, the distance between the evaluated data and its subcentroids, $Dist2_i$, is presented in Eq. (2), where $||D_i - L_k||$ is the Euclidean distance between D_i and L_k, and O is the number of subcentroids in the respective cluster. If the distance between D_i and L_k is 0 (i.e. overlapping), then the distance is reset. The new transformed data, D_i' is then obtained by summing $Dist1_i$ and $Dist2_i$, as provided in Eq. (3). This transformation step is repeated until all D_i have been processed. That is, each data in training set T will be transformed into new training data T' and each data in testing set S will also be transformed into new testing data S'. This is noted by red ($\times$) and blue ($\bullet$) arrows, respectively in Fig. 3. Each new training data T' is then assigned to its respective cluster.

As an alternative, it is also possible to remove the logarithmic calculation, as shown in Eq. (4) where D_i'' is the transformation results. This is because logarithmic calculation may take a little bit longer.

The final step of proposed method is classifying the data in testing set S. For this purpose, we classify the evaluated point D_i as member of the cluster whose centroid is the nearest. Next, the three nearest transformed neighbor points are selected, which D_i is assigned a label similar to the dominant label. That is, if most of those three are normal, than D_i is also normal. If most of those three are attack, than D_i is also attack.

An example of this classification process is presented in Fig. 6, where new data D_i is being classified. In Fig. 6a, the centroid C_j with the smallest distance to D_i is looked for. In this case, C_5 is found in a cluster, whose subcentroids are L_1, L_2 and L_3. The respective cluster has T_1, T_2, T_3, T_4 and T_5 as the members. By using Eq. 3, its transformation value is calculated as depicted in Fig. 6b. Finally, the three closest transformed members are selected, which are: T_3',

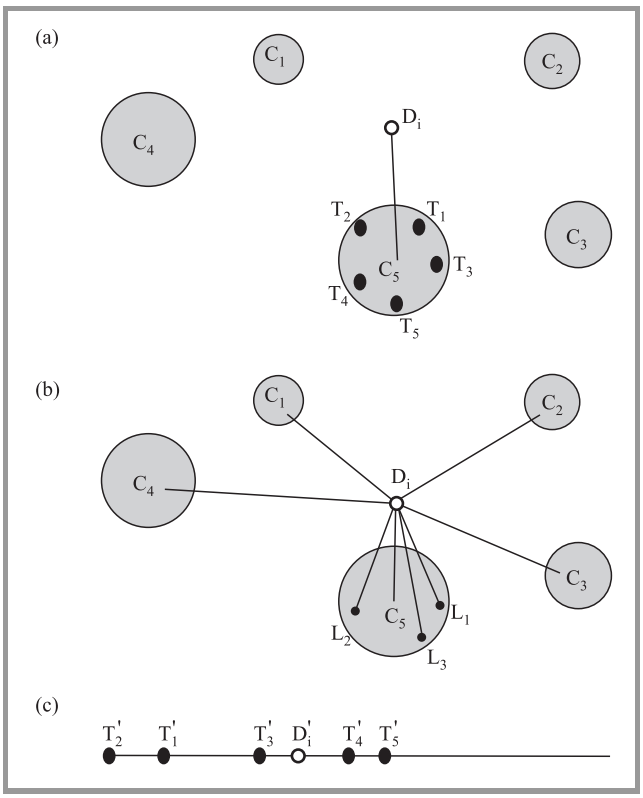

Fig. 6. Example of classification process.

T_4' and T_5', see Fig. 6c. The majority labels of them are then assigned to D_i:

$$Dist1_i = \sum_{j=1}^{n} ||C_j - D_i||, \tag{1}$$

$$Dist2_i = \sum_{L=1}^{O} \begin{cases} \ln(||D_i - L_k||), & \text{if } D_i \neq L_k \\ 0, & \text{otherwise} \end{cases}, \tag{2}$$

$$D_i' = Dist1_i + Dist2_i. \tag{3}$$

$$D_i'' = \sum_{j=1}^{n} ||C_j - D_i|| + \sum_{L=1}^{O} ||D_i + L_k||. \tag{4}$$

4. Experimental Design

The experiment is carried out in Python 2.6 with scipy and numpy package in 64-bit Ubuntu Linux using Intel Core i5-2410M processor with 4 GB of RAM.

In the modified bisecting k-means, we use an impurity index as the stopping criteria in finding clusters. That is, Gini impurity index, entropy, and their combination as provided in Eqs. (5)–(7) respectively, where m is the number of class labels and f_i is the frequency of i-th label. Those first two are common index while the third is our proposed combination method. The Eq. (7) is designed based on the facts that gini index has a range between 0 to 0.5 in two label cases, and the entropy index has a range between 0 to 1 in any case. In addition, we use two labels, normal and attack. For a deeper analysis, the attack is further divided into subclasses (sublables) for NSL-KDD.

$$I_G = 1 - \sum_{i=1}^{m} f_i^2, \tag{5}$$

$$H = -\sum_{i=1}^{m} f_i log_2 f_i, \tag{6}$$

$$Combined = \frac{H + 2I_G}{2}. \tag{7}$$

4.1. Dataset

In the experiment, we use NSL-KDD 20% [22] and a subset of Kyoto 2006 [23] datasets. In NSL–KDD, we remove protocol_type, service and flag because those three are categorical types. In Kyoto 2006, we use a subset which was taken in 20 July 2009 whose unused attributes are removed, i.e. flag, start_time, and duration. Additionally, redundant records from Kyoto 2006 are then removed. At the end, we have 25192 records in NSL-KDD and 107213 records in Kyoto 2006. The composition of NSL-KDD and Kyoto 2006 is available in Table 1.

Table 1
Dataset composition

NSL-KDD			
Label	Sublabel	Number	
Attack	Dos	9234	11743
	Probe	2289	
	U2R	11	
	R2L	209	
Normal	Normal	13449	

Kyoto 2006	
Label	Number
Attack	52554
Normal	64659

4.2. Parameter Tested

The proposed method requires two parameters to work. Those are the impurity index U, and the assumption number of subcentroids O. We define $U \in \{0.1, 0.2, 0.3\}$ and $O \in \{4, 5, 6\}$. In the experiment, we combine all possibilities of those values, such that, we have 9 combinations. The number of subclusters is not more than 6 in order to ensure that the cluster with lower number members is homogeneous. The value of impurity index is not larger than 0.3 because it is over half of Gini impurity index, whose range is between 0 and 0.5, for 2 labels. Here, three types of impurity index as previously described are used.

4.3. Evaluation Criteria

The proposed method is evaluated in terms of accuracy, sensitivity, and specificity as specified in Eqs. (8), (9), and (10), respectively. In this case, TP is true positive (correctly classified attack), TN is true negative (correctly classified normal), FP is false positive (misclassified normal), and FN is false negative (misclassified attack). Another evaluation criterion is running time, to see how search-space reduction affect the speed of the algorithm.

$$\text{Accuracy} = \frac{TP + TN}{TP + TN + FP + FN}, \tag{8}$$

$$\text{Sensivity} = \frac{TP}{TP + FN}, \tag{9}$$

$$\text{Specificity} = \frac{TN}{TN + FP}. \tag{10}$$

5. Experimental Results

The experiment results are provided in this section. These comprise that of proposed method as well as TANN for the comparison purpose. In this case, we firstly present the results of TANN in order to make it easier to compare.

5.1. TANN

Accuracy, sensitivity, and specificity of TANN on NSL-KDD and Kyoto 2006 can be observed in Table 2, where Acc, Sen and Spe represent accuracy, sensitivity and specificity respectively (in percent) and time depicts processing time (in hour).

In NSL-KDD dataset, increasing the value k of kNN leads to raising the value of accuracy and sensitivity but reducing specificity. The table also shows that the processing time is not affected by k. When it goes up from 3 to 5, the processing time drops. However, when it then grows to 7, the time also increases.

It is depicted that the best results is achieved by using $k=5$ where accuracy, sensitivity and specificity are 96.80%, 95.92% and 97.64%, respectively with processing time 9.15 hours. It is worth noting that the processing time raises about 16 times when the dataset is 4 times larger than the size of NSL-KDD.

Table 2
Performance of TANN on different dataset

NSL-KDD				
k	Acc [%]	Sen [%]	Spe [%]	Time (hour)
3	93.08	94.85	91.53	0.47
5	93.36	95.86	91.17	0.39
7	93.51	96.32	91.05	0.56
9	93.56	96.48	91.02	0.42
11	93.60	96.60	90.99	0.50
13	93.61	96.66	90.95	0.53
15	93.54	96.62	90.86	0.53
Kyoto 2006				
3	96.73	95.79	97.63	9.12
5	96.80	95.92	97.64	9.15
7	96.69	95.84	97.51	9.14

5.2. Proposed Method with Gini Impurity Index

The experimental results of the proposed method which uses the gini impurity index on NSL-KDD can be observed in Table 3, where Clu represents the average number of generated clusters. Based on this result, we find that the highest accuracy, sensitivity and specificity level is achieved when the impurity threshold and the number of subcentroids are 0.1 and 4, respectively. It is also shown that increasing the impurity value results to decreasing those performances, and raising the number of subcentroids may cause the performances go up to some extent. It can be inferred that smaller number of both impurity index and subcentroids holds the best performance.

Compared to the performance of TANN, proposed method produces significantly higher result in terms of accuracy and specificity, but slightly lower in sensitivity. At the same time, the time needed to process the whole dataset goes down.

The experimental results which are obtain on Kyoto 2006 are depicted in Table 3. It shows that increasing the impurity index leads to decreasing the performance. In addition, higher number of clusters results to a little higher level of accuracy and sensitivity. However, this causes the specificity slightly lower. As specified in Table 3, it also found that proposed method is able to decrease the processing time from 9 to 2 hours for 100,000 records.

This result represents the characteristics of dataset we used. In this case, the average number of generated clusters in NSL-KDD is much higher than that of Kyoto 2006. It is very likely that NSL-KDD comprises heterogeneous data, which are more sparsely distributed across the initial clusters than that of Kyoto 2006. Furthermore, it is also found that in NSL-KDD, most clusters ($>50\%$) are small with 3 or lower members, while those in Kyoto 2006 mostly ($>50\%$) have 6 or more members.

5.3. Proposed Method with Entropy Index

The experimental result of the proposed method by using entropy index on NSL-KDD can be observed in Table 4. It depicts that an increase of impurity threshold results to a decrease of accuracy, sensitivity, and specificity; and raising the number of subcentroids, on the other hand, slightly change the accuracy, sensitivity, and specificity.

Similar to the experiment on NSL-KDD, the use of entropy on Kyoto 2006 dataset presents better results than that of gini index, as shown in Table 4. Furthermore, it also gives similar trends, that higher entropy values result in slightly lower performance. In addition, the number of subcentroids does not much affect the performance.

Based on this experimental result, it can be inferred that in general, the use of entropy in the proposed method is more appropriate to the performance than Gini impurity index. This is because by using entropy, the number subcentroids resulted from the clustering process is much higher than that of Gini index. Furthermore, the overall performance is also better than that of TANN.

5.4. Proposed Method with Combined Index

The experimental results with combination of Gini and entropy indexes are in Table 5. Similar to the results with either Gini or entropy indexes, that with their combination is, in general, down due to rising this index. Also, an increase of the number of subcentroids leads to slightly changes in the performances.

The overall performance resulted from the use of this combination index in both NSL-KDD and Kyoto 2006 datasets is lower than that of entropy, depending on the environment, which is represented by the parameter values. It is possible that this performance is affected by the resulted cluster numbers. That is, the accuracy, sensitivity and specificity are more or less proportional to the the number of generated clusters.

Table 3
Results of proposed method using Gini impurity index on different dataset

NSL-KDD															
Subcentroid	Gini impurity index														
	0.1					0.2					0.3				
	Acc [%]	Sen [%]	Spe [%]	Clu	Time [h]	Acc [%]	Sen [%]	Spe [%]	Clu	Time [h]	Acc [%]	Sen [%]	Spe [%]	Clu	Time [h]
4	94.95	91.71	97.78	541.70	0.32	94.11	90.53	97.23	354.00	0.23	93.13	88.93	96.80	218.40	0.16
5	94.49	90.73	97.78	546.70	0.29	93.33	88.79	97.29	351.60	0.21	93.48	89.54	96.92	217.50	0.15
6	94.50	90.83	97.71	539.00	0.31	93.33	88.66	97.41	347.80	0.27	92.97	88.33	97.03	217.20	0.16
Kyoto 2006															
4	98.40	98.09	98.70	58.40	1.975	98.28	98.03	98.52	42.1	2.031	97.45	97.52	97.38	24.8	2.08
5	98.41	98.13	98.69	58.50	1.956	98.29	98.07	98.07	42	2.036	97.49	97.62	97.36	24.8	2.105
6	98.43	98.16	98.69	58.40	2.001	98.31	98.07	98.53	41.9	2.04	97.51	97.67	97.35	24.8	2.061

Table 4
Results of proposed method using entropy index on different datasets

NSL-KDD															
Subcentroid	Entropy														
	0.1					0.2					0.3				
	Acc [%]	Sen [%]	Spe [%]	Clu	Time [h]	Acc [%]	Sen [%]	Spe [%]	Clu	Time [h]	Acc [%]	Sen [%]	Spe [%]	Clu	Time [h]
4	98.28	98.68	97.93	716.4	0.343	95.28	92.64	97.58	593.4	0.353	94.71	91.20	97.78	540.6	0.336
5	98.28	98.65	97.95	715.9	0.348	95.70	93.41	97.70	596	0.348	94.96	91.74	97.78	541.3	0.341
6	98.26	98.63	97.94	716	0.386	95.02	91.71	97.91	596.7	0.415	94.47	90.70	97.76	542.4	0.356
Kyoto 2006															
4	98.93	98.64	99.21	199.7	1.525	98.65	98.50	98.80	68.5	1.7525	98.38	98.06	98.69	58.5	1.72
5	98.93	98.64	99.21	197.3	1.58	98.60	98.50	98.70	69.5	1.821	98.39	98.08	98.69	58.5	1.863
6	98.94	98.65	99.22	199.4	1.58	98.64	98.48	98.79	68.4	1.848	98.41	98.10	98.70	58.5	1.83

Table 5
Results of proposed method using combined index on different dataset

NSL-KDD															
Subcentroid	0.1					0.2					0.3				
	Acc [%]	Sen [%]	Spe [%]	Clu	Time [h]	Acc [%]	Sen [%]	Spe [%]	Clu	Time [h]	Acc [%]	Sen [%]	Spe [%]	Clu	Time [h]
4	98.31	98.57	98.09	705.1	0.361	94.37	90.45	97.80	569	0.348	94.57	91.08	97.62	507.7	0.331
5	98.30	98.69	97.96	704.2	0.36	94.23	90.21	97.75	565.2	0.366	94.08	89.94	97.69	512	0.331
6	98.28	98.63	97.98	703.2	0.293	94.53	90.85	97.74	565.8	0.278	94.84	91.55	97.70	510.8	0.261
Kyoto 2006															
4	98.86	98.57	99.13	152.7	1.598	98.59	98.38	98.78	65	1.726	98.38	98.09	98.66	57.7	1.73
5	98.87	98.60	99.13	153	1.795	98.54	98.31	98.77	64.7	1.968	98.31	97.95	98.66	57.7	1.978
6	98.91	98.69	99.12	152.9	1.806	98.57	98.36	98.78	65.2	2.035	98.41	98.14	98.66	57.7	2.006

5.5. Proposed with k-Means

From the previous experiments we find that the best result is achieved when the number of subclusters is 705 and 200 for NSL-KDD and Kyoto 2006 datasets. Based on these numbers and the previous cluster number of TANN (i.e. 5), we perform experiments by using the common *k*-means method whose result is provided in Table 6 for NSL-KDD and Kyoto 2006, respectively. It is depicted that the overall performance is lower than that of the proposed method with Gini impurity index, entropy index and their combination.

Table 6
Results of proposed method using *k*-means

NSL-KDD				
Cluster	Acc [%]	Sen [%]	Spe [%]	Time [h]
5	94.99	95.89	94.20	0.51
705	97.44	97.54	97.33	0.27
Kyoto 2006				
5	97.70	97.49	97.91	8.84
200	98.39	97.83	98.93	2.01

5.6. Correlation between the Number of Clusters and Performance

Correlation between the number of clusters and performance (accuracy, sensitivity, and specificity) on NSL-KDD and Kyoto 2006 datasets can be observed in Figs. 7–12. In general, it is shown that the number of clusters is proportional to the performance. In more details, NSL-KDD produces an exponential graph for accuracy and sensitivity, and linear for specificity, as depicted in Figs. 7, 8 and 9, respectively. For accuracy and sensitivity, the number of 4 subcentroids is better than others when the number of clusters is less than 600, and 5 subcentroids is for more than 600 clusters. Differently, 6 subcentroids is the best for almost all numbers of clusters.

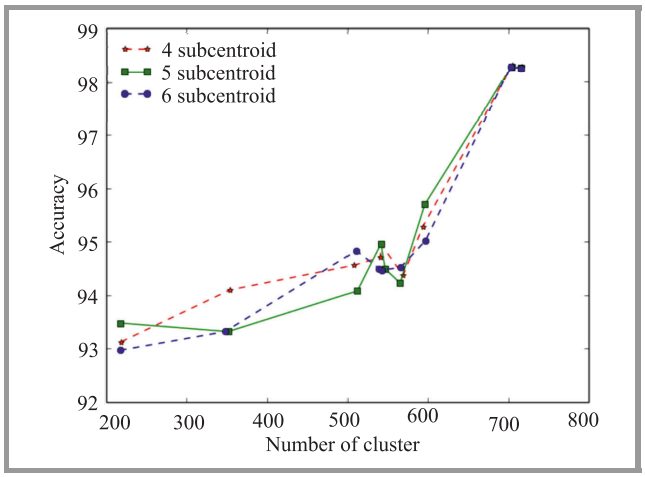

Fig. 7. Correlation between number of cluster and accuracy on NSL-KDD.

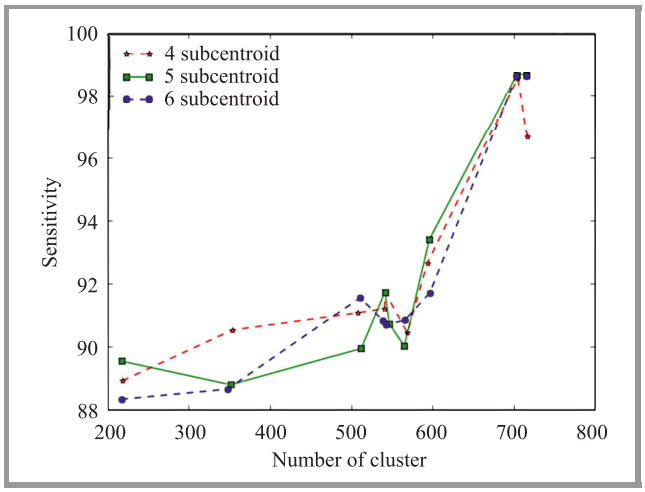

Fig. 8. Correlation between number of cluster and sensitivity on NSL-KDD.

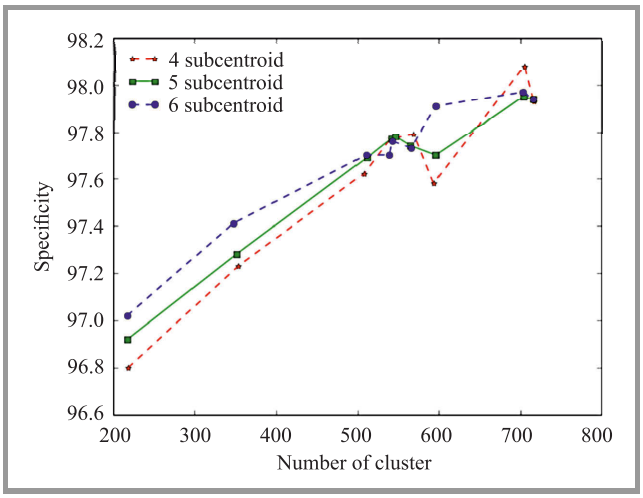

Fig. 9. Correlation between number of cluster and specificity on NSL-KDD.

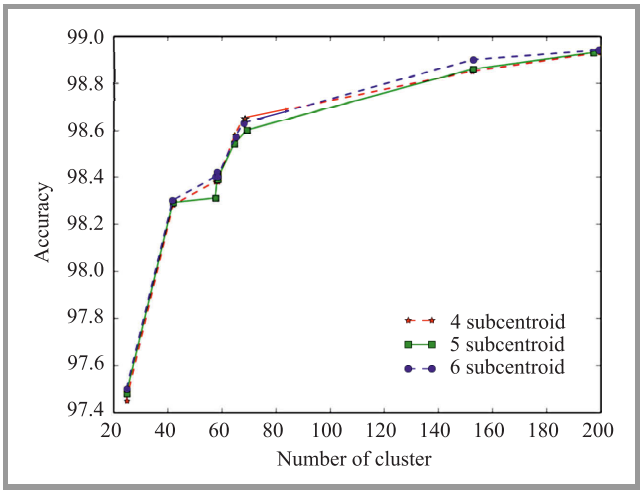

Fig. 10. Correlation between number of cluster and accuracy on Kyoto 2006.

Slightly different from the experiment on NSL-KDD, that on Kyoto 2006 generates logarithmic graphs, as presented in Figs. 10–12. It also shows that increasing the number of clusters means raising the performance, for the same number of subcentroids.

Nevertheless, there is a drawback of this increasing number of clusters. That is, more numbers of clusters need more time to transform the data. This is because each distance between the data and centroids must be calculated. An advantage of this condition is that the time to classify the data drops since the size of each cluster is very likely to be smaller.

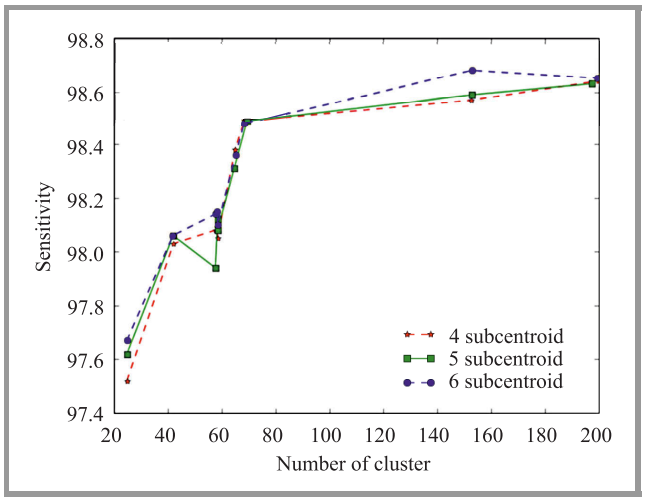

Fig. 11. Correlation between number of cluster and sensitivity on Kyoto 2006.

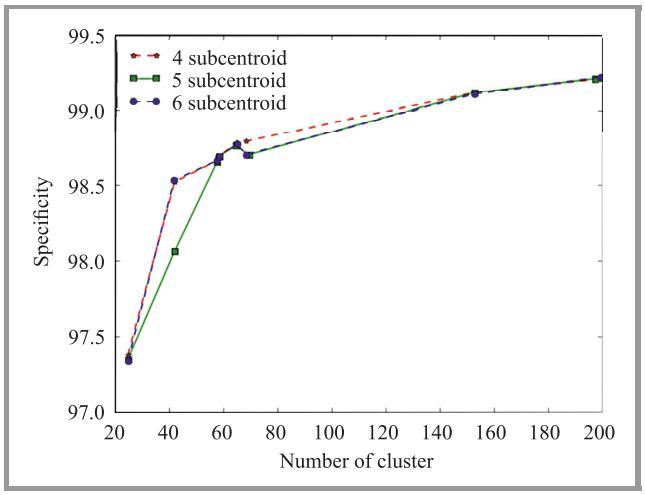

Fig. 12. Correlation between number of cluster and specificity on Kyoto 2006.

5.7. Classification Results

The classification results of our proposed method using combined index = 0.1 and the number of subcentroids = 4 is presented in Table 7. These parameter values are selected because we believe that this combination delivers better results than others, as described in previous tables. In addition, the results of the proposed method with *k*-means whose number of clusters is 5 and 705 as previously specified are in Tables 8 and 9.

Table 7
Classification results of proposed method using combined impurity index 0.1 and subcentroid 4

Actual		Detected				
		Attack				Normal
		Dos	Probe	U2R	R2L	
Attack	Dos	8823	350	0	0	61
	Probe	302	1907	0	1	79
	U2R	0	1	0	2	8
	R2L	0	0	0	189	20
Normal		60	134	1	61	13192

Table 8
Classification results of proposed method with 5 clusters

Actual		Detected				
		Attack				Normal
		Dos	Probe	U2R	R2L	
Attack	Dos	8649	190	0	0	302
	Probe	352	1780	0	0	123
	U2R	0	1	0	0	10
	R2L	3	2	0	155	47
Normal		568	149	0	43	12669

Table 9
Classification results of proposed method with 705 clusters

Actual		Detected				
		Attack				Normal
		Dos	Probe	U2R	R2L	
Attack	Dos	8933	191	0	0	95
	Probe	305	1799	0	2	159
	U2R	0	0	2	0	9
	R2L	0	1	0	182	23
Normal		120	193	3	19	13091

The result shows that the U2R class can only be classified by using *k*-means with 705 clusters. Here, 2 out of 11 have been correctly classified. The classification result of probe and normal classes, however, drops significantly. This hard-classification of U2R class may happen because their coordinate in the cluster is sparsely distributed. Therefore, a relatively high number of clusters are required in order to be able to classify the data correctly.

6. Conclusion

In this paper we have investigated the classification method of data in an IDS. We propose the use of impurity indexes such as the entropy. In addition, we also examine the effect of bisecting *k*-means and logarithmic distance. Based on the experimental results, the use of those parameters and methods gives better performance in terms of accuracy, sensitivity, and specificity than TANN. Overall, we also find that there is correlation between the number of clusters and the performance. That is, more numbers of clusters may result to higher performance.
In the future, we would like to do further research in order to increase the performance. This may be done by normalizing the data in the preprocessing step. Additionally, the

parameter for deciding whether a cluster must be split or not, is to be refined.

References

[1] B. Czaplewski, M. Dzwonkowski, and R. Rykaczewski, "Digital fingerprinting based on quaternion encryption scheme for gray-tone images", *J. Telecommun. & Inform. Technol.*, no. 2, pp. 3–11, 2014.

[2] T. Ahmad and J. Hu, "Generating cancelable biometric templates using a projection line", in *Proc. 11th Int. Conf. on Control, Autom., Robot. & Vision ICARCV 2010*, Singapore, 2010, pp. 7–12.

[3] M. Holil and T. Ahmad, "Secret data hiding by optimizing general smoothness difference expansion-based method", *J. Theor. & Appl. Informa. Technol.*, vol. 72, no. 2, pp. 155–163, 2015.

[4] P. García-Teodoro, J. Díaz-Verdejo, G. Macia-Fernández, and É. Vazquez, "Anomaly-based network intrusion detection: Techniques, systems and challenges", *Comput. Secur.*, vol. 28, no. 1–2, pp. 18–28, 2009.

[5] R. Sommer and V. Paxson, "Outside the closed world: On using machine learning for network intrusion detection", in *Proc. IEEE Symp. on Secur. & Priv.*, Oakland, CA, USA, 2010, pp. 305–316.

[6] I. H. Witten and E. Frank, *Data Mining: Practical Machine Learning Tools and Techniques*, 2nd ed. San Francisco, CA, USA: Morgan Kaufmann Publ. Inc., 2005.

[7] W.-C. Lin, S.-W. Ke, and C.-F. Tsai, "CANN", *Know.-Based Syst.*, vol. 78, no. C, pp. 13–21, 2015.

[8] C.-F. Tsai and C.-Y. Lin, "A triangle area based nearest neighbors approach to intrusion detection", *Pattern Recogn.*, vol. 43, no. 1, pp. 222–229, 2010.

[9] K. Muchammad and T. Ahmad, "Detecting intrusion using recursive clustering and sum of log distance to subcentroid", *Procedia Comp. Sci.*, vol. 72, no. 1, pp. 446–452, 2015.

[10] C. Guo, Y. Zhou, Y. Ping, Z. Zhang, G. Liu, and Y. Yang, "A distance sum-based hybrid method for intrusion detection", *Appl. Intellig.*, vol. 40, no. 1, pp. 178–188, 2014.

[11] J. Parkinson and M. Blaxter, "Simitri-visualizing similarity relationships for groups of sequences", *Bioinformatics*, vol. 19, no. 3, pp. 390–395, Feb. 2003.

[12] B. Luo and J. Xia, "A novel intrusion detection system based on feature generation with visualization strategy", *Expert Syst. Appl.*, vol. 41, no. 9, pp. 4139–4147, 2014.

[13] E.-H. Han and G. Karypis, "Centroid-based document classification: Analysis and experimental results", in *Proceedings of the 4th European Conference on Principles of Data Mining and Knowledge Discovery*. London, UK: Springer, 2000, pp. 424–431.

[14] S. Varuna and P. Natesan, "An integration of *k*-means clustering and nave bayes classifier for intrusion detection", in *Proc. 3rd Int. Conf. on Sig. Process., Commun. & Netw. ICSCN 2015*, Chennai, India, 2015, pp. 1–5.

[15] W. Wang, T. Guyet, R. Quiniou, M.-O. Cordier, F. Masseglia, and X. Zhang, "Autonomic intrusion detection: Adaptively detecting anomalies over unlabeled audit data streams in computer networks", *Knowl.-Based Syst.*, vol. 2014, no. 70, 2014.

[16] X. Zhang, C. Furtlehner, C. Germain-Renaud, and M. Sebag, "Data stream clustering with affinity propagation", *IEEE Trans. on Knowl. & Data Engin.*, vol. 26, no. 7, pp. 1644–1656, 2014.

[17] B. J. Frey and D. Dueck, "Clustering by passing messages between data points", *Science*, vol. 315, no. 5814, pp. 972–976, 2007.

[18] V. Garcia, E. Debreuve, and M. Barlaud,"Fast k-Nearest Neighbor Search using GPU", ArXiv e-prints, Apr. 2008.

[19] J. Heinermann, O. Kramer, K. L. Polsterer, and F. Gieseke, "On GPU based nearest neighbor queries for large-scale photometric catalogs in astronomy", in *KI 2013: Advances in Artificial Intelligence*, I. J. Timm and M. Thimm, Eds. *LNCS*, vol. 8077, pp. 86–97. Springer, 2013.

[20] M. Steinbach, G. Karypis, and V. Kumar, "A comparison of document clustering techniques", in *Proc. KDD Workshop on Text Mining*, Boston, MA, USA, 2000.

[21] A. Demiriz, K. Bennett, and M. J. Embrechts, "Semi-supervised clustering using genetic algorithms", in *Proc. Conf. on Artificial Neural Networks in Engineering ANNIE'99*, St. Louis, MO, USA, 1999, pp. 809–814.

[22] M. Tavallaee, E. Bagheri, W. Lu, and A. A. Ghorbani, "A detailed analysis of the KDD cup 99 data set", in *Proc. 2nd IEEE Symp. on Computat. Intellig. for Secur. & Defense Appl. CISDA'09*, Ottawa, Canada, 2009, pp. 53–58.

[23] J. Song, H. Takakura, Y. Okabe, M. Eto, D. Inoue, and K. Nakao, "Statistical analysis of honeypot data and building of Kyoto 2006+ dataset for NIDS evaluation", in *Proc. 1st Worksh. on Build. Analysis Datasets and Gathering Exper. Returns for Secur. BADGERS 2011*, Salzburg, Austria, 2011, pp. 29–36.

Tohari Ahmad is a lecturer at Institut Teknologi Sepuluh Nopember (ITS) Surabaya, Indonesia. He received his Bachelor, Master and Doctorate degrees from ITS, Monash University (Australia) and RMIT University (Australia), respectively. His research interest is in network security, data hiding and pattern recognition.

E-mail: tohari@if.its.ac.id
Department of Informatics
Institut Teknologi Sepuluh Nopember (ITS)
Surabaya, Indonesia

Kharisma Muchammad received the Bachelor and Master of Computer from Institut Teknologi Sepuluh Nopember (ITS), Surabaya, Indonesia in 2013 and 2016, respectively. His research interest is in applied machine learning, computer security and data hiding. Currently, he is also a software developer in an IT industry.

E-mail: kharisma_muchammad@yahoo.co.id
Department of Informatics
Institut Teknologi Sepuluh Nopember (ITS)
Surabaya, Indonesia

Paper

Closed-form Distribution and Analysis of a Combined Nakagami-lognormal Shadowing and Unshadowing Fading Channel

Rupender Singh and Meenakshi Rawat

Indian Institute of Technology, Roorkee, India

Abstract—The realistic wireless channels face combined (time shared) Nakagami-lognormal shadowing and unshadowing fading because of time varying nature of radio channel and mobile user. These channels can be modeled as time-shared sum of multipath-shadowing and unshadowing Rician distributions. These fading create severe problems in long distance wireless systems where multipath fading is superimposed on shadowing fading (called multipath-shadowing fading). The multipath effect can be modeled using Rayleigh, Rician, Nakagami-m or Weibull distribution and shadowing effect is modeled using lognormal distribution. In this paper, authors present a new closed-form probability distribution function of a Nakagami-lognormal fading channel. Using this result, the closed-form expression of combined Nakagami-lognormal shadowing and unshadowing fading is presented. The obtained closed-form result facilitates to derive the important performance metrics of a communication system such as amount of fading, outage probability, and average channel capacity in closed-form expressions.

Keywords—multipath shadowing fading, outage probability, propagation, wireless communication system.

1. Introduction

The propagation of radio wave through wireless channels is intricate phenomenon characterized by multipath and shadowing effects [1]. This scenario frequently observed with slow moving or stationary user [2]. So the resultant signal at receiver is observed as multipath-shadowing faded signal. Several multipath-shadowing fading models have been presented in [3]–[5]. The precise mathematical expressions and descriptions of this phenomenon are either too complex or unknown for using in real communication system. Based on different experimental observations, lognormal distribution can be used to model shadowing effects [5]–[7] and multipath effect can be captured by using distribution such as Nakagami-m, Rayleigh and Rician distribution [8].

A multipath-shadowing fading scenario are often encountered in a real scenarios. Modeling of composite fading attracts attention due to its role in analyzing the wireless systems such as MIMO and cognitive radio and in the modeling of interferences in cellular phone network. Further, due to mathematical complexity in the closed-form expressions of lognormal based composite models, various approximations to log normal have been suggested. In [9], the Gamma distribution is suggested as an alternative approach to lognormal to model shadowing effect. In [10], a composite Nakagami/N-Gamma distribution is considered and performance metrics such as outage probability and biterror rate for receiver are analyzed. The work in [2] analyses the composite Nakagami-lognormal (NL) fading approximating lognormal shadowing as an Inverse Gaussian (IG) distribution, thus, ensuring the resultant expression in the closed-form. In [11], [12] a multipath-shadowing fading is represented as a series of Nakagami-Mixtures of Gamma distribution. In [13], considering Nakagami-lognormal composite fading, second-order statistics of fading channel has been studied. They expressed probability distribution function in closed form using Gauss-Hermite quadrature function. However, combined NL shadowing and unshadowing fading scenario has got little attention till date in terms of closed-form PDF and is not reported in literature and thus, hampering further analytical derivation of important performance metric such as amount of fading (AOF), average channel capacity, and outage probability.

In the case of mobile user there is the possibility of receiving signal from both line of sight (LOS) and shadowing path. This concept was discussed in [1], [14]. In early 1990s, Lutz *et al.* [15] and Barts and Stutzman [16] found that total fading for land-mobile satellite systems can be viewed as combination of unshadowed fading and a multipath-shadowing fading [1]. Statistical modeling of this realistic scenario has also received a little attention in research community until date.

In this paper, the goal is to obtain the closed-form expression of Nakagami-lognormal (NL) distribution using Holtzman approximation [17] for the expectation of the function of a normal variant. The closed-form expression facilitates to obtain a simple analytical approximation of the probability density function (PDF) of combined NL shadowing and unshadowing (Rician) fading. Further, the proposed closed-form PDF leads to the derivation of the closed-form solution of the performance metrics of communication system such as AOF, outage probability P_{out} and channel capacity C/B using Meijer G function for both multipath-shadowing fading as well as combined shadowing and unshadowing fading channel.

The remainder of the paper is organized as follows. In Section 2 the closed-form expression of NL distribution is obtained and using it, the distribution of combined fading is expressed. AOF for the composite fading channels is derived followed by combined fading using Kummer confluent hyper geometric function in Section 3. In Section 4, performance measure such as P_{out} of the communication system is analyzed. The derivation of average channel capacity for both the composite fading as well as combined fading is derived in Section 5. This is followed by results and discussion in Section 6. Finally conclusions are given in Section 7.

2. The PDF of Combined NL Shadowing and Unshadowing Distribution

2.1. PDF of NL Shadowing

In this section, a closed-form of Nakagami-lognormal composite fading is derived where Nakagami-m represents multipath effect and lognormal model capture the effect of shadowing. PDF of signal to noise ratio (SNR) of NL shadowing can be obtained by averaging the conditional PDF of NL distribution over lognormal fading. Conditional Nakagami-m distribution is given as [1], [2]:

$$p\left(\frac{\gamma}{w}\right) = \frac{m^m \gamma^{m-1}}{w^m \Gamma(m)} \mathrm{e}^{-\frac{m\gamma}{w}}; \qquad \gamma \geq 0, \tag{1}$$

where $\Gamma(\cdot)$ is Gamma function and m is the Nakagami-m fading parameter. The parameter γ is the average SNR at the receiver. Here, w is slowly varying power and modeled using lognormal distribution:

$$p(w) = \frac{1}{\sigma w \sqrt{2\pi}} \mathrm{e}^{-\frac{(\log_e w - \mu)^2}{2\sigma^2}}; \qquad w \geq 0, \tag{2}$$

where the parameters μ and σ are mean and standard deviation, respectively of random variable (RV) $\log_e w$. They can be expressed in decibels by $\sigma_{dB} = \xi\sigma$ and $\mu_{dB} = \xi\mu$, where $\xi = 10/\ln 10$ [6]. Averaging the PDF of Eq. (1) w.r.t. Eq. (2), we have PDF of composite NL fading:

$$p(\gamma) = \int_0^\infty p\left(\frac{\gamma}{w}\right) p(w) \mathrm{d}w. \tag{3}$$

Substituting the PDFs from Eqs. (1) and (2), into Eq. (3), we have

$$p(\gamma) = \int_0^\infty \left\{ \frac{m^m \gamma^{m-1}}{w^m \Gamma(m)} exp\left(-\frac{m\gamma}{w}\right) \right\} \times \\ \times \left\{ \frac{1}{\sigma w \sqrt{2\pi}} \mathrm{e}^{-\frac{(\log_e w - \mu)^2}{2\sigma^2}} \right\} \mathrm{d}w. \tag{4}$$

It is difficult to calculate the result in closed-form. In this work, the approach proposed by Holtzman [17], [18]. Taking $\log_e w = x$ in Eq. (2):

$$p(\gamma) = \int_0^\infty \psi(\gamma; x) \left\{ \frac{1}{\sigma\sqrt{2\pi}} \mathrm{e}^{-\frac{(x-\mu)^2}{2\sigma^2}} \right\} \mathrm{d}x. \tag{5}$$

Then, finally PDF of NL fading is:

$$p(\gamma) = \tfrac{2}{3}\psi(\gamma;\mu) + \tfrac{1}{6}\psi(\gamma;\mu+\sigma\sqrt{3}) + \\ + \tfrac{1}{6}\psi(\gamma;\mu-\sigma\sqrt{3}), \tag{6}$$

where

$$\psi(\gamma;x) = \frac{m^m \gamma^{m-1}}{\mathrm{e}^{x^m} \Gamma(m)} \mathrm{e}^{-\frac{m\gamma}{\mathrm{e}^x}}. \tag{7}$$

Using Eqs. (6) and (7), CDF of NL fading is derived as:

$$P(\gamma) = \sum_{i=1}^{3} d_i \Gamma(\gamma, m), \tag{8}$$

where, $\Gamma(\cdot,\cdot)$ is incomplete Gamma function and $d_i\,(i = 1,2,3)$ are $\frac{2}{3}$, $\frac{1}{6}$, $\frac{1}{6}$.

2.2. PDF of the Combined NL Shadowing and Unshadowing Fading

Considering the case of mobile user there is a possibility of receiving signal from both LOS and shadowing path. So combined PDF of instantaneous SNR γ is [14]

$$p(\gamma) = (1-A) \times \text{PDF of Rician fading} + \\ + A \times \text{PDF of NL composite shadowing fading}, \tag{9}$$

where A is shadowing time-share factor and $0 \leq A \leq 1$. When $A = 1$, only NL shadowing exists and for $A = 0$, only unshadowing (Rician) exists. For $0 < A < 1$, a mobile user moves between unshadowing and composite shadowing fading.

Rice distribution of γ (SNR per symbol) is given as [14]

$$p_{rice}(\gamma) = \frac{(1+K)\mathrm{e}^{-K}}{\overline{\gamma}} \mathrm{e}^{-\frac{(1+K)\gamma}{\overline{\gamma}}} I_o \quad 2\sqrt{\frac{K(1+K)\gamma}{\overline{\gamma}}}\Bigg), \tag{10}$$

where $I_0(\cdot)$ is modified Bessel function of first kind with zero order, $\overline{\gamma}$ is average SNR per symbol and K is Rician factor [1]. Rice distribution is often used to model the propagation channel consisting of LOS and some multipath components. Using $p(\gamma)$ from Eqs. (6), (7), (9), and (10), PDF of combined NL and unshadowing fading is given as:

$$p(\gamma) = (1-A) \times \frac{(1+K)\mathrm{e}^{-K}}{\overline{\gamma}} \mathrm{e}^{-\frac{(1+K)\gamma}{\overline{\gamma}}} \\ \times I_o \quad 2\sqrt{\frac{K(1+K)\gamma}{\overline{\gamma}}}\Bigg) + A\sum_{i=1}^{3} d_i \psi(\gamma; x_i), \tag{11}$$

where $x_i (i = 1,2,3)$ are $\mu, \mu+\sigma\sqrt{3}, \mu-\sigma\sqrt{3}$, $\psi(\gamma;x_i)$ is defined in Eq. (7) and $d_i\,(i = 1,2,3)$ are $\frac{2}{3}$, $\frac{1}{6}$, $\frac{1}{6}$.

3. Amount of Fading

Amount of fading is a measure of severity of fading of the channel. In this section, the AOF of the NL fading is computed. The amount of fading is defined as [1]:

$$AOF = \frac{E[\gamma^2]}{(E[\gamma])^2} - 1. \tag{12}$$

Considering the closed-form expressions given in Eqs. (6) and (7), k-th moment of γ is given as:

$$E[\gamma^k] = \int_0^\infty \gamma^k \frac{m^m \gamma^{m-1}}{\overline{\gamma}^n \Gamma(m)} \mathrm{e}^{-\frac{m\gamma}{\overline{\gamma}}} \mathrm{d}\gamma, \tag{13}$$

where $\overline{\gamma} = \mathrm{e}^x$.

Substituting $\frac{m\gamma}{\overline{\gamma}} = R$ in Eq. (13) and after some simple calculations:

$$E[\gamma^k] = \frac{\Gamma(m+k)}{\Gamma(m)} \left(\frac{\mathrm{e}^x}{m}\right)^k. \tag{14}$$

Thus, considering all the three terms of Eq. (6):

$$E[\gamma^k] = \sum_{i=1}^{3} \frac{d_i \Gamma(m+k)}{\Gamma(m)} \left(\frac{e^{x_i}}{m}\right)^k. \tag{15}$$

From Eq. (12), AOF for NL fading is given as:

$$\mathrm{AOF} = \left[\ dfrac\Gamma(m+2)\Gamma(m)(\Gamma)^2(m+1)m\right] \times \times \left[\frac{\left\{\frac{2}{3}\mathrm{e}^{2\mu} + \frac{1}{6}\mathrm{e}^{2\mu+2\sigma\sqrt{3}} + \frac{1}{6}\mathrm{e}^{2\mu-2\sigma\sqrt{3}}\right\}}{\left\{\frac{2}{3}\mathrm{e}^{\mu} + \frac{1}{6}\mathrm{e}^{\mu+\sigma\sqrt{3}} + \frac{1}{6}\mathrm{e}^{\mu-\sigma\sqrt{3}}\right\}^2}\right] - 1, \tag{16}$$

k-th moment of output SNR of combined fading is:

$$E[\gamma^k] = (1-A)\int_0^\infty \gamma^k p_{rice}(\gamma) d\gamma + A\int_0^\infty \gamma^k p_{comp}(\gamma) \mathrm{d}\gamma. \tag{17}$$

The k-th moment of Rice distribution is given as [1]:

$$E[\gamma^k] = \frac{\Gamma(1+k)}{(1+k)^k} {}_1F_1(-k,1;-K)\overline{\gamma}^k, \tag{18}$$

where ${}_1F_1(\cdot,\cdot;\cdot)$ is Kummer confluent hyper geometric function.

Thus, the k-th moment of combined NL and unshadowing fading is obtained by substituting Eqs. (15) and (18) in Eq. (17):

$$E[\gamma^k] = (1-A)\frac{\Gamma(1+k)}{(1+k)^k} {}_1F_1(-k,1;-K)\overline{\gamma}^k + + \sum_{i=1}^{3} \frac{d_i \Gamma(m+k)}{\Gamma(m)} \left(\frac{\mathrm{e}^{x_i}}{m}\right)^k. \tag{19}$$

Amount of fading can be obtained using Eqs. (19) and (12).

4. Outage Probability

The outage probability P_{out} is one of the standard performance criterion of communication systems operating over fading channels and it is defined as [1]:

$$P_{out}(\gamma_{th}) = \int_0^{\gamma_{th}} p(\gamma) \mathrm{d}\gamma. \tag{20}$$

Substitution of Eq. (10) into Eq. (20) yields P_{out} of Rician fading channel and is expressed as:

$$P_{out}(\gamma_{th})_{rice} = \int_0^{\gamma_{th}} \frac{(1+K)\mathrm{e}^{-K}}{\overline{\gamma}} \mathrm{e}^{-\frac{(1+K)\gamma}{\overline{\gamma}}} \times \times I_o\left(2\sqrt{\frac{K(1+K)\gamma}{\overline{\gamma}}}\right) \mathrm{d}\gamma. \tag{21}$$

To solve this, $I_0(z)$ is replaced in (21) using [19] $a = \frac{1+K}{\overline{\gamma}}$, $P_{out}(\gamma_{th})_{rice}$ is given as:

$$P_{out}(\gamma_{th})_{rice} = \sum_{n=0}^{\infty} \frac{a^{n+1} e^{-K} K^n}{n!^2} \int_0^{\gamma_{th}} \gamma^n \mathrm{e}^{-a\gamma} \mathrm{d}\gamma. \tag{22}$$

Using Appendix 1, Eq. (22) can be computed as:

$$P_{out}(\gamma_{th})_{rice} = \sum_{n=0}^{\infty} \frac{a^{n+1} e^{-K} K^n}{n!^2} \times \times \Big[(-a)^{n-1}(-1)^n \Gamma[1+n, a\gamma_{th}] - (-a)^{n-1}(-1)^n \Gamma[1+n,0]\Big]. \tag{23}$$

Considering the incomplete Gamma function and its relation with Kummer's confluent hypergeometric function from [20], the Eq. (23) can also be expressed as:

$$P_{out}(\gamma_{th})_{rice} = \sum_{n=0}^{\infty} \frac{a^{n+1} e^{-K} K^n}{n!^2} a^{-n-1}(1+n)^{-1} \times \times (a\gamma_{th})^{n+1} \times {}_1F_1(n+1, 2+n; -a\gamma_{th}). \tag{24}$$

P_{out} of NL fading can be obtained by substituting Eq. (6) into Eq. (20), which yields:

$$P_{out}(\gamma_{th})_{NL} = \sum_{i=1}^{3} d_i \Gamma(\gamma_{th}, m). \tag{25}$$

Using the results of Eqs. (23) and (25), P_{out} of combined NL and unshadowing channel can be written in closed form as:

$$P_{out}(\gamma_{th}) = \sum_{n=0}^{\infty} \frac{(1-A)a^{n+1} e^{-K} K^n}{n!^2} \times \times \Big[(-a)^{n-1}(-1)^n \Gamma[1+n, a\gamma_{th}] - (-a)^{n-1}(-1)^n \times \times \Gamma[1+n,0]\Big] + \sum_{i=1}^{3} d_i \Gamma(\gamma_{th}, m). \tag{26}$$

5. Average Channel Capacity

The average channel capacity for fading channel is a significant performance metric as it gives an estimation of the information rate that the channel can support with small probability of error. Channel capacity is defined as [21]:

$$\frac{C}{B} = \int_0^\infty \log_2(1+\gamma) p(\gamma) \mathrm{d}\gamma. \tag{27}$$

Using Eq. (10) into Eq. (27), the average channel capacity of Rician fading channel is given as:

$$\frac{C}{B}_{rice} = \int_0^\infty \log_2(1+\gamma) \frac{(1+K)\mathrm{e}^{-K}}{\overline{\gamma}} \mathrm{e}^{-\frac{(1+K)\gamma}{\overline{\gamma}}} \times \times I_o\left(2\sqrt{\frac{K(1+K)\gamma}{\overline{\gamma}}}\right) \mathrm{d}\gamma. \tag{28}$$

After substituting the modified Bessel function from [19] into Eq. (28) and noting the Meijer G functions from Appendix 1, an average channel capacity for Rician fading may be written as:

$$\frac{C}{B}_{rice} = \sum_{n=0}^{\infty} \frac{a^{n+1}\mathrm{e}^{-K}K^n}{\ln(2)n!^2} \int_0^{\infty} \gamma^n \mathrm{G}_{2,2}^{1,2}\left[\gamma \middle| \begin{matrix} 1,1 \\ 1,0 \end{matrix}\right] \times \times \mathrm{G}_{0,1}^{1,0}\left[a\gamma \middle| 0\right] \mathrm{d}\gamma, \quad (29)$$

where $a = \frac{1+K}{\bar{\gamma}}$, replacing n by $n-1$ in Eq. (29) and using Appendix 1 and [21], the average channel capacity of Rician fading channel is expressed as:

$$\frac{C}{B}_{rice} = \sum_{n=-1}^{\infty} \frac{a^n \mathrm{e}^{-K}K^{n-1}}{\ln(2)(n-1)!^2} \mathrm{G}_{2,3}^{3,1}\left[a \middle| \begin{matrix} -n,1-n \\ 0,-n,-n \end{matrix}\right]. \quad (30)$$

After substituting Eq. (6) in Eq. (27), the channel capacity for the NL shadowing fading is given as:

$$\frac{C}{B}_{NL} = \int_0^{\infty} \log_2(1+\gamma)\left\{\left(\frac{2}{3}\psi(\gamma;\mu\right) + \right. \left. + \frac{1}{6}\psi(\gamma;\mu+\sigma\sqrt{3}) + \frac{1}{6}\psi(\gamma;\mu-\sigma\sqrt{3})\right\}\mathrm{d}\gamma. \quad (31)$$

From Eq. (7):

$$\frac{C}{B}_{NL} = \sum_{i=1}^{3} \frac{{b_i}^m d_i}{ln(2)\Gamma(m)} \int_0^{\infty} \gamma^{m-1} \ln(1+\gamma)\mathrm{e}^{-\gamma b_i}\mathrm{d}\gamma, \quad (32)$$

where $b_i = m \cdot \mathrm{e}^{-x_i}$.

Using Meijer G function from Appendix 1 in Eq. (32):

$$\frac{C}{B}_{NL} = \sum_{i=1}^{3} \frac{{b_i}^m d_i}{\ln(2)\Gamma(m)} \int_0^{\infty} \gamma^{m-1} \mathrm{G}_{2,2}^{1,2}\left[\gamma \middle| \begin{matrix} 1,1 \\ 1,0 \end{matrix}\right] \mathrm{G}_{0,1}^{1,0}\left[b_i\gamma \middle| 0\right] \mathrm{d}\gamma. \quad (33)$$

Using Appendix 1, average channel capacity of NL fading is expressed as:

$$\frac{C}{B}_{NL} = \sum_{i=1}^{3} \frac{{b_i}^m d_i}{ln(2)\Gamma(m)} \mathrm{G}_{2,3}^{3,1}\left[b_i \middle| \begin{matrix} -m+1,-m \\ 0,-m+1,-m+1 \end{matrix}\right]. \quad (34)$$

From Eqs. (30) and (34), average channel capacity of combined NL and unshadowing channel is given in closed form as:

$$\frac{C}{B}_{rice} = \sum_{n=-1}^{\infty} \frac{(1-A)a^n e^{-K}K^{n-1}}{\ln(2)(n-1)!^2} \mathrm{G}_{2,3}^{3,1}\left[a \middle| \begin{matrix} -n,1-n \\ 0,-n,-n \end{matrix}\right] + + \sum_{i=1}^{3} \frac{A{b_i}^m d_i}{\ln(2)\Gamma(m)} \mathrm{G}_{2,3}^{3,1}\left[b_i \middle| \begin{matrix} -m+1,-m \\ 0,-m+1,-m+1 \end{matrix}\right]. \quad (35)$$

6. Results and Discussion

In Figs. 1, 2, and 3 exact plot using Eq. (4) and proposed closed-form solution using Eq. (11) are plotted. The proposed closed-form solution perfectly matches the exact solution, which confirms accuracy of proposed closed-form solution. In Figs. 1 and 2, values of A and K are fixed (0.25 and 11.9 dB, respectively) and m takes values 0.5, 2, and 4. In Fig. 3, m takes value 2 whereas values of K and A as per Table 1. Values of μ and σ are taken as -3.914 and 0.806, respectively for heavy shadowing and -0.115 and 0.161, respectively for average shadowing [2]. Different shadowing cases given in [22] have been considered such as urban, sub-urban and highway scenarios. The corresponding values of A (parameter showing occurrence of shadowing) and Rice factor K, for these scenarios are presented in Table 1. It is observed from the PDF of the combined NL shadowing and unshadow-

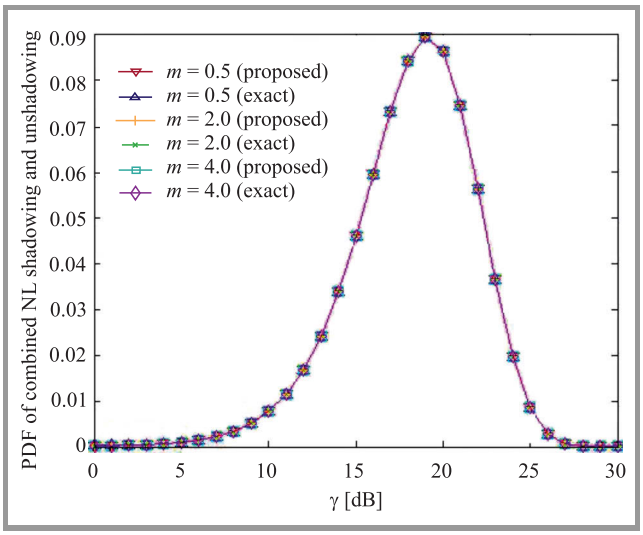

Fig. 1. PDF of combined NL shadowing and unshadowing for heavy shadowing ($\mu = -3.914$, $\sigma = 0.806$, $A = 0.25$, $K = 11.9$ dB.
(See color pictures online at www.nit.eu/publications/journal-jtit)

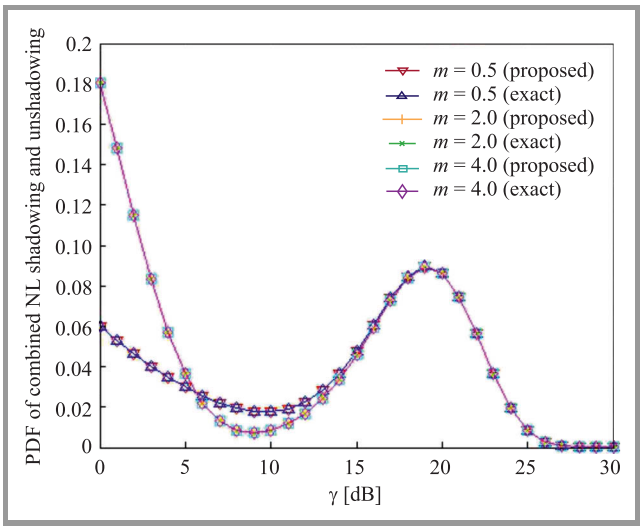

Fig. 2. PDF of combined NL shadowing and unshadowing for average shadowing ($\mu = -0.115$, $\sigma = 0.0.161$, $A = 0.25$, $K = 11.9$ dB.

ing fading that for urban scenario, the PDF is closer to NL fading and as the user moves from urban to highway, the combined PDF gets closer to Rician distribution. Thus, for highway scenario, the fading is dominated by Rician distribution. Hence, the PDF approaches the perfect Rician curve.

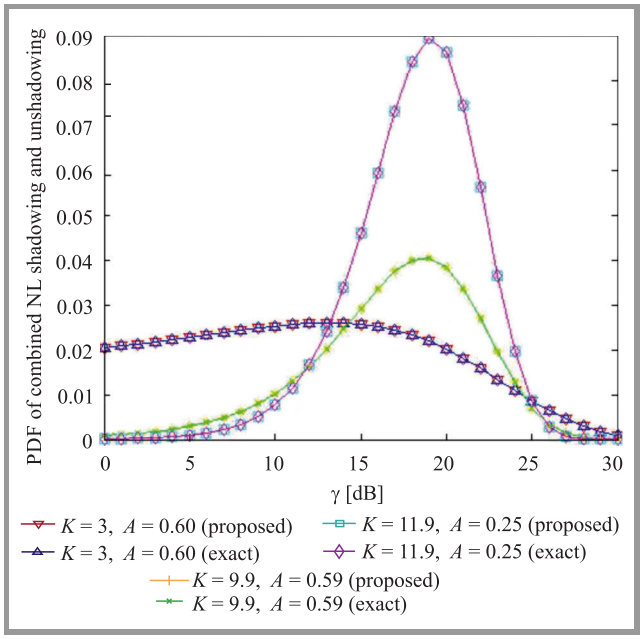

Fig. 3. PDF of combined NL shadowing and unshadowing for urban, suburban and highway ($\mu = -3.914$, $\sigma = 0.806$, $m = 2$).

In Fig. 4, AOF has been plotted for different time-share factor A. This figure gives details about variation in the total amount of fading with variation in probabilistic change in the fading conditions for a combined fading scenario. Initially, with $A = 0$, only Rician condition dominates and hence AOF remains very low. With increase in A, fading is dominated by multipath shadowing condition and hence

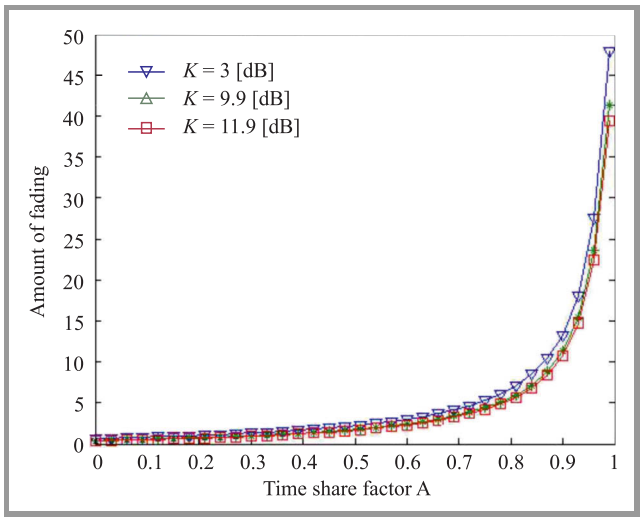

Fig. 4. Amount of fading for combined NL shadowing and unshadowing ($\mu = -3.914$, $\sigma = 0.806$, $m = 0.5, \overline{\gamma} = 10$ dB.

Table 1
Parameters A and K for various scenarios

Environment	A	K [dB]
Urban	0.60	3
Suburban	0.59	9.9
Highway	0.25	11.9

AOF increases with increase in A. One can also observe that AOF slightly decreases with increase in Rice factor K due to obvious reason.

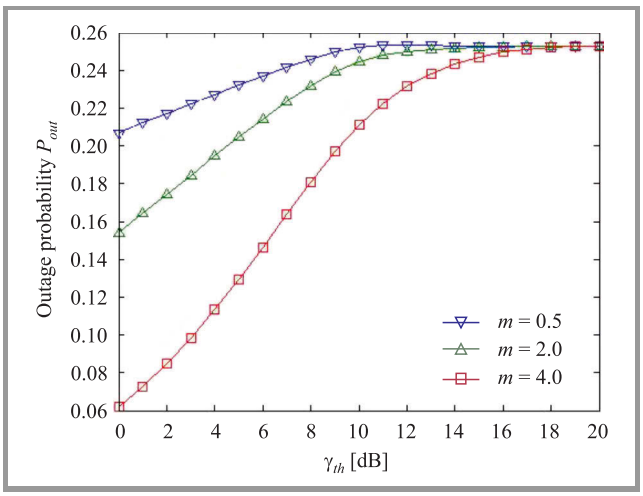

Fig. 5. Outage probability for heavy shadowing($\mu = -3.914$, $\sigma = 0.806$, $\overline{\gamma} = 10$ dB, $A = 0.25$ and $K = 11.9$ dB.

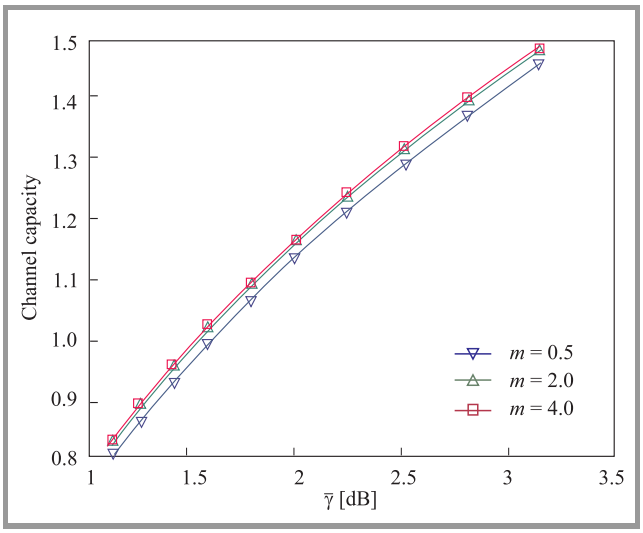

Fig. 6. Average channel capacity for combined NL shadowing and unshadowing for different values of m parameter ($\mu = -0.115$, $\sigma = 0.161$, $A = 0.25$, $K = 11.9$ dB.

P_{out} of combined fading is illustrated in Fig. 5 for different threshold level γ_{th}. As expected P_{out} increases with increase in threshold level γ_{th}. Increasing m indicates the less fluctuation of the multipath effect of composite fading, so P_{out} is expected to decrease with increase in m parameter and it is observed from the Fig. 5.

Figure 6 gives the numerical results for the average channel capacity vs average SNR $\overline{\gamma}$ for combined fading for different m parameter. As is observed the channel capacity increases with $\overline{\gamma}$ and also there is a shift in upwards direction with increase in value of m parameter. At high value of m, NL shadowing fading moves towards deterministic, which results into better channel capacity.

7. Conclusion

In this paper, the closed-form expressions for PDF of instantaneous SNR, amount of fading, outage probability, and average channel capacity of the Nakagami-lognormal fading and combined (time shared) NL shadowing and unshadowing (Rician) fading are derived. The approach uses the Holtzmanian approximations to estimate the closed-form of PDF of NL fading. The resulting Holtzman approximation for NL fading has the advantage of being in closed-form, thereby facilitating the performance evaluation of communication links over combined NL shadowing and unshadowing fading channel.

Appendix 1

$I_0(z)$ from [19]

$$I_0(z) = \sum_{n=0}^{\infty} \frac{\left(\frac{z}{z}\right)^{2n}}{n1^2}.$$

For any z [20]:

$$\int z^n \mathrm{e}^{-az} \mathrm{d}z = a^{-n-1}(-1)^n .\Gamma(1+n,-z)$$

For any z [20]:

$$\mathrm{e}^{-z} = \mathrm{G}_{0,1}^{1,0}\left[z\middle|0\right].$$

For any z [20]:

$$\ln(1+\gamma) = \mathrm{G}_{2,2}^{1,2}\left[z\middle|\begin{matrix}1,1\\1,0\end{matrix}\right].$$

Meijer's integral from two G functions [20]:

$$\int_0^{\infty} z^n \mathrm{G}_{2,2}^{1,2}\left[z\middle|\begin{matrix}1,1\\1,0\end{matrix}\right] \mathrm{G}_{0,1}^{1,0}\left[z\middle|0\right] \mathrm{d}z = \mathrm{G}_{2,3}^{3,1}\left[a\middle|\begin{matrix}-n,1-n\\0,-n,-n\end{matrix}\right].$$

References

[1] M. K. Simon and M. S. Alouini, *Digital Communication over Fading Channels: A Unified Approach to Performance Analysis*. New York: Wiley, 2000.

[2] A. Laourine, M.-S. Alouini, S. Affes, and A. Stephenne, "On the performance analysis of composite multipath/shadowing channels using the G-distribution", *IEEE Trans. on Commun.*, vol. 57, no. 4, pp. 1162–1170, 2009.

[3] F. Hansen and F. I. Mano, "Mobile fading-rayleigh and lognormal superimposed", *IEEE Trans. Vehic. Technol.*, vol. VT-26, no. 4, pp. 332–335, 1977.

[4] N. C. Sagias, G. K. Karagiannidis, P. S. Bithas, and P. T. Mathiopoulos, "On the correlated weibull fading model and its applications", in *Proc. 62nd IEEE Veh. Techol. Conf. VTC-2005-Fall*, Dallas, USA, 2005, vol. 4, pp. 2149–2153 (doi: 10.1109/VETECF.2005.1558500).

[5] W. C. Jakes, *Microwave Mobile Communication*, 2nd ed. Piscataway, NJ: IEEE Press, 1994.

[6] V. Khandelwal and Karmeshu, "A new approximation for average symbol error probability over log-normal channels", *IEEE Wireless Commun. Lett.*, vol. 3 no. 1, pp. 58–61, 2014.

[7] H. Hashemi, "Impulse response modeling of indoor radio propagation channels", *IEEE J. Select. Areas Commun.*, vol. SAC-11, pp. 967–978, 1993.

[8] S. Al-Ahmadi and H. Yanikomeroglu, "On the approximation of the generalized-k distribution by a gamma distribution for modeling composite fading channels", *IEEE Trans. on Wireless Comm.*, vol. 9, no. 2, pp. 706–713, 2010.

[9] A. Abdi and M. Kaveh, "On the utility of Gamma PDF in modeling shadow fading (slow fading)", in *Proc. 49th IEEE Veh. Technol. Conf.*, Houston, TX, USA, 1999, vol. 3, pp. 2308–2312 (doi: 10.1109/VETEC.1999.778479).

[10] P. M. Shankar, "A Nakagami-N-gamma Model for shadowed fading channels", *Wireless Personal Commun.*, vol. 64, p. 665–680, 2012 (doi: 10.1007/s11277-010-0211-5).

[11] S. Atapattu, Ch. Tellambura, and H. Jiang, "Representation of composite fading and shadowing distributions by using mixtures of gamma distributions", in *Proc. of IEEE Wireless Commun. & Network. Conf. WCNC 2010*, Sydney, Australia, 2010 (doi: 10.1109/WCNC.2010.5506173).

[12] W. Cheng, "On the Performance of Multi-node Cooperative Networks over Composite Nakagami-lognormal Fading Channels using Mixture Gamma Distribution", *Journals of Computers*, vol. 8, no. 10, pp. 2607–2614, 2013.

[13] X. Wang, W. Wang, and Z. Bu, "Fade statistics for selection diversity in Nakagami-lognormal fading channels", *IEEE Electron. Lett.*, vol. 42, no. 18, pp. 1046–1048, 2006 (doi: 10.1049/el:20061744).

[14] M.-S. Alouini and A. J. Goldsmith "A unified approach for calculating error rates of linearly modulated signals over generalized fading channels", *IEEE Trans. on Commun.*, vol. 47, no. 9, pp. 1324–1334, 1999.

[15] E. Lutz, D. Cygan, M. Dippold, F. Dolainsky, and W. Papke, "The land mobile satellite communication channel: recording, statistics, and channel model", *IEEE Trans. Veh. Technol.*, vol. VT-40, pp. 375–386, 1991.

[16] R. M. Barts and W. L. Stutzman, "Modeling and simulation of mobile satellite propagation", *IEEE Trans. Antennas Propagat.*, vol. AP-40, pp. 375–382, 1992.

[17] J. M. Holtzman, "A simple, accurate method to calculate spread multiple access error probabilities", *IEEE Trans. Commun.*, vol. 40, no. 3, pp. 461–464, 1992.

[18] Karmeshu and V. Khandelwal, "On the applicability of average channel capacity in log-normal fading environment", *Wireless Personal Commun.*, vol. 68, no. 4, pp. 1393–1402, 2012 (doi: 10.1007/s11277-012-0529-2).

[19] I. S. Gradshteyn and I. M. Ryzhik, *Table of Integrals, Series, and Products*, 7th ed. Academic Press, 2007.

[20] "Wolfram. The Wolfram functions site" [Online]. Available: http://functions.wolfram.com (last visited on 20th Oct, 2015).

[21] F. El Bouanani, H. Ben-Azza, and M. Belkasmi, "New results for Shannon capacity over generalized multipath fading channels with MRC diversity", *EURASIP J. on Wireless Commun. & Network.*, 2012:336, Nov. 2012 (doi: 10.1186/1687-1499-2012-336).

[22] J. Goldhirsh and W. J. Vogel, *Handbook of Propagation Effects for Vehicular and Personal Mobile Satellite Systems*, Johns Hopkins University Applied Physics Laboratory and the University of Texas at Austin, Dec. 1998.

Rupender Singh has done his M.Tech. from Delhi Technological University (formerly Delhi College of Engineering), Delhi, India. He has received his B.Tech. from MJP Rohilkhand University, Bareilly, India. Currently he is working towards his Ph.D. from Indian Institute of Technology, Roorkee, India, with specialization in wireless communication. He has published one book and presented 20 papers in national and international journals. His current research interest is focused on wireless communication.

E-mail: rupendersingh04cs39@gmail.com
Indian Institute of Technology
Roorkee, India

Meenakshi Rawat received the B.Tech. degree in Electrical Engineering from the Govind Ballabh Pant University of Agriculture and Technology, Uttarakhand, India, in 2006, and the M.Sc. and Ph.D. degrees in Electrical and Computer Engineering from the University of Calgary, Calgary, Canada, in 2012. From September 2012 to June 2013, she was a Post-Doctoral Research Fellow with the University of Calgary. From July 2013 to June 2014, she was a Post-Doctoral Project Researcher/Scientist with the Ohio State University. She is currently an Assistant Professor with the Indian Institute of Technology (IIT), Roorkee, India.

E-mail: rawatfec@iitr.ac.in
Indian Institute of Technology
Roorkee, India

Paper

Long-term Absolute Wavelength Stability of Acetylene-stabilized Reference Laser at 1533 nm

Tomasz Kossek[1], Dariusz Czułek[2], and Marcin Koba[1]

[1] *National Institute of Telecommunications, Warsaw, Poland*
[2] *Central Office of Measures, Warsaw, Poland*

Abstract—The second harmonic generation process in Periodically Poled Lithium Niobate (PPLN) has been applied in order to measure frequency of reference laser locked to acetylene absorption peak $^{12}C_2H_2$ (P13) (1533 nm) against optical frequency synthesizer. The measurement results have been compared to the results obtained using different techniques for the same reference laser during the past 10 years in other laboratories.

Keywords—laser, optical comb generator, optical frequency standard, second harmonic generation.

1. Introduction

Accurate optical frequency standards are important tool in various technological domains. This is most important in high accuracy distance measurement, spectroscopy, and recently in development of fiber optic telecommunications.

A new definition of meter directly related to speed of light in vacuum and time has been proposed. It was possible due to progress in building more accurate atomic time and optical frequency standards. During last decades, a lot of research has been done in the area of spectroscopy of reference materials, which can be used as a reference for optical frequency standards. There are several practical realizations of optical frequency standards and they were summarized by BIPM [1]. In most cases the optical frequency standards in visible and near infrared regions are built as He-Ne (543 nm, 633 nm) lasers locked to absorption lines of iodine, or DFB laser diodes locked to rubidium two-photon transition (778 nm).

The rapid development of Dense Wavelength Division Multiplexing (DWDM) fiber optic networks stimulates research on optical frequency standards in wavelengths range around 1550 nm. The best candidates to meet the increasing demand on these standards seem isotopomers of acetylene $^{12}C_2H_2$ and $^{13}C_2H_2$ which cover wavelength range of 1520–1550 nm. The measurement accuracy at the level of 10^{-9}–10^{-10} of optical frequencies of absorption lines has been achieved in case of molecular absorption cells [2], [3]. The lasers stabilized to acetylene $^{13}C_2H_2$ have been put by Consultative Committee for Length (CCL) of the Metric Convention in 2001 into the list of radiation sources, which realize the definition of SI meter. Especially, the P(16) 1542.384 nm absorption peak has been chosen as most accurate. A lot of specific solutions have been proposed over the years of development up to compact fiber-based solutions [4]–[8].

The commercially available stabilized lasers offer wavelength accuracy of ±0.0001 nm in wavelength domain. In such systems, the dithering of output signal can be observed due to the electronic way of wavelength locking which usually is better than ±0.05 pm (±6 MHz), while the linewidth of DFB laser diodes used in optical frequency standards is not broader than 1 MHz.

The development of optical frequency standards stimulates progress in wavelength/optical frequency measurement methods and measurement equipment. In practice, the interferometric setups, beating of laser signals, and femtosecond laser comb generators are used [9]–[12]. Especially the latter ones [12] facilitate measurement of optical frequencies at highest accuracies. At the beginning, the optical comb generators were driven by Ti:Sapphire femtosecond lasers and did not cover 1550 nm wavelength region. The next generation combs based on Er-doped mode-locked fiber lasers, apart from reducing cost of such system and its complexity, gave the possibility of direct optical frequency measurements in 1550 nm wavelength region without the need of second harmonic generation (SHG). Nevertheless only few laboratories offer measurement of optical frequency against comb generators in full wavelength range.

The authors motivations was to measure frequency of their reference laser against optical frequency comb generator and then compare measurement results with results obtained earlier using different methods.

The application of SHG technique in case of frequency measurement of laser emitting light in 1550 nm region against optical frequency comb generator was reported in [13]. In conducted experiment, in contrast to the cited work we did not use "lab developed" technology but commercially available comb generator which is installed in Central Office of Measures (Warsaw, Poland). The tested laser was also delivered by commercial company and its parameters were not as good as the best of its kind. Thus, we were particularly interested in the behavior of the device parameters over relatively long period.

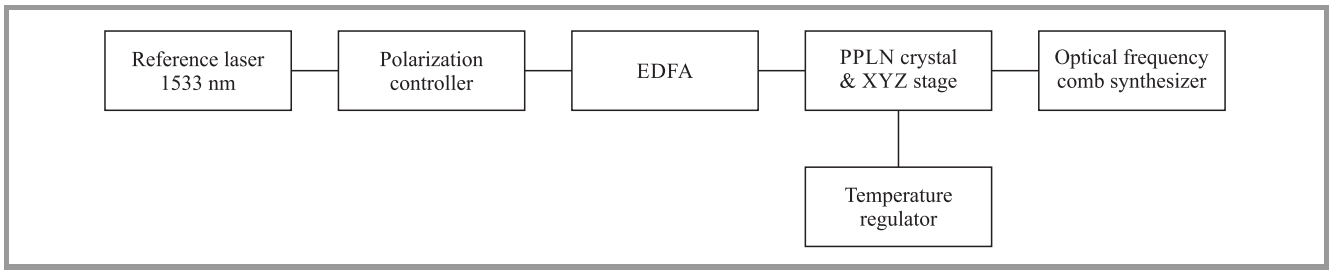

Fig. 1. Schematic block diagram of the measurement setup.

2. Measurement Setup

In Fig. 1 the schematic block diagram of a measurement setup is presented. The general idea of the setup was to measure second harmonic of light emitted from the reference laser.

The object of the measurement was a reference laser locked to acetylene reference $^{12}C_2H_2$ (P13) line (195580979.3711 MHz ±10 kHz, 1532.8307 nm), which might operate in three wavelength stabilization modes: "left", "right" and "center". Which mean that the laser wavelength may be stabilized to the left or right slope of the absorption peak or to the highest point of the absorption peak, respectively. The manufacturer stated the laser frequency in center mode as 195.58097 THz (1532.8304 nm ±0.0003 nm), which is slightly different from the reference wavelength of $^{12}C_2H_2$ (P13) line. On the other side of the setup the optical frequency comb synthesizer FC8004 made by Menlosystems driven with Ti:Sapphire femtosecond laser was used. It has been designed to measure frequencies of optical signals in visible and near infrared regions, i.e., in the wavelength range 532–1074 nm. It is usually used for realizing definition of meter and calibration of the stabilized metrological lasers.

In order to measure 1533 nm reference laser we decided to use second harmonic generation (SHG) technique using Periodically Poled Lithium Niobate (PPLN) crystal to get 766.4 nm signal, which is in the measurement range of the optical frequency comb synthesizer. Similar solution has been reported in case of 1542 nm laser stabilized to P(16) absorption line of $^{13}C_2H_2$ [13].

In our case the maximum output power of the reference laser was only 0.5 mW, which is too low to achieve effective frequency conversion in PPLN crystal. Its efficiency is only 0.5%. As a solution for low power problem, an Erbium Doped Fiber Amplifier (EDFA) was applied. Furthermore, the optical frequency synthesizer can measure optical signals only with power greater than 100 μW. Taking this limitation into account as well as losses caused by reflections and light launching into the optical fibers the maximum output power of EDFA has to be greater than 23 dBm.

The frequency conversion is possible only when the phase matching condition of pump signal and second harmonic signal is fulfilled. This condition strongly depends on polarization of input signal and temperature of PPLN crystal. For that reason the polarization controller and dedicated thermally controlled oven has been used (Fig. 1).

The maximum conversion efficiency can be achieved when the focusing conditions of optical beam fulfils the Boyd and Kleinman requirement: $L/b = 2.84$, where L is the crystal length and b is the confocal parameter. Our optical setup was close to this condition. The PPLN crystal was relatively long (i.e. 40 mm) with input aperture 0.5×0.5 mm. This implicated precise optomechanical setup elements in order to properly focus and adjust the laser beam. Our setup delivers 0.5 mW of converted power, which is enough to be measured with optical comb (frequency synthesizer).

In Figs. 2 and 3 a photo and block diagram of setup of the optical frequency synthesizer are shown, respectively.

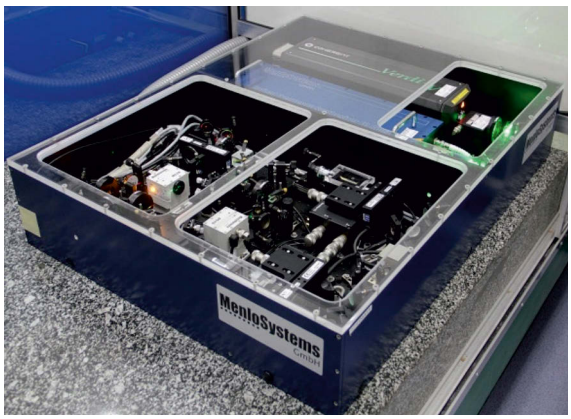

Fig. 2. Photo of optical frequency synthesizer.

The main advantage of the comb synthesizer is an efficient technique of locking of the f_r repetition frequency and f_o offset frequency. Both parameters are synchronized with cesium clock and subsequently phase locked by controlling the cavity length and the pump power. An example of spectrum of the optical frequency synthesizer is shown in Fig. 4.

The f_0 frequency is defined according to following formula:

$$2f_n - f_{2n} = 2(f_o + nf_r) - (f_o - 2nf_r) = f_o\,, \qquad (1)$$

where: f_n – frequency of the synthesizer n-mode, f_{2n} – frequency of the synthesizer 2n-mode, f_o – offset frequency, n – integer number, f_r – repetition rate.

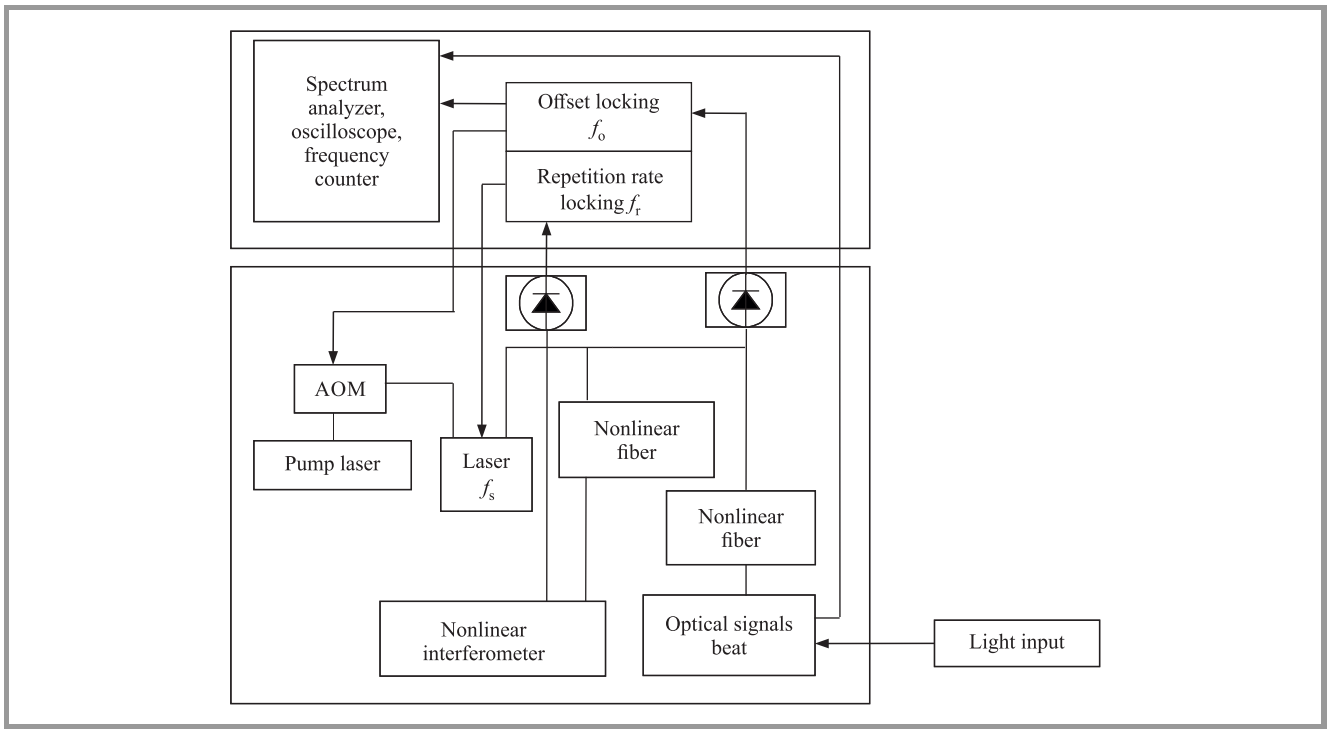

Fig. 3. Block diagram of the optical frequency synthesizer.

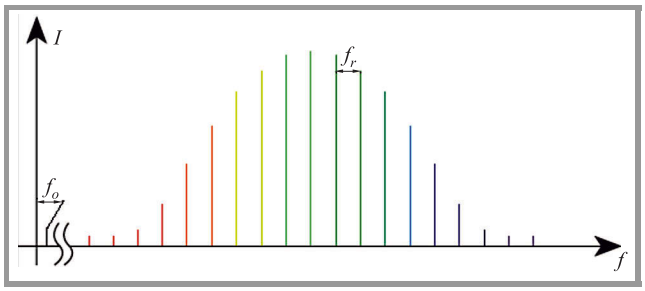

Fig. 4. Frequency synthesizer spectrum example. (See color pictures online at www.nit.eu/publications/journal-jtit)

The reference frequency signal from the cesium clock allows achieving a relative uncertainty at the level of 10^{-13}.

3. Results

The raw measurement results in frequency and wavelength domains of the reference laser after frequency doubling recorded during almost 2.5 h session are presented in Fig. 5. The corresponding Allan deviation is plotted in Fig. 6. The tested laser was operating in the "left" mode which, as mentioned earlier, means that it was stabilized on the left slope of the absorption peak. In this mode the smallest frequency dithering is observed, and it is smaller than in case of stabilization to the highest point of the absorption peak.

The mean value of frequency and wavelength of the stabilized laser for all operating modes obtained during this experiment (year 2016) as well as the measurement results of the same laser obtained from other laboratories over the past ten years are presented in Table 1.

Over mentioned decade three different measurement methods have been applied in order to verify the laser's frequency stability, namely: imposition of signals from our laser with higher accuracy laser, interferometric method, and method presented here based on optical frequency comb synthesizer.

In 2006 the method of imposition of signals from our laser with higher accuracy laser locked to the same absorption line of acetylene $^{12}C_2H_2$ and measurement of beat signal has been applied. The uncertainty of mean frequency measurement results was ±2.8 MHz for "center" and "right" laser operating mode and ±2.0 MHz for "left" laser operating mode.

In 2011 and 2014 the laser has been compared with primary wavelength standard 1542 nm – acetylene $^{13}C_2H_2$ stabilized laser using interferometric method – absorption line P(16). The uncertainty of mean frequency measurement results in 2011 were ±1.3, ±7.3, and ±8.9 MHz for "centre", "left", and "right" operation modes, respectively. Similarly, the uncertainty of mean frequency measurement results in 2014 were ±3.5, ±8.4, and ±8.4 MHz for "centre", "left", and "right" mode of operation, respectively.

Finally, in 2016 the measurement results, which are the subject of this work, have been obtained. The relative expanded uncertainty of the mean frequency measurement results were $U_w = \pm 3.5$ MHz for all operating modes of the tested laser.

The reported expanded uncertainties in all cases were stated as the standard uncertainties multiplied by the coverage factor $k = 2$, which corresponds to a coverage probability of approximately 95%.

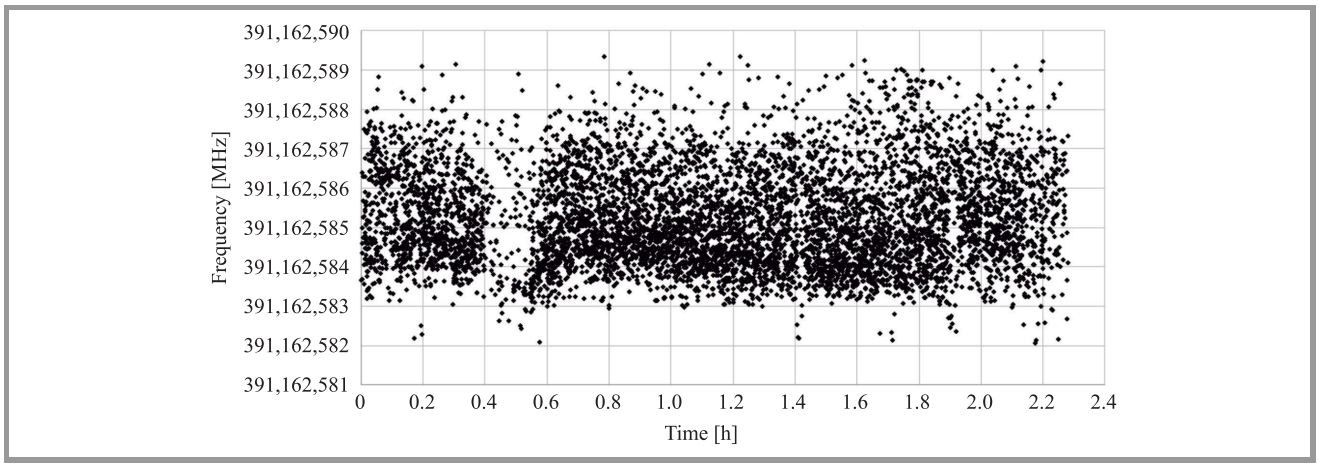

Fig. 5. Frequency of stabilized laser (operating in the "left" mode).

Table 1
Summary of calibration results

Laser stabilization mode	Unit	Year of measurement			
		2006	2011	2014	2016
Left	λ [nm]	1532.827839	1532.827880	1532.827921	1532.827880
	f [MHz]	195,581,297.8	195,581,292.5	195,581,287.4	195,581,292.6
Right	λ [nm]	1532.832912	1532.832856	1532.832829	1532.832867
	f [MHz]	195,580,650.5	195,580,657.7	195,580,661.0	195,580,656.2
Center	λ [nm]	1532.830387	1532.830390	1532.830410	1532.830378
	f [MHz]	195,580,972.6	195,580,972.2	195,580,969.8	195,580,973.8

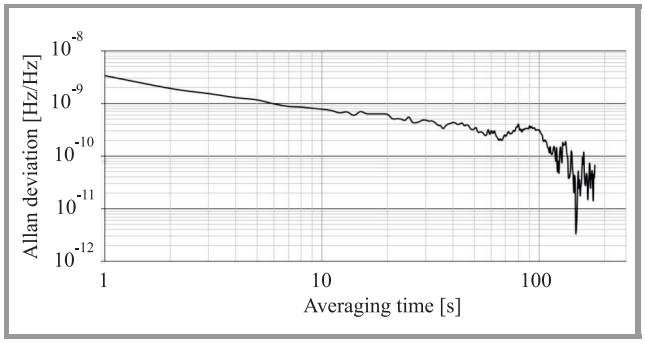

Fig. 6. Allan deviation of frequency measurement of stabilized laser (operating in the "left" mode).

The environmental conditions of the measurements were well controlled in all cases in the range 23.0 ±0.4°C in 2006, 20.0 ±1.0°C in 2011 and 2014, and 23.0 ±0.5°C in 2016. Influence of the temperature on absorption peak has been investigated previously [3] and is relatively small and less than ±100 Hz.

It has to be noticed that the reported dominant uncertainty component was a result of laser modulation, which caused frequency excursions as large as 10 MHz in the worst cases.

The results summarized in this paper can be treated in the sense of interlaboratory comparison. All three methods were applied by highest-level laboratories, which offer uncertainties as good as ±10 kHz. So, in order to investigate accuracy of the methods or its application in particular laboratories the better comparison object is needed.

4. Conclusions

The frequency of a laser locked to the absorption line (P13) of acetylene $^{12}C_2H_2$ against optical frequency comb synthesizer was evaluated. Namely, the signal from the stabilized laser has been amplified, its frequency doubled using second harmonic generation process in PPLN, and finally its stability compared against the frequency generated by the comb synthesizer

Conducted experiments showed that the wavelength accuracy of the stabilized laser is better than ±0.0003 nm (ca. ±38 MHz), which complies with the parameters stated by its manufacturer. Judging upon available literature we can state that the main advantages of the measuring method involving optical frequency comb synthesizer are the direct reference to atomic frequency standards (high accuracy) and wide range of the measurable wavelengths (high flexibility).

Moreover, the differences in results obtained from all the laboratories for the past 10 years are within uncertainty ranges, which also indirectly confirms the validity of used

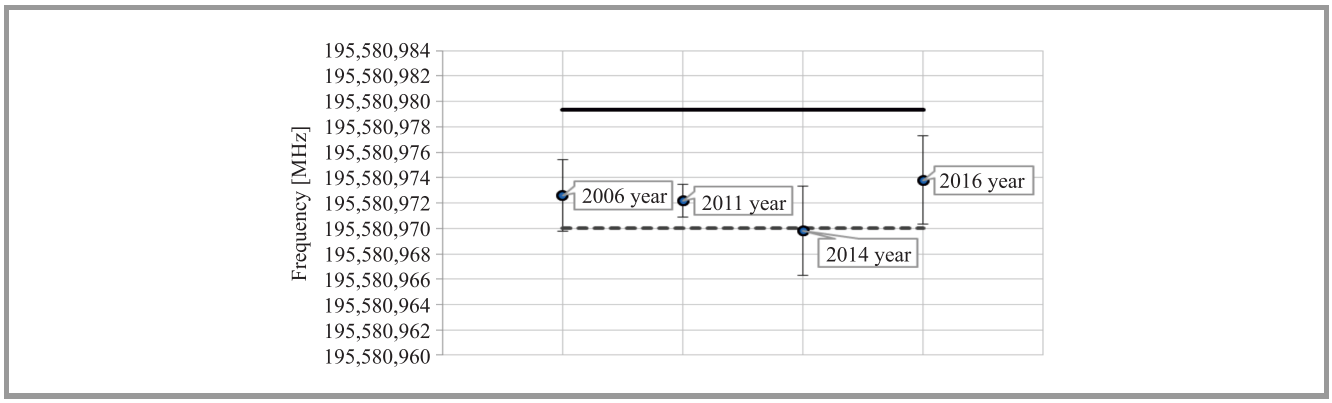

Fig. 7. Comparison of measurement results of laser wavelength ("center" mode), solid line represents reference frequency 195,580,979.3711 MHz of absorption line of P(13) $^{12}C_2H_2$, dashed line represents declared by manufacturer frequency of measured laser 195.58097 THz.

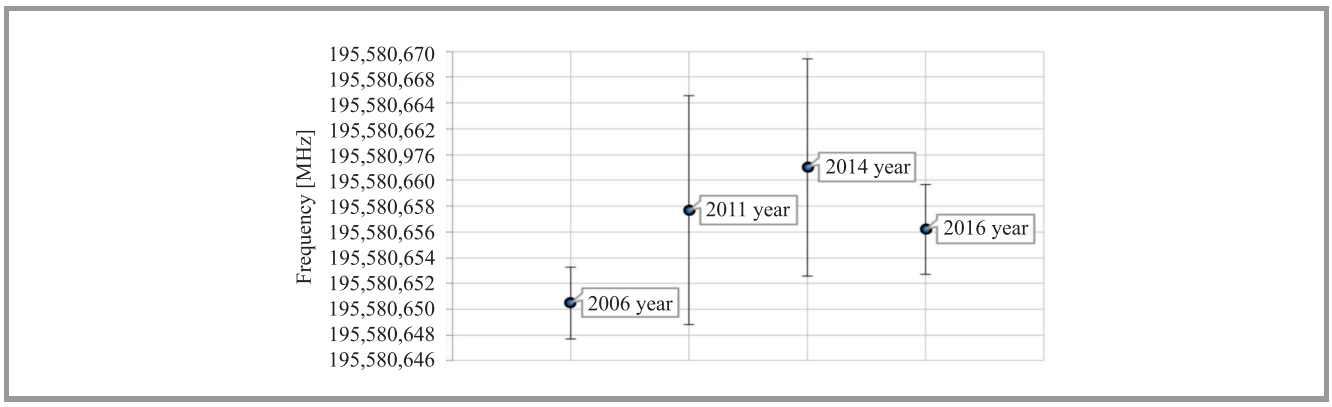

Fig. 8. Comparison of measurement results of laser wavelength ("right" mode).

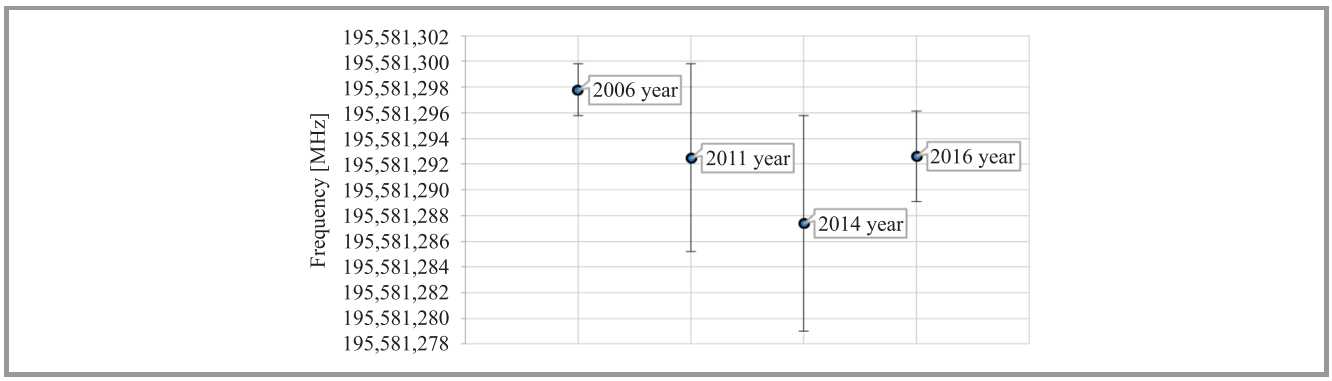

Fig. 9. Comparison of measurement results of laser wavelength ("left" mode).

approach and methods. In general, the influence of pressure or temperature on operation of a stabilized laser with absorption cells has been investigated by many laboratories, but in relatively short periods of time. Nevertheless, according to our knowledge, the long term stability of such lasers, which is an important issue in case of using it as a wavelength standard for calibration of measurement equipment, has not been presented in such a long timescale. The outcomes broaden the information on aging effects of the device and might allow the user to prolong the recalibration period.

References

[1] T. J. Quinn, "Practical realization of the definition of the metre, including recommended radiations of other optical frequency standards (2001)", *Metrologia*, vol. 40, no. 2, pp. 103–133, 2003 (doi: 10.1088/0026-1394/40/2/316).

[2] K. Nakagawa, M. de Labachelerie, Y. Awaji, and M. Kourogi, "Accurate optical frequency atlas of the 1.5 μm bands of acetylene", *J. Opt. Soc. of America B*, vol. 13, no. 12, pp. 2708–2714, 1996 (doi: 10.1364/JOSAB.13.002708).

[3] W. C. Swann and S. L. Gilbert, "Pressure-induced shift and broadening of 1510-1540 nm acetylene wavelength calibration lines", *J. Opt. Soc. of America B*, vol. 17, no. 7, pp. 1263–1270, 2000.

[4] S. Sudo *et al.*, "Frequency-stabilized DFB laser module using 1,53159 μm absorption line of C2H2", *IEEE Photon. Technol. Lett.*, vol. 1, no. 10, pp. 281–284, 1989 (doi: 10.1109/68.43345).

[5] M. Labachelerie, K. Nakagawa, Y. Awaji, and M. Ohtsu, "High-frequency-stability laser at 1.5 μm using Doppler-free molecular lines", *Opt. Lett.*, vol. 20, no. 6, pp. 572–574, 1995.

[6] V. Ahtee, M. Merimaa, and K. Nyholm, "Fiber-based acetylene stabilized laser", *IEEE Trans. on Instrumen. Measur.*, vol. 58, no. 4, pp. 1211–1216, 2009 (doi: 10.1109/TIM.2008.2008476).

[7] C. S. Edwards *et al.*, "Development and evaluation of compact acetylene frequency standards", in *Proc. Conf. on Precision Electromag. Measur. CPEM 2012*, Washington , USA, 2012, pp. 610–611 (doi: 10.1109/CPEM.2012.6251077).

[8] J. Seppä, M. Merimaa, A. Manninen, M. Triches, J. Hald, and A. Lassila, "Interference cancellation for hollow-core fiber reference cells", *IEEE Trans. on Instrument. & Measur.*, vol. 64, no. 6, pp. 1595–1599, 2015 (doi: 10.1109/TIM.2015.2408800).

[9] P. Balling, M. Fischer, P. Kubina, and R. Holzwarth, "Absolute frequency measurement of wavelength standard at 1542 nm: acetylene stabilized DFB laser", *Optics Express*, vol. 13, no. 23, pp. 9196–9201, 2005 (doi: 10.1364/OPEX.13.009196).

[10] J. L. Hall and S. A. Lee, "Interferometric real-time display of cw dye laser wavelength with sub-Doppler accuracy", *Appl. Phys. Lett.*, vol. 29, no. 6, pp. 367–369, 1976 (doi: 10.1063/1.89089).

[11] C. S. Edwards, G. P. Barwood, H. S. Margolis, P. Gill, and W. R. C. Rowley, "High-precision frequency measurements of the v1 + v3 combination band of $^{12}C_2H_2$ in the 1.5 μm region", *J. of Molecular Spectr.*, vol. 234, no. 1, pp. 143–148, 2005 (doi: 10.1016/j.jms.2005.08.014).

[12] T. Udem, R. Holzwarth, and T. Hänsch, "Optical frequency metrology", *Nature*, vol. 416, pp. 233–237, 2002 (doi: 10.1038/416233a).

[13] F.-L. Hong *et al.*, "Absolute frequency measurement of an acetylene-stabilized laser at 1542 nm", *Optics Lett.*, vol. 28, no. 23, pp. 2324–2326, 2003 (doi: 10.1364/OL.28.002324).

Tomasz Kossek received the M.Sc. degree in Optoelectronics and the Ph.D. degree from the Warsaw University of Technology, Warsaw, Poland, in 1996 and 2002, respectively. He is currently an Assistant Professor at the National Institute of Telecommunications Poland, Warsaw. His current research interests include optoelectronic measurements and their calibration, laser physics, optical communication.

E-mail: T.Kossek@itl.waw.pl
National Institute of Telecommunications
Szachowa st 1
04-894 Warsaw, Poland

Dariusz Czułek received his M.Sc. from Technical University of Łódź, Faculty of Technical Physics, Information Technology and Applied Mathematics. From 2002 he is working in Length and Angle Department of Central Office of Measures, Warsaw, Poland. His current interests include laser physics, practical realization of the length unit, optical comb generators.

E-mail: d.czulek@gum.gov.pl
Central Office of Measures
Elektoralna st 2
00-139 Warsaw, Poland

Marcin Koba received his M.Sc. and Ph.D. in Engineering in the field of Electronics from the Warsaw University of Technology (WUT), Poland, in 2006, and 2011, respectively. He is currently an Assistant Professor at WUT and the National Institute of Telecommunications, Poland. He held an Assistant Professor position at the Institute of Experimental Physics, University of Warsaw from December 2011 to June 2013. From July 2013 to July 2015 he has been a Postdoctoral Fellow at Photonics Research Center, UQO, Canada. His current interests include general photonics, comprising fiber optic sensing structures, laser physics, solid state physics, optical communication, metrology, and thin films.

E-mail: M.Koba@itl.waw.pl
National Institute of Telecommunications
Szachowa st 1
04-894 Warsaw, Poland

Paper

Verification of Staff Proficiency in the Calibration Laboratory on Voltage, Frequency, Resistance and Capacity Measurements

Anna Warzec, Michał Marszalec, and Marzenna Lusawa

National Institute of Telecommunications, Warsaw, Poland

Abstract—The Laboratory of Electrical, Electronic and Optoelectronic Metrology is accredited by the Polish Center of Accreditation for nearly two decades. Over time, the requirements of proficiency verification are growing continuously. In order to satisfy higher and higher of reliability demands the most promising staff proficiency verification estimators were examined for voltage, frequency, resistance and capacity measurements. The article presents measurement systems used for verification, analysis of results or simulations, and shows conclusion for selecting the best solution.

Keywords—Calibration and Measurement Capability, staff proficiency verification.

1. Introduction

The Laboratory of Electrical, Electronic and Optoelectronic Metrology within National Institute of Telecommunications (NIT-LMEEiO) is divided into four divisions (Fig. 1):

- Basic Parameters Metrology Team, which works on the metrology of basic measurements, such as DC&AC, LF voltage and current, resistance, capacitance, inductance, impedance and power,
- Telecommunication Parameters Metrology Team, which works on the measurements of RF and microwave signals and also on transmission parameters of telecommunication networks, e.g. PDH/SDH, Ethernet, SONET etc.,
- Optoelectronic Metrology Team, which works on optoelectronic metrology of such parameters as optical power, wavelength, chromatic and polarization dispersion, optical attenuation and optical fiber length,
- Time and Frequency Metrology Team, which is responsible for accurate measurements of frequency, time, phase time, interval, TIE and conducts science works.

Today's market demands complete offer in electronic area, which NIT-LMEEiO laboratory is trying to fulfill. The work on improvement the quality and CMC (Calibration and Measurement Capability) in every division is continuously ongoing. Every metrology area has its own specifics and in situation of wide range of measured parameters, assurance of proficiency verification and choosing appropriate estimators is not an easy task.

Based on long-term experience the most convenient solution for proficiency verification would be all known and well tested E_n scores. Unfortunately, during the experts discussion and accreditation audits there have been many critical remarks, that for statistically dependent value sets it is not correct solution. In the following discussions, various test and scores have been recommended. In addition, a review of standardization documents [1], [2] (some of them are recently revised) have indicated solutions that could be helpful in solving the proficiency verification problem.

2. Research Plan

For mentioned reasons, following estimators have been analyzed:

- F-Snedecor test [1],
- Bartlett test [1],
- E_n scores [2],
- Morgan test [1],
- ζ scores [2],
- "simple test" – difference of individual measurements should be lower than uncertainty of measurement.

Research was conducted in the following areas of measurements:

- voltage,
- frequency,
- resistance,
- capacity.

In order to detect strong dependence in individual data, for voltage and frequency, the correlation coefficient was calculated for compared pairs of extended result sets (1000 individual measurements). For data set average value, the standard deviation and uncertainty have been calculated. The tables of the critical values for F-Snedecor, Bartlett

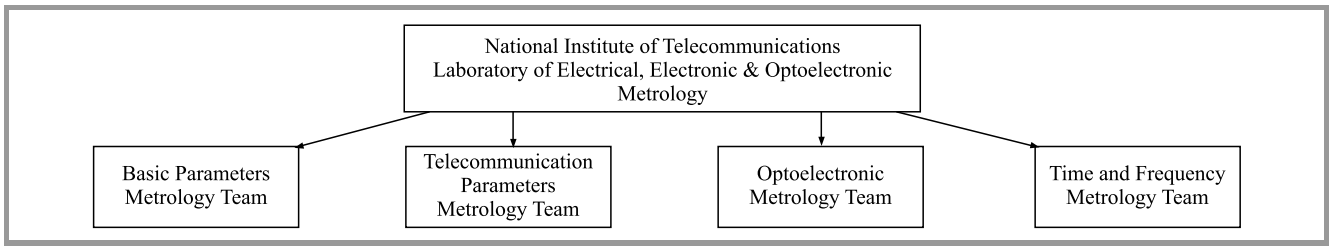

Fig. 1. Actual NIT-LMEEiO laboratory structure.

and Morgan tests have been taken from Excel spreadsheet and verified with statistical tables [1], [3], [4].

2.1. F-Snedecor Test

The F-Snedecor is used to compare standard deviation for two result data sets. It is assumed that both sets have normal distribution. At the beginning standard deviation [5] for both results sets should be calculated. Then F-Snedecor parameter is calculated according to:

$$F = \frac{\frac{n_1}{n_1 - 1} s_1^2}{\frac{n_2}{n_2 - 1} s_2^2}, \tag{1}$$

where for both results sets s_1 and s_2 are standard deviations, n_1 and n_2 are numbers of measurements.

For further analysis, $s_1 > s_2$ constraint must be ensured. The next step is to find appropriate critical value F_{cr} from F-Snedecor distribution table for assumed significance level and calculated degrees of freedom ($f_1 = n_1 - 1$ and $f_2 = n_2 - 1$).

Finally, the comparison between F and F_{cr} has to be made. If calculated value F is lower or equal than F_{cr} ($F \leq F_{cr}$) then conclusion that difference between calculated standard deviation values should not be statistically significant is allowed and the result of proficiency verification is confirmed. In other case ($F > F_{cr}$) the difference is clearly statistically significant and verification of proficiency is unconfirmed.

2.2. Bartlett Test

This test is used to compare standard deviation for many result sets. It is applicable if number of measurements is higher than 3. First, the standard deviation for every result set should be calculated. Then Q parameter is calculated according to:

$$Q = \frac{2.303}{c}\left[(N-k)\log\left(\overline{s}_0^2\right) - \sum_{i=1}^{k}(n_i - 1)\log\left(s_i^2\right)\right], \tag{2}$$

where:

$$c = 1 + \frac{1}{3(k-1)}\left(\sum_{i=1}^{k}\frac{1}{n_i - 1} - \frac{1}{N-k}\right),$$

$$\overline{s}_0^2 = \frac{1}{N-k}\sum_{i=1}^{k} s_i^2 (n_i - 1).$$

In presented tests, the same number of measurements in all data sets have been used. Therefore, a simplified following formula is applicable:

$$\overline{s}_0^2 = \frac{1}{k}\sum_{i=1}^{k} s_i^2. \tag{3}$$

In Eqs. (2) and (3): N – summary number of all samples used in calculations, k – number of compared measurement sets, n_i – number of samples in individual data set, s_i – standard deviation for results of method i.

At the end comparison between Q and χ^2_{kr} has to be made. If calculated value Q is lower or equal than χ^2_{kr} ($Q \leq \chi^2_{kr}$) then conclusion that the difference between calculated standard deviation values should not be statistically significant is allowed and the result of proficiency verification is confirmed. In other case ($Q > \chi^2_{kr}$) the difference is clearly statistically significant and verification of proficiency is unconfirmed.

2.3. E_n Scores

The E_n scores is mainly used in calibration processes to evaluate inter-laboratory comparisons. The process of evaluation begins of calculation E_n scores according to formula:

$$E_n = \frac{x_i - x_{pt}}{\sqrt{U_i^2 + U_{pt}^2}}, \tag{4}$$

where: x_i and x_{pt} – measured laboratory and reference result values, U_i and U_{pt} – expanded laboratory and reference uncertainties of measured values.

By definition, the final evaluation is done by comparing calculated E_n scores. If $|E_n| < 1$, the evaluation is positive and if $|E_n| \geq 1$ evaluation is negative. Unfortunately this criterion is applicable only if individual data set is statistically independent. In other case scores E_n should be compared to appropriately selected value other than 1. In laboratory practice this critical value is often specified as 0.5 or 0.32.

2.4. Morgan Test

This test is used to compare standard deviation for two correlated result sets.

First, standard deviation for both results sets should be calculated. Then regression parameter r (Pearson prod-

uct – moment correlation coefficient) is calculated according to:

$$r = \frac{k\sum_{i=1}^{k} x_{1i}\,x_{2i} - \sum_{i=1}^{k} x_{1i}\sum_{i=1}^{k} x_{2i}}{\sqrt{\left[k\sum_{i=1}^{k} x_{1i}^2 - \left(\sum_{i=1}^{k} x_{1i}\right)^2\right]\left[k\sum_{i=1}^{k} x_{2i}^2 - \left(\sum_{i=1}^{k} x_{2i}\right)^2\right]}}\,. \quad (5)$$

Next, the test parameters L and t should be calculated:

$$L = \frac{4s_1^2 s_2^2(1-r^2)}{(s_1^2+s_2^2)^2 - 4r^2 s_1^2 s_2^2}\,, \quad (6)$$

$$t = \sqrt{\frac{(1-L)(k-2)}{L}} = \frac{|s_1^2 - s_2^2|}{2s_1 s_2}\sqrt{\frac{k-2}{1-r^2}}\,, \quad (7)$$

where: k – number of pairs of measurements x_1 and x_2 – individual measurements for compared results sets.

In the next the critical value t_{cr} step is read from Student's t-distribution table for assumed level of significance α (5%) and degree of freedom level to compare calculated t and t_{cr}.

If $t \le t_{cr}$, then the difference between calculated standard deviation values should not be statistically significant and the verification of staff proficiency is confirmed. In other case ($t > t_{cr}$) the difference between compared values is clearly statistically significant and the staff proficiency is verified negatively.

2.5. ζ Scores

ζ (zeta) scores could be useful in proficiency evaluation when the goal is to verify if one participant is able to obtain results close to assigned value within their claimed uncertainty. The second participant's measurement set becomes a source of assigned reference value and standard uncertainty.

$$\zeta = \frac{x_i - x_{pt}}{\sqrt{u_i^2 + u_{pt}^2}}\,, \quad (8)$$

where: x_i – are participant measured value and $u(x_i)$ – standard uncertainty, x_{pt} and $u(x_{pt})$ have assigned value and standard uncertainty for proficiency testing, e.g. second series of measurements from another participant.

If $|\zeta| \le 2$ the final evaluation is positive, while $2 < |\zeta| < 3$ the evaluation is doubtful, and if $|\zeta| \ge 3$ evaluation is negative. Unfortunately, those constraints are applicable only if individual data sets are statistically independent. Otherwise, the scores ζ should be compared to appropriately selected value other than 1. In practice this critical limits are specified respectively as 0.64 and 1, i.e. $|\zeta| < 0.64$ result is positive.

It could be noted that for uncertainty coverage factor $k = 2$, which is due to its normal distributions most popular in measurements ζ scores is equivalent to $2E_n$.

2.6. "Simple test"

The simple test is based on basic comparison of individual measurements, which difference should be lower than quarter of arithmetically added expanded uncertainties of both sets of measurements.

$$|x_1 - x_2| < \frac{U_1 + U_2}{4}\,. \quad (9)$$

This procedure could be useful if none of recommended tests proved to be applicable for specific unit of measure proficiency verification.

2.7. Correlation Coefficient

In most cases for determination of dependencies in individual measurements series correlation coefficients, the Pearson product – moment correlation coefficient was used. It is also a base for Morgan test calculations and it was determined for the cases where series of data were recorded. The result has been presented in few separate tables to avoid unnecessary misunderstandings.

$$r = \frac{cov(x_1, x_2)}{s_1 s_2}\,, \quad (10)$$

which is equivalent notation of Eq. (5), where s_1 and s_2 are standard deviations for both results sets.

3. Voltage Measurements

In voltage measurements a precise multimeter was used as the object of study. Three independent calibrators were used as a voltage source (Fig. 2). One of them was used in both cases for AC and DC measurements and the other two were used for AC or DC measurement only. Because the equipment used in research provides an opportunity for automated measurements, at least 1000 samples for set have been saved. For such typical measuring systems in the metrological practice, the behavior of the individual tests for different numbers of samples could be observed. It allows more precise statistical characterization of each data set.

Each series of measurements were conducted independently one after another with both calibrators usage. To

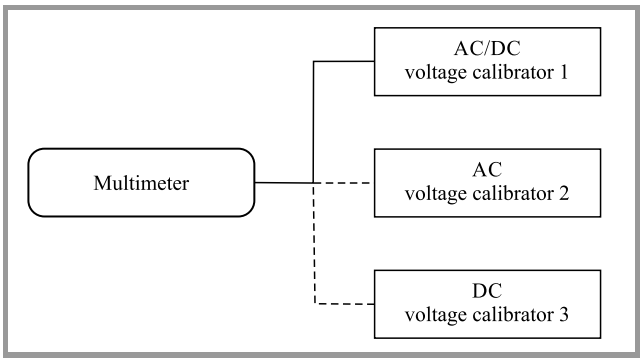

Fig. 2. Measuring system block diagram.

achieve precise statistical analysis the number of individual measurements were set to $N = 1000$. Three different cases were analyzed. The first set was constructed from all of 1000 samples retrieved from both calibrators. In the second case 20 samples from the end of measurement series were used. The last case was set of $N = 10$ samples from the end of measurement series.

3.1. AC Test

The individual series of measurements were saved one after another. The time interval between data sets acquisition was lower than two hours. For measured data, calculations for different numbers of measurements have been done. Figures 3 and 4 show distribution of both result sets while Table 1 presents calculated correlation coefficient for AC voltage measurements.

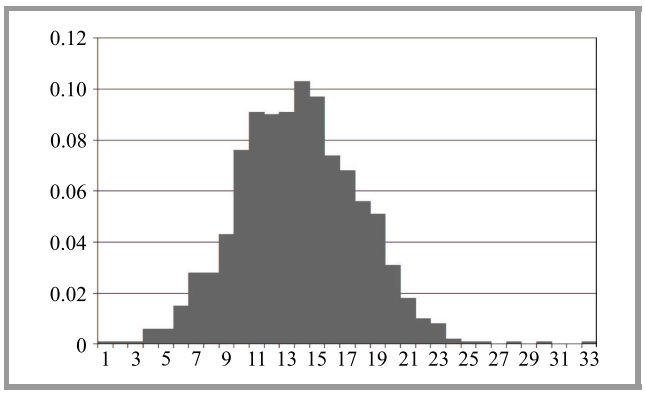

Fig. 3. Distribution graph of the first result set for AC measurements.

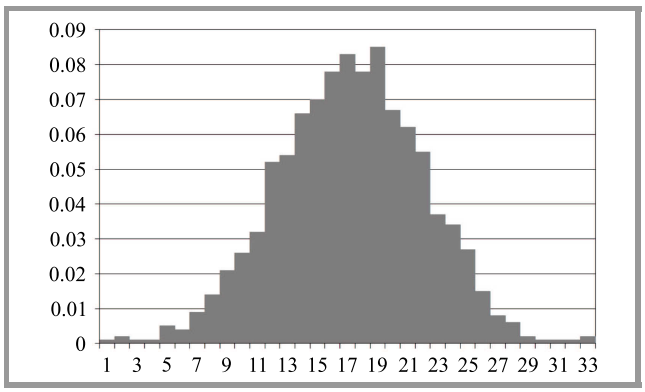

Fig. 4. Distribution graph of the second result set for AC measurements.

Table 1
Correlation coefficients for AC measurement

Number of individual measurements N	Correlation coefficient
1000	3.8%
20	–4.6%
10	12.0%

In Tables 1 and 2 below calculated test results and estimators for N individual measurements have been presented. Value of test parameter: F for F-Snedecor, Q for Bartlett, t for Morgan, $|x_1 - x_2|$ for simple test (ST). Value of estimators: ζ, E_n.

Table 2
Results of analyzed tests for AC voltage measurements

Test name	N	Test result	Critical value	Proficiency verification
F-Snedecor	1000	1.61	1.11	Fail
Bartlett		56.45	3.84	
Morgan		7.62	1.96	
ζ		0.26	0.64	Pass
E_n		0.13	0.32	
ST		0.000046	0.00012	
F-Snedecor	20	2.10	2.17	
Bartlett		2.51	3.84	
Morgan		1.61	2.10	
ζ		0.26	0.64	
E_n		0.13	0.32	
ST		0.000047	0.00012	
F-Snedecor	10	3.00	3.18	
Bartlett		2.50	3.84	
Morgan		1.65	2.31	
ζ		0.25	0.64	
E_n		0.13	0.32	
ST		0.000045	0.00012	

3.2. DC Test

During this measurements sets were also saved one after another. The interval time was lower than two hours. For measured data, calculations for different numbers of measurements have been done. Figures 5 and 6 show distribution of both result sets and Table 3 presents calculated correlation coefficient for DC voltage measurements.

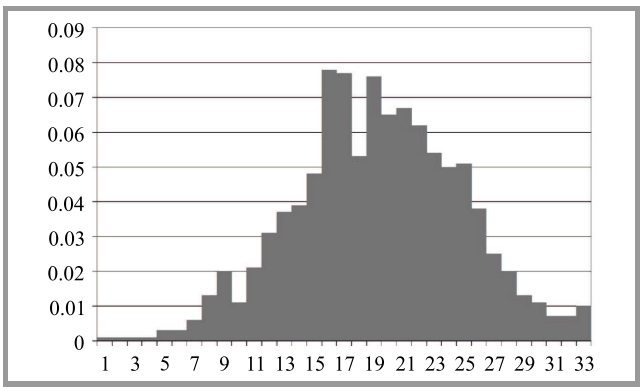

Fig. 5. Distribution graph of the first result set for DC measurements.

In the Table 4 calculated test results and estimators for N individual measurements have been presented.

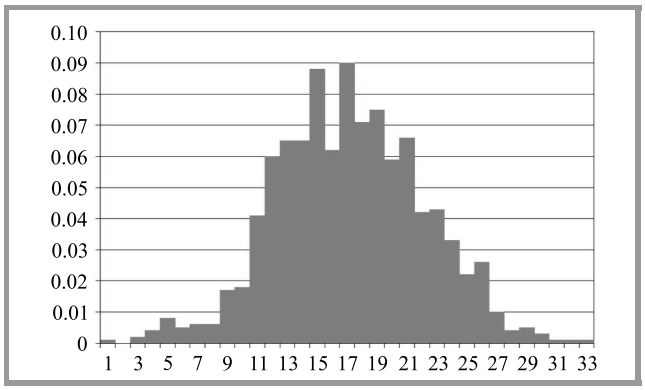

Fig. 6. Distribution graph of the second result set for DC measurements.

Table 3
Correlation coefficients for DC measurement

Number of individual measurements N	Correlation coefficient
1000	6.2%
20	44.1%
10	29.2%

Table 4
Results of conducted tests for DC voltage measurements

Test name	N	Test result	Critical value	Proficiency verification
F-Snedecor	1000	1.13	1.11	Fail
Bartlett		3.92	3.84	
Morgan		1.99	1.97	
ζ		0.17	0.64	Pass
E_n		0.086	0.32	
ST		0.0000022	0.0000090	
F-Snedecor	20	1.18	2.17	
Bartlett		0.13	3.84	
Morgan		0.39	2.10	
ζ		0.21	0.64	
E_n		0.10	0.32	
ST		0.0000026	0.0000090	
F-Snedecor	10	1.10	3.18	
Bartlett		0.021	3.84	
Morgan		0.15	2.31	
ζ		0.22	0.64	
E_n		0.11	0.32	
ST		0.0000028	0.0000090	

4. Frequency Measurements

In the area of frequency measurements a typical signal from internal quartz-driven oscillator was used. Proficiency verification has been analyzed for two persons case. Two independent precise frequency meters synchronized to atomic cesium reference clock were used as a source of standard (Fig. 7). For more precise statistical analysis the number of measurements was set to $N = 1000$ and the gate open time to 1 s. In the research, three different cases were analyzed. To characterize short-term stability of reference oscillator typically the set of 1000 samples is measured with gate open for 1 s. The second case is frequency measurements with assumed normal distribution or with low resolution where many laboratories is using set of 10 samples. For more precise measurements set of $N = 20$ samples is used.

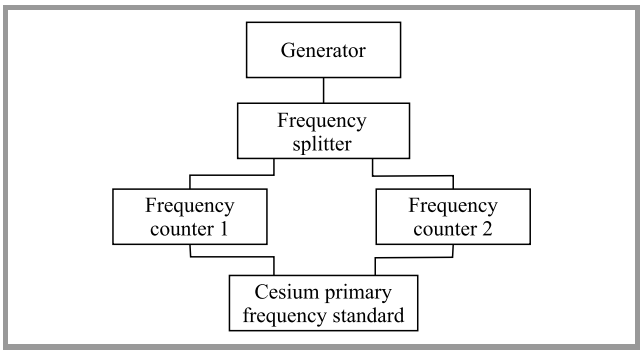

Fig. 7. Block diagram of measuring system.

Because of non-stationary nature of frequency generation process both counters where connected to same source through signal splitter (frequency distribution amplifier)

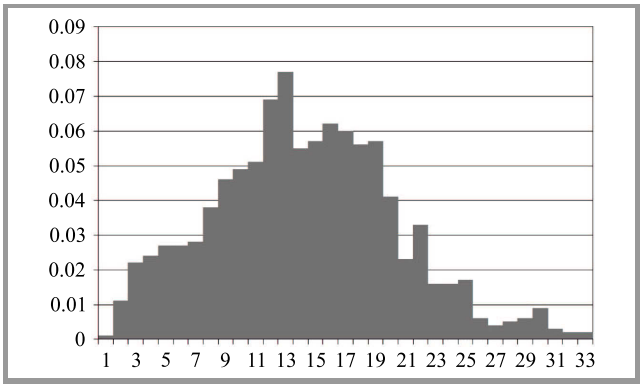

Fig. 8. Distribution graph of the first result set for frequency measurements.

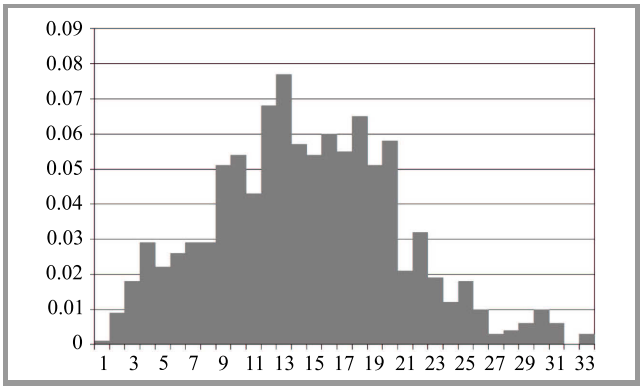

Fig. 9. Distribution graph of the second result set for frequency measurements.

and all measurements were started at the same moment. Figures 8 and 9 show distribution of both result sets and Table 5 presents calculated correlation coefficient for frequency measurements.

Table 5
Correlation coefficients for frequency measurement

Number of measurements N	Correlation coefficient
1000	62.1%
20 (set 1)	99.6%
20 (set 2)	–79.9%
10 (set 1)	96.3%
10 (set 2)	–95.8%

For measured data, calculation for different numbers of measurements have been done. Set 1 was constructed from data from the beginning of measurement series for both participants (for $N = 10$ and $N = 20$). Set 2 was constructed from data from the beginning for one participant and from the end of measurement series for second participant (for $N = 10$ and $N = 20$). The data in this case was expected to be statistically dependent.

Table 6
Test results for frequency measurements

Test name	N	Test result	Critical value	Proficiency verification
F-Snedecor	1000	1.01	1.11	Pass
Bartlett		0.052	3.84	
Morgan		0.29	1.96	
ζ		0.015	0.64	
E_n		0.0074	0.32	
ST		0.000041	0.0019	
F-Snedecor	20 (set 1)	1.12	2.17	
Bartlett		0.057	3.84	
Morgan		2.61	2.10	Fail
ζ		0.21	0.64	Pass
E_n		0.10	0.32	
ST		0.0013	0.0044	
F-Snedecor	20 (set 2)	2.92	2.17	Fail
Bartlett		5.11	3.84	
Morgan		3.96	2.10	
ζ		5.38	0.64	
E_n		2.69	0.32	
ST		0.046	0.0058	
F-Snedecor	10 (set 1)	1.03	3.18	Pass
Bartlett		0.0019	3.84	
Morgan		0.16	2.31	
ζ		0.12	0.64	
E_n		0.062	0.32	
ST		0.00047	0.0027	
F-Snedecor	10 (set 2)	2.99	3.18	
Bartlett		2.48	3.84	
Morgan		5.68	2.31	Fail
ζ		14.55	0.64	
E_n		7.28	0.32	
ST		0.087	0.0041	

In the Table 6 calculated results and estimators for N individual measurements have been presented.

A good example of problems with usage of advanced statistic test is set 1 for $N = 20$ measurements. The data seems to be almost identical, which is confirmed by correlation coefficient calculation (99.6%). It is the biggest obtained correlation coefficient during all tests (Fig. 10). The Morgan test according to theory [1] should be especially useful for statistically dependent data in staff proficiency verification. Unfortunately, it seems it is the only one test that gave a negative result. The research shows that a positive Morgan test result can be obtained, if with an increase of correlation coefficient the difference between standard deviations values is decreasing.

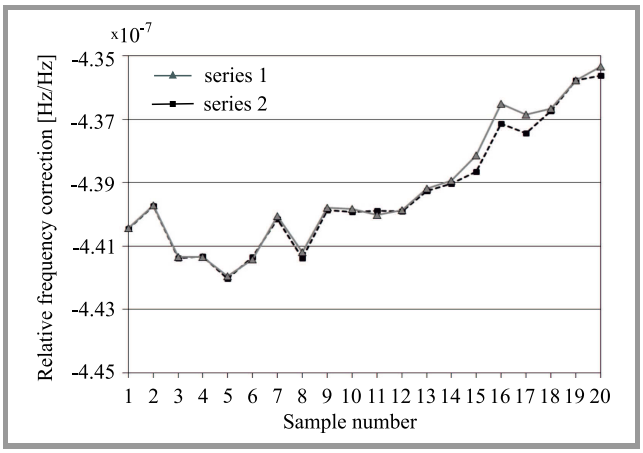

Fig. 10. Results for frequency tests for set 1 and $N = 20$ measurements.

5. Resistance Measurements

In this case the object of study was standard reference resistor. Two series of measurements ($N = 10$ samples) was obtained one after another with usage of two independent precise multimeters (Fig. 11). Authors experience from many years in this area shows that $N = 10$ samples is sufficient to proper characterization of an object, i.e. resistor, because high stability measurements. The limited number of samples and the fact that the dominant component of uncertainty is type B (from the specifications of the instrument), allow to limit the analysis to three last tests (ζ, E_n, ST). Three skipped tests, i.e. F-Snedecor,

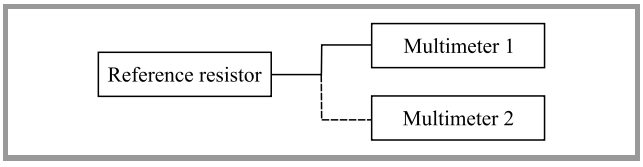

Fig. 11. Block diagram of measurements system.

Bartlett, Morgan, require the usage of a standard deviation (a component of uncertainty of type A).
In the Table 7 calculated test results and estimators have been presented. The set for every value of resistance comes from original measurements.

Table 7
Test results of analyzed tests for resistance measurements

Test name	Value	Test result	Critical value	Proficiency verification
ζ	10 Ω	0.44	0.64	Pass
E_n		0.22	0.32	
ST		0.00006	0.0000925	
ζ	100 Ω	0.045	0.64	
E_n		0.023	0.32	
ST		0.00005	0.000738	
ζ	1 kΩ	0.50	0.64	
E_n		0.25	0.32	
ST		0.00004	0.0000558	
ζ	10 MΩ	0.37	0.64	
E_n		0.19	0.32	
ST		0.00014	0.000245	

6. Capacity Measurements

The object of study (capacity calibrator) was measured on the same measurement station (precise capacity bridge) within the period of four days ($N = 3$ samples) (Fig. 12). The sample number was set to $N = 3$, because measurements process took a long time. For this reason, it seems to be a reasonable choice to characterize the object (capacitor) with good accuracy. As in the previous case, the following discussion was limited to analysis of three tests, i.e. ζ , E_n, ST, due the limited number of measurement samples and the dominant component of uncertainty is type B (information retrieved from the specifications of the instrument).

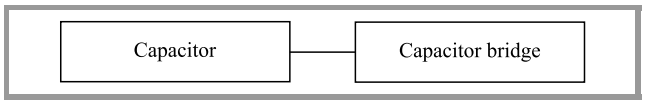

Fig. 12. Block diagram of measurement system.

Table 8
Test results for capacity measurements

Test name	Value	Test result	Critical value	Proficiency verification
ζ	10 pF	0	0.64	Pass
E_n		0	0.32	
ST		0	0.00055	
ζ	100 pF	0.13	0.64	
E_n		0.064	0.32	
ST		0.0010	0.0055	
ζ	1000 pF	0.12	0.64	
E_n		0.059	0.32	
ST		0.010	0.060	

Table 8 shows calculated test results and estimators. The set for every value of capacity comes from original measurements.

7. Conclusions

To determine the most appropriate algorithm for staff proficiency verification few different examples have been tested. First, the voltage measurement were taken one after another, in short (two hours) period of time with usage of two individual high-class reference standards like precise calibrators. The only issue that could affect statistic dependency was the object of study. Due to automation of data acquisition big samples were taken and reliable statistical analysis were done.
The similar process was possible in the frequency case. The measurements were done in parallel at the same time. That is why high correlation factors were expected. Therefore, additional Morgan test was taken under consideration.
The resistance and capacity areas are the examples of typical proficiency verification in the laboratory. Limited number of individual measurements and two different procedures were proceed. For resistance the same object, different precise multimeters and short time interval between measurements was used. For capacity the same object of study and the same measuring equipment was used. However the time between measurements was very large. For those cases the limited number of samples and the fact that the dominant component of uncertainty is type B the analysis was limited to only three tests (ζ, E_n, ST). Three abandoned tests, i.e. F-Snedecor, Bartlett, Morgan require the usage of a standard deviation (a component of uncertainty of type A) which in some cases is not dominant factor of complex uncertainty. For this reason they can be used with particular caution.
As it has been marked, selection one test valid for entire laboratory turns out to be quite difficult. The collected data lead to ambiguous conclusions. In that case, it seems that the most appropriate is to use solutions directly recommended by standardization documents [2], which could be the ζ scores. As it was mention before, for uncertainty coverage factor $k = 2$, which is most popular in measurements due to its normal distributions, ζ scores is equivalent to $2E_n$. Because of statistical dependency, it is suggested to use safer critical limits. In this example limits are specified respectively as 0.64 for ζ.
The good way out of this difficult situation would be usage of proposed simple test or similar equation that matches accuracy level and specificity of individual laboratory.
The results seem to be very promising, but it was worth it to expand the scope of the study in the future. That extension could concern increasing the number of measurements for e.g. capacity (very time-consuming), make study of other physical measures and a comparison between two or more laboratories. That would be the case of inter-

laboratory comparisons and not only the verification of staff proficiency.

References

[1] P. Konieczka and J. Namieśnik, Eds., *Ocena i Kontrola Jakości Wyników Porównań Analitycznych*. Warsaw, Poland: Wydawnictwa Naukowo Techniczne, 2007 (in Polish).

[2] ISO 13528:2015(E) "Statistical methods for use in proficiency testing by interlaboratory comparison", 2nd ed. ISO 2015, Switzerland 2015.

[3] R. Zieliński, *Tablice Statystyczne*. Warsaw, Poland: Państwowe Wydawnictwa Naukowe, 1972 (in Polish).

[4] A. D. Aczel, *Complete Bussiness Statistics*, 2nd ed. Irwin, Burr Ridge, Illinois; Boston Massachusetts; Sydney, Australia; 1989 and 1993.

[5] JCGM 100:2008, "Evaluation of measurement data – Guide to the expression of uncertainty in measurement", Bureau International des Poids et Mesures, Joint Committee for Guides in Metrology, Sept. 2008 [Online]. Available: www.bipm.org/utils/common/documents/jcgm/JCGM_100_2008_E.pdf

[6] ISO/IEC 17025:2005 General requirements for the competence of testing and calibration laboratories, 2nd ed. Switzerland 2005.

Anna Warzec is a Head of Central Chamber for Telecommunications Measurements and Laboratory of Electrical, Electronic and Optoelectronic Metrology in National Institute of Telecommunications since 1998. Graduation on Faculty of Electrical Engineering of Warsaw University of Technology. She is responsible for supervising the quality management system in the laboratory and on the development of new measurement methods in the area of basic electrical parameters (voltage, resistance, capacity etc.)
E-mail: A.Warzec@itl.waw.pl
Central Chamber for Telecommunications Measurements
National Institute of Telecommunications
Szachowa st 1
04-894 Warsaw, Poland

Michał Marszalec is a Chief of Time and Frequency Metrology Team in Laboratory of Electrical, Electronic and Optoelectronic Metrology in National Institute of Telecommunications. He received the M.Sc. degree in Telecommunications from Faculty of Electronics and Information Technology of Warsaw University of Technology in 2000. He specializes in time and frequency metrology, both measuring techniques and in timescale ensemble algorithms development in Database for Polish Atomic Timescale TA(PL).
E-mail: M.Marszalec@itl.waw.pl
Central Chamber for Telecommunications Measurements
National Institute of Telecommunications
Szachowa st 1
04-894 Warsaw, Poland

Marzenna Lusawa is a Specialist in the Time and Frequency Metrology Team in Laboratory of Electrical, Electronic and Optoelectronic Metrology in National Institute of Telecommunications. She received M.Sc. degree in Faculty of Physics of University of Warsaw in 2008. She specializes in time and frequency metrology, both measuring techniques and in timescale ensemble algorithms development in Database for Polish Atomic Timescale TA(PL).
E-mail: M.Lusawa@itl.waw.pl
Central Chamber for Telecommunications Measurements
National Institute of Telecommunications
Szachowa st 1
04-894 Warsaw, Poland

Information for Authors

Journal of Telecommunications and Information Technology **(JTIT)** is published quarterly. It comprises original contributions, dealing with a wide range of topics related to telecommunications and information technology. **All papers are subject to peer review**. Topics presented in the JTIT report primary and/or experimental research results, which advance the base of scientific and technological knowledge about telecommunications and information technology.

JTIT is dedicated to publishing research results which advance the level of current research or add to the understanding of problems related to modulation and signal design, wireless communications, optical communications and photonic systems, voice communications devices, image and signal processing, transmission systems, network architecture, coding and communication theory, as well as information technology.

Suitable research-related papers should hold the potential to advance the technological base of telecommunications and information technology. Tutorial and review papers are published only by invitation.

Manuscript. TEX and LATEX are preferable, standard Microsoft Word format (.doc) is acceptable. The author's JTIT LATEX style file is available:
http://www.nit.eu/for-authors

Papers published should contain up to 10 printed pages in LATEX author's style (Word processor one printed page corresponds approximately to 6000 characters).

The manuscript should include an abstract about 150–200 words long and the relevant keywords. The abstract should contain statement of the problem, assumptions and methodology, results and conclusion or discussion on the importance of the results. Abstracts must not include mathematical expressions or bibliographic references.

Keywords should not repeat the title of the manuscript. About four keywords or phrases in alphabetical order should be used, separated by commas.

The original files accompanied with pdf file should be submitted by e-mail: redakcja@itl.waw.pl

Figures, tables and photographs. Original figures should be submitted. Drawings in Corel Draw and PostScript formats are preferred. Figure captions should be placed below the figures and can not be included as a part of the figure. Each figure should be submitted as a separated graphic file, in .cdr, .eps, .ps, .png or .tif format. Tables and figures should be numbered consecutively with Arabic numerals.

Each photograph with minimum 300 dpi resolution should be delivered in electronic formats (TIFF, JPG or PNG) as a separated file.

References. All references should be marked in the text by Arabic numerals in square brackets and listed at the end of the paper in order of their appearance in the text, including exclusively publications cited inside. Samples of correct formats for various types of references are presented below:

[1] Y. Namihira, "Relationship between nonlinear effective area and mode field diameter for dispersion shifted fibres", *Electron. Lett.*, vol. 30, no. 3, pp. 262–264, 1994.

[2] C. Kittel, *Introduction to Solid State Physics*. New York: Wiley, 1986.

[3] S. Demri and E. Orłowska, "Informational representability: Abstract models versus concrete models", in *Fuzzy Sets, Logics and Knowledge-Based Reasoning*, D. Dubois and H. Prade, Eds. Dordrecht: Kluwer, 1999, pp. 301–314.

Biographies and photographs of authors. A brief professional author's biography of up to 200 words and a photo of each author should be included with the manuscript.

Galley proofs. Authors should return proofs as a list of corrections as soon as possible. In other cases, the article will be proof-read against manuscript by the editor and printed without the author's corrections. Remarks to the errata should be provided within one week after receiving the offprint.

Copyright. Manuscript submitted to JTIT should not be published or simultaneously submitted for publication elsewhere. By submitting a manuscript, the author(s) agree to automatically transfer the copyright for their article to the publisher, if and when the article is accepted for publication. The copyright comprises the exclusive rights to reproduce and distribute the article, including reprints and all translation rights. No part of the present JTIT should not be reproduced in any form nor transmitted or translated into a machine language without prior written consent of the publisher.
For copyright form see: http://www.nit.eu/for-authors

A copy of the JTIT is provided to each author of paper published.

Journal of Telecommunications and Information Technology has entered into an electronic licencing relationship with EBSCO Publishing, the world's most prolific aggregator of full text journals, magazines and other sources. The text of *Journal of Telecommunications and Information Technology* can be found on EBSCO Publishing's databases. For more information on EBSCO Publishing, please visit www.epnet.com.

(*Contents Continued from Front Cover*)

Closed-form Distribution and Analysis of a Combined Nakagami-lognormal Shadowing and Unshadowing Fading Channel

R. Singh and M. Rawat — *Paper* — *81*

Long-term Absolute Wavelength Stability of Acetylene-stabilized Reference Laser at 1533 nm

T. Kossek, D. Czułek, and M. Koba — *Paper* — *88*

Verification of Staff Proficiency in the Calibration Laboratory on Voltage, Frequency, Resistance and Capacity Measurements

A. Warzec, M. Marszalec, and M. Lusawa — *Paper* — *94*

Editorial Office

National Institute
of Telecommunications
Szachowa st 1
04-894 Warsaw, Poland

tel. +48 22 512 81 83
fax: +48 22 512 84 00
e-mail: redakcja@itl.waw.pl
http://www.nit.eu

INSTYTUT ŁĄCZNOŚCI
PAŃSTWOWY INSTYTUT BADAWCZY

JOURNAL OF TELECOMMUNICATIONS AND INFORMATION TECHNOLOGY 4/2016